EFFECT OF TRANSITION METAL COMPOUNDS ON THE UV DEGRADATION OF POLYMERS

BY

RAMANEE P. R. RANAWEERA

A thesis submitted for the degree
of Doctor of Philosophy of the
University of Aston in Birmingham.

SEPTEMBER 1975

SUMMARY

The effects of typical nickel complex light stabilisers as UV screens and as additives were compared in model systems initiated by hydroperoxides or carbonyl compounds. Oxygen absorption studies showed the nickel oxime and nickel dithiocarbamate complexes to impart a stability additional to UV screening in the hydroperoxide initiated photo-oxidation and only screening in the triplet initiated oxidant. On the other hand, cyasorb UV(1084) was found to stabilise photo-oxidation only by screening of ultra violet radiation. The order of effectiveness of the additives is $Ni(DBDC)_2$ > $Ni(OX)_2$ > cyasorb UV(1084).

The stability of these complexes to UV radiation was compared by measuring the changes in the UV absorption spectra of these complexes. Their stabilities to UV radiation was found not to be effected by the presence of carbonyl compounds. The determination of the extinction coefficients of typical UV stabilisers in the range 230 mm - 400 mm enabled a comparison to be made of their theoretical screening ability. These values correlated well with their screening ability in the above tests.

The reactions of $Ni(DBDC)_2$ and $Ni(OX)_2$ with cumene hydroperoxide were examined kinetically, and by subsequent product analysis some of the kinetic parameters were determined. $Ni(DBDC)_2$ decomposed hydroperoxides by a first order ionic reaction to give phenol and acetone,

whereas the reaction of $Ni(OX)_2$ with hydroperoxide was rather slower and produced the corresponding alcohol in a stoichiometric reaction. An analysis of the products of this reaction by TLC, IR and GLC produced evidence to suggest that the first step in the stabilising mechanism is the attack of hydroperoxide on a Ni(OX)molecule giving rise to O-hydroxy acetophenone and salicylic acid as the major oxidation products.

An attempt was made to correlate the results obtained on the above solution studies with the behaviour of same stabilisers as screens and additives in high density polyethylene, low density polyethylene and polystyrene. It was found that all three complexes retarded the breakdown of hydroperoxide to ketone, when used as screens when used as an additive Ni(DBDC), a typical peroxide decomposer completely eliminated the formation of hydroperoxide derived carbonyl. $Ni(OX)_2$ and cyasorb UV(1084), which have previously been reported to quench excited states retarded but did not eliminate hydroperoxide derived carbonyl formation.

On the basis of the above results it is concluded that the stabilising activity of these nickel complexes is primarily due to a screening of the UV radiation. In addition, interaction with hydroperoxides is considered to be an auxiliary stabilising mechanism. No evidence was found that excited state quenching was an important stabilising mechanism.

The work described herein was carried out at The University of Aston in Birmingham between October 1972 and July 1975. It has been done independently and submitted for no other degree.

SEPTEMBER 1975

R.P.R. RANAWEERA

ACKNOWLEDGEMENTS

I wish to express my gratitude to my supervisor Professor Gerald Scott for his guidance and encouragement throughout the course of this study.

I also acknowledge with thanks the co-operation of technical and Library staff of the University of Aston in Birmingham.

My thanks are due to the technical assistance training department of the British Government and to the Government of Sri Lanka for providing financial support under the Colombo Plan. I am also grateful to the Vidyalankara Campus of the University of Sri Lanka for sponsoring the scholarship and granting study leave.

CONTENTS

CHAPTER 3: GENERAL EXPERIMENTAL TECHNIQUES

CHAPTER 4: OXYGEN ABSORPTION STUDIES OF MODEL COMPOUNDS

CHAPTER 5: ULTRA-VIOLET SPECTRA OF THE METAL CHELATES AND THEIR STABILITIES TO UV LIGHT.

SUPPORTING PUBLICATIONS

Ramanee P.R. Ranaweera and Gerald Scott. Chemistry & Industry, 5 Oct'74, p.774.

Ramanee P.R. Ranaweera and Gerald Scott. J.P.S. (Polymer letters ed^{n}) 13 p.71 (1975).

LIST OF ABBREVIATIONS USED IN THE PRESENT WORK

CHP - cumene hydroperoxide

BP - Benzophenone

BMK - iso-Butyl methyl ketone

TBH - Tertiary butyl hydroperoxide

AZBN- Azobis-isobutyro-nitrile

$Ni(OX)_2$ - Ni(II)bis (orthohydroxy acetophenone oxime)

$Cu(OX)_2$ - Cu(II)bis (orthohydroxy acetophenone oxime)

$Fe(OX)_3$ - Fe(III)tris (orthohydroxy acetophenone oxime)

$Ni(DBDC)_3$ - Ni(II)bis (dibutyl dithiocarbamate)

UV 531 - 2-hydroxy, 4-octoxy benzophenone

UV 1084 Ni(II)-n-butylamino [2-2'-thiobis (4-tert-octyl-phenolate)]

CHAPTER I

1.1 INTRODUCTION

Plastics are degraded by heat, light, chemical or bacterial attack, or simply by long storage their properties can change, and this may result in a loss in desirable physical,mechanical and electrical properties.

The end result of photodegradation is normally embrittlement due to decay of the above properties when exposed to bright sunlight or an accelerated environmental exposure process (i.e. ultraviolet light of wavelength greater than 280 nm). This deterioration is thought to be due to photocatalysed oxidation. Polymers with alphatic backbones should not dissociate, however the presence of a chromophore in the system will initiate photodegradation.

Almost all plastic material except polytetrafluoroethylene are degraded by tropical exposure within two years, but in some cases their useful life may be increased to three years or more by incorporating light stabilisers or carbon black. Typical examples of this last group are polyethylene, polyvinyl, chloride and nylon.

The sun has an approximate Botlzmann distribution of energy with a peak maximum at a wavelength of approximately 500 nm. However the shorter wavelengths are not available at the earths surface because they are absorbed by the ozone layer in the upper atmosphere. As a general rule

only light having a wave length exceeding 280 nm reaches the earths surface. This will restrict the number of reactions which may occur.

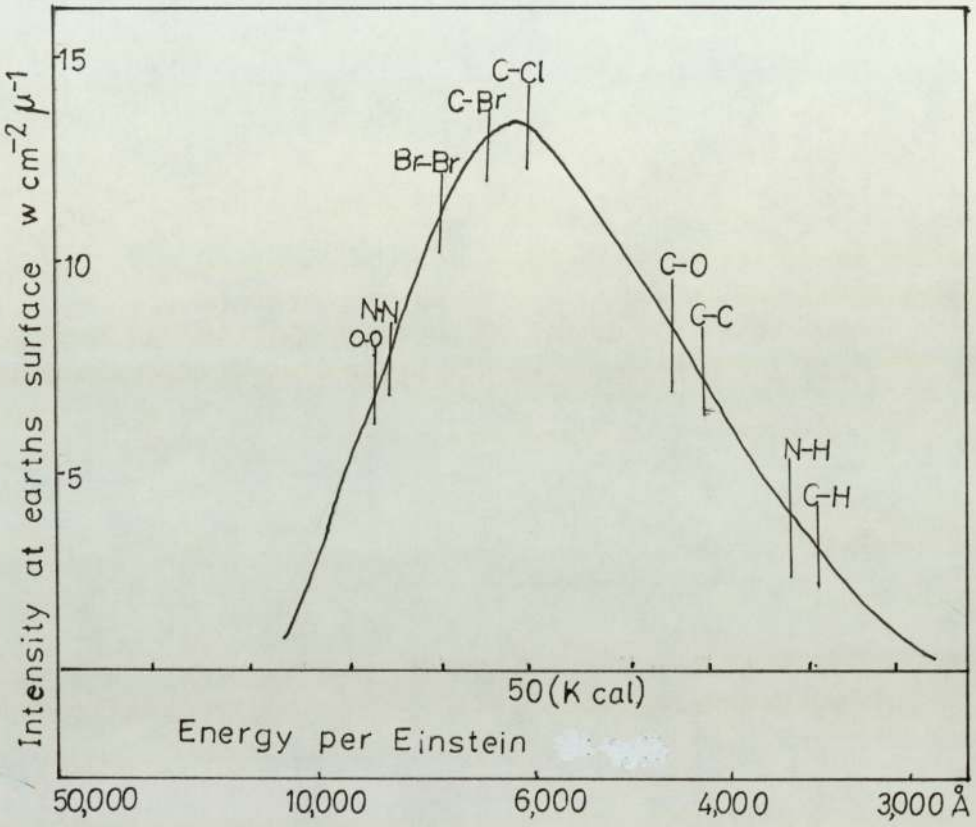

FIGURE 1.1

A plot of distribution of energy from the sun in terms of the intensity at the earths surface, with the bond strengths of a number of typical covalent bonds are shown above. The major reaction in the degradation of physical properties is usually the breaking of chemical bonds in the back bone of the polymer. It is evident from the figure that although a large portion of the suns radiation is sufficiently energetic to break weak bonds such as the O-O bond in a peroxide or an

N-N bond, very little of the total radiation is sufficiently energetic to break strong bonds such as the C-C bond and none is available to break bonds such as C=O or C=C which have energies greater than 100 k cal/mole. The chemical bonds involved in the formation of the back bones of most stable polymers usually have strengths comparable to those of the C-C bond and since biphotonic processes are rather rare in organic photochemistry it could be expected from the data shown in the above figure that radiation with wavelengths longer than about 400 nm will be ineffective in bond breaking processes. Since the radiation of wavelengths shorter than 280 nm is filtered out by the earths atmosphere, for many practical purposes the photochemistry could be restricted to the wavelength range of 280 nm to 400 nm.

Polymers are known to undergo nearly all of the typical photochemical reactions exhibited by small molecules having the same chromophoric groups; however the quantum yields are modified and usually reduced by the fact that these reactions must now take place in the solid state.

1.1.1 Initiation

Polymer oxygen interactions in the excited states may be responsible for initiation of oxidation in some systems. New UV absorption bands have been reported for hydrocarbon-oxygen complexes which is not present in the hydrocarbon alone[1,2,3,4]. These absorptions have been identified[3] as contact charge transfer absorptions. Several authors have suggested that the excited charge transfer states could initiate photooxidation. Hence possible initiation mechanisms in initiated hydrocarbons could be

$$RH + O_2 + h\nu \rightarrow 2R\cdot$$

$$R\cdot + O_2 \rightarrow RO_2\cdot \text{ etc.}$$

However Chien found the quantum yield of radical formation to be low during the induction period observed in the oxidation of cumene. Since the singlet triplet transition is more easily perturbed in aromatic compounds than in olefins the low value for quantum yield may be due to the chemistry of the oxygen perturbed triplet aromatic ^3A state which has low intrinsic reactivity because of electron delocalisation, and hence an oxygen perturbed triplet could be more important in the initiation of aromatic hydrocarbons.

$$3A + O_2 \rightarrow \text{peroxide}$$

Carlsson and Robb[6] proposed that the same process is responsible for the oxygen-tetralin and oxygen-indene spectra. A recent study of the p-cymene-oxygen system led to similar conclusions[7].

Common chromophores that are present in polymers, which are also responsible for initiation are carbonyl groups, peroxides and vinyl groups thermaly produced during processing. The first oxidation product is the peroxide[8] which could subsequently decompose to give carbonyl[9].

$$RCH_2R' \xrightarrow{O_2} \begin{array}{c} HOO \\ | \\ R - C - R' \\ | \\ H \end{array} \longrightarrow \begin{array}{c} O \\ \| \\ R - C - R' \end{array}$$

Several workers[10,18] suggested the possibility of the formation of peroxide by the attack of singlet oxygen on saturated carbon atom or vinyl groups.

$$\text{ketone} \xrightarrow{h\nu} (\text{ketone})^3_n - \pi^* + O_2 \longrightarrow \text{ketone} + {}^1O_2$$

$$RCH_2CH = CH_2 + {}^1O_2 \longrightarrow R - CH = CHCHOOH$$

further reactions

Although the absorption maximum of alkyl hydro-peroxides is around 210 nm, the tail of this band extends beyond 300 nm. Thus absorption of solar radiation can occur. The photochemical reaction brought about by this absorption involves cleavage of the O-O bond[11].

$$ROOH \xrightarrow{h\nu} RO\cdot + \cdot OH$$

The quantum efficiency for this reaction is found to be near unity.

1.1.2 Mechanism

Oxidation of most polymers occurs by a reaction of low activation energy and is very susceptible to inhibition by conventional antioxidants, it is generally assumed to proceed by means of kinetic chains propagated by free radicals. Hydroperoxides are the key initiators for the oxidative degradation of polymers both during thermal and photoinitiated degradation and the mechanisms can be summarised as follows.

Initiation.

$$2ROOH \xrightarrow{Ri} ROO\cdot + RO\cdot + H_2O \quad \text{thermal}$$

$$\text{or} \quad ROOH \xrightarrow{h\nu} RO\cdot + \cdot OH \quad \text{photo}$$

$$\left.\begin{matrix} ROO\cdot \\ RO\cdot \\ \cdot OH \end{matrix}\right\} + RH \longrightarrow \begin{matrix} ROOH \\ ROH + R \\ H_2O \end{matrix}$$

Propagation

$$R\cdot + O_2 \xrightarrow{k_2} ROO\cdot$$

$$ROO\cdot + RH \xrightarrow{k_5} ROOH + R\cdot$$

Termination

$$2ROO\cdot \xrightarrow{k_4}$$

$$2R\cdot \xrightarrow{k_5} \text{Inactive products}$$

$$ROO\cdot + R\cdot \xrightarrow{k_6}$$

Under steady state conditions or under high oxygen pressure, a general expression for the rate of oxidation of this reaction scheme was derived by Bolland[12] and is given as

$$\frac{-do_2}{dt} = \sqrt{Ri}\ \frac{k_3}{k_4}\ [RH]$$

Under these circumstances the reaction rate depends on the chemistry of the hydrocarbon RH. The easier it is for hydrogen to be abstracted from RH, the higher will be the value of k_3, and faster will be the rate of oxidation. The ease of abstraction of H from different types of carbon atom has been shown by Bolland[13] to increase in the followong order.

primary C-H < secondary C-H < tertiary C-H < allylic H

< H in α position to aromatic ring.

Therefore it might be expected that small amounts of chain branching or unsaturation in polymers might be responsible for initiating degradation by slowly peroxiding or by providing easily oxidisable sites.

Another possible initiation process is through aliphatic ketones. These show a weak absorption in the near UV with a peak around 280 nm and tails extending beyond 300 nm up to about 320 to 330 nm. The known photochemistry of these ketones suggests that the principal routes available for chain scission are Norrish type I and Norrish type II reactions.

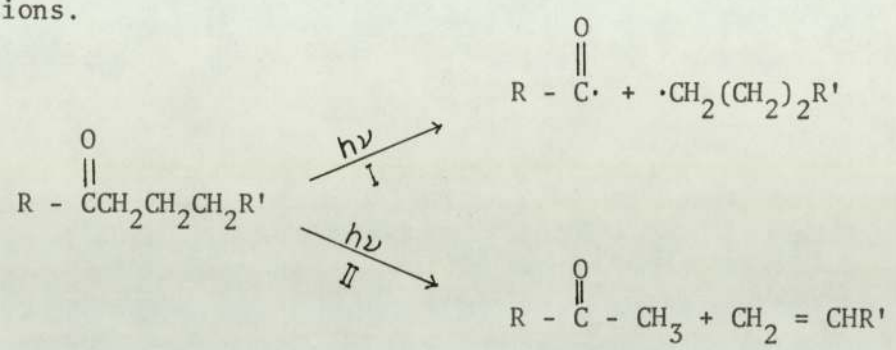

Quantum yield measurements show that the type II cleavage occurs more readily than type I. Thus the effects of the absorbed UV light on the polymers have been interpreted as free radical chain oxidations which finally lead to the cleavage of the polymer back bone with the formation of molecular fragments.

A sequence of reactivity was drawn up by Naarman [49] relating the induction time during thermal oxidation to the type of functional group as

$$-OOH > C{=}O > CH_2CH{=}CH_2 > -O-CH{=}CH_2 > -C{=}C- > \overset{CH_3}{\underset{|}{C}}-H > CHOH > CHOR$$

1.1.3 Stabilisation

The stabilisation of polymers against weathering damage involves the retardation of or elimination of primary photochemical processes similar to those discussed above, for this photostabilisers are used. There are in principal, four general ways in which these could act.

1. By simply acting as a UV absorber.
2. Quenching of the excited states
3. Trapping of radicals

or 4. Decomposing peroxides.

A good UV absorber should have a high absorptivity in the region of wavelengths harmful to the polymer. Since this region of maximum sensitivity varies from one polymer system to another, therefore a universal stabiliser should absorb in the entire solar UV region, thereby weakening its action on the polymer. A good UV absorber will harmlessly dissipate the absorbed energy and this should proceed at a faster rate than side reactions, leading to the formation of free radicals.

Recently it was suggested[14 - 23] that compounds that do not act as UV screens can stabilize polymers by abstracting the excited state energy from the polymer molecule. This process is known as energy transfer or quenching. This could be either a long range energy transfer or contact transfer. For either process to occur the quencher should reach within quenching distance of the excited sensitizer within its life time, and should possess high diffusion constants in the substrate. But this process is rather unlikely[24], in polymers containing

alphatic back bones as this would require an extinction coefficient greater than 5000 to 10,000 for the rate of quenching of excited singlet states to exceed the fluorescence decay rate.

It is worth pointing out that a method of stabilisation like this, although interesting would have very little or no significance in practice. In fact under real conditions Norrish type II breaking may still occur via the singlet state, also oxygen being one of the most effective triplet quenches will completely eliminate the action of added triplet quencher producing molecules of singlet oxygen which may promote oxidation[10].

The mechanism of action of some organometallic stabilisers has been associated with their ability to quench the excited singlet and triplet states[14-23] of the carbonyl groups that are present at random in the polymer chain. This mechanism is based on inference rather than direct experimental evidence.

Briggs and McKellar[14-16] showed that there is a possibility that metal oxime chelates having the general formula

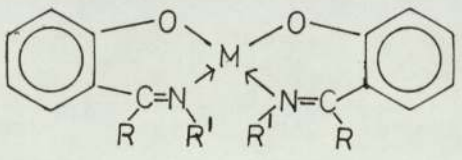

might act as triplet quenchers. They investigated the effect of these on triplet anthracene by the flash photolytic technique. They found that the chelates that are more effective as UV stabilisers generally reduce both the intensity and the life time of the triplet anthracene

to a greater extent under similar photolysis conditions. For example the Ni(II) chelate of syn methyl-2hydroxy-4-methyl phenyl N-butyl ketimine which is a moderate quencher of triplet anthracene is a better stabiliser than 2-hydroxy-4-n-octoxy benzophenone, the well known commercial UV absorber. However in their experiments they found no apparent effect on the fluorescence emission of anthracene. They concluded from their results that the quenching effect is primarily dependent on the spacial configuration of the ligands round the central metal atom in the chelate.

Some of these chelates are also found to be effective UV stabilisers for polypropylene[25]. However anthracene cannot be expected to be an adequate model for polypropylene or any other polyolefine or carbonyl chromophore. Particularly the energy of transition for anthracene triplet is ∿ 42k cal/mole, (26,100 cm^{-1}) whereas the value for an aliphatic ketone is ∿ 74k cal/mole[26,30] (31,200 cm^{-1}).

Usually energy transfer takes place from a donor at higher energy level than that of the acceptor. Therefore it is possible for an additive incapable of quenching anthracene triplets to quench ketone triplets. The inadequacy of the anthracene triplet model is seen in the failure of the Ni(II) complex of 2,2'thio bis 4-tert octyl phenol to quench triplet anthracene, whereas the same Ni(II) complex is found to be an effective stabiliser by Chien and Conner[17] who used a system of cumene photosensitized by diethyl ketone. Further to this it was also shown to be an effective stabiliser in polypropylene[27].

Porter and Wright[28] discussed a possible mechanism for quenching. They used an aqueous and alcoholic solutions of paramagnetic metallic ions, which were found to be quenchers. This quenching process is the same as that suggested by McConnell[29] for the catalysis of cis trans isomerisation via triplet transitions states by NO.

Similar inferences were made by Linschitz and coworkers[33,31,32] for the quenching activity of metal chelates of ethylene diamene, o-phenanthrolene using triplet anthracene as a model system.

Hammond et al[34] found that some organometallic compounds act in solution as quenchers of representative triplets of high excitation energy and to the same extent as of triplets with a low electronic energy. Their conclusions were similar to those by Linschitz and coworkers. Their results indicate that the transition metal chelates are far more reactive than the solvated ions. They pointed out the importance of the presence of unsaturated systems in the chelate.

The results published by Wiles et al.[27] are consistent with those published by Guillory and coworkers[35]. They concluded from their results that there could be an energy transfer from the carbonyl chromophores to the stabiliser, but this is not the sole protective action of all effective additives, or necessarily the most important mechanism and suggest that the effectiveness of the oxime and the zinc diisopropyl dithiophosphate is due to their ability to act as effective traps for OH and alkoxy radicals[36].

However the dominant processes involved in photostabilisation are still open to speculisation. The quenching as discussed above has now been shown to be of only minor importance for certain Ni(II) chelates[37]. Recent studies by Carlsson and Wiles[21,38] too showed the Ni(II) chelates to be an ineffective quencher of model ketones excited by ultra-violet radiation[21]. This supports the evidence by Guillory and Cook[37] who used a more sensitive test to show that quenching can occur in the liquid phase but at well below the rates suggested in previous work.

Recent work by Wiles et al.[22,39] showed that many Ni(II) chelates which are effective stabilisers for polypropylene are very effective singlet oxygen quenchers. This is also supported by other workers[40,41,42] Trozzolo and Winslow[18] suggested the possibility of formation of singlet oxygen from excited macrocarbonyl impurities which could react rapidly with back bone aklyl methylene groups to yield hydroperoxides. Kaplan and Kelleher[10] showed the possibility for the singlet oxygen to attack saturated carbon atoms as well to form hydroperoxides.

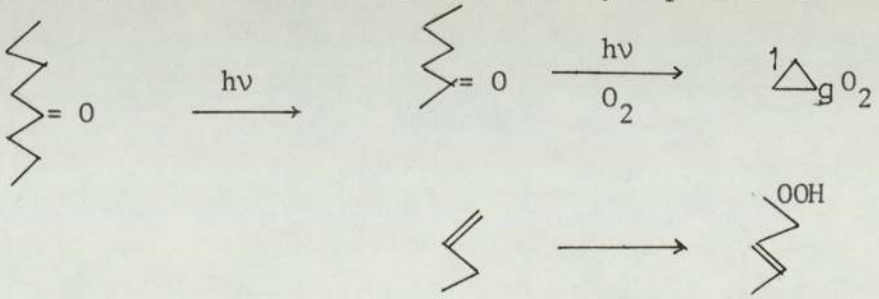

However the true importance of the singlet oxygen route to hydro-peroxides is uncertain in comparison with other photoinitiation processes.

Antioxidants acting as radical traps.

Any substance capable of reacting with free radicals to form products that do not reinitiate the oxidation reaction could be considered to function as a free radical trap, for example, quinones are known to scavenge alkyl free radicals as evidenced by their effectiveness as inhibitors of polymerisation. Many polynuclear hydrocarbons too show activity as inhibitors of oxidation and are thought to function by trapping free radicals[46].

The most clear cut examples of inhibitors by trapping of radicals are the phenols and amine type of antioxidants which function primarily by removing alkyl-peroxy radicals from an autoxidising system and hence by interfering with the kinetic chain reaction[4,3,6].

$$R\cdot + O_2 \longrightarrow ROO\cdot$$

$$ROO\cdot + RH \longrightarrow ROOH + R\cdot \quad \Big\} \text{ chain reaction}$$

$$ROO\cdot + AH \longrightarrow ROOH + A\cdot$$

$$A\cdot \longrightarrow \text{inert product} \quad \Big\} \text{ chain termination}$$

in which RH is the substrate and AH is the antioxidant which is competing with the substrate for alkyl-peroxy radicals.

Peroxide decomposing Antioxidants.

Some antioxidants achieve their effect by decomposing hydroperoxides into inactive products without the intervention of free radicals whereby they destroy the initiators of oxidation chain reactions, examples are metal dithiocarbomates and phosphites which can reduce peroxides to alcohols[44,45].

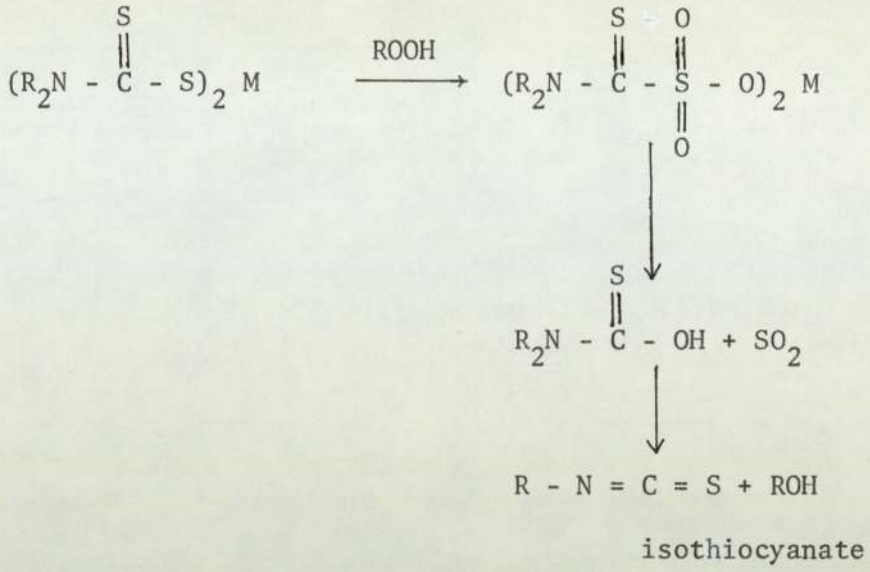

Here a Lewis acid possibly sulphur dioxide or sulphur trioxide is formed which is found to be formed by the oxidation of the dithiocarbomate complexes[44]. Scott et al. accounted for the catalytic effect of sulphur dioxide on the decomposition of cumene hydroperoxide on the basis of the following scheme.

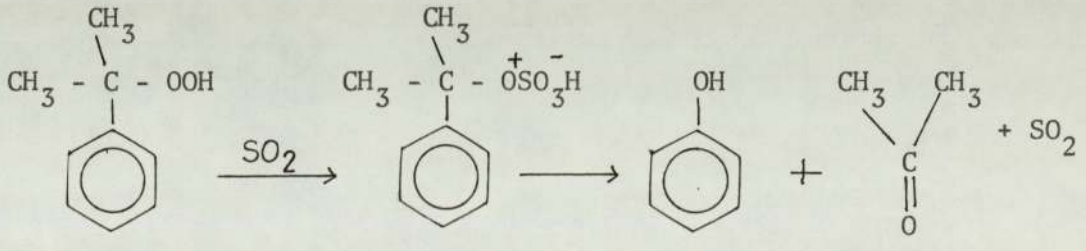

These antioxidants were distinguished from the phenolic type of antioxidants by comparing the oxygen absorption profile obtained with hydroperoxide and azobis-isobutyro-nitrile (AZBN) initiated oxidation[44]. Sulphur containing antioxidants prevented the initiation of oxidation by removing the hydroperoxide. With phenol inhibited oxidation initiated by

AZBN an initial induction period was observed even at very low anti-oxidant concentrations. This shows that the reaction

$$ROO\cdot + AH \rightleftharpoons ROOH + A\cdot$$

is reversible and the reverse reaction can compete with the reaction

$$A\cdot \longrightarrow \text{Inactive products.}$$

1.2 SCOPE AND OBJECT OF THE PRESENT WORK

Much of our present knowledge of stabilisation of polymers and related materials against photo-oxidation under various environmental conditions has been obtained by direct experimental observations rather than based on theory. The continued development of improved antioxidants and synergistic combinations of stabilisers of different types will depend increasingly upon a better understanding of the mechanisms by which these materials function to inhibit or retard the autoxidation reaction.

Although a lot of work has been done on the mechanism of action of ultra-violet stabilisers the dominant processes involved in photo-stabilisation are still the subject of speculation. Furthermore, from the foregoing survey it is seen that most of the nickel complexes used as photostabilisers were earlier thought to be acting as quenchers of triplet carbonyl groups. These conclusions were based more or less on inference rather than on direct experimental evidence. Recent work by Carlsson and Wiles[38] showed that this type of stabilisation by a quenching of the triplet states of carbonyl is no more important than the other possible mechanisms, including hydroperoxide decomposition radical scavenging, and singlet oxygen quenching.

Therefore additional studies both qualitative and quantitative are needed to provide more complete information, particularly with regard to the detailed reactions involved in the action of the several types of preventive antioxidants.

Recent studies in these laboratories have suggested that hydroperoxides rather than carbonyl is the more important photoinitiator present in polyolefins[8,47,48] based on this, model compound studies were carried out with various initiators and the effect of transition metal compounds were studied in more detail, paying some attention to the reasons for the unexplained aspects of the processes occurring in these systems.

The complexes used are

1. with Nitrogen-Oxygen Ligands.

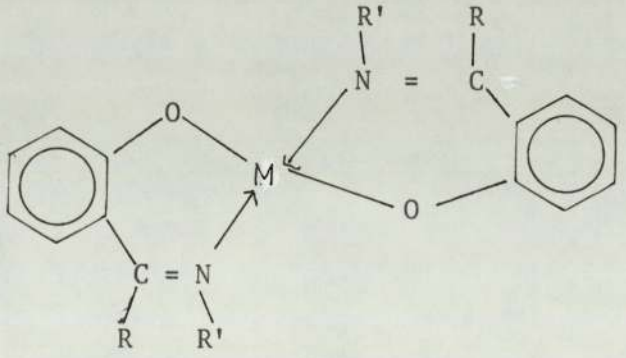

2. Sulphur-sulphur Ligands

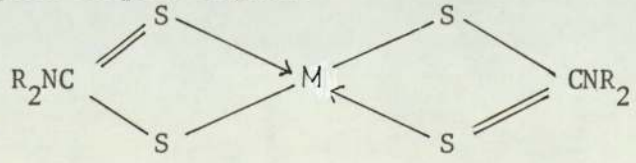

3. Oxygen-sulphur Ligands

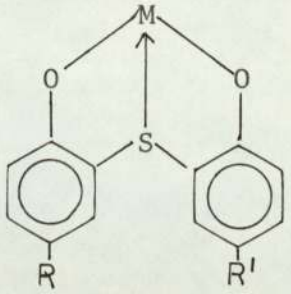

The model compound studies were followed by some studies with some polyolefines so that their effects could be inter-related in an attempt to explain some of the unexplained aspects.

CHAPTER 2

SYNTHESIS AND CHARACTERIZATION OF METAL CHELATES USED AS ADDITIVE COMPOUNDS

2.1.1 Preparation of O-hydroxy acetophenone oxime.

The oxime was first prepared[50] and subsequently used in the preparation of the respective complexes.

0.5 gm of hydroxyl amine hydrochloride in water was added to a solution of 0.2 gm α-hydroxy acetphenone in alcohol containing 2 ml of 10% sodium hydroxide. Sufficient alcohol was added to this solution to give a clear solution. This mixture was refluxed for ten to fifteen minutes, cooled in ice, and recrystallised the white solid formed with dilute alcohol.

Reaction mechanism

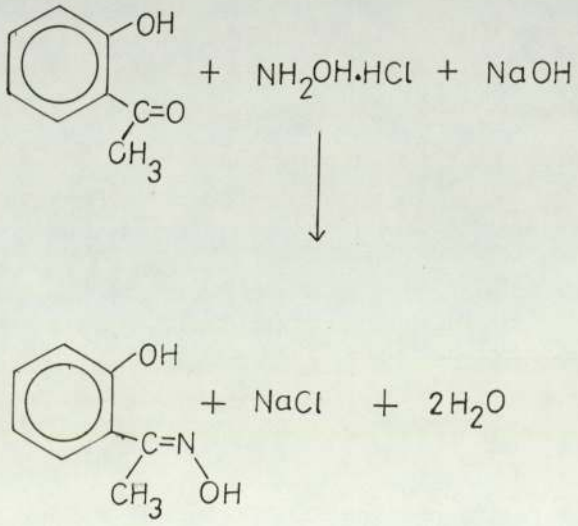

2.1.2 Preparation of the Nickel oxime chelate.

Reaction mechanism

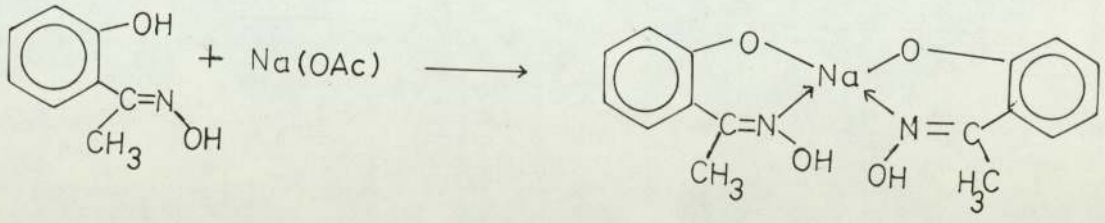

12.5 gms (0.05 mole) of hydrated Nickel acetate [$Ni(OAc)_2.4H_2O$] in water was refluxed for one hour with 15 gm (0.1 mole) α-hydroxy acetophenone oxime in ethanol. The green crystals separated on cooling were recrystallised with benzene. The compound when heated above 250°C.

2.1.3 Preparation of Cupper Oxime Chelate[51]

The above procedure was repeated with 6 gms (0.05 mole) of cupric acetate [$Cu(OAc)_2H_2O$] instead of 12.5 gm of nickel acetate.

2.1.4 Preparation of Ferric Oxime Chelate

The same procedure as for the nickel chelate was repeated with 0.54 gm (0.03 mole) of Ferric chloride (anhydrous) instead of 12.5 gm of nickel acetate.

2.1.5 Characterization of the Nickel and Copper complexes

The composition of the Ni(II) and Cu(II) complexes were found to be 1.2 (metal ligand) table (2.1.1). The structures were confirmed from the IR spectra. figures (2.1.1), (2.1.2) and (2.1.3). In the complexes the absorption band due to the free phenolic group is absent, while the

TABLE 2.1.1

Elemental Analysis of the Complexes

Compound	Molecular formula	Molecular weight	Theoretical			Experimental		
			%C	%H	%N	%C	%H	%N
O-hydroxy acetophenone	$C_8H_9NO_2$	151	63.6	5.9	9.27	65.04	6.00	9.93
Ni(II)bis O-hydroxy acetophenone oxime	$C_{16}H_{16}N_2O_4Ni$	359	53.41	4.45	7.79	54.71	4.54	7.8
Cu(II)bis O-hydroxy acetophenone oxime	$C_{16}H_{16}N_2O_4Cu$	364	52,71	4.39	7.69	53.2	4.30	7.6
Fe(III)bis O-hydroxy acetophenone oxime	$C_{24}H_{24}N_3O_6Fe$	510	44.70	4.70	8.23	45.8	4.84	8.12

Figure (2.1.1) Infra-Red spectrum of ortho hydroxy acetophenone oxime.

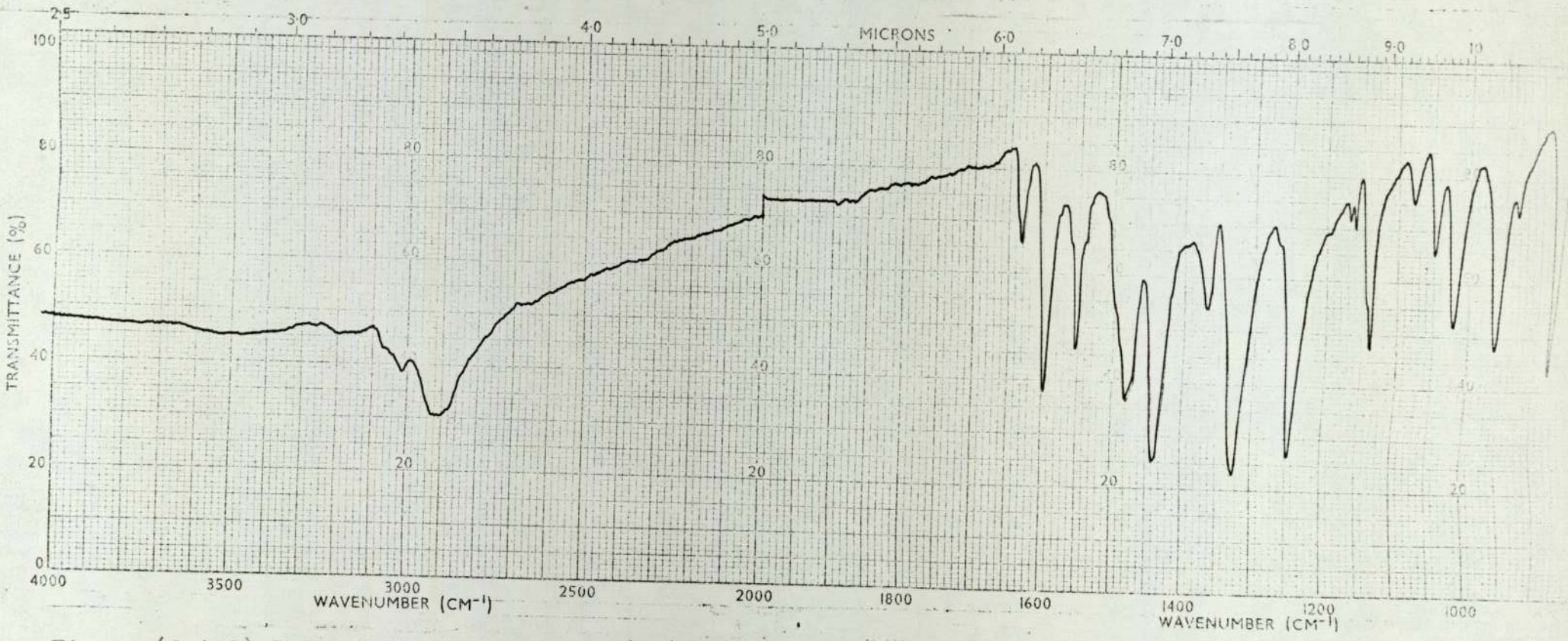

Figure (2.1.2) Infra-Red spectrum of $Ni(OX)_2$

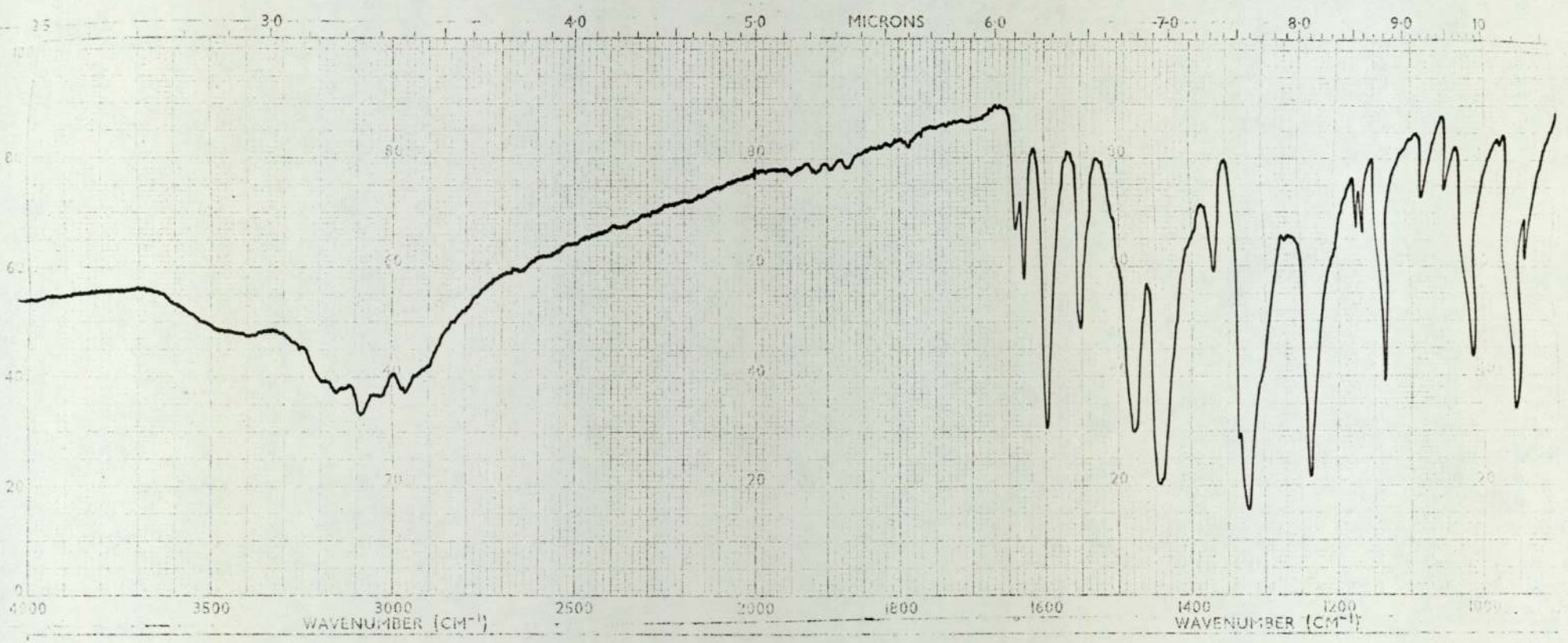

Figure (2.13) Infra-Red spectrum of $Cu(OX)_2$

TABLE 2.1.2

Absorption frequencies of ligands and their metal complexes

	Phenotic OH (cm^{-1})	Aromatic C=C (cm^{-1})	Oxime C=N (cm^{-1})	M - O (cm^{-1})	M - N (cm^{-1})
Oxime	3340	1575,1450	1615	-	-
Ni(II) complex	-	1600	1550	640,605	465,498
Cu(II) complex	-	1605	1550	640,600	465,498
Fe(III)complex	-	1610	-	640,600	428,460

bands due to =N-OH of the oxime group are intact, showing thereby that the phenolie hydrogen is replaced by the metal during complex formation. The stretching frequency of C=N is also lowered in the complexes, thus pointing to the co-ordination of the metal to the nitrogen of the oxime group. The low frequency of OH of the oxime group indicates strong intermolecular hydrogen bonding of the complexes.

In the complexes a band at 3260cm^{-1} is observed. This band is assigned to OH of the oxime group. This lower OH frequency is attributed to intramolecular hydrogen bonding OH.....O in the complexes[52,53,54].

2.1.6 Preparation of Nickel di-n-butyl dithiocarbomate

$[Cn\text{-}C_4H_9)_2.NCS_2]_2Ni$

Reaction mechanism.

$$Ni(SO_4) + 2[(n\text{-}C_4H_9)_2.NCS_2Na]$$

$$\downarrow$$

$$[(n\text{-}C_4H_9)_2.NCS_2]_2Ni + Na_2SO_4$$

A solution of 15.4 gm of nickel sulphate (AR grade) (0.05 mole) in 25 ml of water was added to 50.5 gm of a 45% W/N (22.7 gm) solution of the sodium salt of di-n-butyl dithiocarbamic acid. The crude nickel complex was filtered off and dissolved in 100 ml of chloroform by warming. This solution was filtered to remove the suspended green powder of nickel hydroxide, the solution in chloroform was washed three times with 100 ml portion of water, dried over anhydrous magnesium sulphate and the chloroform was evaporated on a rotary evaporator. (The water bath was maintained at 80°C).

Molecular formula $C_{18} H_{36} N_2 S_4 Ni$

Calculated C = 52.94 H = 8.82 N = 6.86 S = 31.37

Experimental C = 51.83 H = 7.80 N = 6.80 S = 30.21

Ferric dibutyl dithiocarbamate complex & UV 531 were supplied by R.P.Brueton.

Cyasorb UV 1084 was obtained from the Cyanamid company and was used without further purification.

2.2 Purification of solvents and reagents

2.2.1 Cumene

Technical grade cumene was washed with concentrated sulphuric acid, water, sodium bicarbonate and finally with water and was then dried, before fractionally distilling under nitrogen. The fraction boiling at 152°C was collected and stored at 5°C in a well stoppered flask (b.pt 152.39/ 760 mm)[55].

2.2.2 Cumene hydroperoxide

Cumene hydroperoxide stabilised with 6% of 15% W/W slurry of aqueous Na_2CO_3 (koch Light Ltd.) was purified by a modification of Kharasch's method[56]. 50 gm (1.25 mole) of caustic soda in 100 ml of water was added to 152 gm (1.0 mole) of hydroperoxide in ligroin at 0°C. The sodium salt was filtered, washed with 25% caustic soda solution, then with petroleum ether, and suspended in 500 ml of water. A stream of carbon dioxide was bubbled through the suspension and when all the hydroperoxide has been reliberated the solution became opaque, and separated into two layers. The lower aqueous layer was extracted

three times with pet ether and the combined ethereal fraction was washed with dilute sodium carbonate solution, and dried over anhydrous sodium carbonate. After removal of solvent the product was distilled at 52-55°C / 0.01 mm Hg, as a colourless liquid; purity by iodometric titration was better than 99%.

Tertiary butyl hydroperoxide was also purified via its sodium salt in a similar manner to boiling point 40°C / 19 mm Hg.

2.2.3 Purification of Solvents

Chlorobenzene: was fractioned from phosphorous pentoxide and the fraction boiling at 132°C collected.

Carbon Tetrachloride: spectroscopic grade was used without further purification.

Benzene: spectroscopic grade was used without further purification.

Benzophenone: recrystallised from 1:1 mixture of benzene and ligroin (m.pt. 47°C)

CHAPTER 3

3.1 INSTRUMENTAL TECHNIQUES

Infra-red spectra were recorded using a Perkin Elmer grating infra-red spectrophtotmeter Model 457.

Ultra-violet spectra were obtained from Perkin Elmer double beam ultra-violet spectrophotometer.

3.2 Oxygen absorption measurements using a pressure transducer

3.2.1 The apparatus for thermal studies

The oxygen absorption of the solutions studied were followed continuously and automatically using the apparatus[57] shown diagramatically in figure (3.2.1a). The reaction vessel is a 50 ml three necked quick-fit round bottom flask fitted with a tap which has a luer needle fitted at the opening. This allows the flask to be vented to the atmosphere and for calibration of the equipment. To the second neck the bucket dropping device figure (3.2.1b) is fixed. This allows the additive to be added at will to an autoxidising solution. The reaction vessel is charged with the oxidising solution, purged with oxygen, and placed in a thermostated bath and is then connected by a capillary glass tubing to the wet side of the pressure transducer. The dry side of the pressure transducer is connected to the ballast flask, having the same volume as the reaction vessel, and is placed alongside the reaction vessel in the bath. Capillary tubing is used for connections outside the bath and the distance is kept small so that the volume of the apparatus not thermostated is negligible to the total volume of the apparatus. Any pressure difference

Figure (3.2.1a)

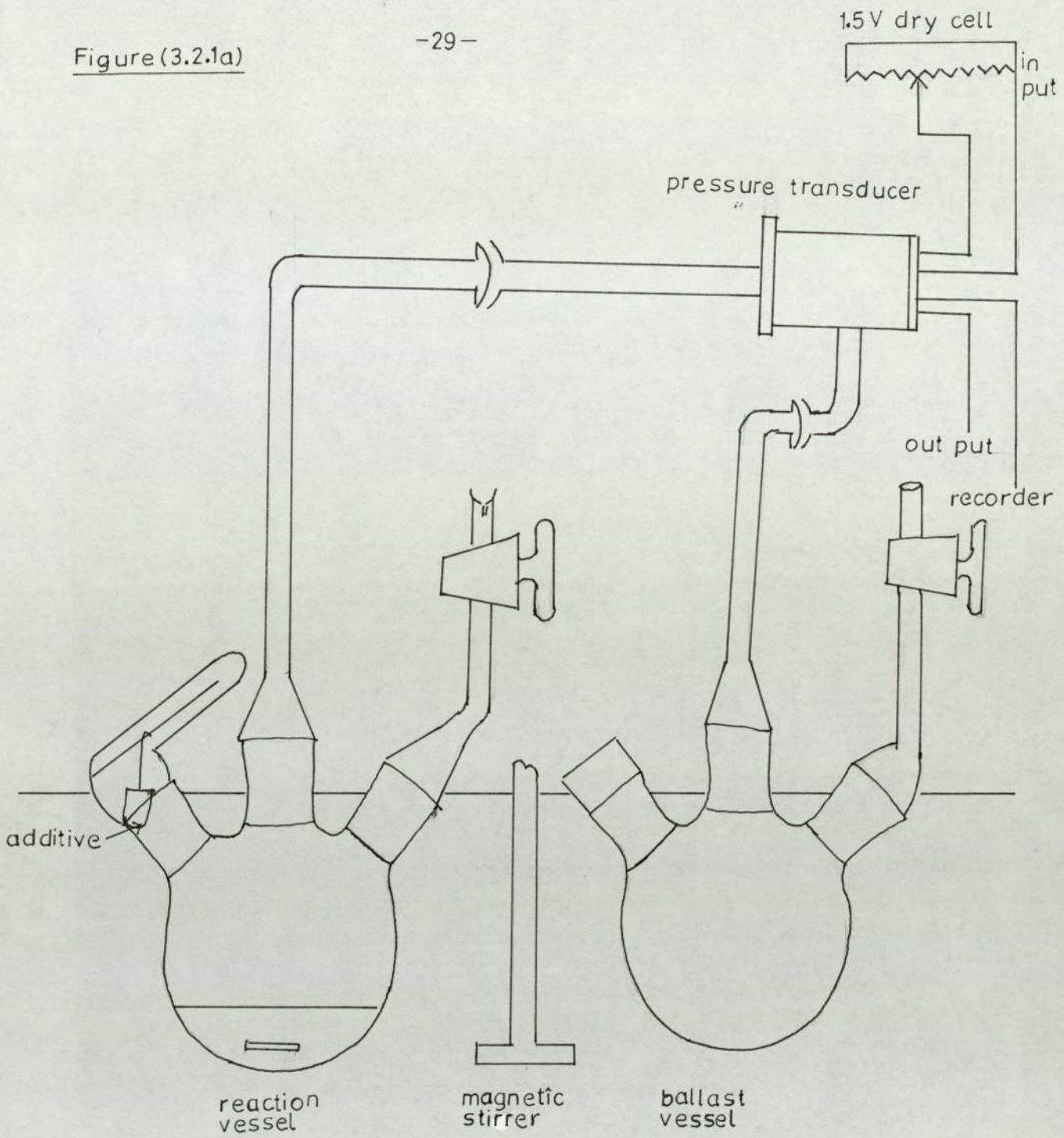

OXYGEN ABSORPTION APPARATUS

Figure (3.2.1b)

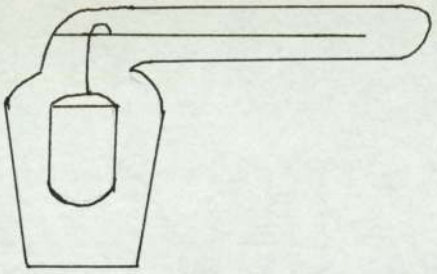

iron wire withdrawn with magnet to drop the bucket containing additive

between the reaction vessel and the ballast flask is proportional to the voltage output of the pressure transducer, and this is recorded using a millivolt recorder.

The transducer used was a strain gauge type manufactured by Pye Ether Ltd. Model UP1 (±10" WG).

The size of the output voltage is proportional to the input voltage therefore by varying the input voltage the sensitivity of the transducer to pressure fluctuations can be varied. To determine the amount of gas that is absorbed or evolved a syringe is fitted to the luer needle attached to the tap, volumes of air are withdrawn and the corresponding deflection on the recorder is recorded.

The maximum pressure change which was allowed to occur was 8%. If the oxygen was still absorbed oxygen was simply added by carefully opening the tap to an atmosphere of oxygen. Thus the reaction is carried out at constant pressure even though the rate of oxygen absorption above 100 mm pressure is independent of oxygen pressure [58].

3.2.2 Oxygen absorption under ultra-violet

A modification of the above system was used for oxygen absorption studies under ultra violet photograph. I. A rocking ultra-violet cabinet was used where the oxygen absorption system as shown in figure (3.2.2) is fitted to a hard board, which could move in front of a series of ultra-violet tubes. These were once used lamps and it consists of alternate sun lamps and black lamps, the energy output is maintained by a staggered replacement of the tubes.

Figure (3.2.2)

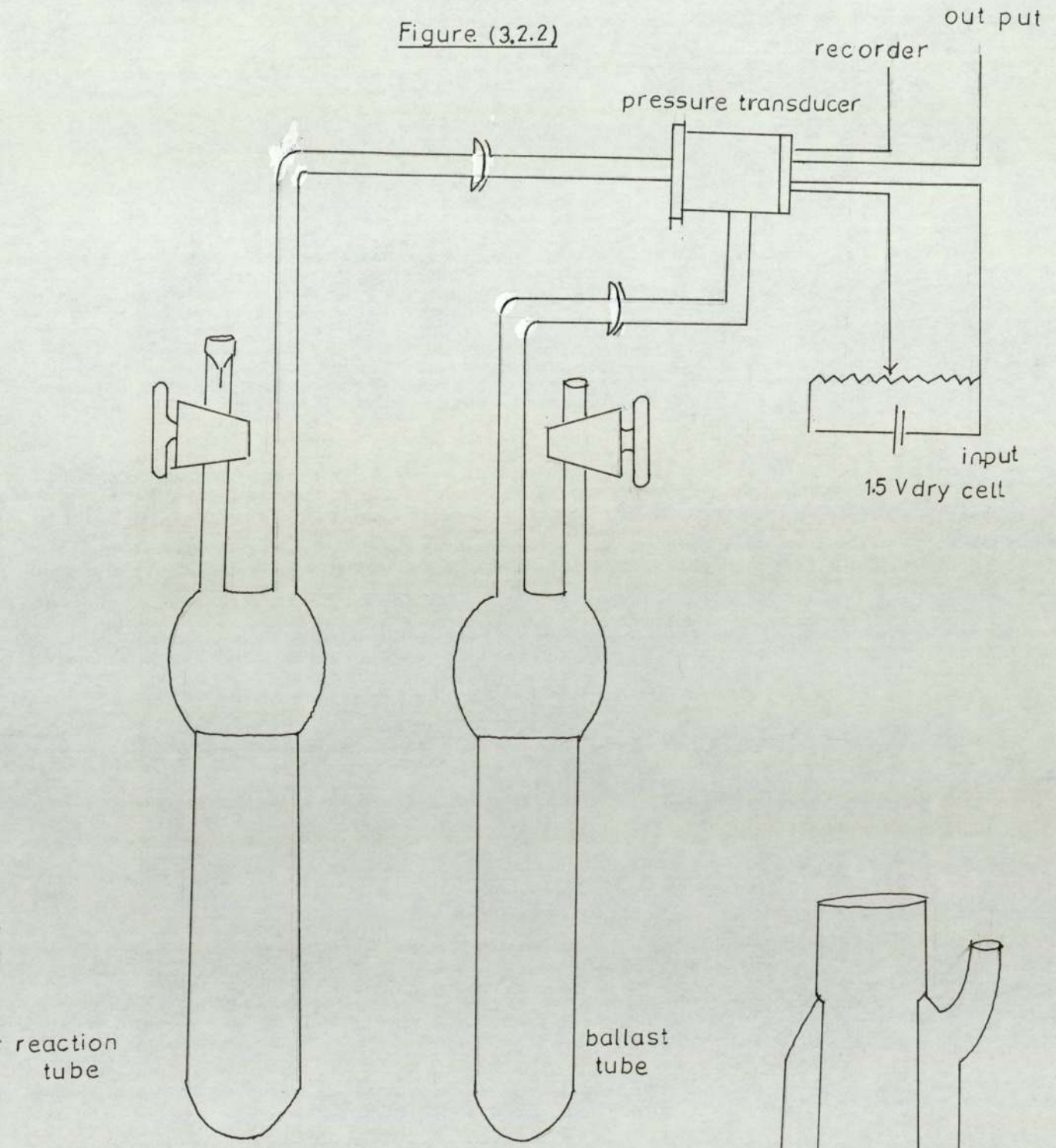

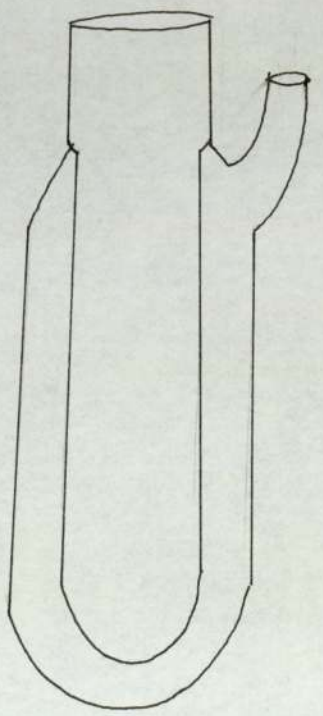

Fig (3.2.2.b)

PHOTOGRAPH I

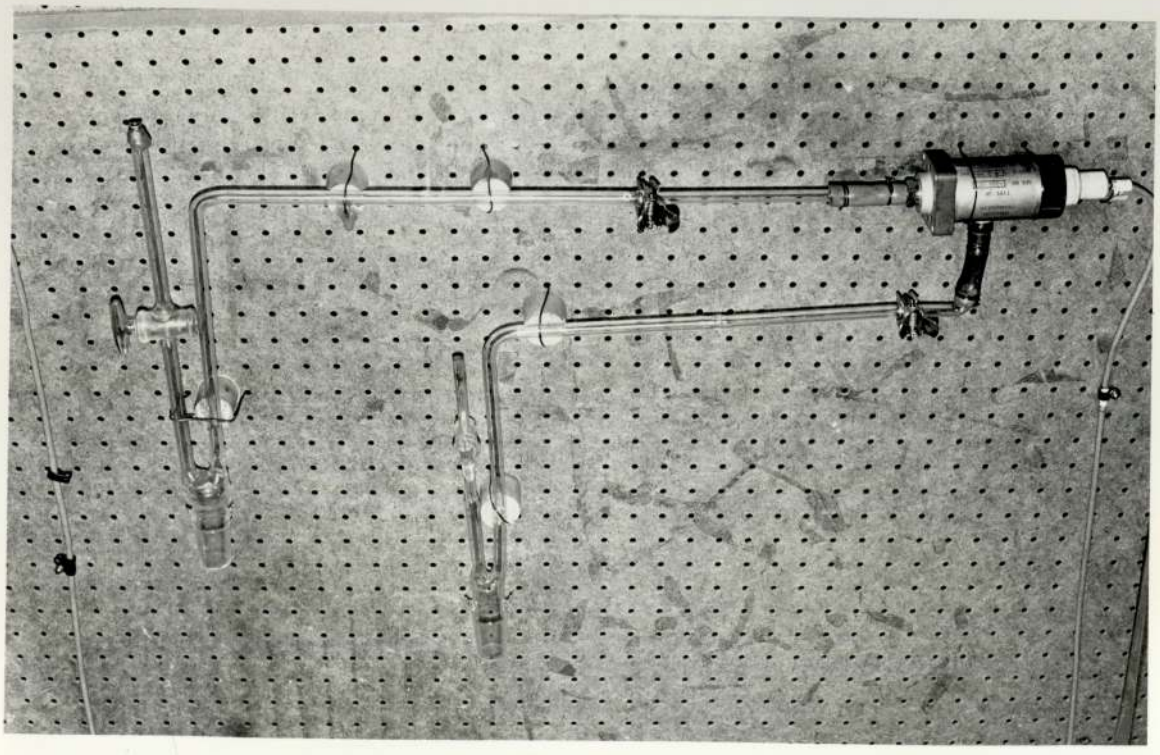

As before any pressure change in the reaction vessel is recorded on a multivolt recorder by means of a transducer.

The ultra-violet light emitted by the fluorescent sun lamp has a peak intensity at 3130°A and shows little resemblance to sun light (figure 3.2.13) in addition the emission extends to shorter wavelengths than sun light. Therefore the use of the fluorescent black lamps in conjunction with the fluorescent sun lamp was recommended by Hirt[59] in an attempt to improve the deficiency in the long wavelength ultra-violet region compared with sun light. The emission of this lamp peaks at 3520°A (figure 3.2.4), and in combination with the sun lamp provides closer approximation to sun light.

3.2.3 Apparatus for hydroperoxide decomposition studies

The apparatus used for the decomposition studies of cumene hydroperoxide is as shown in figure (3.2.5). Here the reaction vessel is a 50 ml, three necked round bottom flask. One neck of this is fitted with a bucket dropping device and a water condenser is fixed to the middle neck, closed with a silica drying tube. The third neck is closed with a rubber stopper, so that a known volume of liquid could be withdrawn using a syringe needle. The whole system is placed in a thermostated bath, and the liquid inside is stirred throughout the reaction.

3.2.4 Quantitative estimation of Hydroperoxides

The amount of hydroperoxide remaining in the solutions were determined at regular intervals of time so that the kinetics of the reaction could be followed.

Figure (3.2.3)

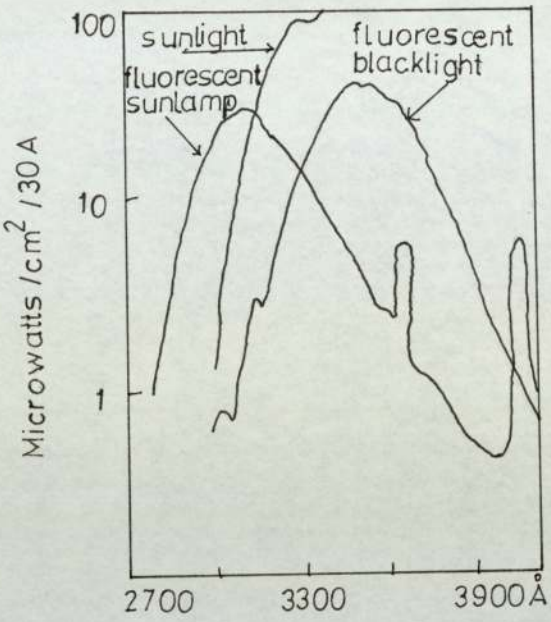

Figure (3.2.4)

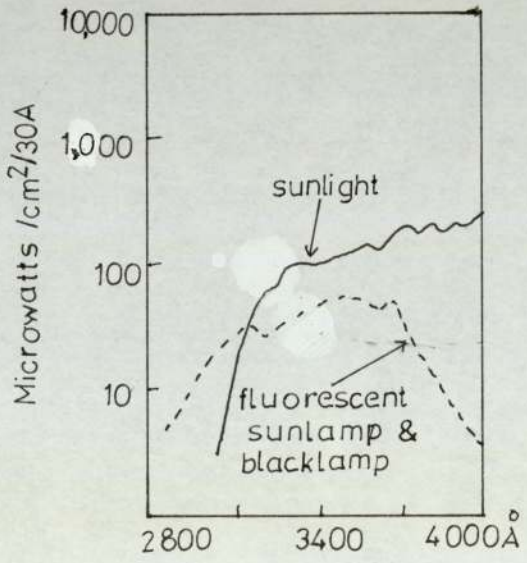

Figure (3.2.5)

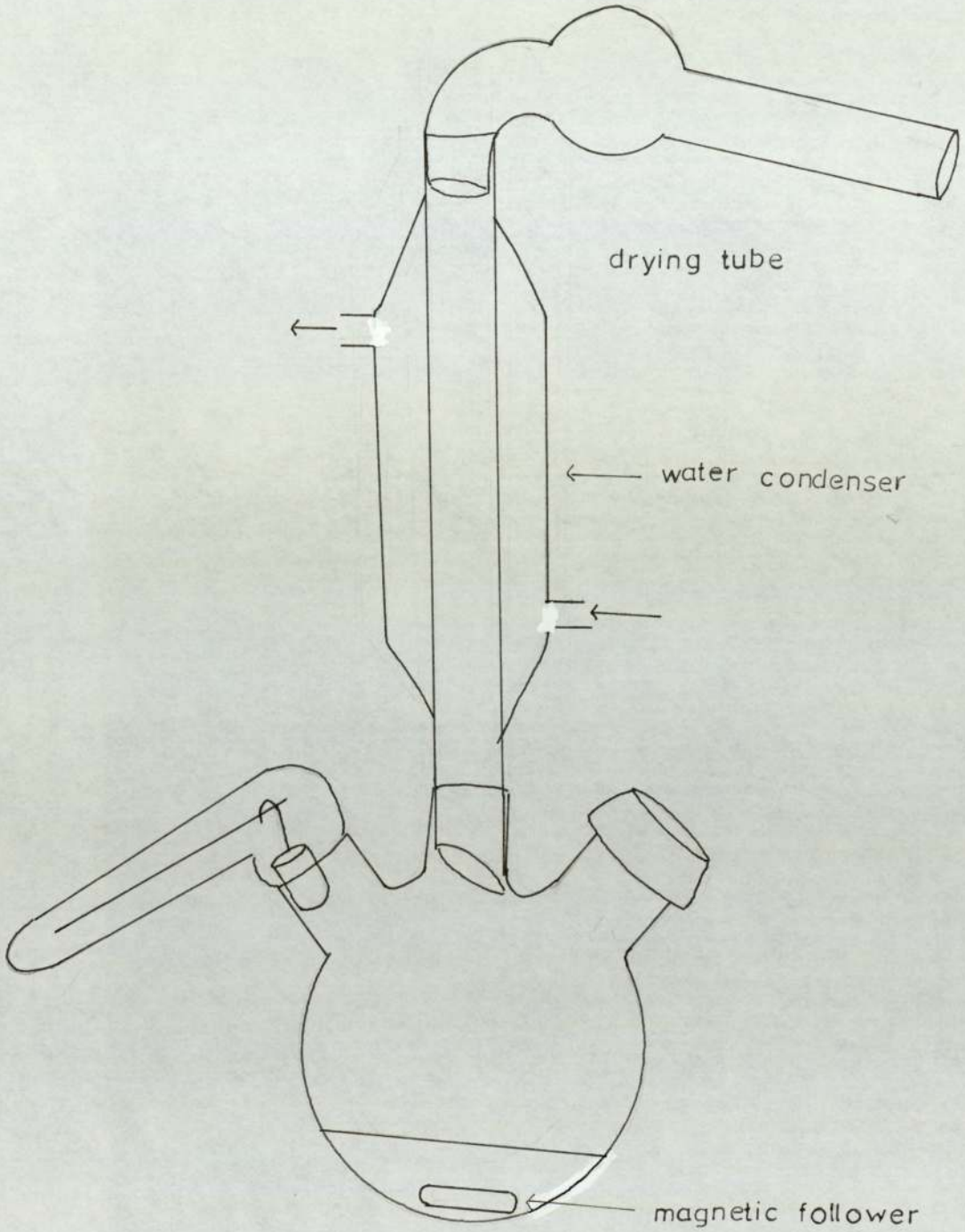

Iodometry is one of the most widely used techniques for the estimation of hydroperoxides. In this method the iodide is oxidised quantitatively to iodine by the hydroperoxide in an acidic medium.

$$ROOH + 2I^- + H^+ \longrightarrow ROH + H_2O + I_2$$

Dialkyl

Peroxides too can oxidise the iodide to iodine, but slowly. The conditions used are important and many modifications of the procedure has been published. The method used in this work is the modified procedure adopted by Mair and Graupnor[60] of the method by Wagner, Smith and Peters[61].

The medium of the reaction is isopropanol containing glacial acetic acid, and sodium iodide is used as the source of iodide instead of potassium iodide. This method has the following advantages.

1. The use of sodium iodide in place of the potassium salt, due to its greater solubility will keep the equilibrium

$$I_2 + I^- \rightleftharpoons I_3^-$$

far to the right with the result that

(a) the loss of liberated iodine due to purging or boiling is prevented as the tri-iodide ion is involatile.

(b) the tri-iodide ion will not add to the double bonds so that errors due to unsaturation are eliminated.

2. The use of isopropanol as solvent and the absence of strong acids eliminates atmospheric oxidation of the iodide.

3. The absence of water in the system avoids low results due to retardation of the iodide-hydroperoxide reaction.

In addition the method is rapid, accurate and needs only simple apparatus.

Reagents.

10% (V/V) acetic acid: isopropanol (AR grade) containing less than 0.1% water.

20% (W/V) sodium iodide in isopropanol.

Sodium thiosulphate (0.01N)

Sodium thiosulphate (0.1N) was prepared with boiled filtered water, stabilised with a few drops of chloroform and stored in flasks covered with aluminium foil. The exact strength of thiosulphate was determined using a standard solution of potassium iodate.

Method.

To 25 ml of 10% acetic acid in isopropanol was added 0.5 ml of the solution under test. This was refluxed for five minutes, allowed to cool. Then five to ten millilitres of water was added and the liberated iodine was titrated against 0.01N sodium thiosulphate.

$$\text{Percentage of hydroperoxide} = \frac{15.2 \times N \times V'}{\rho}$$

V = volume of thiosulphate

N = normality of thiosulphate

ρ = density of the hydroperoxide.

3.3.1 Ultra-Violet Cabinet

The ultra-violet cabinet used to expose the polymer samples is made up of a central rotating sample drum (photograph II) which has a diameter 15 cm less than the inter metal cylinder, on the inside of which an equal number of fluorescent sun lamps and black lamps are alternatively

PHOTOGRAPH II

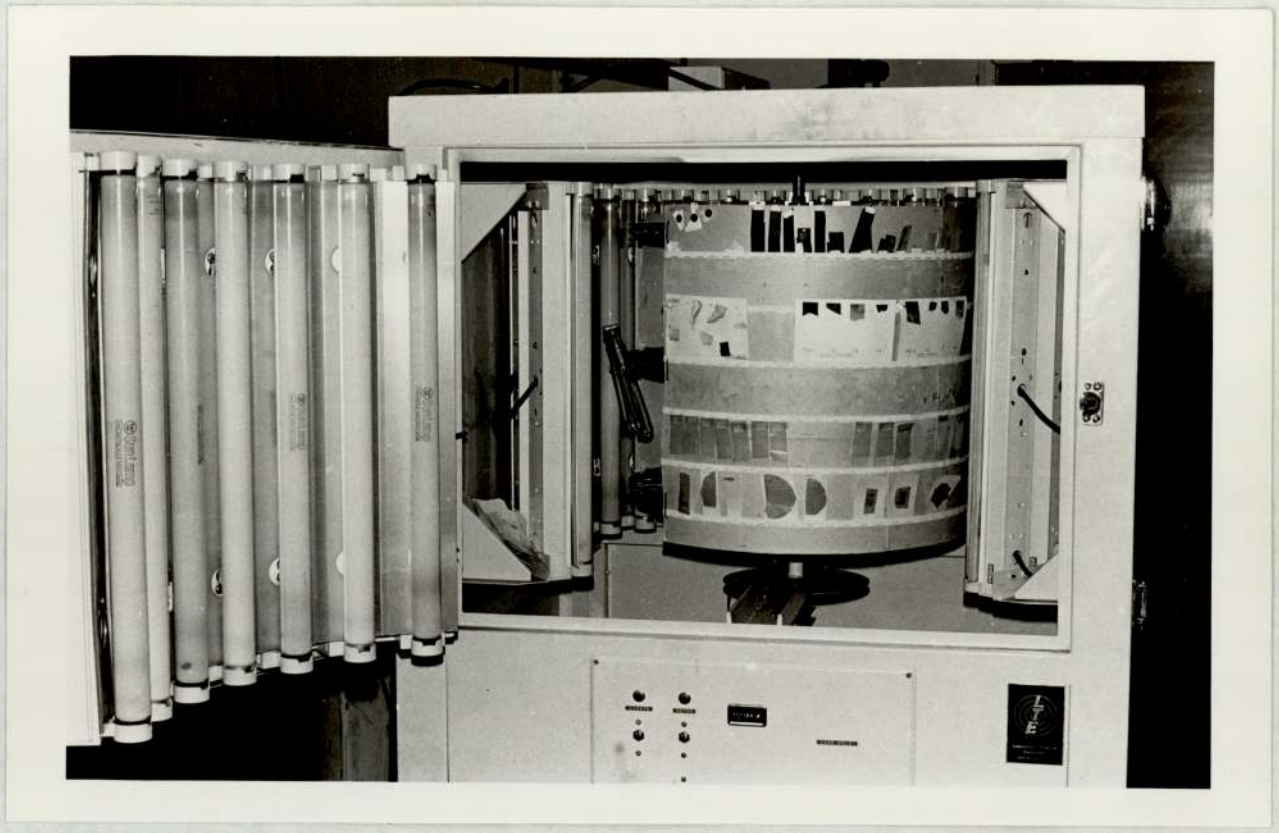

mounted. The energy output of the lamps is maintained relatively constant by a program of staggered replacement of the tubes. The energy drop of the lamps with respect to time is shown in figure (3.2.1.).

The uniform illumination over the entire height of the sample rack is a major advantage because all portions of every sample is now exposed to identical levels of total radiation. This cabinet is housed in a laboratory thermostated at 23±1°C

Preparation of polymer fims.

The polymers used were

1. High density polyethylene (HDPE) Rigidex type 9 supplied by BP Chemicals Ltd. and were completely free from additives. Density was 0.960, and the nominal melt flow index 0.9.

2. Low density polyethylene, commercial material from ICI, Alkathene WJG 47. Completely free from additives and the nominal melt flow index 2.0.

Poly styrene, commercial from Dow Chemicals, Styron. Completely free from additives.

All these polymers were stored in the dark at 0°C.

The additives were initially tumbled with a polymer which is then processed using the prototype RAPRA Torque Rheometer[62], which is essentially a small mixing chamber, containing mixing screws contra-rotating at different speeds. It has good temperature control, and a continuous readout is provided of both melt temperature and the torque

required for mixing. The chamber was operated sealed by a pneumatic ram. The full charge was calculated out for each polymer according to its density, (35 gm of HDPE, 36 gm of LDPE and 40 gm of PS), with this charge the chamber was sealed, and was mixed for five minutes to ensure complete gelation of the polymer.

On completion of mixing, the polymer sample was rapidly removed and quenched in cold water to prevent further thermal oxidation. The material was then compression moulded at 160°C for two minutes into sheets of thickness 0.008 in using a special grade of cellophane as a mould releasing agent, except in the case of polystyrene where a Teflon spray was used instead of the cellophane. Then these were mounted on quartz slides and were exposed in the ultra-violet cabinet described in Section (3.3.1). Infra-red spectra were obtained at regular intervals embrittlement testing was by flexing a fresh piece of the sample through 180°C, the sample being considered brittle if a fracture occurred.

3.4.2 Infra-red Analysis of the Oxidised Films

Infra-Red spectroscopy was used to estimate the oxidation kinetics of polymer samples since photoxidation of polymers results in the build up of different oxidation products for example, hydroxyl, carbonyl, carboxyl, vinyl etc. The kinetics of the growth of these functional groups, as the irradiation proceeds were followed by observing the changes in the characteristic absorption peaks at a definite wave length, and these were assigned by a comparison with the values for long chain ketones, aldehydes etc.[63].

Figure (3.3.1)

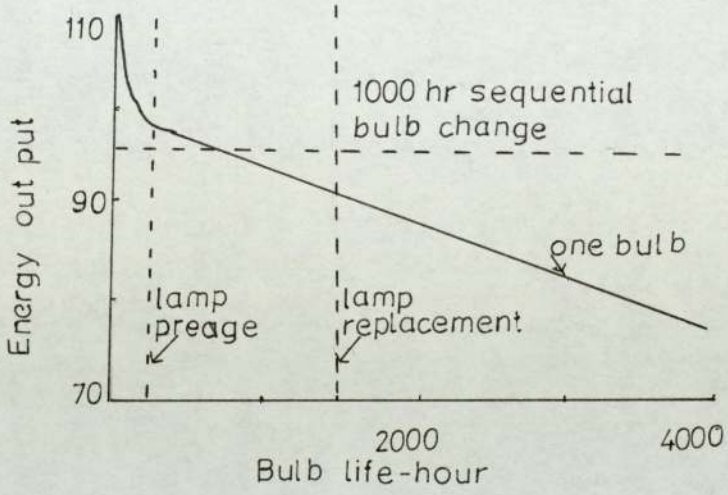

Figure (3.4.1)

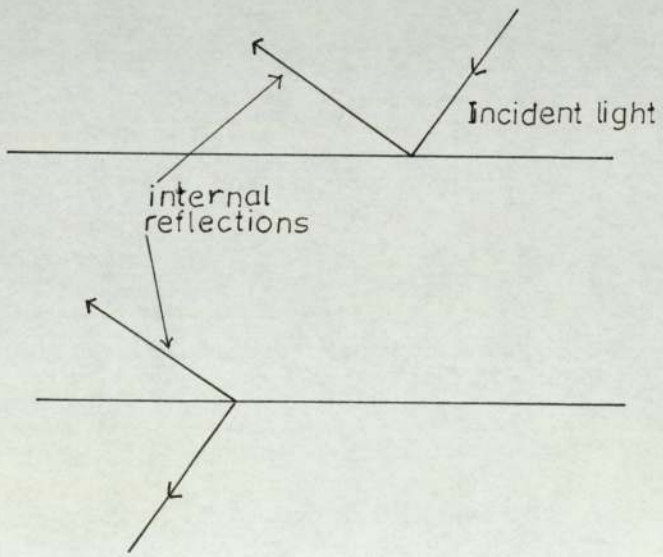

Procedure.

In all these quantitative analysis, the following combined form of Beer-Lamberts equation was used[64].

$$A = \log_{10} \frac{I_o}{I} = ecl.$$

where

A = Absorbance or optical density

I_o = Intensity of radiation falling on the sample.

I = Intensity of radiation emerging from the sample.

e = Molar extinction coefficient.

c = Concentration of the absorbing group present in the sample in moles per litre.

l = Path length of radiation eithin the sample in centimetres.

The samples were exposed for regular intervals of time and the spectra were run on the same chart paper for comparison purposes, chart paper with percentage transmittance scale were used in this work, rather than the one with a logarithmic scale as the former is made to eliminate losses due to internal reflections of the incident light falling on the polymer sample[65], figure (3.4.1.).

The functional group index calculated from these spectra, which is defined as the ratios

$$\frac{\text{Absorbance of the function group}}{\text{Absorbance of a standard peak}}$$

The standard peak used here corresponds to an absorption band that does not change with oxidation of the sample and this will help to minimise errors due to variations of the film thickness as well as errors due to the instrument.

Calculation of Absorbance.

The base line technique[66] was used to calculate the optical density or absorbance due to various functional groups. Suppose it is desired to find the absorbance corresponding to the first band shown in figure 3.4.2. A base line is drawn across the shoulders of this band then the quantities I_o and I can be measured as shown and the absorbance calculated. However with an absorption such as shown in figure (3.4.3) the proper location of the base line is open to much doubt, but in the present work to determine the absorbance of peak A, the base line is taken to be either a, b or c depending on the width of the shoulders B, C and D. If all three shoulders B, C and D are narrow, a is used as the base line and so on. And in this situation which frequently occurs one particular way to draw the line is adopted in all the samples for the same functional group.

3.5 Actinometry

A chemical actinometer was used to measure the intensity of Ultra-violet light,. The principal requirements of an ideal general purpose chemical actinometer are:

(a) constant quantum efficiency and high absorption factor over a wide range of wavelengths on intensities and of total radiation dose;
(b) high sensitivity and precision coupled with simplicity of operation and need availability of the photochemical material. The ferrioxalate actinometer developed by Parker and Hatchard[67,68,69,70] largely fulfils these conditions for wavelengths between 500 and 250 nm, and the indications are that it would be suitable down to at least 200 nm. The photolyte

Figure (3.4.2)

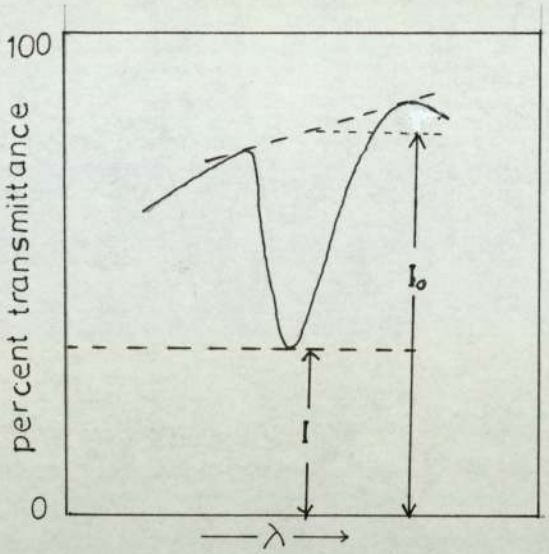

Figure (3.4.3)

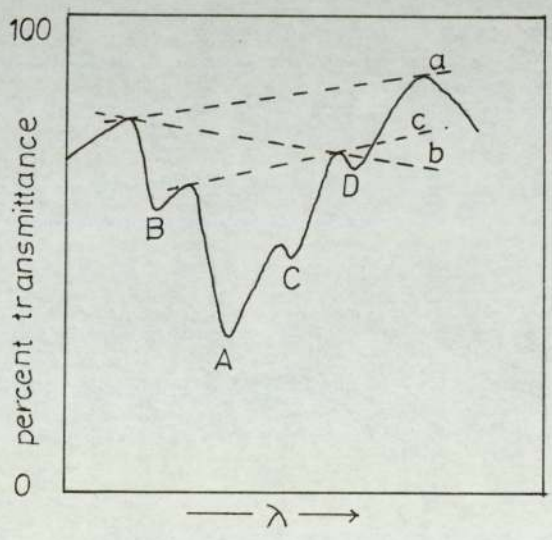

consists of a solution of potassium ferrioxate, $K_3Fe(C_2O_4)_3.3H_2O$ in 0.1N sulphuric acid. In acid solution the trioxalato-ferric ions are largely dissociated into monoxalate and dioxalate complexes. On exposure to light the following reactions occur:

$$[Fe(C_2O_4)]^+ \xrightarrow{h\nu} Fe^{2+} + (C_2O_4)^- \ldots\ldots\ldots \quad (1)$$

$$(C_2O_4)^- + Fe(C_2O_4)^+ \longrightarrow 2CO_2 + Fe^{2+} + (C_2O_4)^{2-} \ldots\ldots\ldots \quad (2)$$

After photolysis the ferrous ion formed is converted to its 1,10-phenenthroline complex and the latter determined absorptiometrically. Both the photolyte and photolysis products are stable in the dark and the procedure is simple and versatile. The versatility of the system depends on the fact that the photolyte itself absorbs strongly, but gives rise to weakly absorbing photolysis products. Accumulation of the latter does not therefore disturb the linearity of response, even wnen the proportion of photolyte decomposed is considerable. Therefore large or small armounts of decomposition could also be measured with equal accuracy by simple dilution before absorptiometric reaction.

Procedure

Pure potassium ferrioxalate was prepared by mixing three volumes of 1.5 AR potassium oxalate with one volume of 1.5 AR ferric chloride with vigorous stirring. The precipitated potassium ferrioxalate was re-crystallised thrice from warm water, and the crystalls so formed were sucked dry. The composition corresponds to $K_3Fe(C_2O_4)_3.3H_2O$. The 0.006 M actinometer solution was prepared by dissolving 2.957 gm of the crystals in 800 ml of water, to this 100 ml of 0.1N sulphuric acid was added, and the solution was diluted 1 litre and mixed. This solution was in an amber bottle in a dark room.

A 1 cm depth of 0.006M solution absorbs about 99% or more of the light of wavelength up to 390 mμ, and in the present work this solution was used.

Calibration graph for ferrous ion.
Solutions used

(a) 0.4×10^{-3} M/litre of Fe^{2+} in 0.1N H_2SO_4 (freshly prepared by dilution from standardized 0.1M in 0.1N H_2SO_4).

(b) 0.1%, 1:10 phenanthroline monohydrate in water.

(c) Buffer solution (150 ml of N-sodium acetate and 360 ml of N-H_2SO_4 diluted to 250 ml.

Into a series of 20 ml volumetric flasks added the following volumes of solution (a) 0, 0.5, 1.0.....4.5,5.0 ml. Added 0.1N H_2SO_4 to the above so as to make the total acidity equivalent to 10 ml of 0.1N H_2SO_4. To the above added in succession 2 ml of solution (b), 5 ml of solution (c), mixing after each addition. These were filled up to the neck, mixed well and allowed to stand for half an hour. The optical densities of these were measured at 510 m in a 1 cm cell with a spectrophotometer (P.E.137), with the blank solution in the reference beam.

If $n_{Fe^{2+}}$ is the number of ferrous ion formed during photolysis.

Using equation $\log \frac{I}{I_o} = -s\,c\,l$

$$c = \frac{\log \frac{I_o}{I}}{El}$$

$$n_{Fe^{2+}} = N \frac{\log \frac{I_o}{I}}{VEl}$$

where V = volume of solution exposed.

N = A agacl ro number i.e. 6.023×10^{20}

= The extinction coefficient of Fe'ferrous ion calculated from the calibration plot and is equal to 0.98×10^{4} litre/mole/cm.

Hence n_{Fe}^{2+} can be calculated.

Quantum yield for Fe^{2+} formation $QFe^{2+} = 1.22$ (69).

The intensity of incident light $I_o = \dfrac{n_{Fe}^{2+}}{QFe^{2+} \times (\text{time})(1-10^{-\varepsilon a l})}$

where, a - concentration of the ferrioxalate solution.

Thus knowing n_{Fe}^{2+}, and Q_{Fe}^{2+}, I_o can be calculated.

CHAPTER 4

OXYGEN ABSORPTION STUDIES OF MODEL COMPOUNDS

Oxygen absorption studies of the model compounds cumene and dodecane were carried out under ultra-violet radiation at 29±1°C and the effect of some transition metal chelates were studied.

The primary sources of initiation in polyolefins are the hydroperoxides, carbonyl, vinyl and vinylidene groups (Section 1.1.1). Therefore attempts were made to initiate the model systems with these chromophores, and the effect of additives in these systems were determined.

In these experiments the additives were added at the beginning of the experiment. Most of the experiments were carried out in 100% oxygen atmosphere. By comparing the oxygen absorption curves obtained in the presence of different additives with the oxygen absorption curve of uncatalysed oxidations the accelerators and retarders of oxidation were distinguished.

A different set of experiments were devised to find out the screening capacity of these additives to ultra-violet radiation. By comparing the oxygen absorption curves obtained when the stabiliser was used as an additive or as a screen. The contribution to stabilisation by screening was obtained.

A few experiments were carried out at 50°C (unirradiated) in a thermostatic bath with the initiator azobis - isobutyro-nitrile, (AZBN), which is a free radical generator[71]. These results were used to eliminate some of the possible mechanisms of stabilisation for the metal oxime and metal dithiocarbamate complexes.

4.1.1 Oxygen absorption of cumene under ultra-violet radiation

Oxygen absorption experiments in pure cumene, in the absence and in the presence of different concentrations of cumene hydroperoxide (CHP) were carried out under ultra-violet radiation at 29±1°C (figure 4.1.1). The amount of CHP formed during oxidation was estimated by iodometric titration (Section 3.2.4) and was plotted against time, figures (4.1.2) and (4.1.3).

Oxygen absorption of cumene initiated with one per cent CHP in the presence of 0.025% of the metal chelates were studied at 29±1°C in an oxygen atmosphere. The rates of retardation with different metal complexes are shown graphically in figure (4.1.4).

A similar set of experiments were carried out with 0.05% benzophenone (BP) (giving an equivalent rate of oxidation to that given with the cumene hydroperoxide), and 1% BP initiated cumene system and the rates of oxidation with the different metal chelates are shown in figures (4.1.5a) and (4.1.5b).

In order to determine the contribution to the ultra-violet stabilising effect of ultra-violet absorption a comparison was made of the rate of

Figure (4.1.1) Photoxidation of Cumene initiated with CHP.

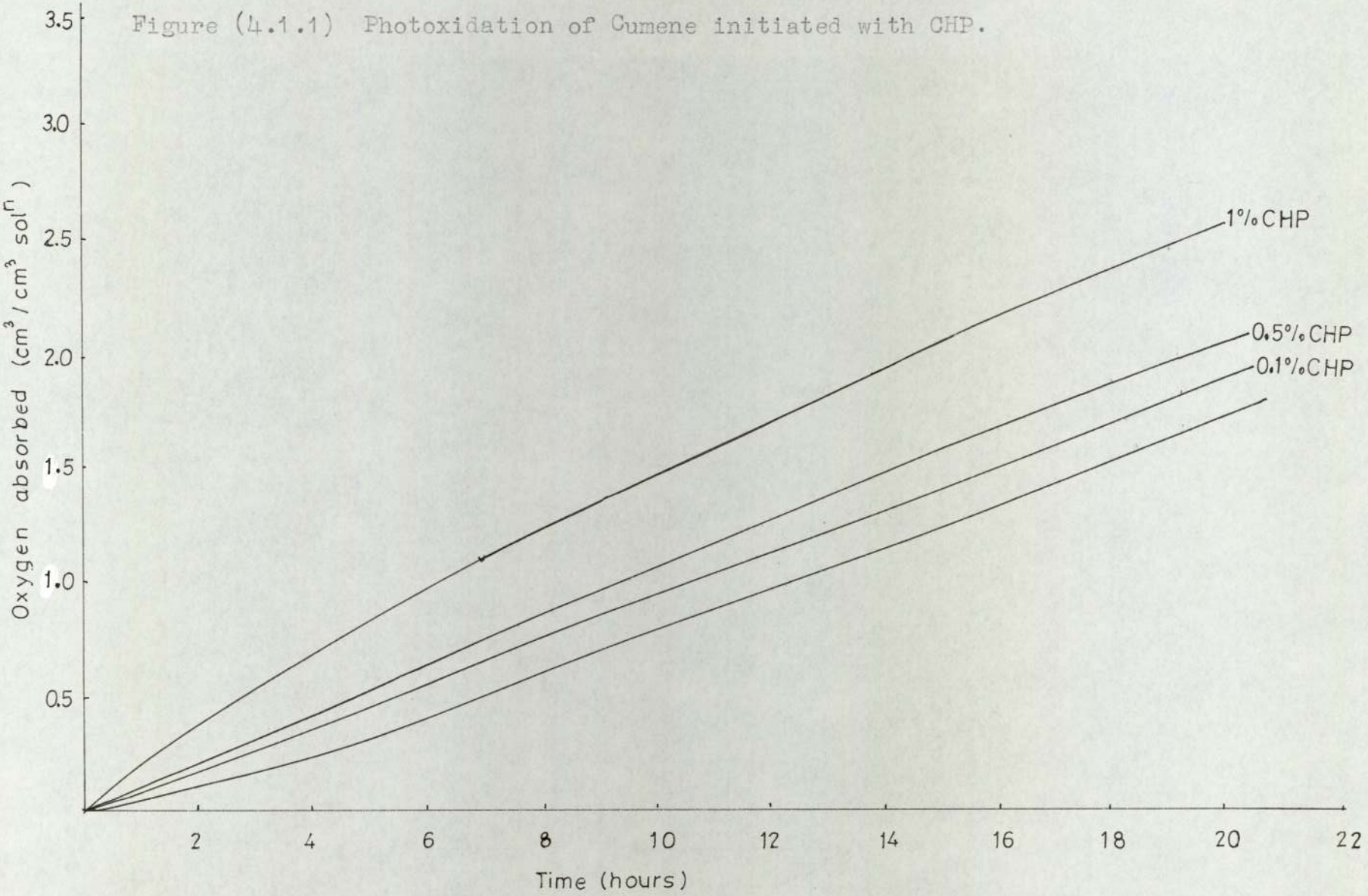

Figure (4.1.2) Amount of CHP formed during the photoxidation of Cumene.

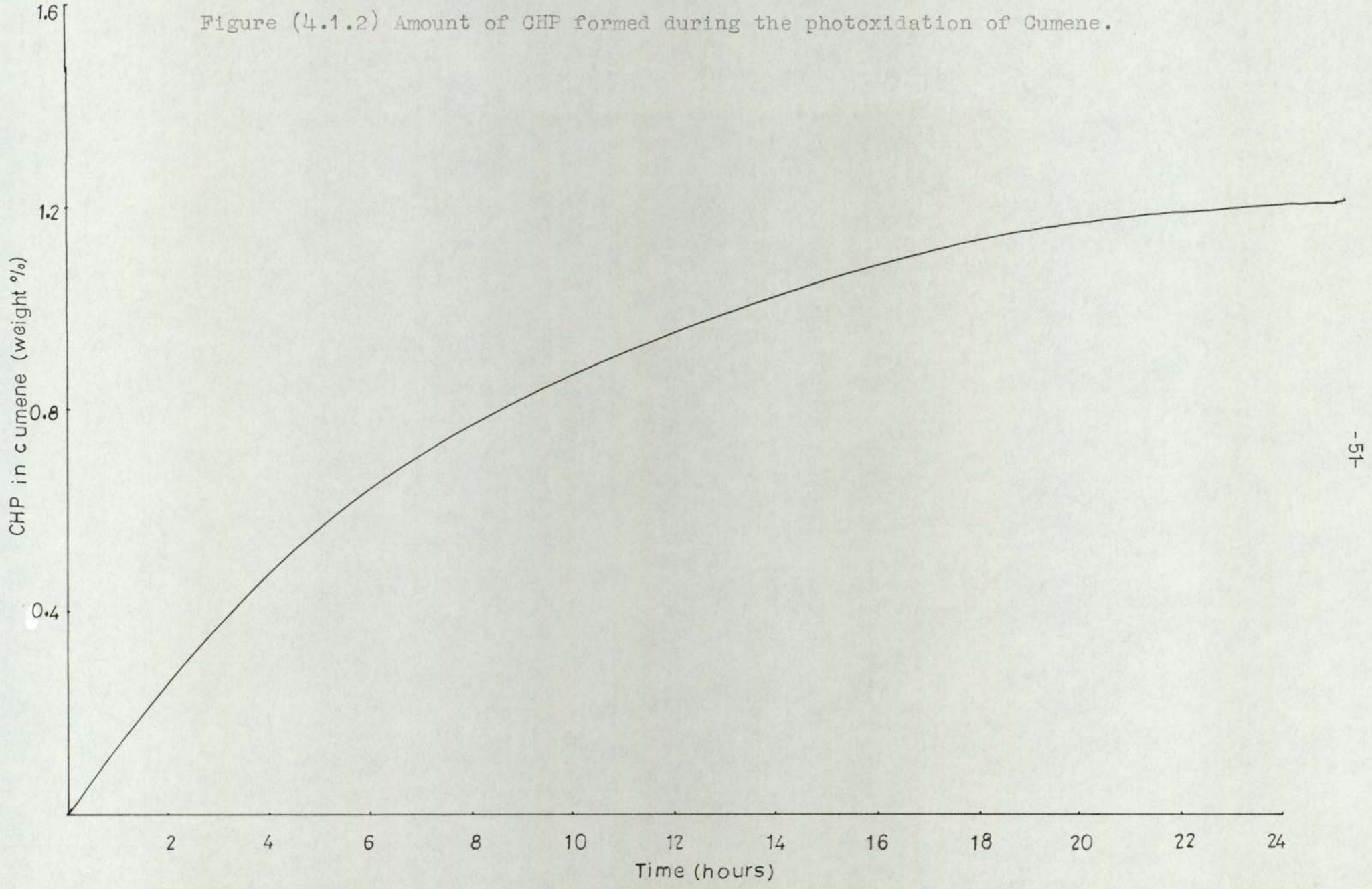

Figure (4.1.3) Photoxidation of Cumene initiated with 1% CHP.

a. Oxygen absorbed with time.

b. Amount of CHP formed during oxidation.

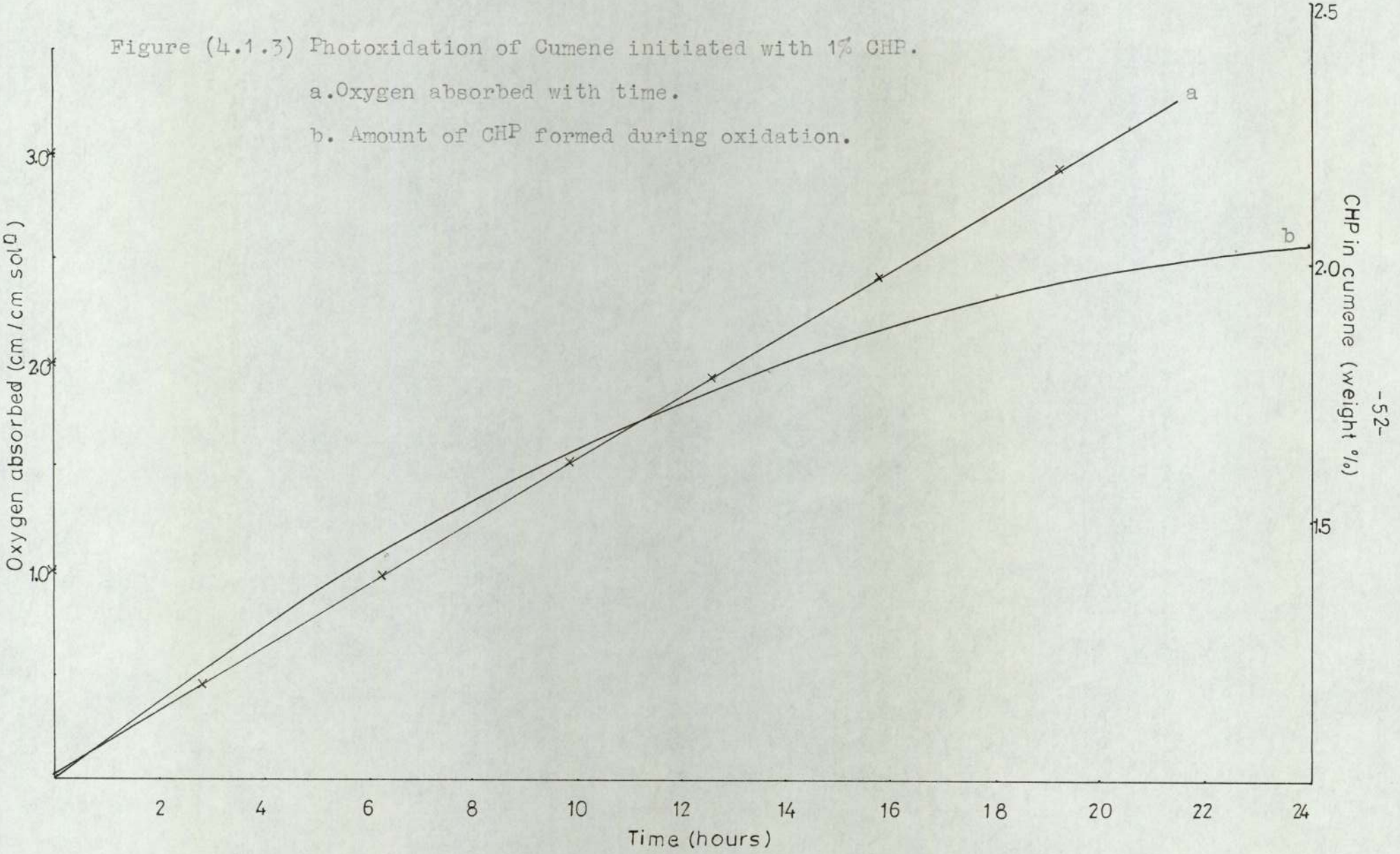

Figure (4.1.4) Oxygen absorption curves for the photoxidation of Cumene initiated by 1% CHP.

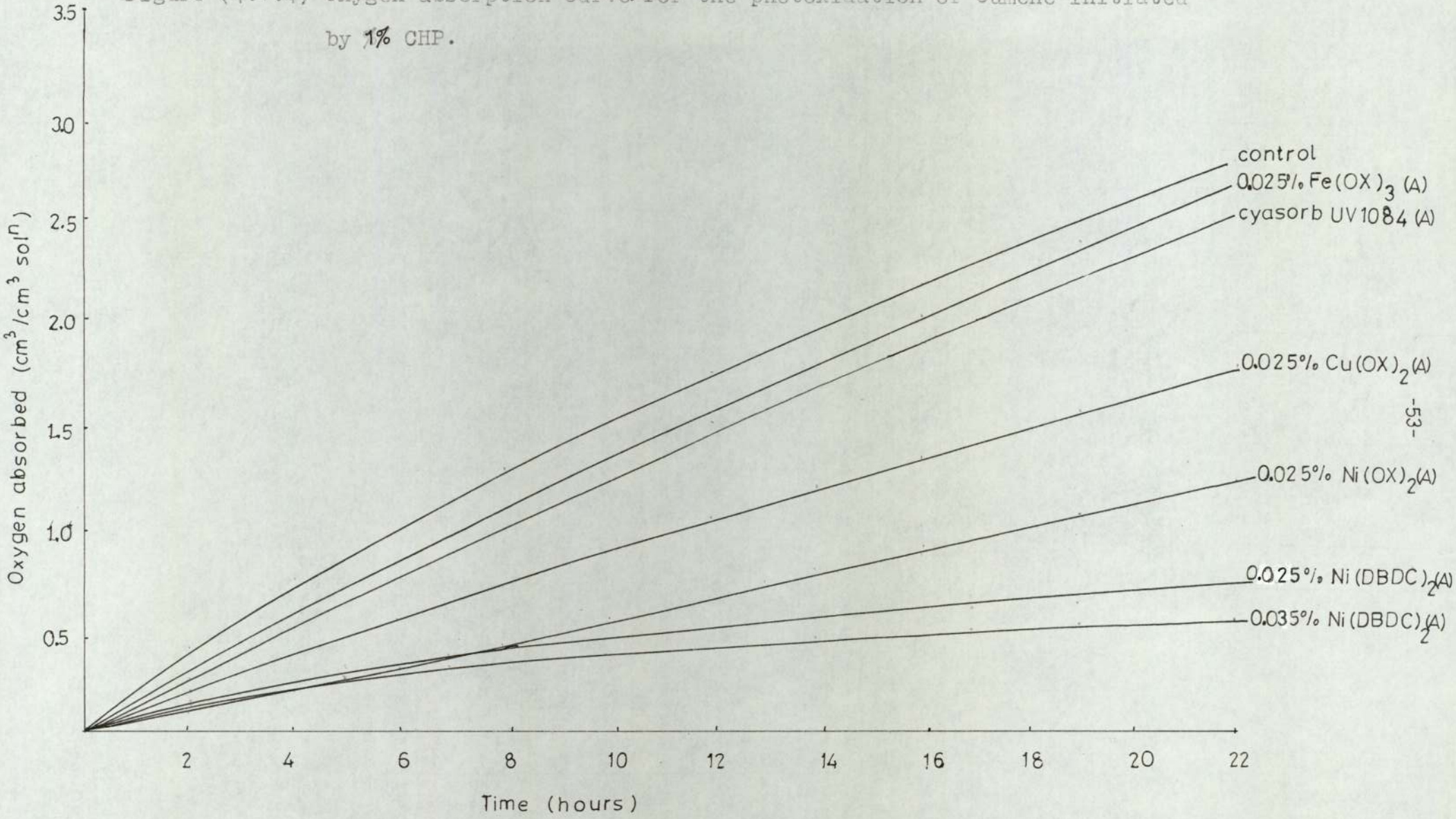

Figure (4.1.5a) Oxygen absorption curves for the photoxidation of Cumene initiated with 0.05% BP.

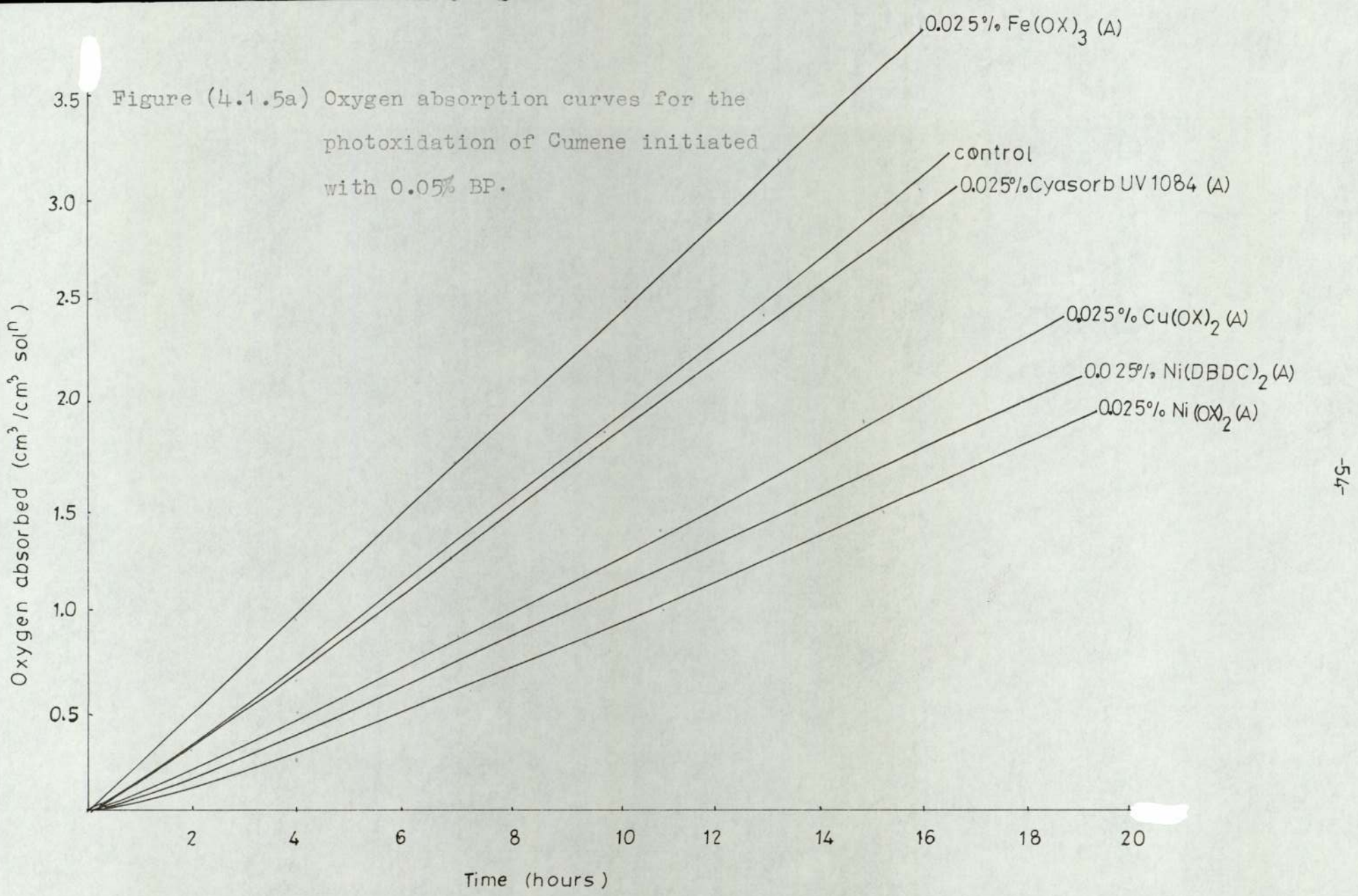

Figure (4.1.5b) Oxygen absorption curve for the photoxidation of Cumene initiated with 1%BP

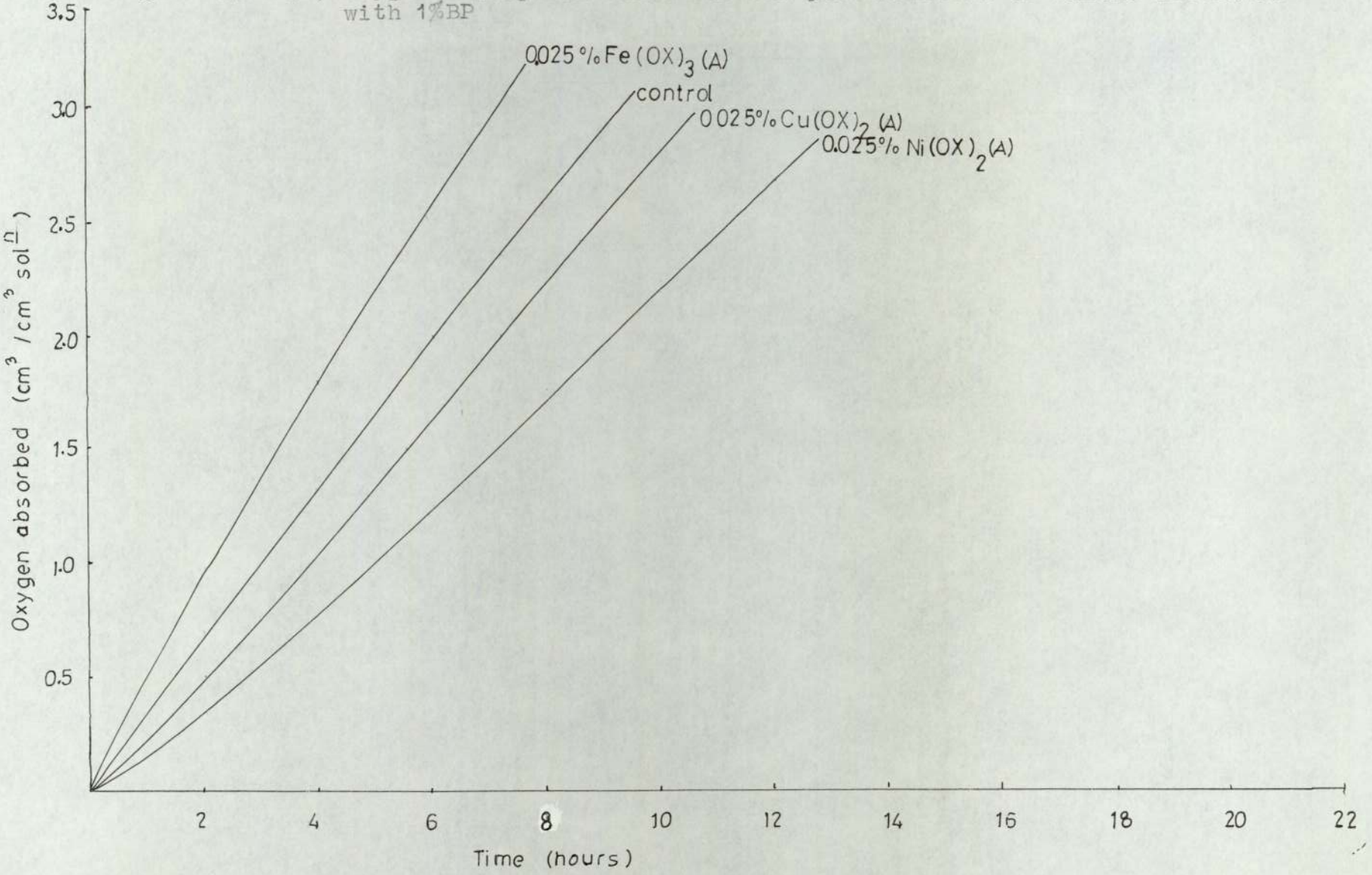

oxidation in the two systems with the nickel complex as an internal stabiliser and as an external screen. This was arranged by having the ultra-violet stabiliser in benzene solution in a separate concentric anulus round the oxygen absorption flask so that now it could act as a screen for the oxidations system.

The vessel used is shown in figure (3.2.2b) where r_i and r_e are the internal and external radii of the two concentric vessels.

Let c_1 be the concentration of the metal complex when used as an additive in the oxidising solution and c_2 be the concentration of the same metal complex when used as a screen. Considering a point at the centre of the vessel (say x) then the absorption of UV light at this point when the complex is used as an additive is given by

$A_1 = \varepsilon c_1 r_1 + a_1 + b_1$.

where a_1 is the absorption due to cumene

b_1 " " " " " benzene

Similarly when the complex is used as a screen the absorption at x,

$A_2 =$ + $a_1 + b_1 + \varepsilon c_2 (r_e - r_i)$

if equivalent screening of UV radiation takes place in the two cases, then $A_1 = A_2$

i.e. $\varepsilon c_1 r_1 + a_1 + b_1 =$ + $a_1 + b_1 + \varepsilon c_2 (r_e - r_i)$

$c_1 r_i = c_2 (r_2 - r_i)$

the dimensions of the vessel are such that

$$r_i = 1.375 \text{ cm and } r_e = 2.061 \text{ cm.}$$

$$c_1(1.375) = c_2\ (2.061 - 1375)$$

$$c_1 = \frac{c_2}{2}$$

twice the concentration of the metal chelate used as an additive had to be used to give an equivalent screening effect.

With the metal complexes used as screens and additives experiments were carried out with cumene initiated with 1% CHP and 0.05% BP. Figures (4.1.6) and (4.1.7). For comparative purposes all these oxygen absorptions were plotted in the same graph, figures (4.1.8a) (4.1.8b),(4.1.9),(4.1.10),(4.1.11) and (4.1.12).

For comparative purposes an experiment was carried out with isobutyl methyl ketone as the initiator and the rates of retardation of the nickel oxime chelate was determined when used as an internal stabiliser and as an external screen. Figure (4.1.13). These rates were then compared with the rates of oxidation with BP initiated system as shown in figure (4.1.14).

Similar oxygen absorption studies were carried out with different concentrations of the nickel oxime chelate figure (4.1.15). The contribution to stabilisation due to screening was determined as before by using the complex in benzene solution in a separate concentric anulus around the oxygen absotption flask; figure (4.1.16). The effect of

Figure (4.1.6) Oxygen absorption curves for the photoxidation of Cumene initiated with 1% CHP, and screened by the respective stabilisers.

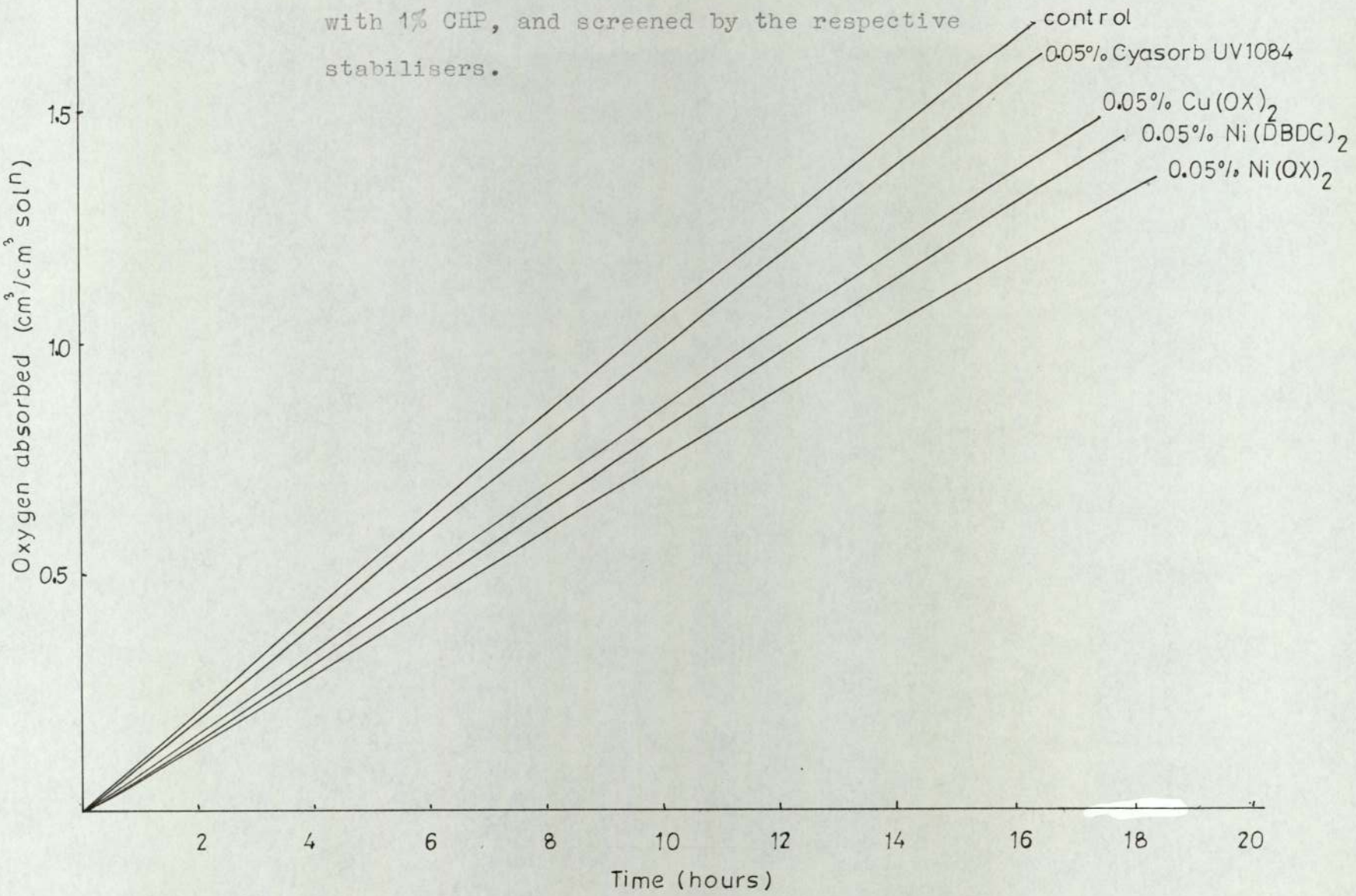

Figure (4.1.7) Oxygen absorption curves for the photoxidation of Cumene initiated with 0.05% BP, and screened by the respective stabilisers.

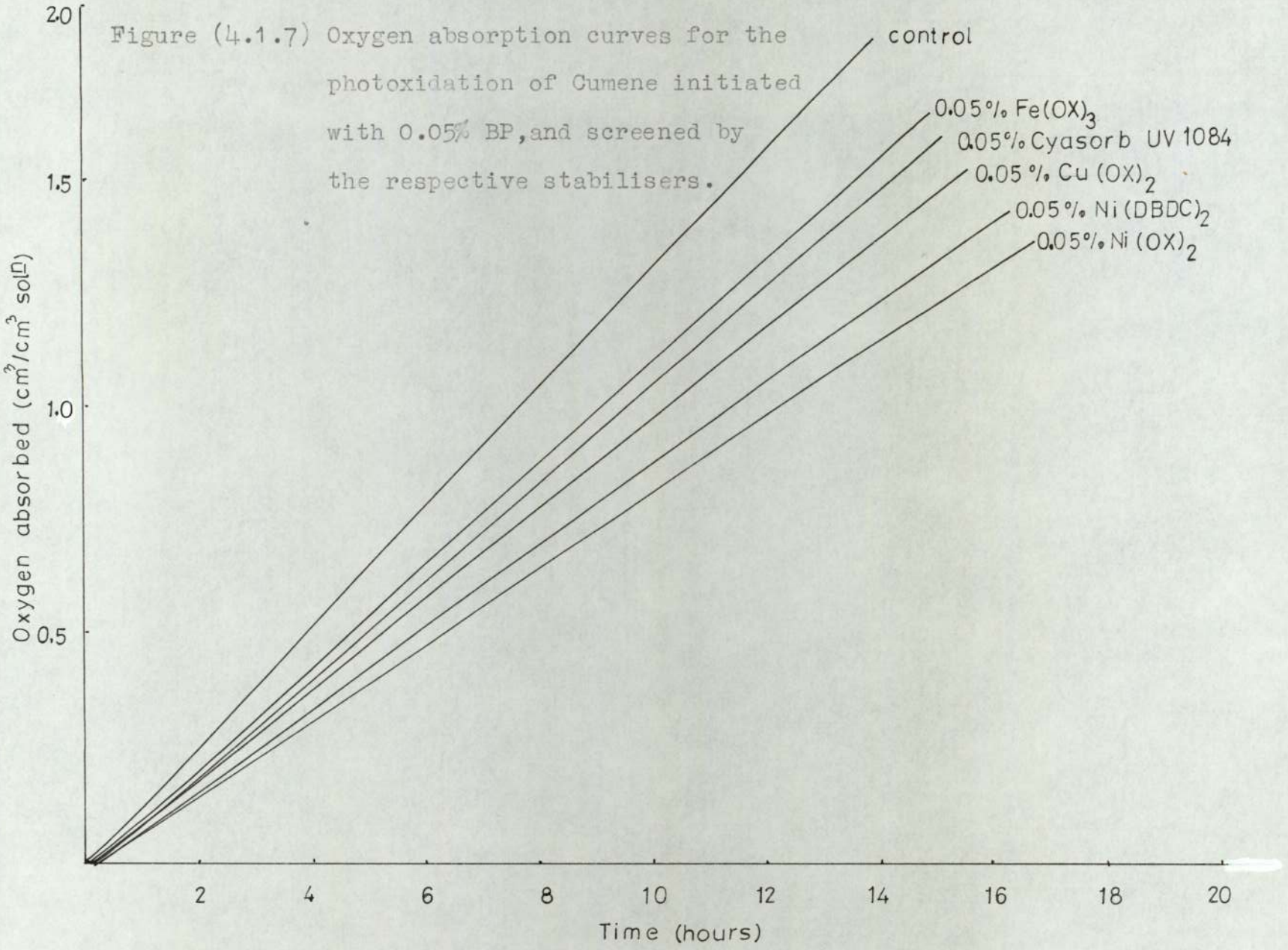

Figure (4.1.8a) Photoxidation of Cumene initiated by 1% CHP,(a) CHP (1%)+0.05% $Cu(OX)_2$(S) (b)CHP (1%)+0.05% $Ni(OX)_2$(S), (c) CHP(1%)+0.025%$Cu(OX)_2$(A), (d) CHP (1%)+ 0.025% $Ni(OX)_2$(A).

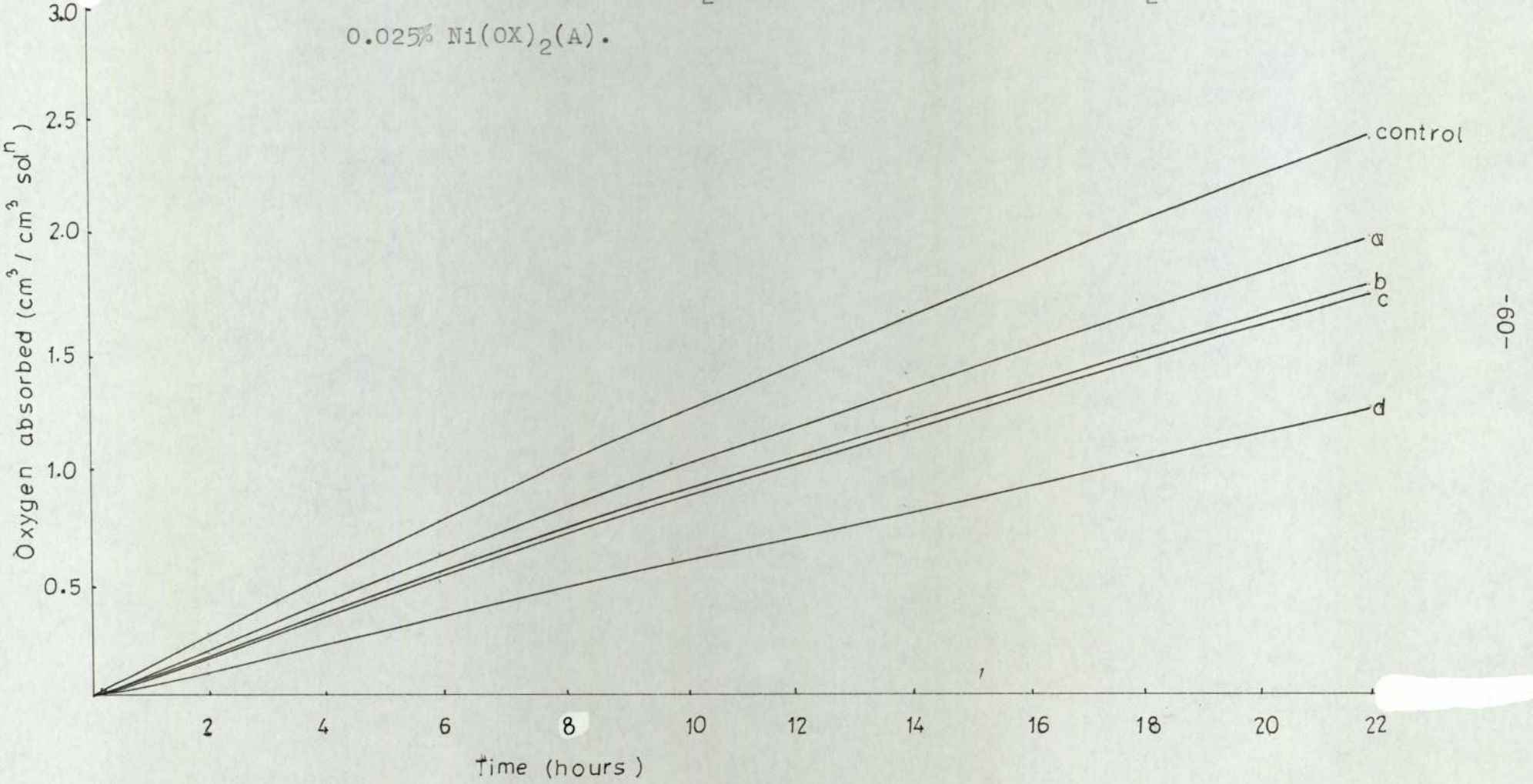

Figure (4.1.8b)Photoxidation of Cumene.(a) CHP (1%), (b) BP (0.05%), (c) BP (0.05%)+0.025% $Cu(OX)_2$(A), (d) CHP (1%)+0.025% $Cu(OX)_2$(A), (e) BP (0.05%)+0.025% $Ni(OX)_2$ (f)CHP (1%)+0.025% $Ni(OX)_2$(A), (g) BP (0.05%)+0.025% $Fe(OX)_3$.

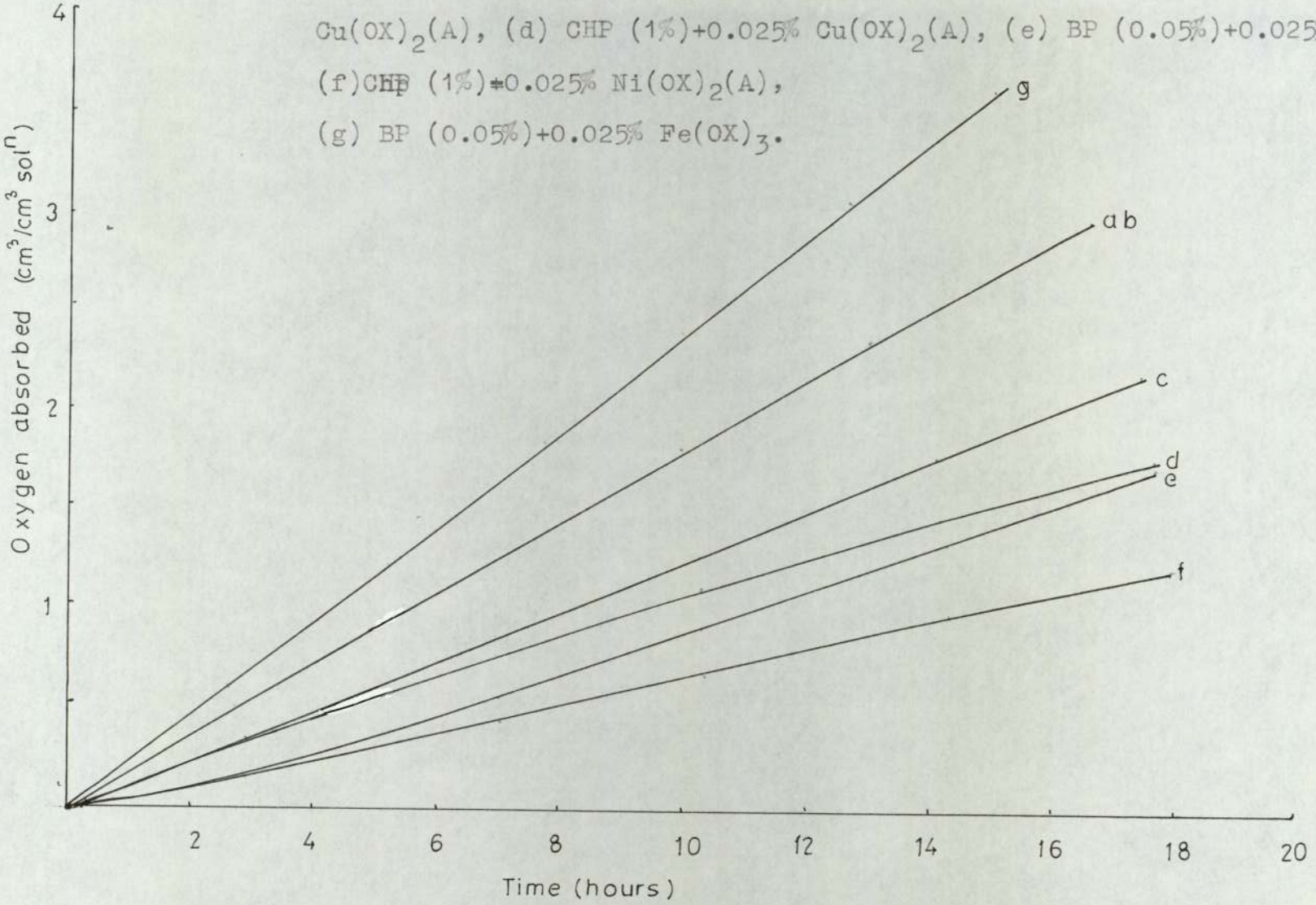

Figure (4.1.9) Photoxidation of Cumene. (a) BP (0.05%), (b) CHP (1%), (c) BP (0.05%)+ 0.025% Ni $(OX)_2$(A), (d) BP (0.05%) + 0.05% $Ni(OX)_2$(S), (e) CHP (1%)+ 0.05% $NI(OX)_2$(S), (f) CHP (1%) + 0.025% $Ni(OX)_2$ (A)

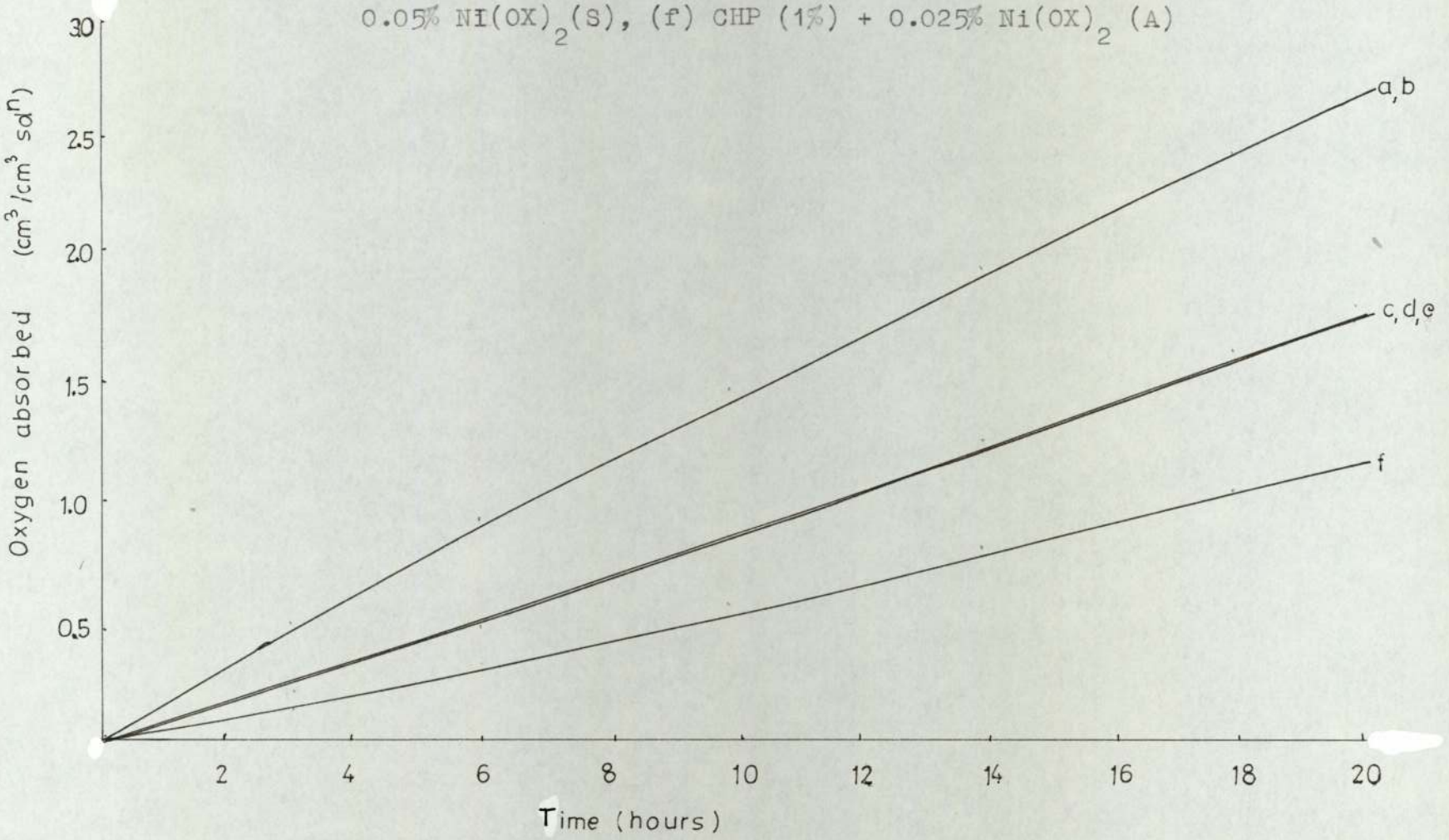

Figure(4.1.10) Photoxidation of Cumene. (a) BP(0.05%), (b) CHP (1%), (c) BP(0.05%)+ 0.025% $Cu(OX)_2$(A) (d) BP (0.05%)+ 0.05% $Cu(OX)_2$(S), (e) CHP.(1%)+ 0.05% $Cu(OX)_2$(S), (f) CHP (1%) + 0.025% $Cu(OX)_2$ (A).

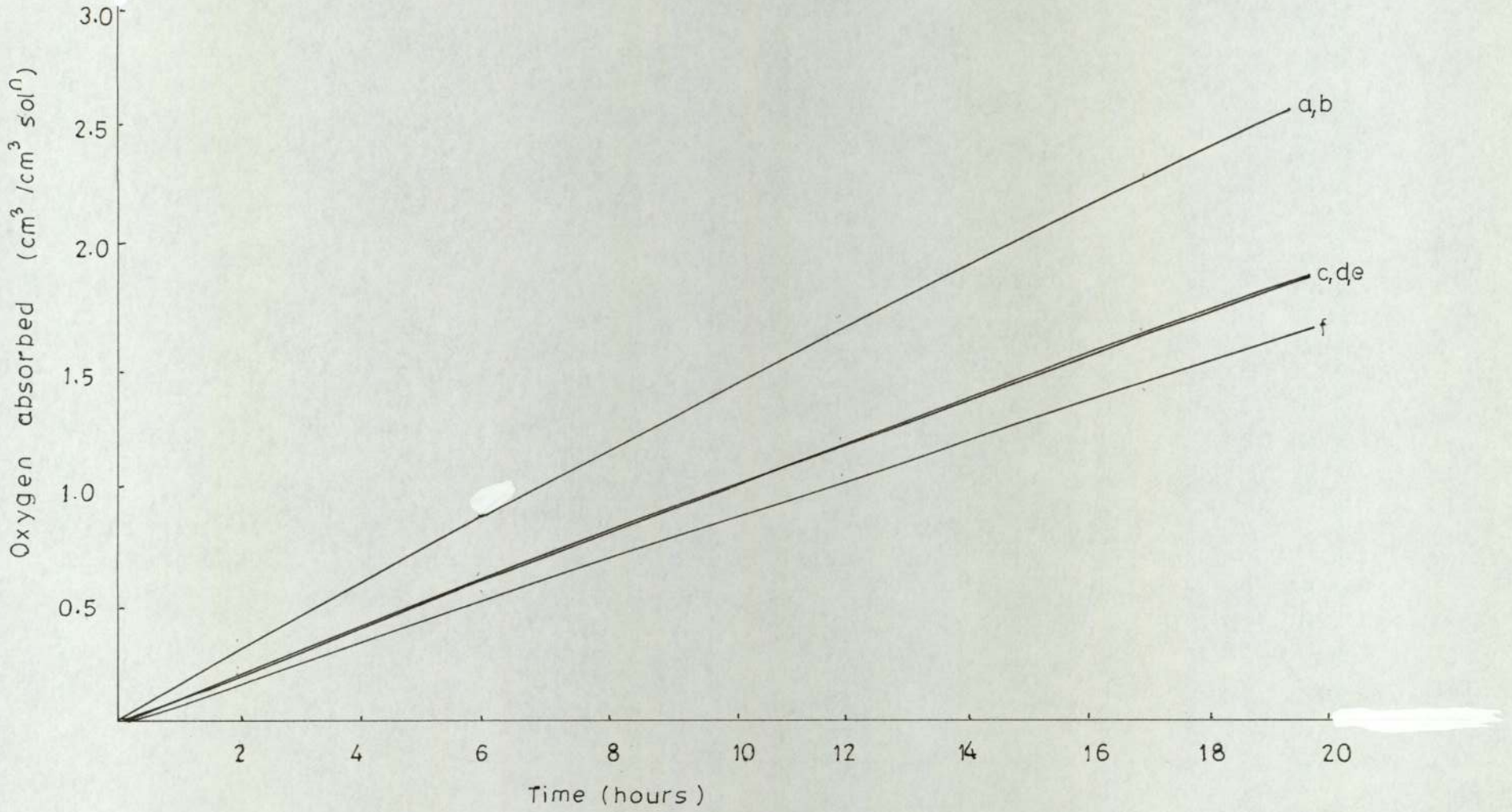

Figure (4.1.11) Photoxidation of Cumene. (a) CHP (1%), (b) BP (0.05%), (c) BP(0.05%)+ 0.05% $Ni(DBDC)_2$(S), (d) CHP (1%) + 0.05% $Ni(DBDC)_2$(S), (e) BP (0.05%)+ 0.025% $Ni(DBDC)_2$ (A), (f) CHP (1%) + 0.025% $Ni(DBDC)_2$(A).

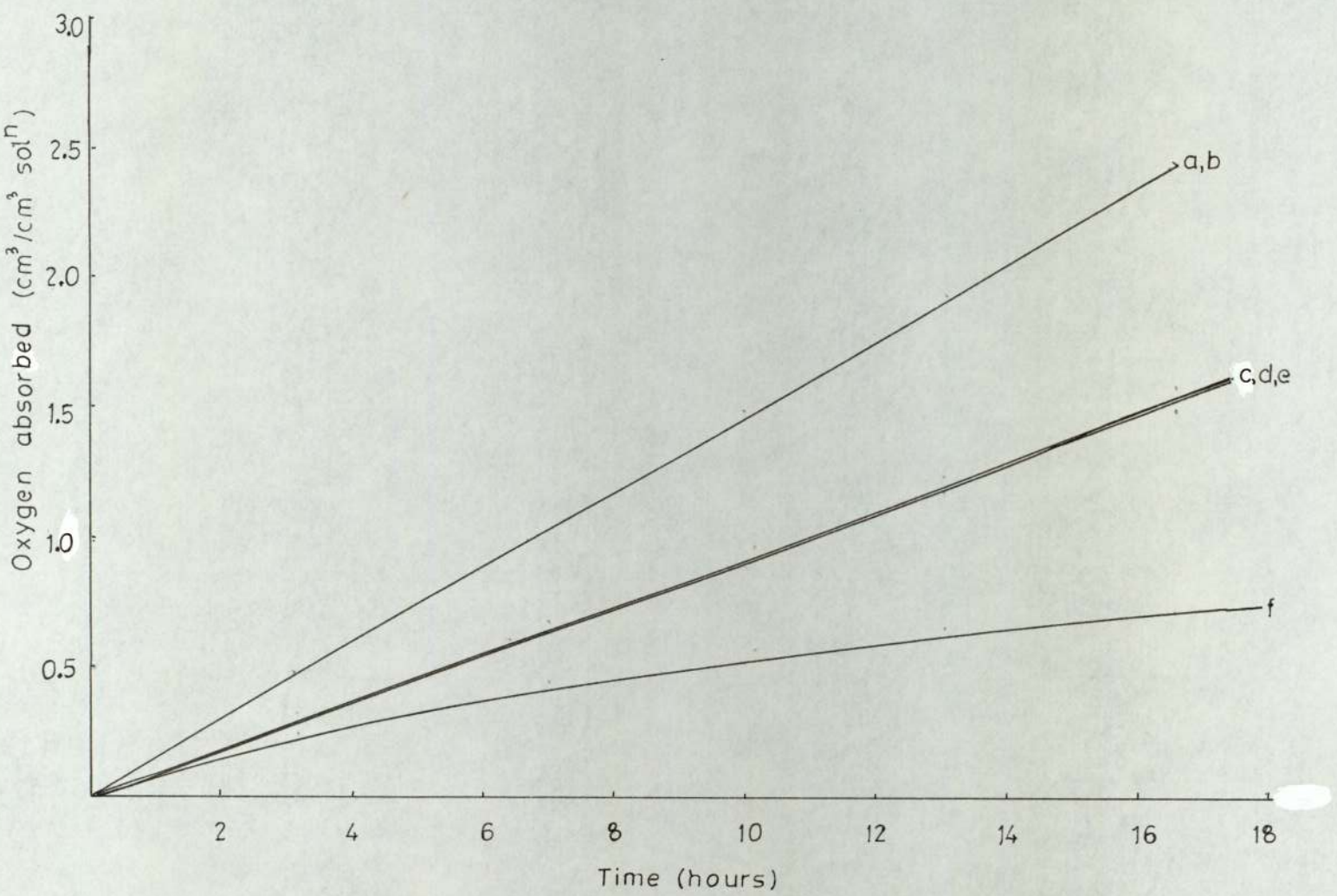

Figure (4.1.12) Photoxidation of Cumene, (a) CHP(1%),(b) BP(0.05%)
(c) BP (0.05%)+0.05% UV 1084 (S), (d)CHP(1%)
+0.05% UV1084 (S), (e)BP (0.05%)+0.025%
UV1084 (A), (f) CHP(1%)+0.025% UV1084(A)

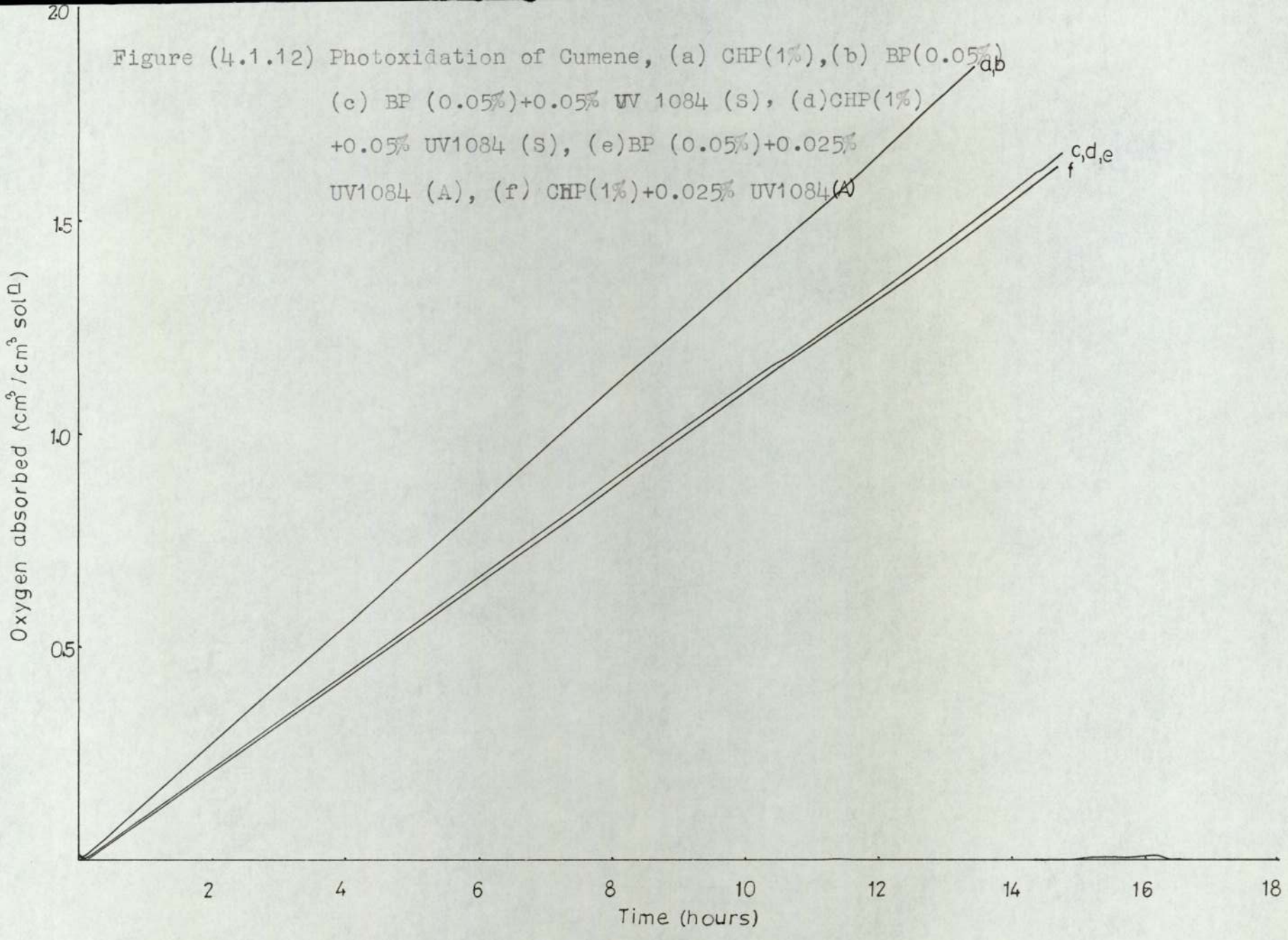

Figure (4.1.13) Photoxidation of Cumene initiated with 2% iso-butyl methyl ketone.

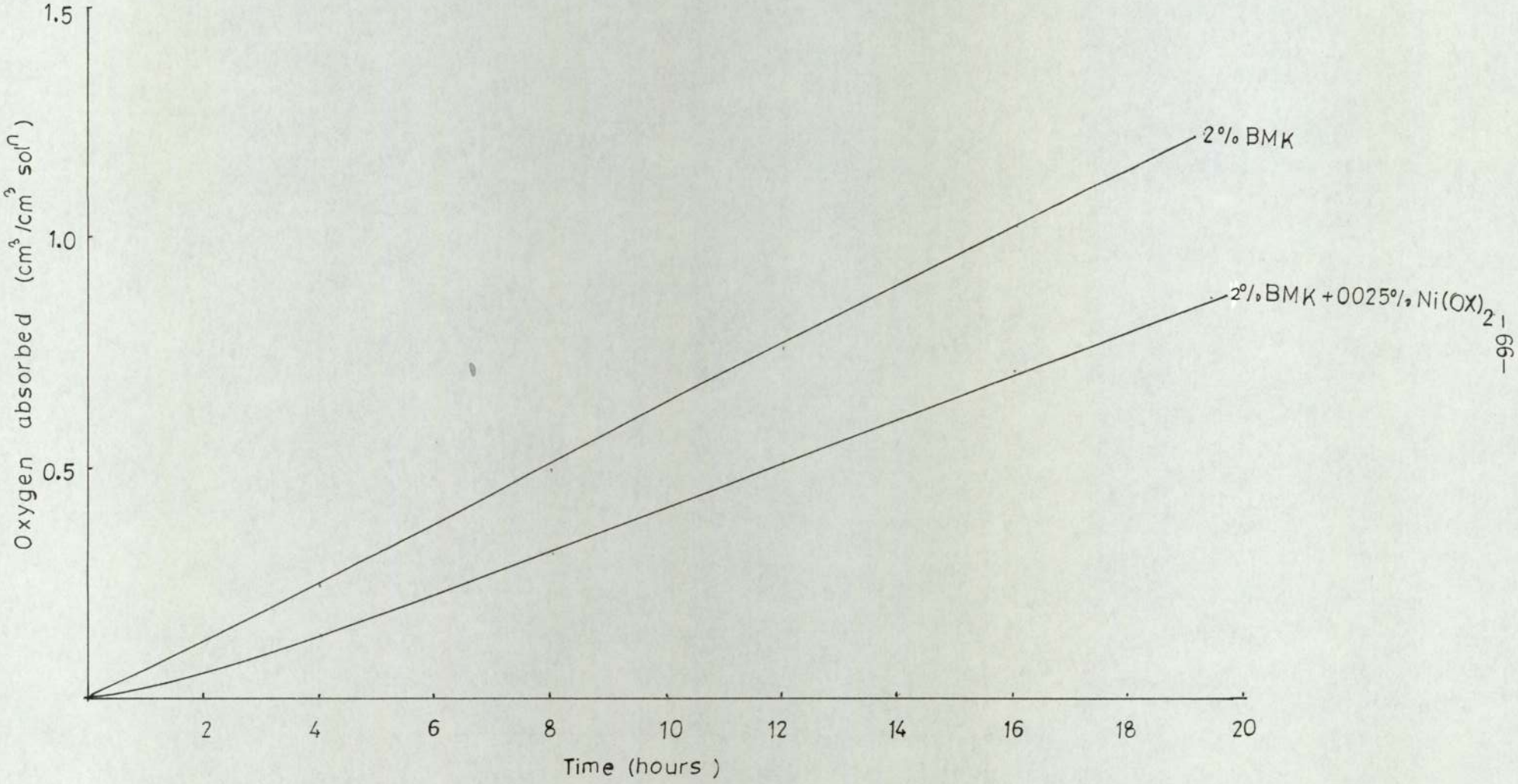

Figure (4.1.14) Photoxidation of Cumene, (a) BMK(2%), (b)BP (0.05%), (c)BMK (2%)+ 0.025% $Ni(OX)_2$, (d) BP (0.05%)+0.025% $Ni(OX)_2$.

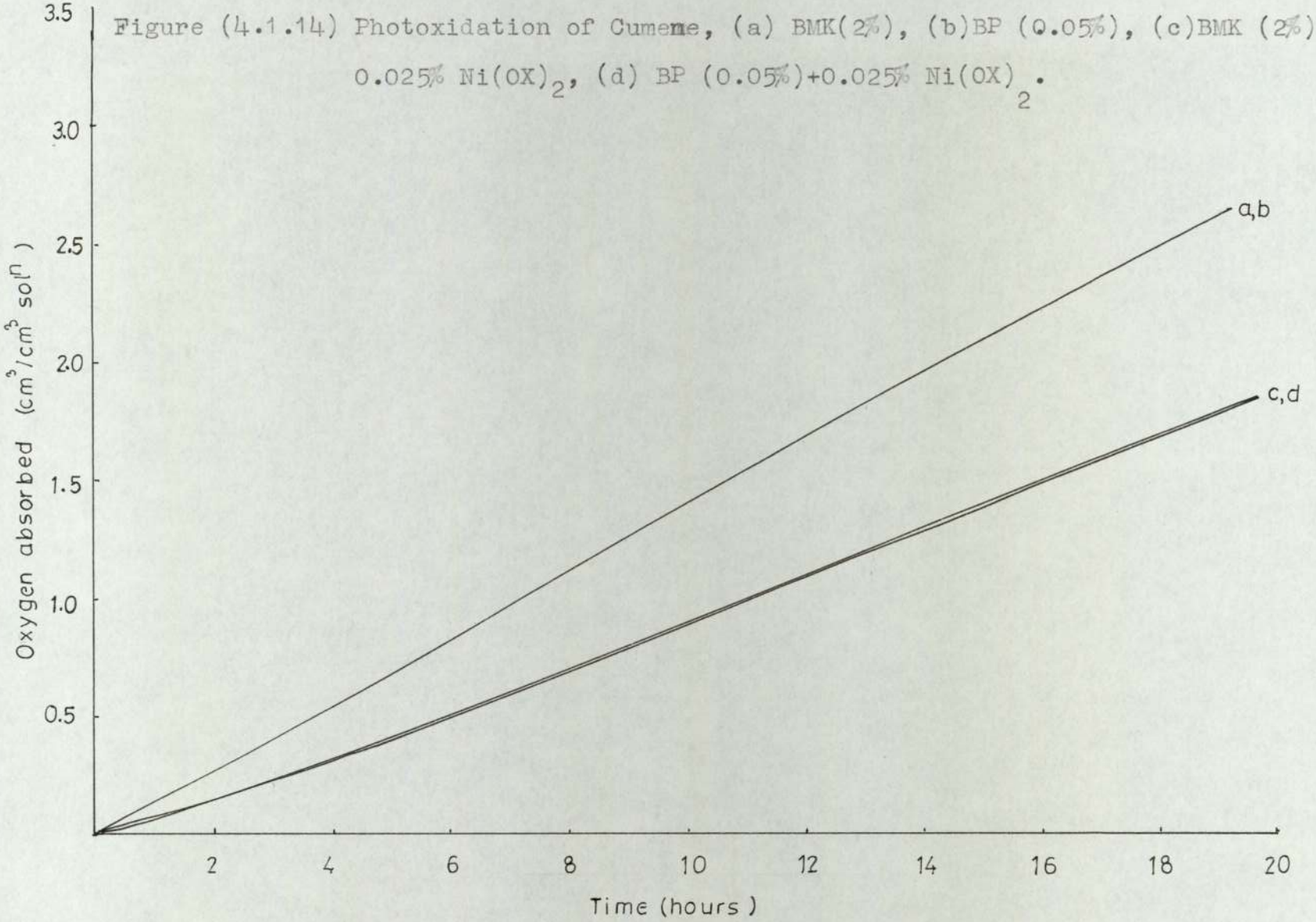

Figure (4.1.15) Photoxidation of Cumene initiated with 1% CHP and stabilised with $Ni(OX)_2$.

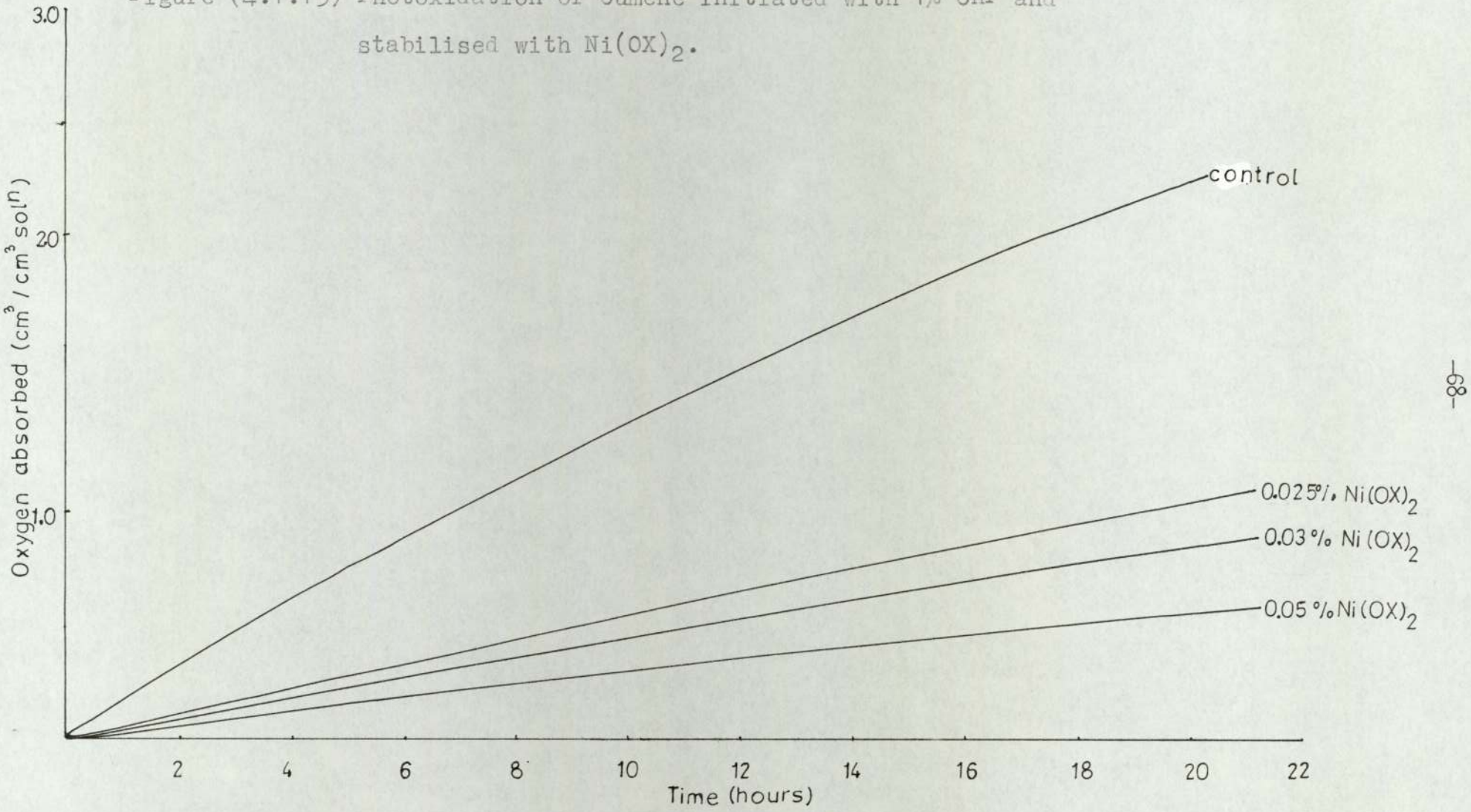

Figure (4.1.16) Photoxidation of Cumene initiated with 1% CHP, control and screened with $Ni(OX)_2$.

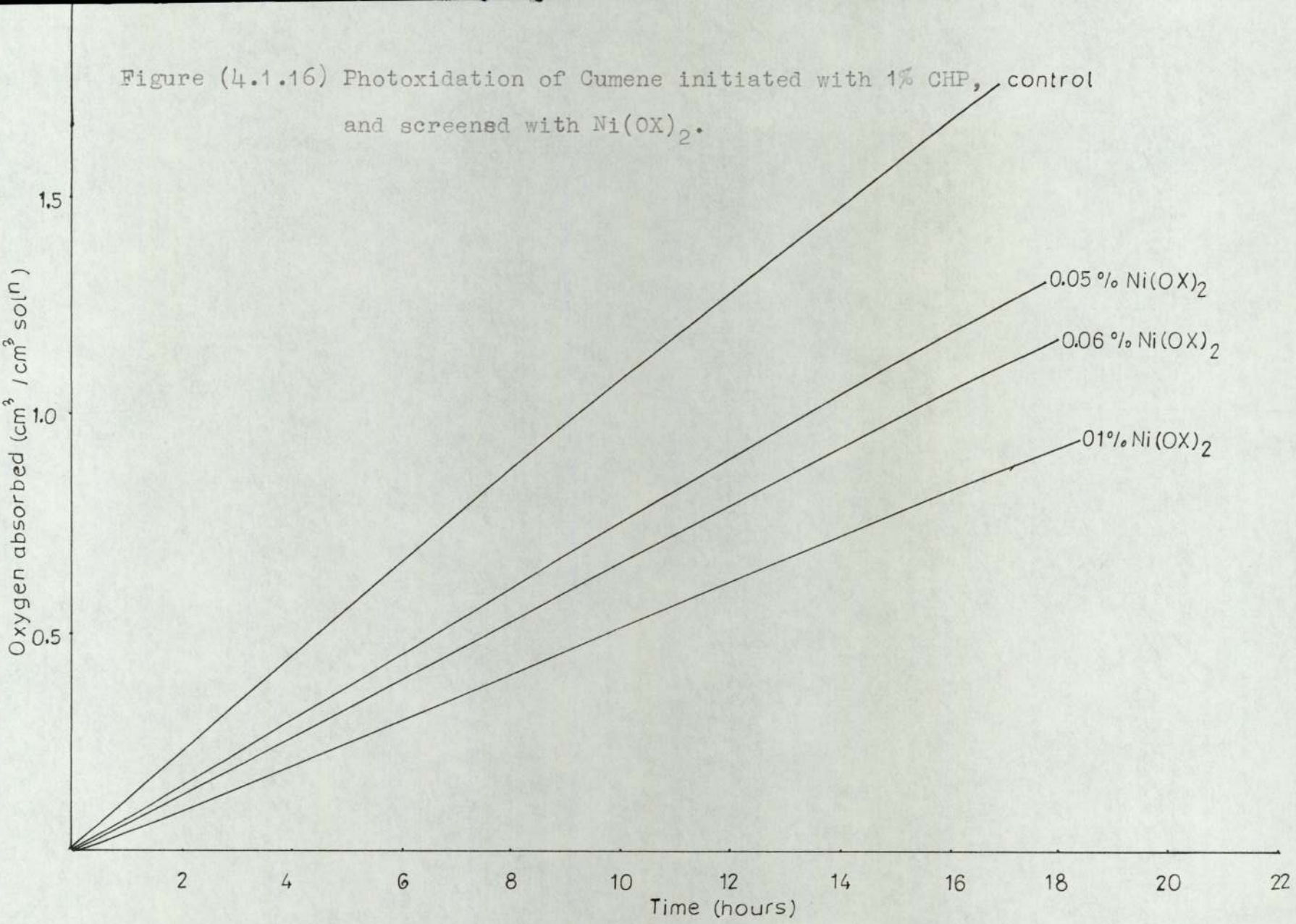

higher concentrations of the $Ni(OX)_2$ chelate when the system of cumene was initiated with 0.5% BP was also studied when used as an additive and as a screen, figures (4.1.17),(4.1.18),(4.1.19) and (4.1.20).

4.1.2 Oxygen absorption studies of uninitiated cumene

The rates of oxidation of cumene in the absence and presence of metal chelates were studied under ultra-violet light, figure (4.1.21). These rates were compared with the rates of oxidation when the stabilisers were used as external screens at equivalent screening concentration. figures (4.1.22) and (4.1.23).

4.1.3 Oxygen absorption studies of dodecane

The rate of absorption of oxygen by dodecane is very small in the absence of an initiator The rate of absorption of oxygen by dodecane was measured with different concentrations of tertiary butyl hydroperoxide (TBH) and benzophenone (BP) and the effect of the metal oxime chelates on the rates of oxidation are shown graphically in figure (4.1.24). These rates were compared with the rates of oxidation at equivalent concentration of the additives when they were used as screens, figures (4.1.25) and (4.1.26).

4.2 Oxygen absorption studies of cumene at 50°C

Oxygen absorption of pure cumene was studied at 50°C, a steady rate of oxidation was obtained when the cumene was initiated with 1% CHP or 0.1% AZBN. These rates were found to be retarded by equal amounts when 0.025% Ni(OX) was used as an additive figure (4.2.1).

Figure (4.1.17) Photoxidation of Cumene initiated with 0.05% BP, and stabilised with $Ni(OX)_2$.

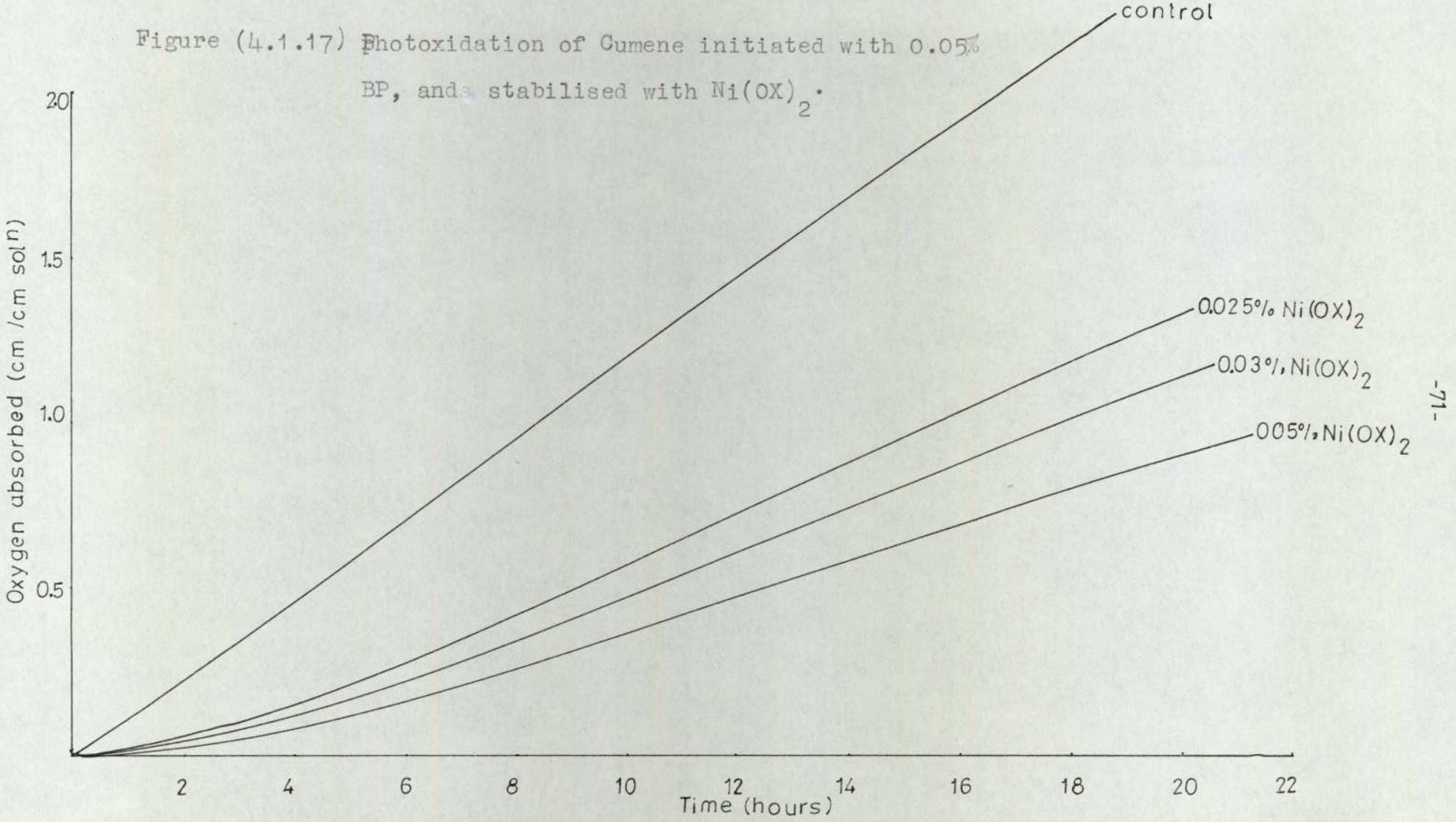

Figure (4.1.18) Photoxidation of Cumene initiated with 0.05% BP and screened by $Ni(OX)_2$.

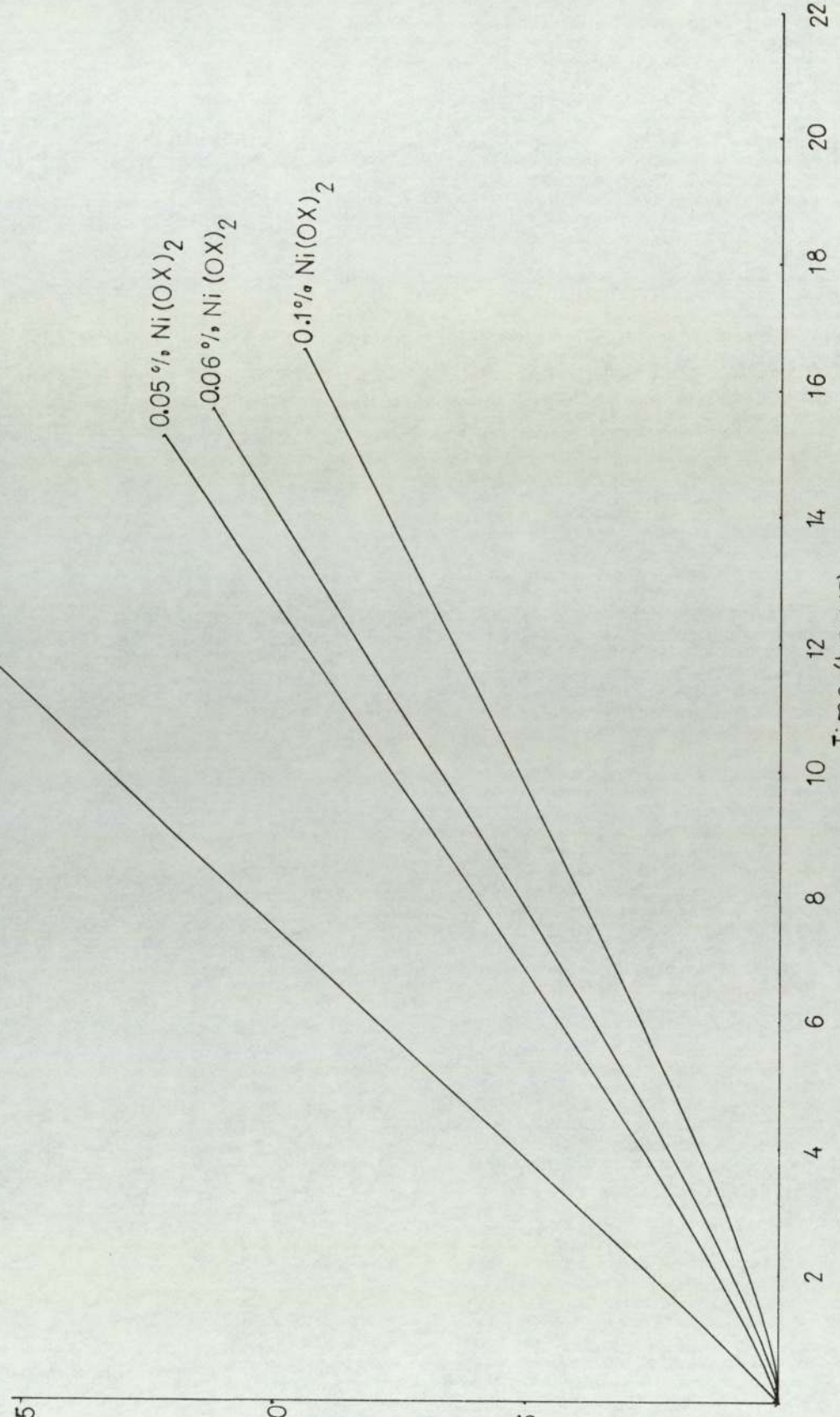

Figure (4.1.19) Photoxidation of Cumene. (a) BP (0.05%), (b) CHP(1%), (c)BP (0.05%)+ 0.03% $Ni(OX)_2$(A), (d) BP (0.05%)+0.06% $Ni(OX)_2$(S), (e) CHP(1%)+0.06% $Ni(OX)_2$(S), (f) CHP(1%) + 0.03% $Ni(OX)_2$(A).

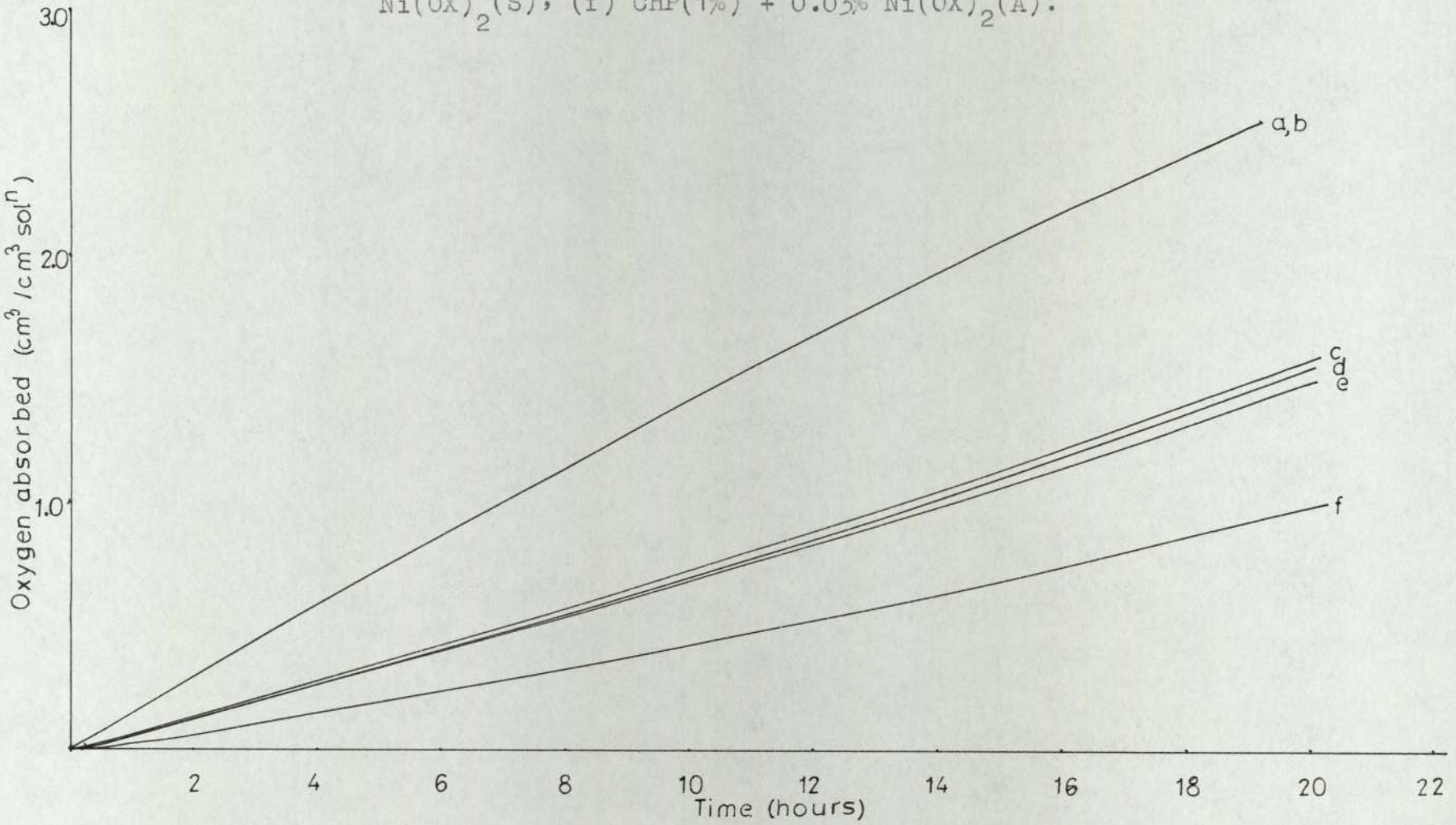

Figure (4.1.20) Photoxidation of Cumene. (a) BP (0.05%), (b) CHP (1%), (c) BP (0.05%)+ 0.05% $Ni(OX)_2$(A), (d) BP(0.05%) + 0.1% $Ni(OX)_2$(S), (e) CHP(1%) + 0.05% $Ni(OX)_2$ (S), (f) CHP(1%) + 0.05% $Ni(OX)_2$(A).

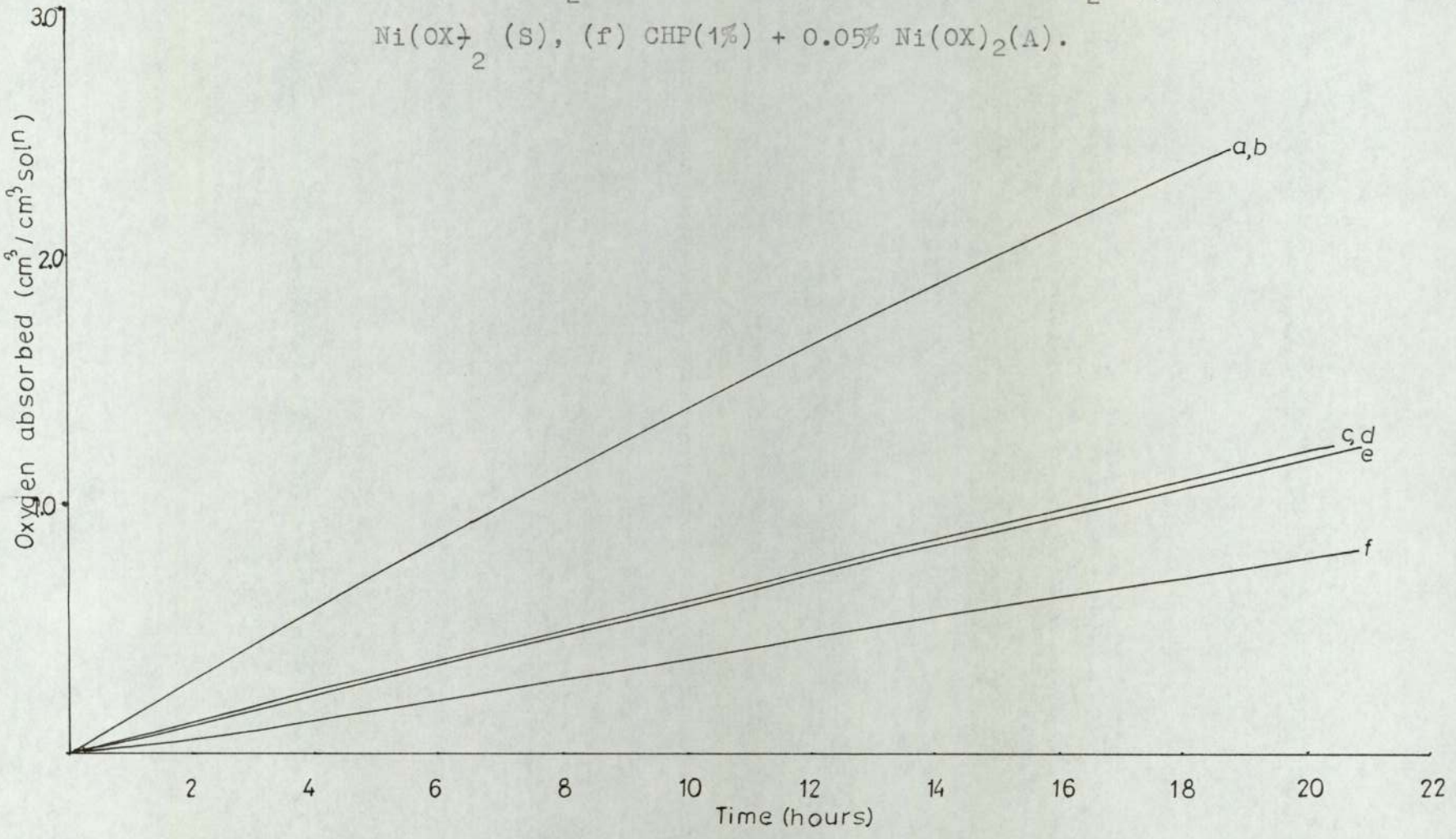

Figure (4.1.21) Oxygen absorption curves for the photoxidation of Cumene

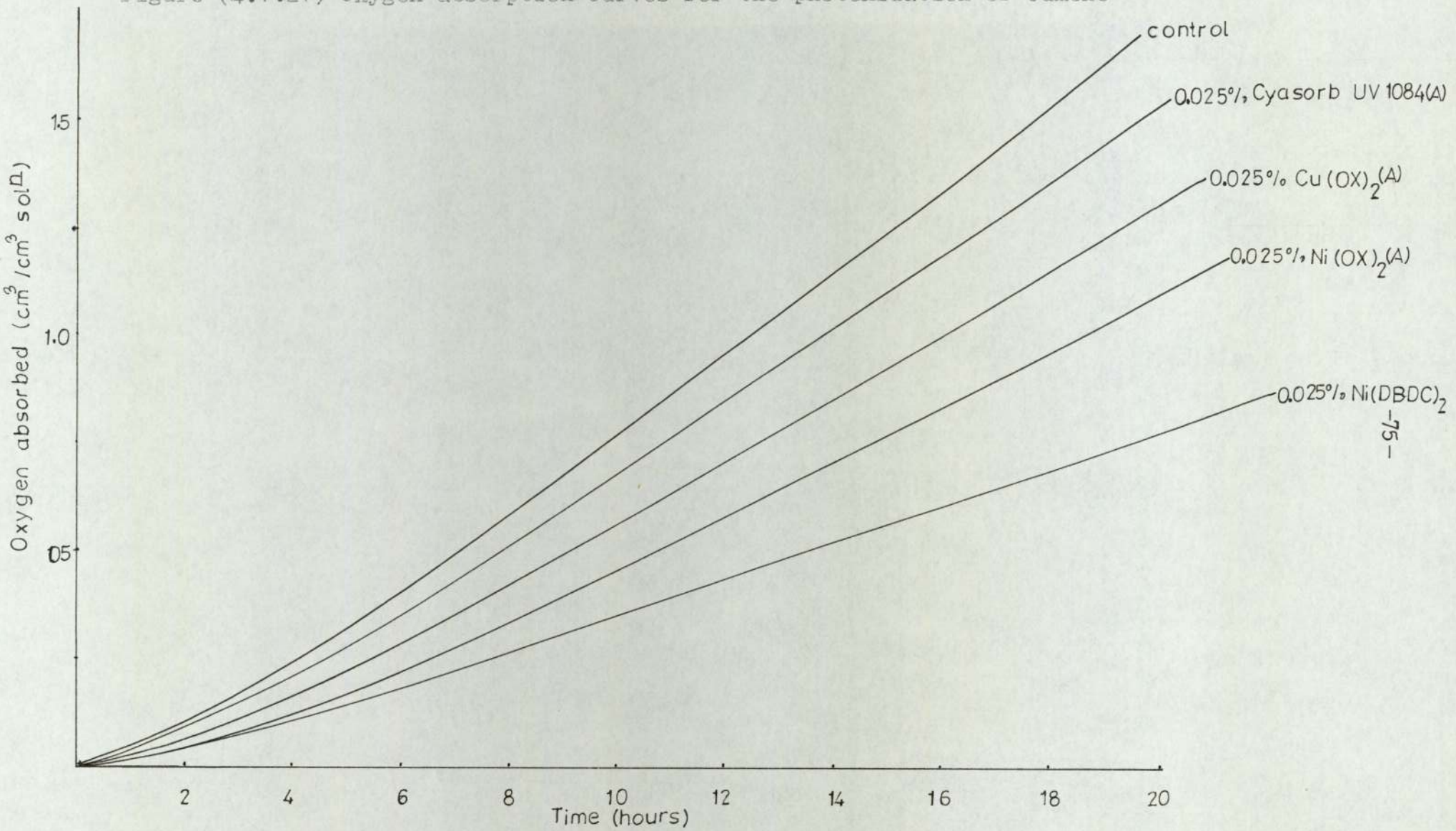

Figure (4.1.22) Oxygen absorption curves for the photoxidation of Cumene screened by the respective stabilisers.

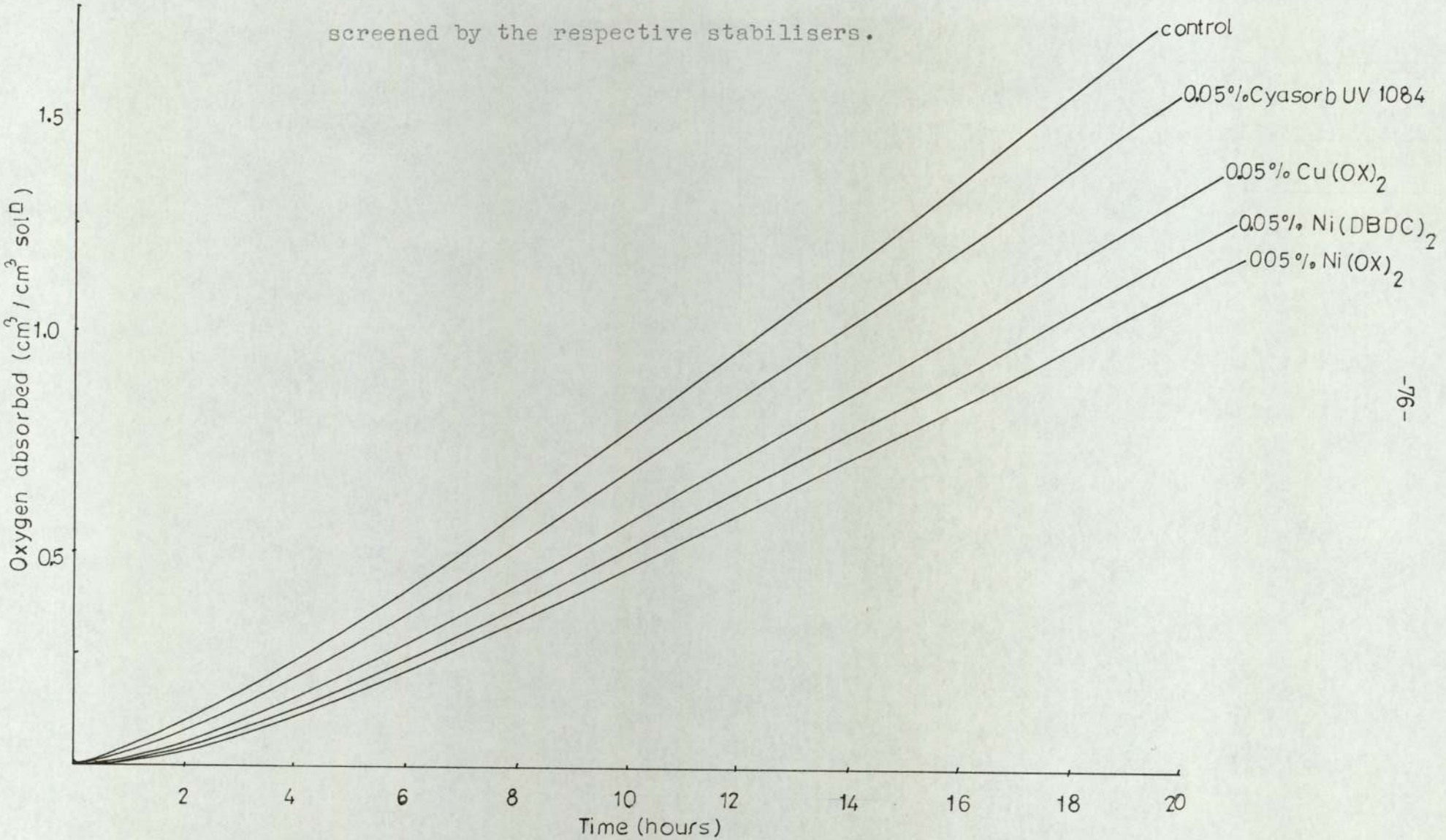

Figure (4.1.23) Photoxidation of Cumene,(a) 0.025% UV 1084 (A), (b) 0.05% VU 1084 (S)
(c) 0.025% $Cu(OX)_2$(A), (d) 0.05% $Cu(OX)_2$(S),
(e) 0.05% $Ni(DBDC)_2$(S), (f) 0.025% $Ni(OX)_2$(A)
(g) 0.05% $Ni(OX)_2$(S), (h) 0.025% $NI(DBDC)_2$(A).

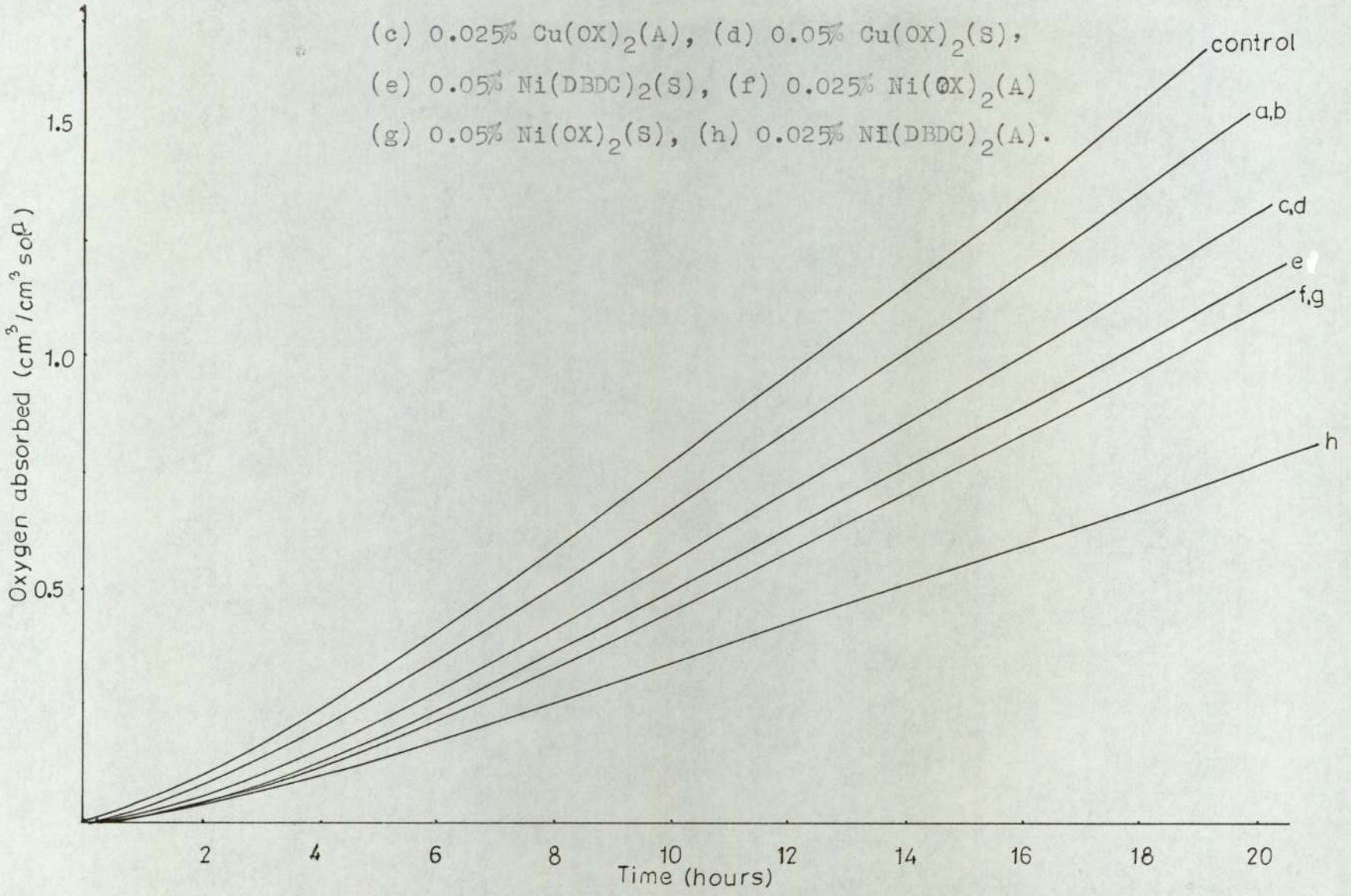

Figure (4.1.24) Photoxidation of dodecane initiated with benzophenone.

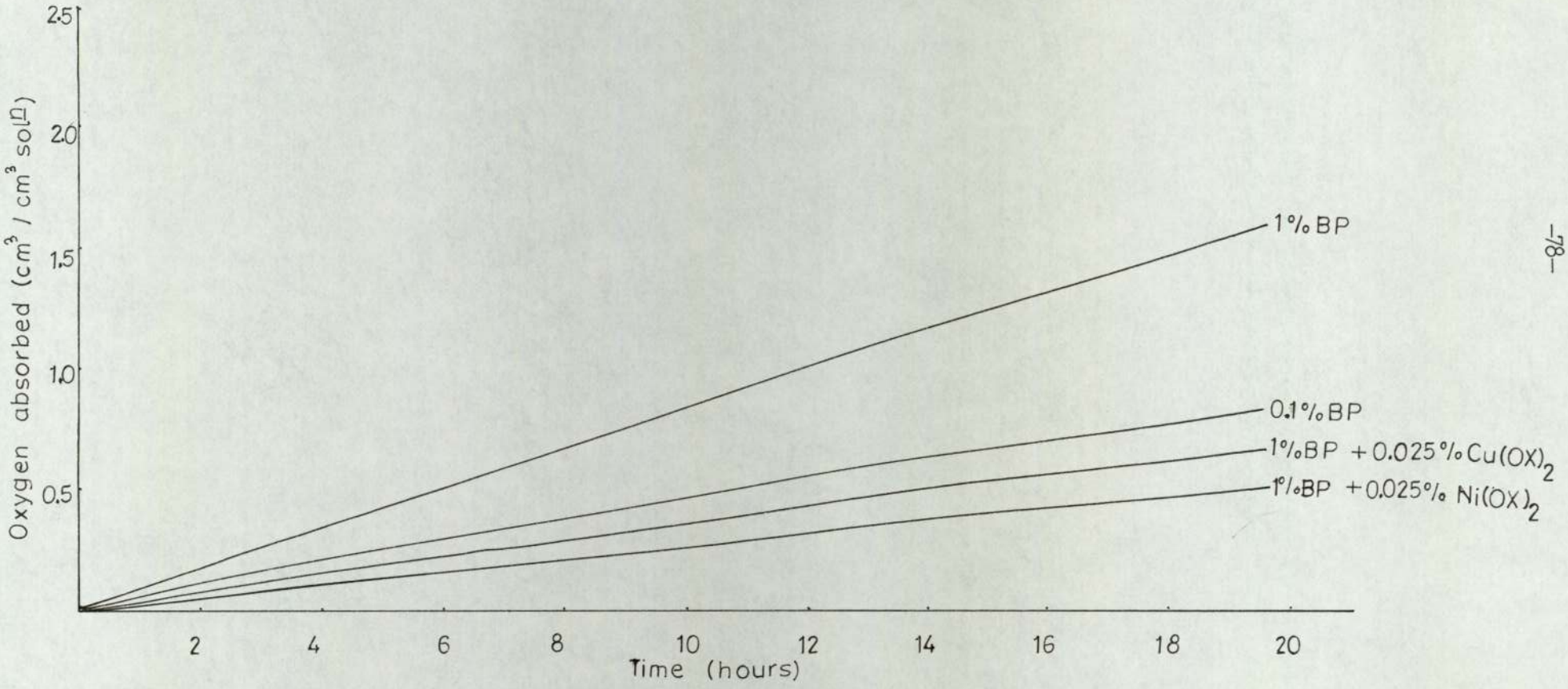

Figure (4.1.25) Photoxidation of Dodecane initiated with 1% benzophenone.

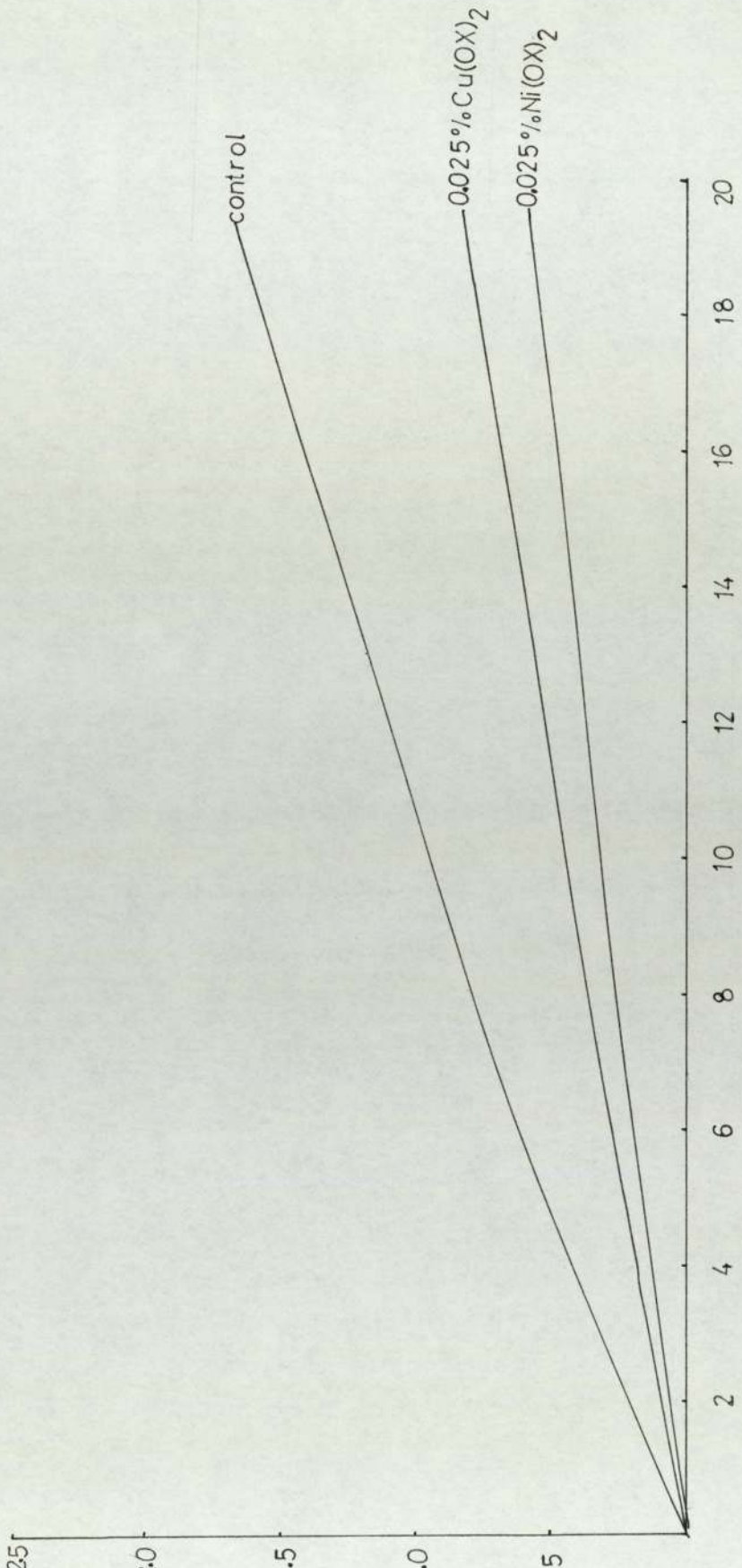

Figure (4.1.26) Photoxidation of Cumene, (a) BP (0.05%), (b) BP (0.05%)+0.05% $Cu(OX)_2$(S) (c) BP (0.05%)+0.05% $Ni(OX)_2$(S).

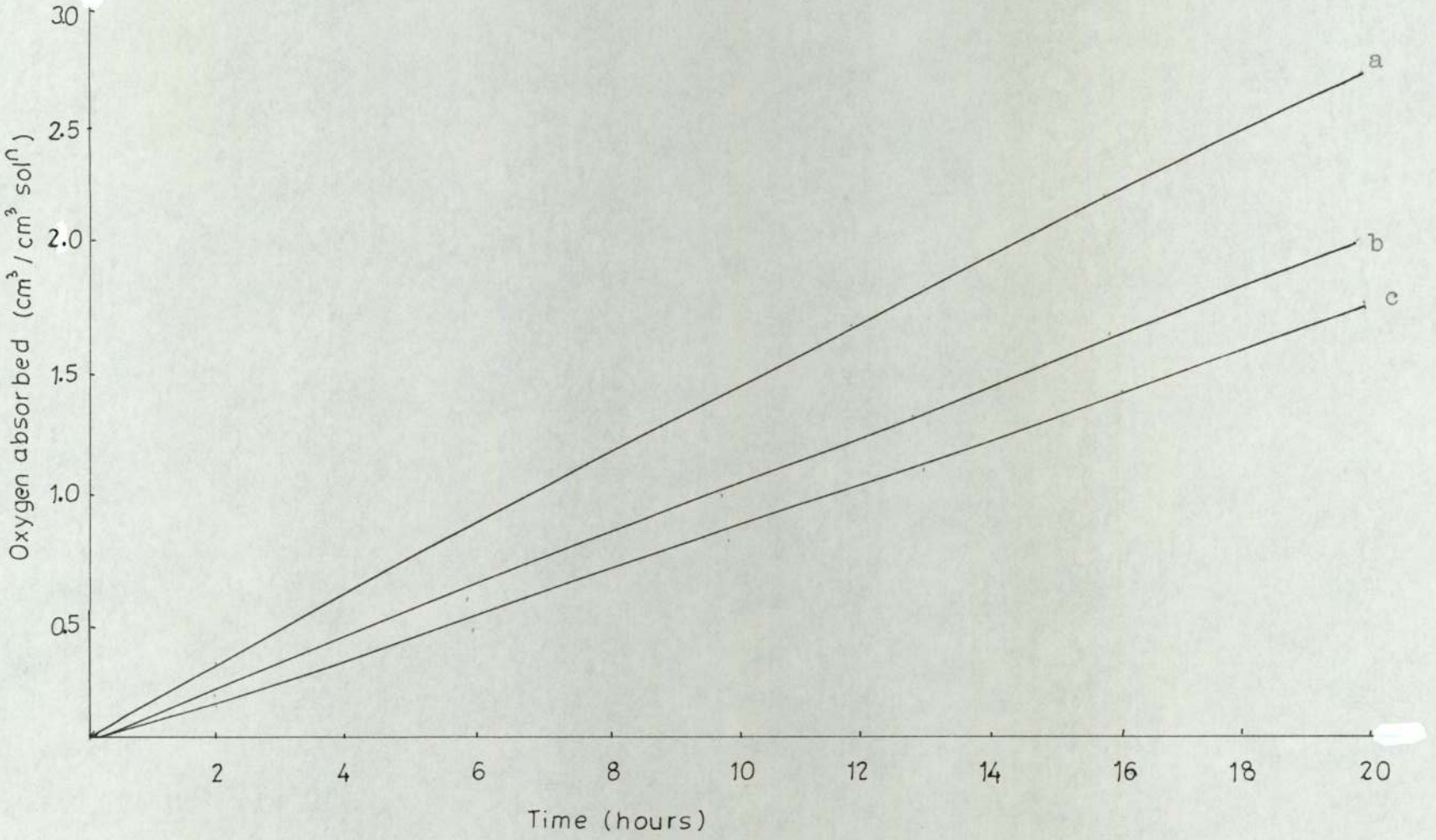

Figure (4.2.1) Thermal oxidation of Cumene.

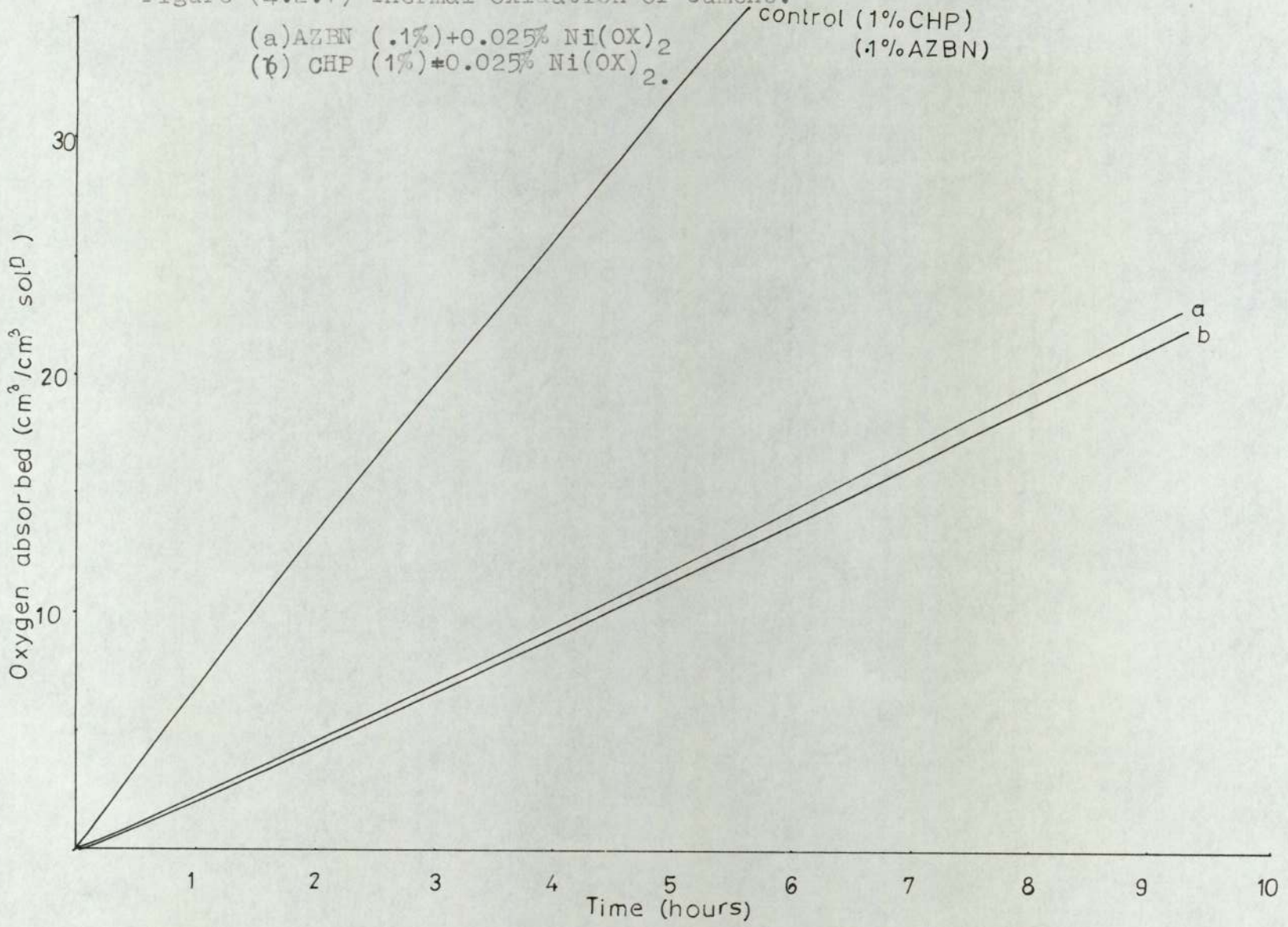

Figure (4.2.2) Thermal oxidation of Cumene,

(a) AZBN (.1%)+0.025% $Ni(DBDC)_2$

(b) CHP (1%)+0.025% $Ni(DBDC)_2$

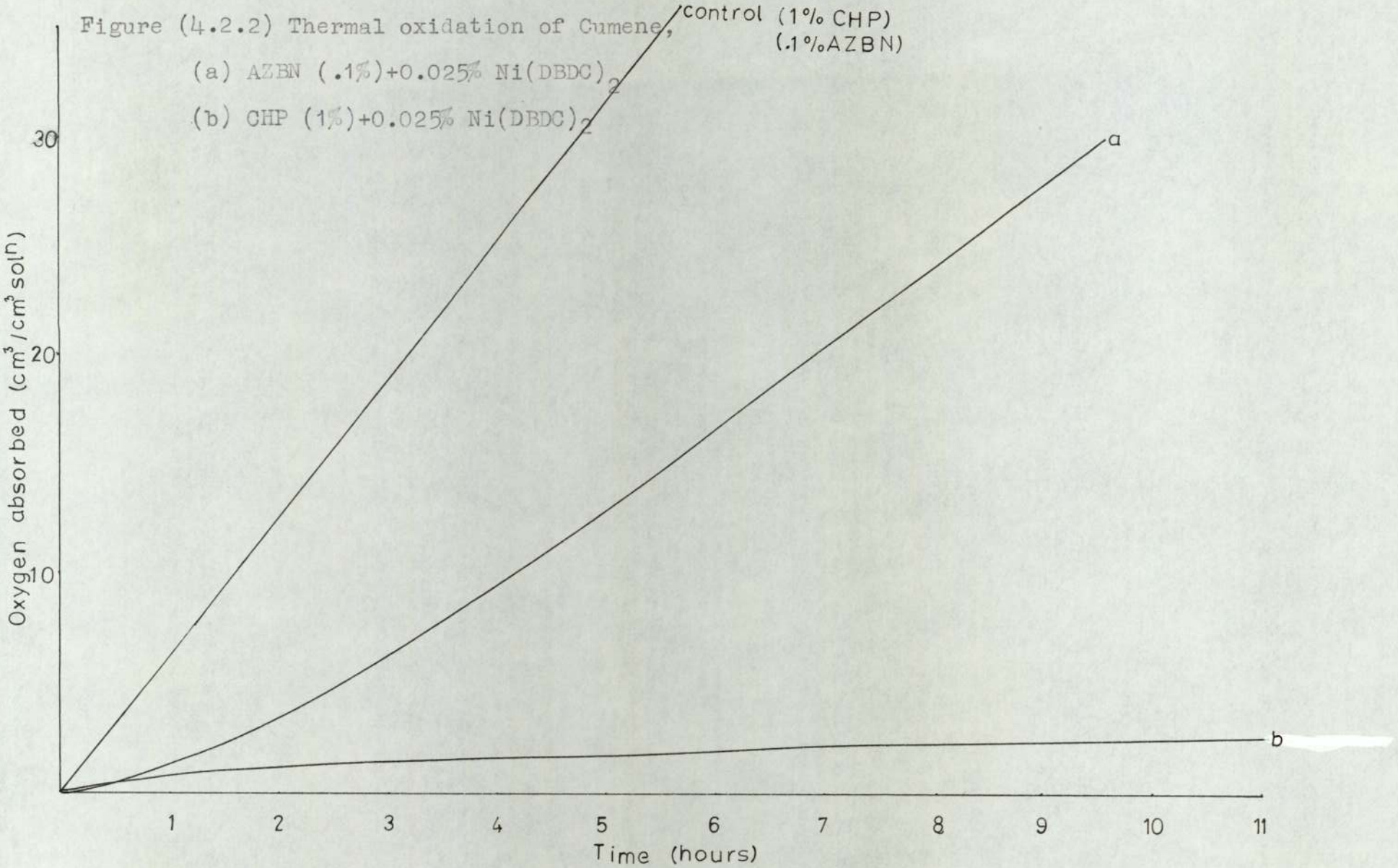

Similar studies were carried out with Ni(DBDC) and the solution did not absorb any oxygen for as long as 70 hours. A measurement of the hydroperoxide content was carried out at regular intervals of time by the iodometric method. However when the system was initiated with 0.1% AZBN the oxidation retarded and complete inhibition did not take place. Figure (4.2.2). This will be discussed in detail in Chapter 6

4.3 Discussion

The photoxidation of cumene in the absence of an initiator shows an autoaccelerating curve figure (4.1.1). This may be due to the fact that cumene oxidises through the interaction of an oxygen perturbed triplet hydrocarbon (3RH) rather than the normal charge transfer complex formed with the hydrocarbon and oxygen[5].

$$3RH + O_2 \xrightarrow{h\nu} \text{peroxide}$$

The triplet state of cumene will have low intrinsic reactivity due to the delocalised π electron system and hence the rate at which the above reaction takes place will be slow giving rise to an induction period.

The photoxidation of cumene in the presence of an initiator I (which could be CHP, BP or AZBN) at moderate temperature is a free radical chain process, which is schematically represented by the following reaction sequence[72], based on the work carried out by Traylor and co-workers[73,74,75].

$$I \longrightarrow R. \quad (1)$$

$$R. + O_2 \longrightarrow RO_2 \quad (2)$$

$$RO_2 + RH \longrightarrow ROOH + R. \quad (3)$$

$$2RO_2 \longrightarrow 2RO. + O_2 \quad (4)$$

or

$$2RO_2 \longrightarrow ROOR + O_2 \quad (5)$$

$$RO + ROOH \longrightarrow ROH + RO_2 \quad (6)$$

$$RO \longrightarrow \text{Products} + CH_3 \quad (7)$$

$$CH_3 + O_2 \longrightarrow CH_3O_2 \quad (8)$$

$$CH_3O_2 + RO_2 \longrightarrow \text{Products} + O_2 \quad (9)$$

Comparing the rates of oxidation of cumene and cumene initiated by 1% CHP, figure (4.1.1), although initially the rate of oxidation is slow, after a few hours the rate becomes almost identical to the rate of oxidation of cumene initiated by 1% CHP, which is evidence for step (2) in the above sequence producing the hydroperoxide.

Figure (4.1.3) compares the rate of oxidation of cumene initiated with 1% CHP, with the rate of formation of CHP during oxidation of cumene. After about 20 hours of oxidation it can be seen that although the rate of oxygen absorption is still unchanged, the peroxide concentration reaches a plateau, this shows that at this stage of oxidation a steady state equilibrium is reached where the rate of formation of CHP is equal to the rate of decomposition of CHP.

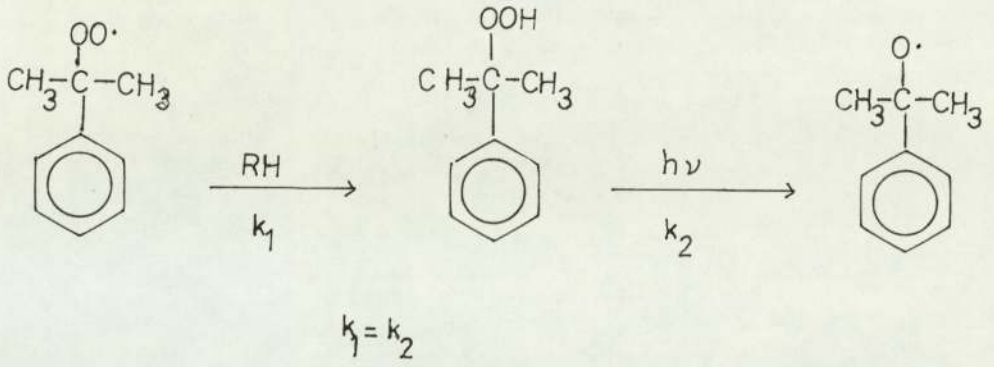

$$k_1 = k_2$$

which is the same as reactions (2) and (4) in the above sequence.

The metal chelates are retarders of photoxidation irrespective of the initiator system used, therefore these act as antioxidants or UV screens. This is described in detail in Section (1.1.3).

Table (4.1) compares the rates of oxidation of cumene initiated by 1% CHP and .05% BP, and how these are effected by the presence of different metal chelates. These rates were calculated by averaging out the rate of oxidation after a steady rate of oxidation is reached.

The linear retardation of oxidation by Ni(II) (o-hydroxy autophenone oxime) [or $Ni(OX)_2$]and Cu(II) (o-hydroxy acetophenone oxime)[or $Cu(OX)_2$] shows that the oxidation reaction is not completely inhibited, but is only retarded to a certain extent. This would mean that there is a gradual removal of the radicals by a chain breaking mechanism rather than a removal of the primary source of radicals which would lead to a total inhibition of the reaction.

The UV activating effects of the iron complex when the system is initiated with BP, seems to be associated with its much lower photo-stability than the nickel and the copper complexes. The radicals thus formed will act as photoactivators as well as the free transition metal ion.

TABLE 4.1

Stabiliser	Initiator	Average rate (Stabilised)	Average rate (Screened)	Initiator	Average rate (Stabilised)	Average rate (screened)
—	1% CHP	0.133	0.133	0.5% BP	0.133	0.133
0.025% nickel oxime	"	0.057	0.084	"	0.084	0.084
0.025% copper oxime	"	0.083	0.097	"	0.097	0.097
0.025% nickel dibutyl dithiocarbomate	"	0.042	0.085	"	0.085	0.085
0.025% cyasorb UV(1084)	"	0.117	0.117	"	0.117	0.117

Rates of oxidation of initiated cumene system with different metal complexes or screens and stabilisers. These rates were calculated as an average of the steady rates of oxidation observed.

The results shown in figures (4.1.9),(4.1.10) and Table (4.1) compare the rates of oxidation of cumene initiated by CHP and BP and stabilised by 0.025% $Ni(OX)_2$ and $Cu(OX)_2$. From these it can be seen that the nickel and copper complexes are at least in part ultra-violet screening agents. The rates of the externally screened oxidations are the same for both initiators when either the nickel or the copper complex is incorporated into the solution at equivalent screening effectiveness, the rate of the BP initiated photoxidation is within experimental limits identical, but that of the hydroperoxide initiated oxidation is more strongly inhibited. Since long lived excited states are not involved in the peroxide decomposition, this would imply that the mechanism involved in the stabilising activity of this nickel complex is not primarily quenching of photoexcited states.

It has been suggested that the antioxidant action by hydroperoxide decomposition could be distinguished from the chain transfer mechanism, by the oxygen absorption profile obtained in hydroperoxide and azobis-isobutyronitrile initiated oxidation of hydrocarbons, in the presence of these antioxidants. A chain breaking antioxidant with hydroperoxide as initiator would only retard the oxidation, as the source of radicals is reversibly removed. However with a peroxide decomposing antioxidant and hydroperoxide initiation, autoretardation is predicted if the antioxidant is in excess or acts catalytically, as the primary source of radicals are removed[44].

Figure (4.2.1) shows that these oxime complexes retard the oxidation of CHP and AZBN initiated cumene to the same extent indicating that the

stabilisation is due to a chain breaking rather than by a decomposition of hydroperoxides and a possible mechanism is a trapping of alkyl or alkyl peroxy radicals (see Chapter 6).

The results in figure (4.1.14) were obtained with a typical aliphatic triplet generator isobutyl methyl ketone (BMK). Aliphatic ketones have higher triplet energy states than aromatic ketones[26], and for energy transfer to take place the donor should be at a higher energy level than the acceptor[30]. The identical retardations observed with both initiators confirms that the system is initiated either with an aliphatic ketone or an aromatic ketone. This supports the conclusions based on figures (4.1.9) and (4.1.10).

Figure (4.1.11) compares the effectiveness of nickel dibutyl dithiocarbamate Ni(DBDC) as an additive and as a screen when present in a separate solution, in the photoxidation of cumene initiated by BP and CHP, It can be seen that the $Ni(DBDC)_2$ is equally effective in a triplet activated photoxidation whether used as an additive or as a screen. This could imply that neither triplet carbonyl or singlet oxygen quenching occurs and only screening is involved under these conditions. However when hydroperoxide is used as an initiator, although the initial effect as an additive appears to be screening the photoxidation rapidly autoretards to give a complete inhibition of the photoxidation process. This behaviour is entirely analogous to that observed in thermal oxidation[44], and could be due to a destruction of hydroperoxides by the Lewis acid catalyst sulphur dioxide. From these it may be concluded that two mechanisms are involved in the ultra-violet

stabilising behaviour of $Ni(DBDC)_2$, namely screening and decomposition of hydroperoxides. This is further confirmed by the complete inhibition of the CHP initiated cumene system when the same reaction was carried out at 50°C in the absence of UV light, whereas the oxidation was only retarded when the system is initiated with 1% AZBN. This proves that the stabilising action of $Ni(DBDC)_2$ is by a process of removing the primary source of radicals. An analysis of the oxidising system for hydroperoxides showed a fast reduction of hydroperoxide with time and was completely removed from the system within a few hours. A detailed study of the kinetics of decomposition of cumene hydroperoxide by $Ni(DBDC)_2$ in the presence and absence of UV light will be discussed in Chapter 7 and the details of the mechanism will also be dealt with in the same chapter.

The results shown in figure (4.1.17) show that the results of similar studies with Ni(II) n-butylamino [2,2'-thiobis(4-tert-octyl) phenolate] (UV 1084). This compares the rate of retardation of cumene initiated with a typical triplet generator BP and hydroperoxide, cumene hydroperoxide. When the stabiliser is used as additive, or as an external screen, with both initiators the rate of retardation is the same, which evidently proves that it acts solely as an ultra-violet screen and does not seem to interact in anyway with the hydro-peroxides or the radical intermediate.

Figures (4.1.21),(4.1.22) and (4.1.23) deals with the same complexes but with uninitiated cumene system. With $Ni(OX)_2$, $Cu(OX)_2$ and UV(1054) as before the stability when used as an additive compares very well with

the stabilising activity when used as a screen. This confirms the conclusions so far obtained. However, with $Ni(DBDC)_2$ the stabilising activity when used as an additive is much more than when used as a screen. From this it is clear that the stabilising activity of Ni(DBDC) by decomposing hydroperoxides is reduced when used in a BP initiated system.

Some of these experiments were carried out with dodecane, this being a long chain hydrocarbon would behave in a manner similar to polyolefins in the presence of chromophores like hydroperoxides, carbonyl and vinylidene which were found to be the active initiating species in polyethylene. Like polyethylene dodecane oxidised readily in the presence of a typical triplet generator BP, with the formation of a carbonyl group absorbing at 1721 cm^{-1}. With low concentrations of hydroperoxide however, the rate of oxidation was too slow for these experiments.

Figures (4.1.25) and (4.1.26) compare the effect of metal oximes on the rate of oxidation of benzophenone initiated dodecane when used as an additive or as a screen. The rates of retardation are the same whether the stabiliser is used in the solution or outside the solution as a screen. This is conclusive evidence that, apart from screening, no other mechanism is involved in a triplet activated system. Furthermore this would eliminate any argument arising due to the fact that BP may be more reactive toward cumene than it would toward a saturated aliphatic hydrocarbon due to the absence of a labile hydrogen in the latter.

CHAPTER 5

The spectral region between 210 nm and 750 nm is that in which many unsaturated aromatic, and heterocyclic, organic compounds have electronic absorption bands.

In this region the important excitations are those of the π-electrons. Excitation of σ electrons require more energy and consequently takesplace at shorter wavelengths. Bonding as well as non-bonding (lone pair) π-electrons may undergo transitions from the ground state to an electronically excited state. The wavelengths corresponding to the energy needed for such a transition is the absorption maximum. (λ_{max}). In many cases more than one such electronic transition is possible and hence many maxima are observed.

5.1 Theory

A combination of the laws by Lambert and Beer states that a proportion of light absorbed by a transparent medium is independent of the intensity of the incident light, and proportional to the number of absorbing molecules through which the light passes.

$$I = I_o\ 10^{-Ecl} \text{ or } \log\left(\frac{I_o}{I}\right) = Ecl$$

I_o = Intensity of the incident light

I = Intensity of light transmitted

E = molar absorptivity

l = path length in centimetres.

c = concentration in moled per litre

Using this equation the molar absorptivity or the extinction coefficient can be calculated.

5.2 Experimental

In the following experiments a PE 137 UV spectrophotometer was used. This covers the ranges 190 to 390 m/μ in the ultra-violet region and 350 to 750 m/μ in the visible region. Most of the spectra were obtained on fast scan which covers one range of wavelengths in two minutes.

In the experiments where the extinction coefficients are calculated dilute solutions of the metal complexes (usually 0.003%) in carbon tetra-chloride were used. This was prepared by diluting a solution containing 0.03% of the complex.

Quartz tubes containing these solutions were placed in the UV cabinet described in section (3.3.1) and were exposed for known intervals of time before their UV spectra were obtained.

Some experiments were carried out to find out the effect of carbonyl compounds on the UV stability of these metal complexes. Here three quartz tubes containing, (i) the desired concentration of the metal complex in carbon tetra-chloride, (ii) a desired concentration of the ketone in carbon tetra-chloride, (iii) a mixture of the appropriate concentrations of the ketone and metal complex were exposed to UV radiation, and at known intervals of time, equal volumes from tubes (i) and (ii) were mixed before scanning a UV spectrum, and at the same time a spectrum of the mixture in tube (iii) too was obtained on the same chart paper.

5.3 Results and Discussion

The ultra-violet spectra of the nickel, cupric and ferric complexes were obtained in two solvents carbon tetra-chloride and benzene. Identical absorption bands were obtained in both solvents, although light was cut off at 270 when benzene was used as a solvent.

The λ_{max} and the extinction coefficients in the two solvents are shown in tables (5.1) and (5.2) and the absorption spectra in carbon tetra-chloride are shown in figures (5.3.1) to (5.3.10). Somewhat different values of absorption maxima were obtained in the two solvents. This is due to the rather broad bands observed which makes an accurate location of the band head difficult.

The different λ_{max} for carbonyl bands in different solvents may be due to different hydrogen bonding or other solvating properties of the different solvents.

All the metal complexes studied absorb within the range 300 to 390 nm and have extinction coefficients of the order of 10^3, this accounts for their ability to screen UV radiation as observed in the oxygen absorption studies (section 4.3).

From figures (5.3.2) and (5.3.3) it is seen that the bands around 360 nm for the nickel oxime and copper oxime are almost insignificant in the parent ligand figure (5.3.1). This could arise from a change in the local symmetry at the nitrogen atom since it cannot be due to electron transfer bands[76].

TABLE 5.1

Extinction coefficients (E) in carbon tetra chloride

Complex	molecular weight	concentration	λ_{max}	absorbance	E_{λ}
Nickel oxime	359	0.003%	269	1.21	1.448×10^4
			304	1.17	1.40×10^4
			385	0.29	3.47×10^3
Nickel di-butyl dithio-carbomate	467	0.001%	262	0.21	9.81×10^3
			328	0.73	3.41×10^4
Copper oxime	364	0.001%	267	0.88	3.204×10^4
			342	0.22	8.01×10^3
Oxime	151	0.003%	267	0.95	4.65×10^3
			312	0.77	3.85×10^3
Ferric oxime	510	0.003%	267	1.22	2.075×10^4
			319	0.81	1.38×10^4
Benzo - phenone	182	0.005%	267	1.27	4.55×10^3
			350	0.03	1.09×10^2
Isobutyl methyl ketone	100	0.5%	285	0.78	1.56×10^2
Cyasorb UV(1084)	544	0.005%	266	0.76	$8,27 \times 10^3$
			305	0.43	4.68×10^3
UV (531)	326	0.0025%	262	0.31	4.044×10^3
			289	1.13	1.474×10^4
			331	0.74	9.65×10^3

TABLE 5.2

Extinction coefficients in benzene

Complex	Molecular weight	concentration gm/100 ml	λ_{max}	Absorbance (am)	Eλ cm^3/mol.
NIckel oxime	359	.001%	306	0.34	1.22×10^4
		.005%	379	0.47	3.375×10^3
Nickel di-butyl di-thiocarbomate	467	.001%	330	0.66	3.08×10^4
			395	0.06	2.8×10^3
Copper oxime	364	0.003%	281	0.53	6.916×10^3
			341	0.33	4.004×10^3
Oxime	151	0.001%	310	0.27	4.0×10^3
Ferric oxime	510	0.003%	382	1.00	1.70×10^6
			316	0.91	1.547×10^4
Benzo-phenone	182	0.005%	282	0.67	2.46×10^3
		0.16 %	350	0.10	1.82×10^2
isobutyl methyl ketone	100	0.5%	287	0.83	2.08×10^3
cyabsorb UV(1084)	544	0.005%	266	0.76	4.896×10^3
			305	0.65	5.113×10^3
UV (531)	326	0.005%	292	1.13	7.366×10^3
			330	0.84	5.476×10^3

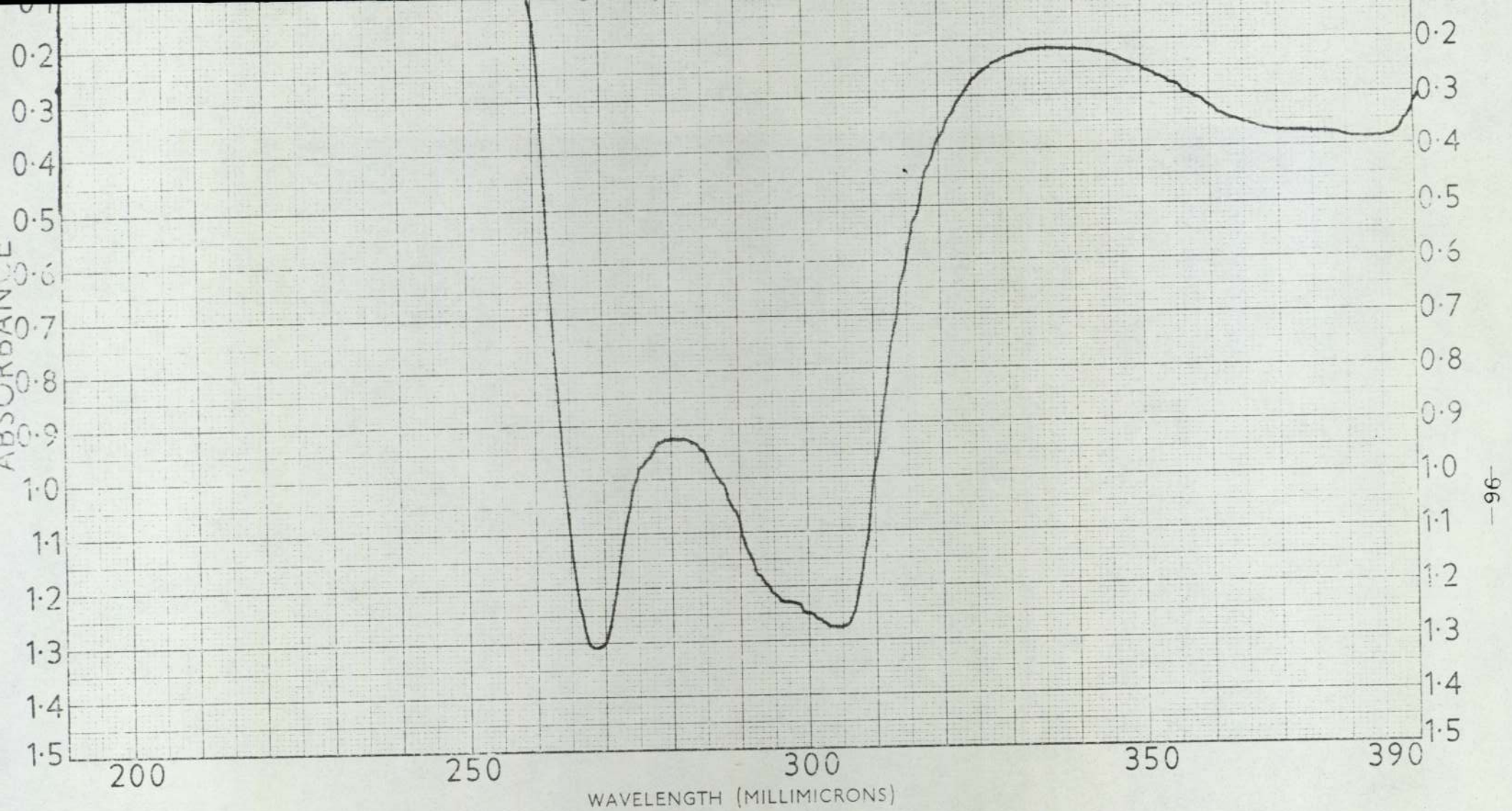

Figure (5.3.1) Ultra-Violet spectrum of 0.003 $Ni(OX)_2$ in carbon tetrachloride.

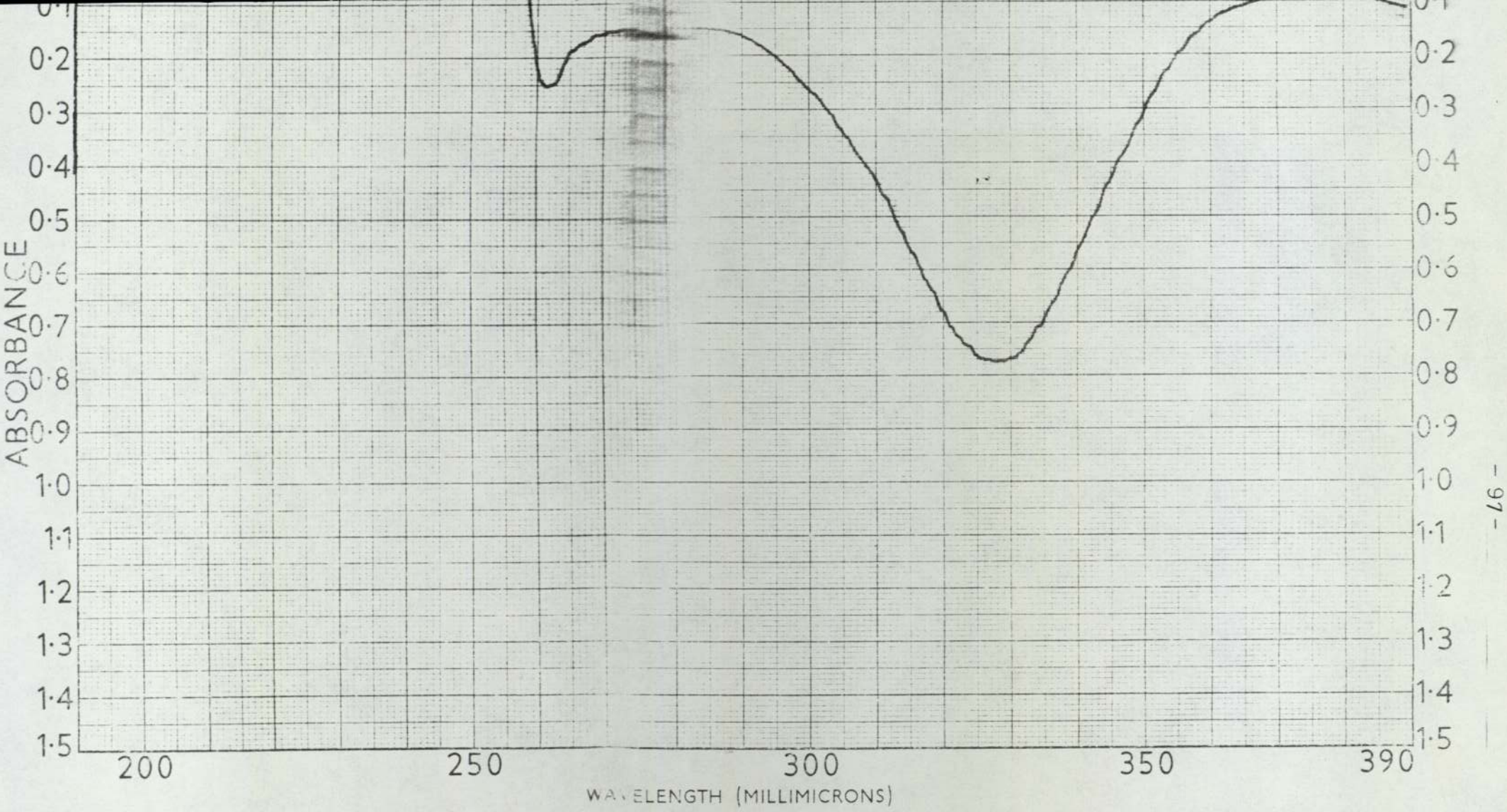

Figure (5.3.2) Ultra-violet spectrum of 0.003% $Ni(DBDC)_2$ in carbon tetrachloride.

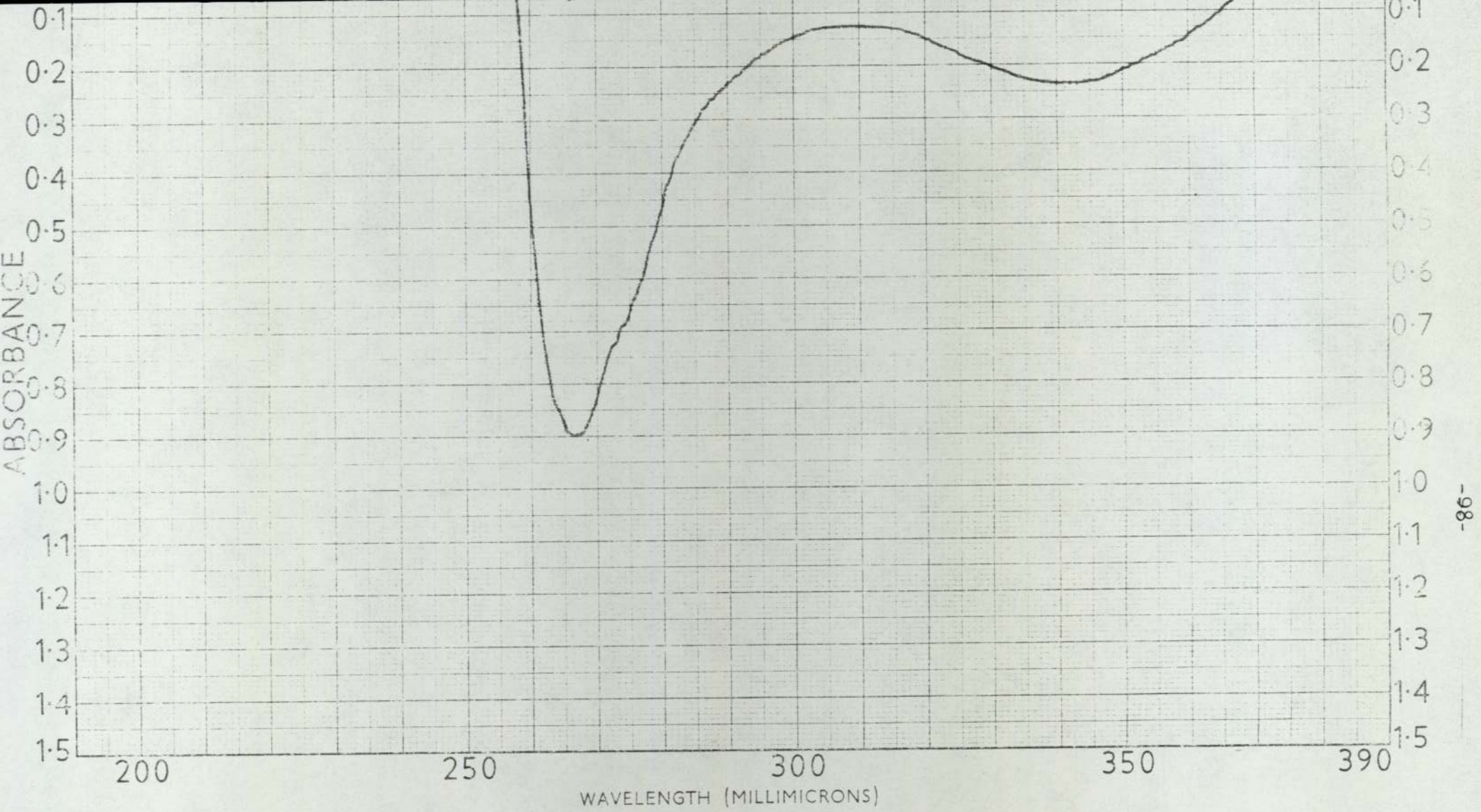

Figure (5.3.3) Ultra-violet spectrum of 0.001 $Cu(OX)_2$ in carbon tetrachloride.

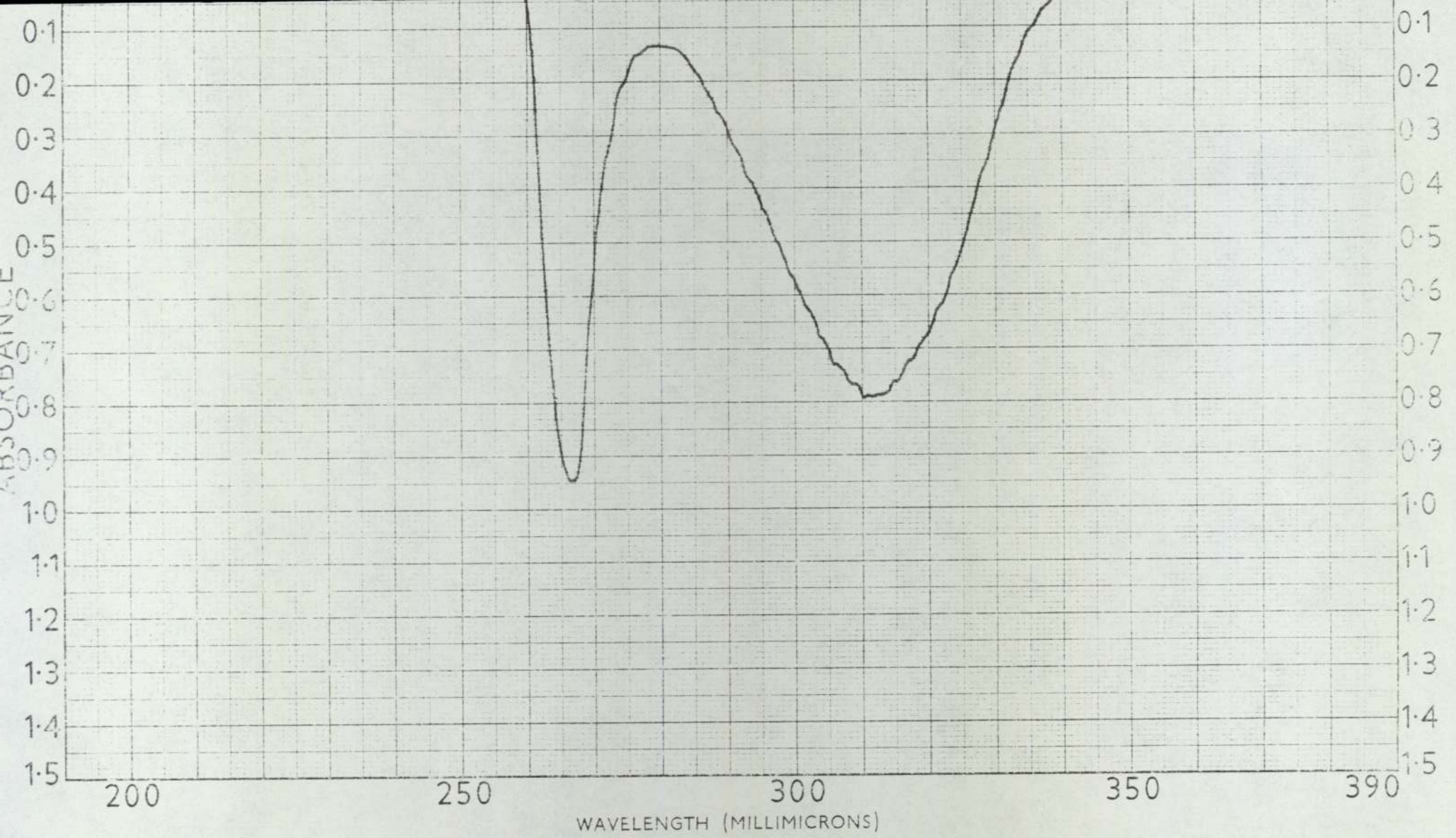

Figure (5.3.4) Ultra-violet spectrum of o-hydroxy acetophenone oxime in carbon tetrachloride

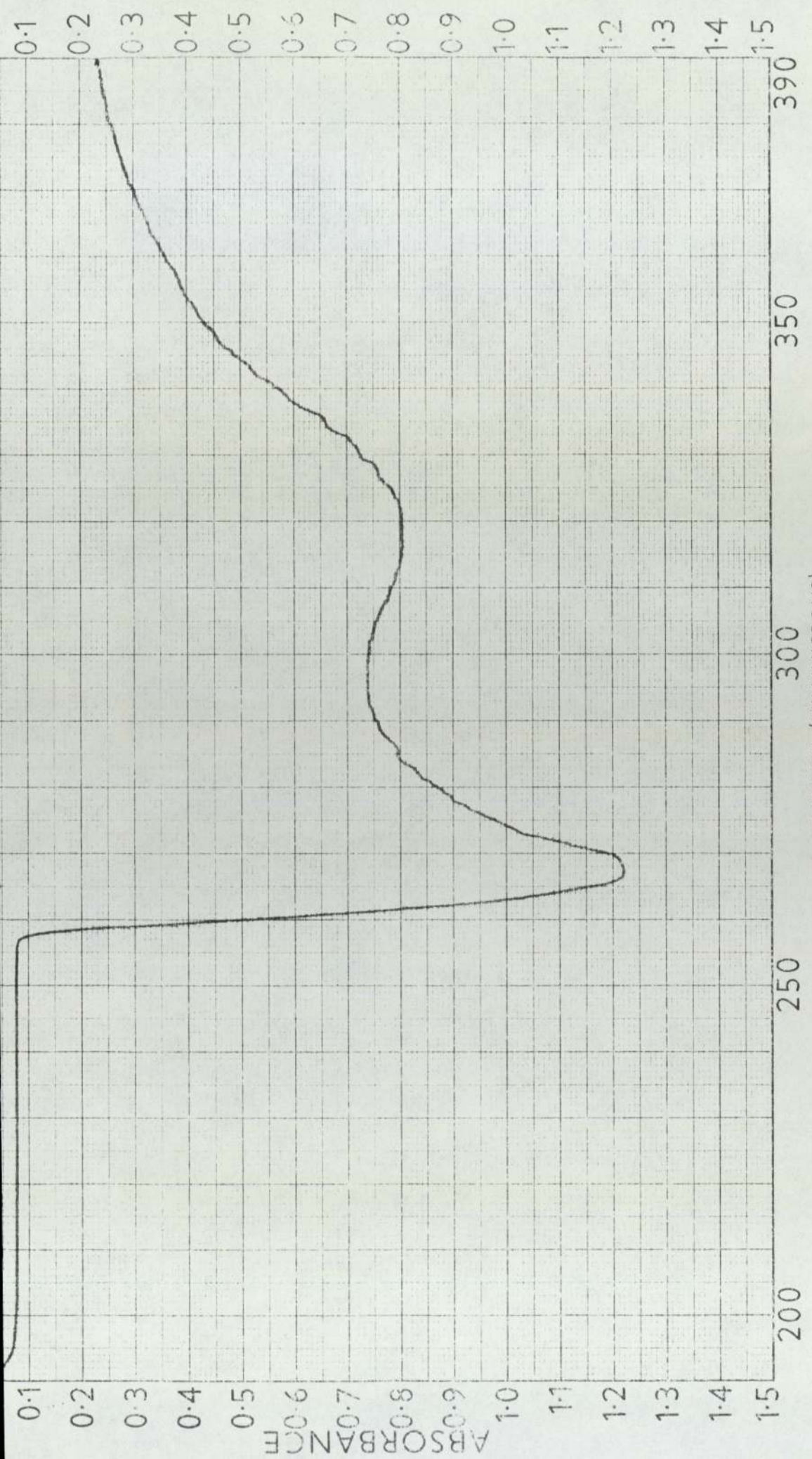

Figure (5.3.5) Ultra-violet spectrum of $Fe(OX)_3$ in carbon tetrachloride.

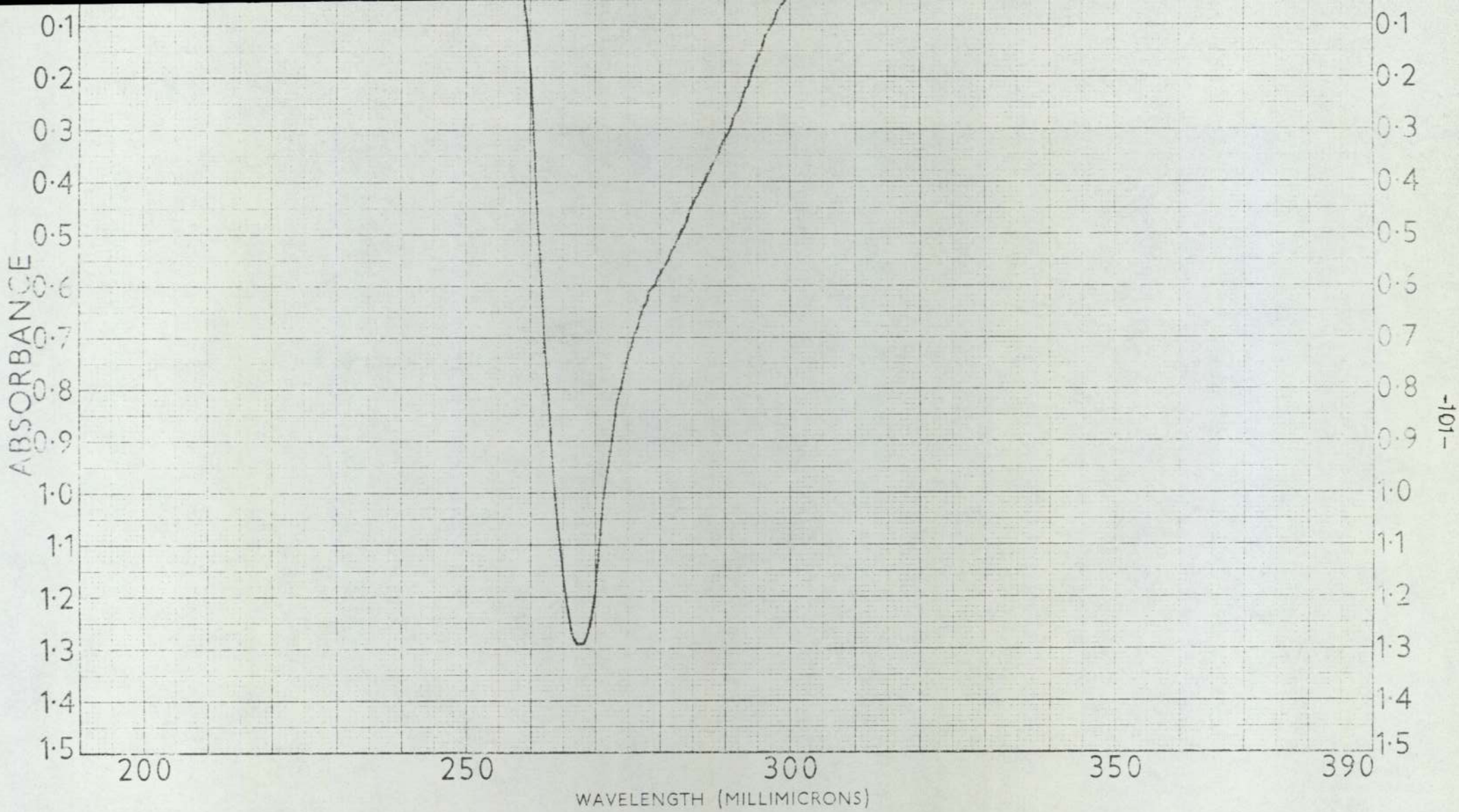

Figure (5.3.6) Ultra-violet spectrum of benzophenone in carbon tetrachloride.

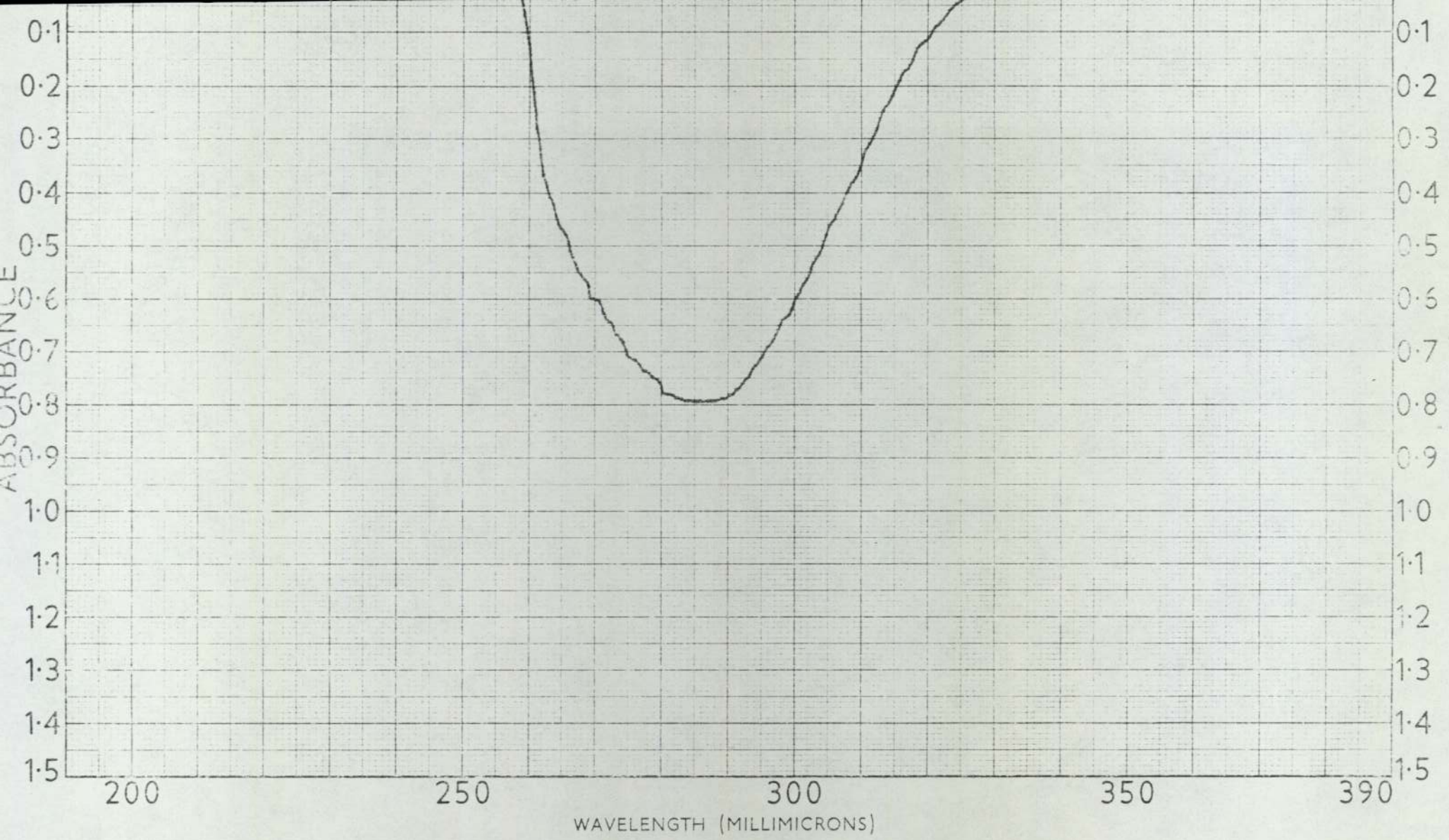

Figure (5.3.7) Ultra-violet spectrum of iso Butyl methyl ketone in carbon tetrachloride.

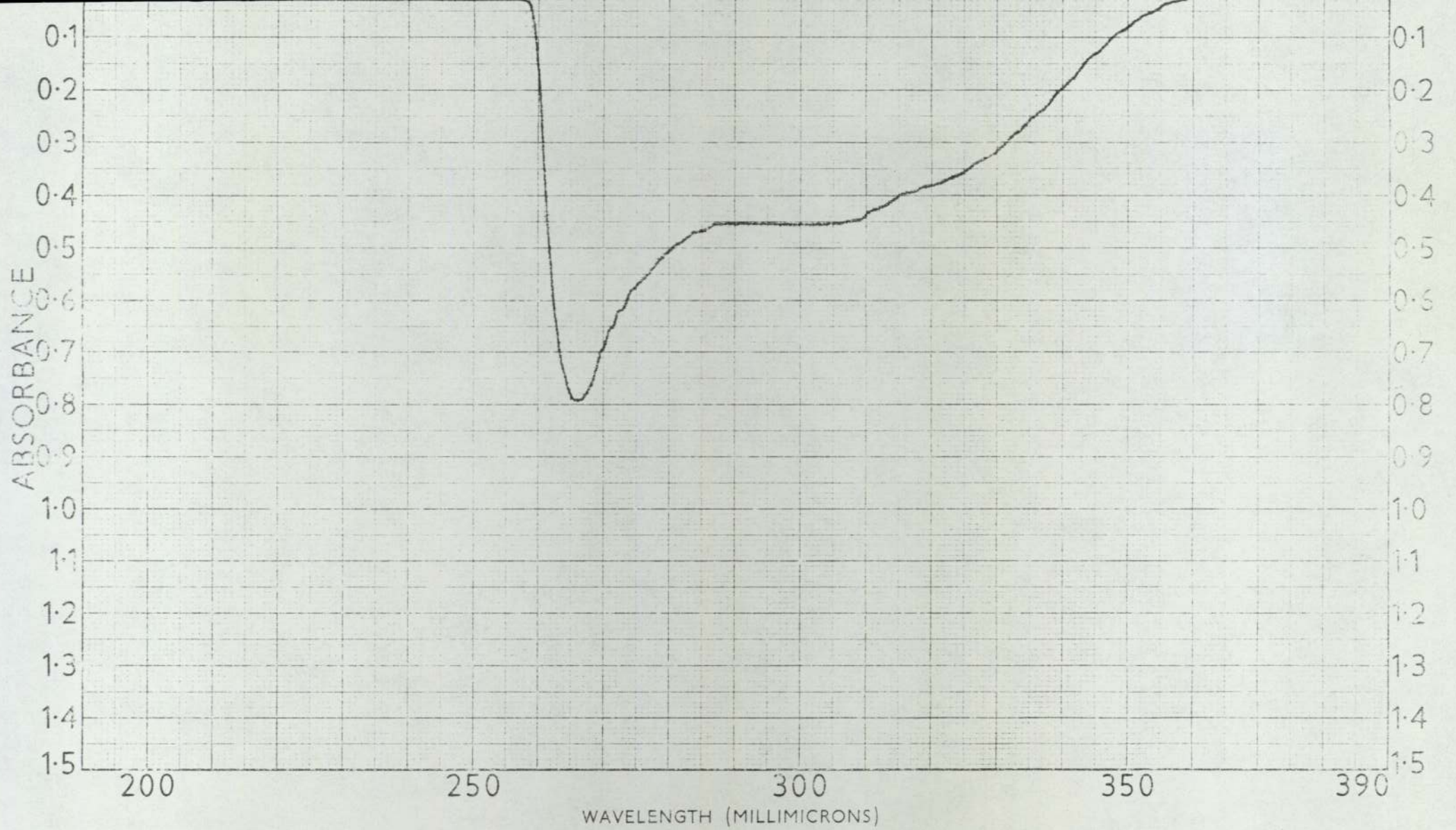

Figure (5.3.8) Ultra-violet spectrum of UV 1084 in carbon tetrachloride.

Figure (5.3.9) Ultra-violet spectrum of UV 531 in carbon tetrachloride.

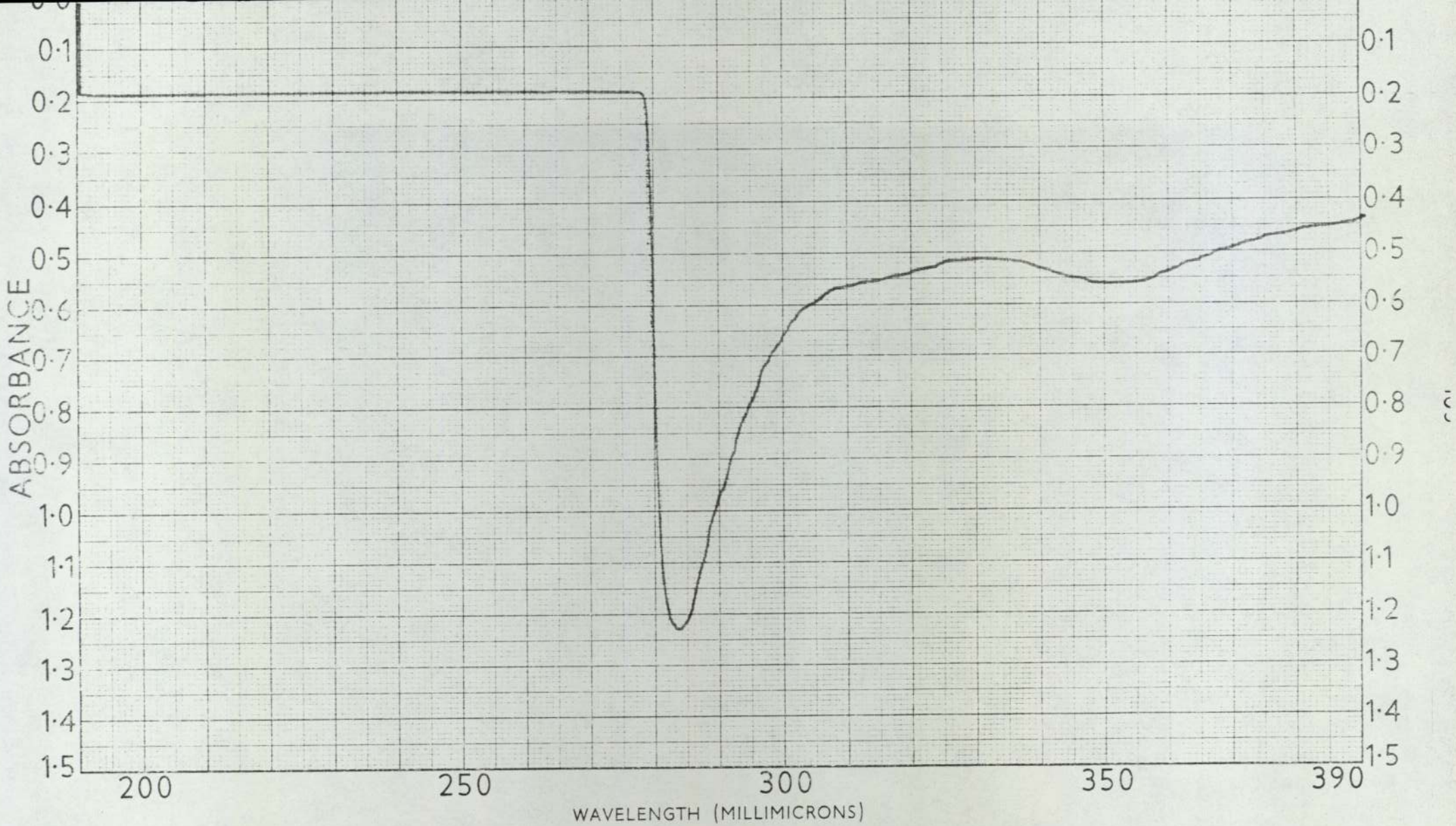

Figure (5.3.10) Ultra-violet spectrum of $Fe(DBDC)_3$ in carbon tetrachloride.

Benzophenone (BP) has two absorption maxima, figure (5.3.9), the one at 267 nm is due to a $\pi \rightarrow \pi^*$ excitation, and the weaker maximum at 360 nm is due to $n \rightarrow \pi^*$ transition, whereas isobutyl methyl ketone (BMK) has only one maximum in carbon tetra chloride at 285 nm due to $n \rightarrow \pi^*$ excitation. The band due to $\pi \rightarrow \pi^*$ transition appears at a wavelength less than 260 nm, and is not observed when carbon tetra chloride is used as a solvent. This lower λ_{max} explains the lower activity of BMK when used as an initiator in the oxidation of cumene [Section (4.1.1)].

The stability of these metal complexes to ultra-violet radiation was tested by scanning ultra-violet spectra of 0.003% of the complexes in carbon tetra chloride, after exposing to UV radiation for a known length of time, figures (5.3.11a), (5.3.11b) and (5.3.11c). All these complexes showed changes and the absorptions in the longer wavelength region due to the ligand completely disappeared within twenty hours of exposure to ultra-violet light. Figures (5.3.11b) and (5.3.11c) show the spectra obtained for $Ni(OX)_2$ and Ni(DBDC) with time. The disappearance of the band at 330 m/μ is rapid in the case of $Ni(DBDC)_2$ and the complex completely disappears within two hours of exposure to ultra-violet radiation. However $Ni(OX)_2$ seems to be much more stable to UV radiation and even after six hours a certain amount of the complex remains undecomposed.

Singlet oxygen could be formed in these systems by a quenching of triplet carbonyl by triplet oxygen

$$^3[\text{x} = \text{o}) + 3O_2 \longrightarrow {}^1[\text{x} = \text{o}] + {}^1O_2$$

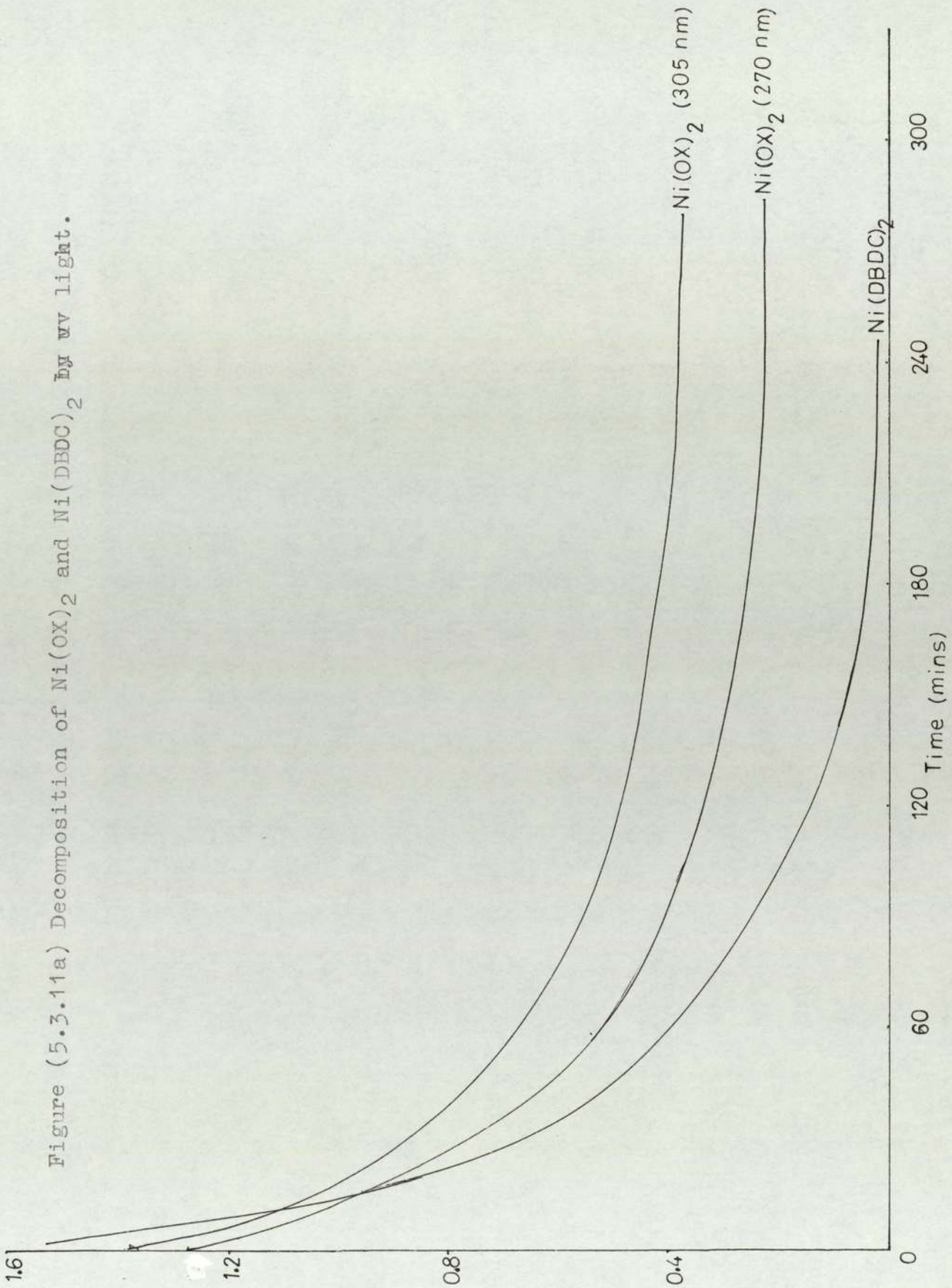

Figure (5.3.11a) Decomposition of $Ni(OX)_2$ and $Ni(DBDC)_2$ by uv light.

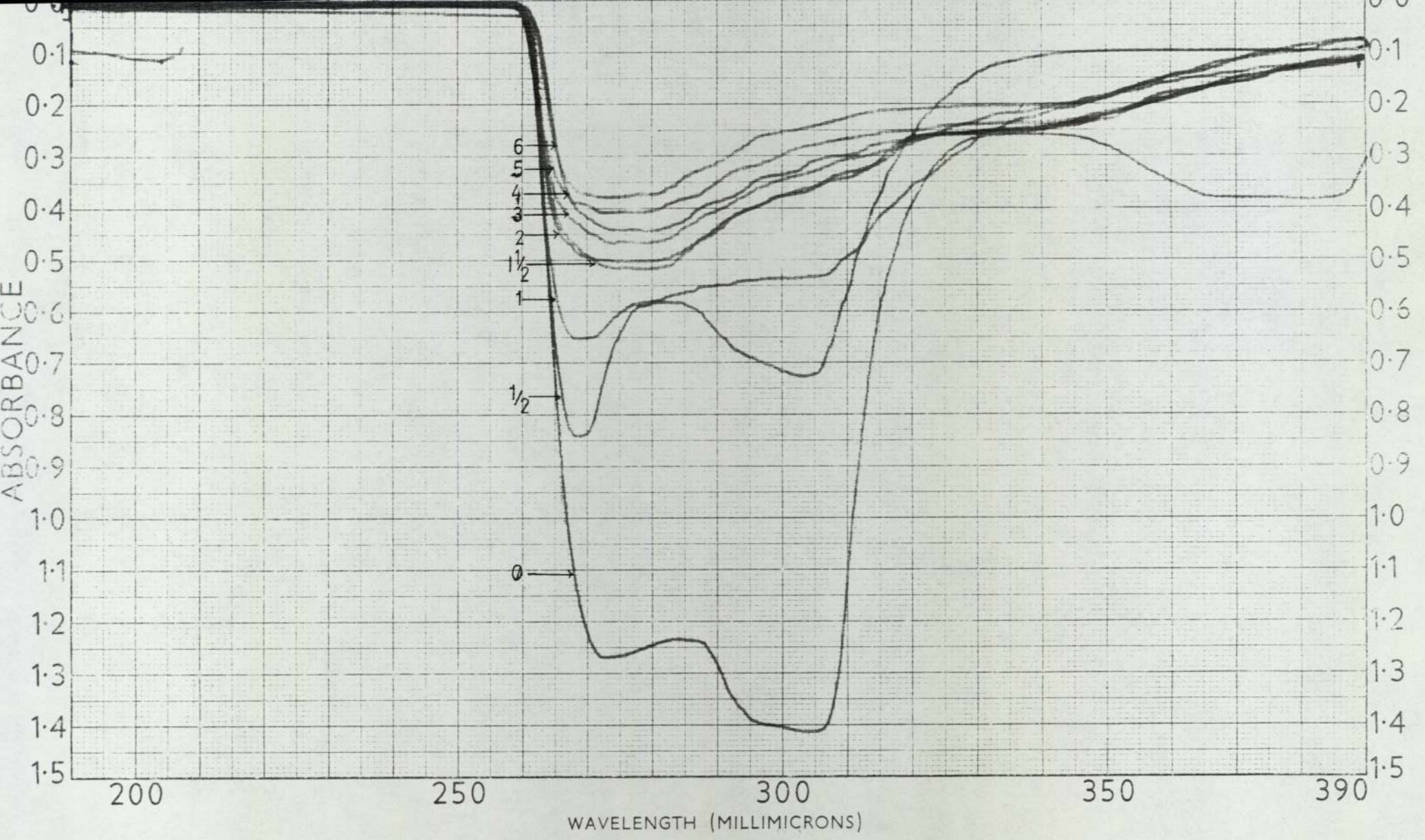

Figure (5.3.11b) Ultra-violet spectra of 0.003% $Ni(OX)_2$ in carbon tetrachloride, when exposed to UV (numbers denote the time of exposure.)

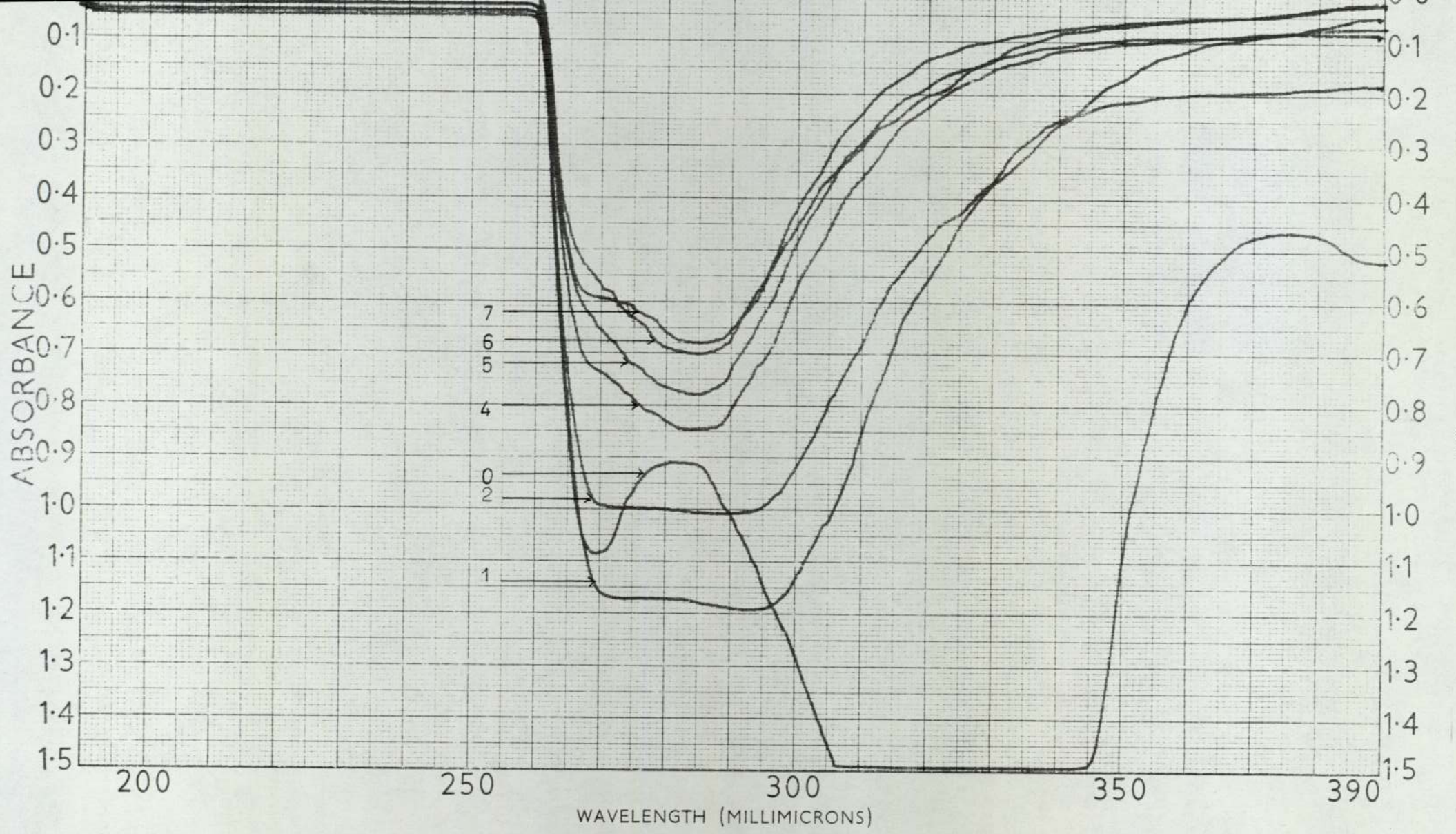

Figure (5.3.11c) Ultra-violet spectra of 0.003% $Ni(DBDC)_2$ in carbon tetrachloride, when exposed t to UV. (numbers denote the time of exposure.)

To find out the effect of carbonyl compounds and singlet oxygen on the stability of these compounds the following experiments were carried out. 0.003% of $Ni(OX)_2$ in carbon tetra chloride was exposed with 0.005% BP in carbon tetra chloride. Ultra-violet spectra of the solutions were scanned before it was exposed to ultra-violet radiation and after exposure in an atmosphere of oxygen. Also the two solutions were exposed individually under oxygen for identical periods of time and were mixed just before scanning a spectrum, this is shown in (5.3.14a) and (5.3.14b).

Identical changes in the absorptions were observed in both cases at half an hour, one and a half hours and 24 hours, showing that the presence of BP in the system has no effect on the stability of $Ni(OX)_2$. The same sort of spectral changes were observed when the experiments were repeated in an atmosphere of nitrogen, figure (5.3.15). If this quenching of triplet carbonyl by $Ni(OX)_2$ is an important mechanism in the stabilisation process (Chapter I), the acceptance of energy by $Ni(OX)_2$ would be observed in the ultra-violet spectrum. However the above results shows no such change. Furthermore the instability of these complexes themselves to ultra-violet light confirms the inadequacy of such a theory to explain the stabilising activity of the metal complexes. Furthermore the identical changes in spectra obtained when the above experiment was carried out in oxygen, shows that the role played by singlet oxygen too is not important as far as the stability of the complex and hence its stabilising activity is concerned.

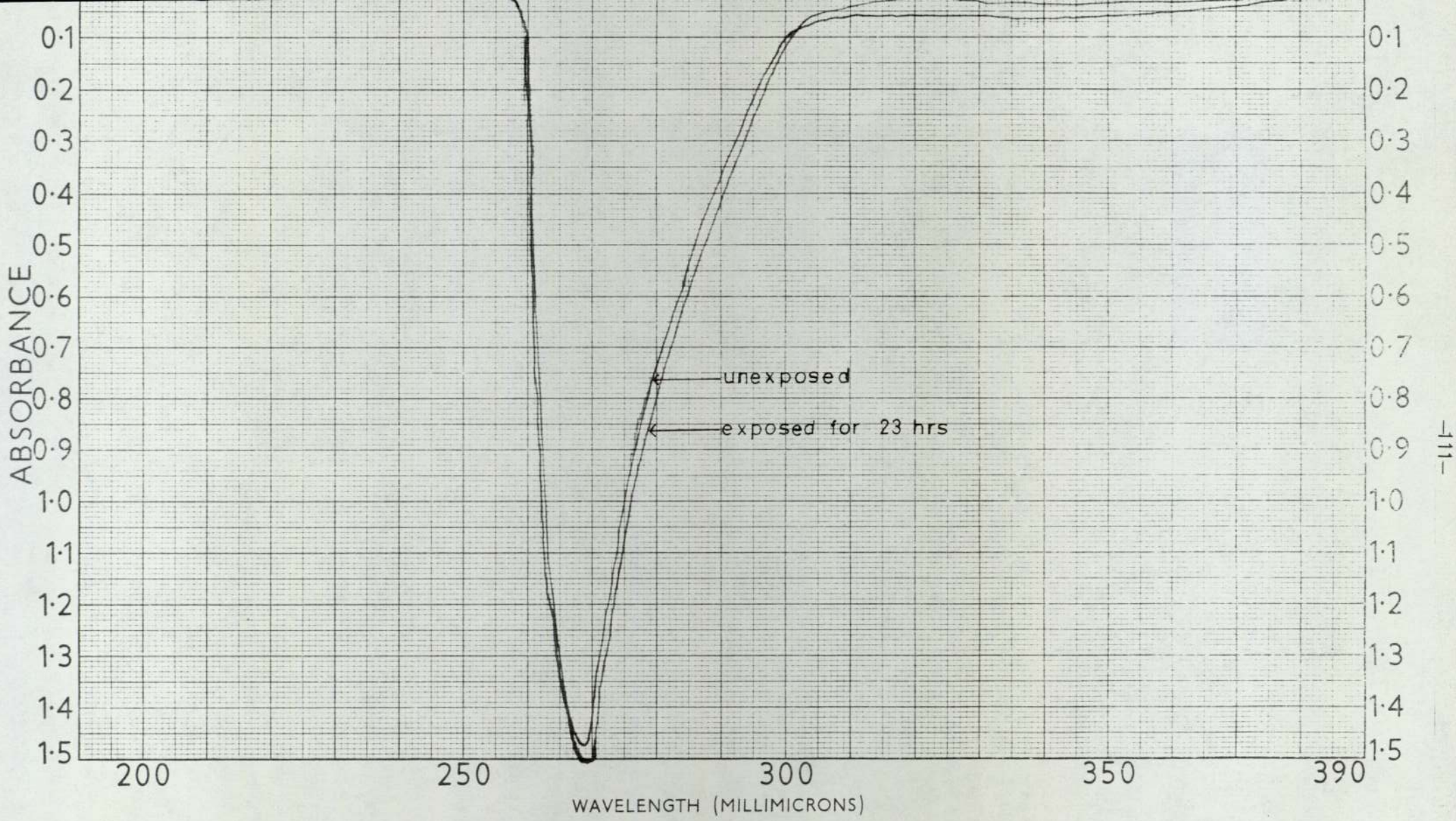

Figure (5.3.12) Ultra-violet spectrum of BP when exposed to UV light.

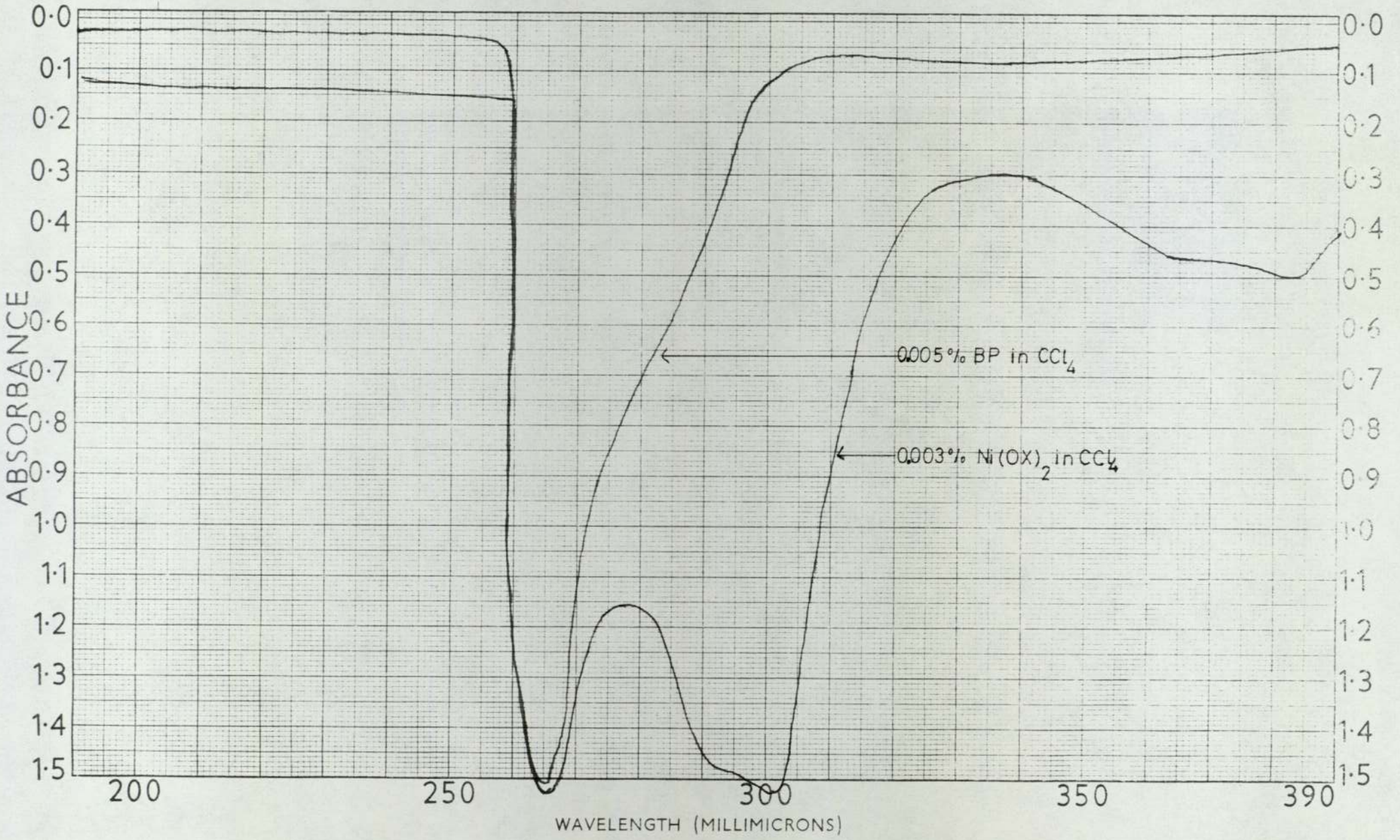

Figure (5.3.13) Ultra-violet spectra of BP and $NI(OX)_2$

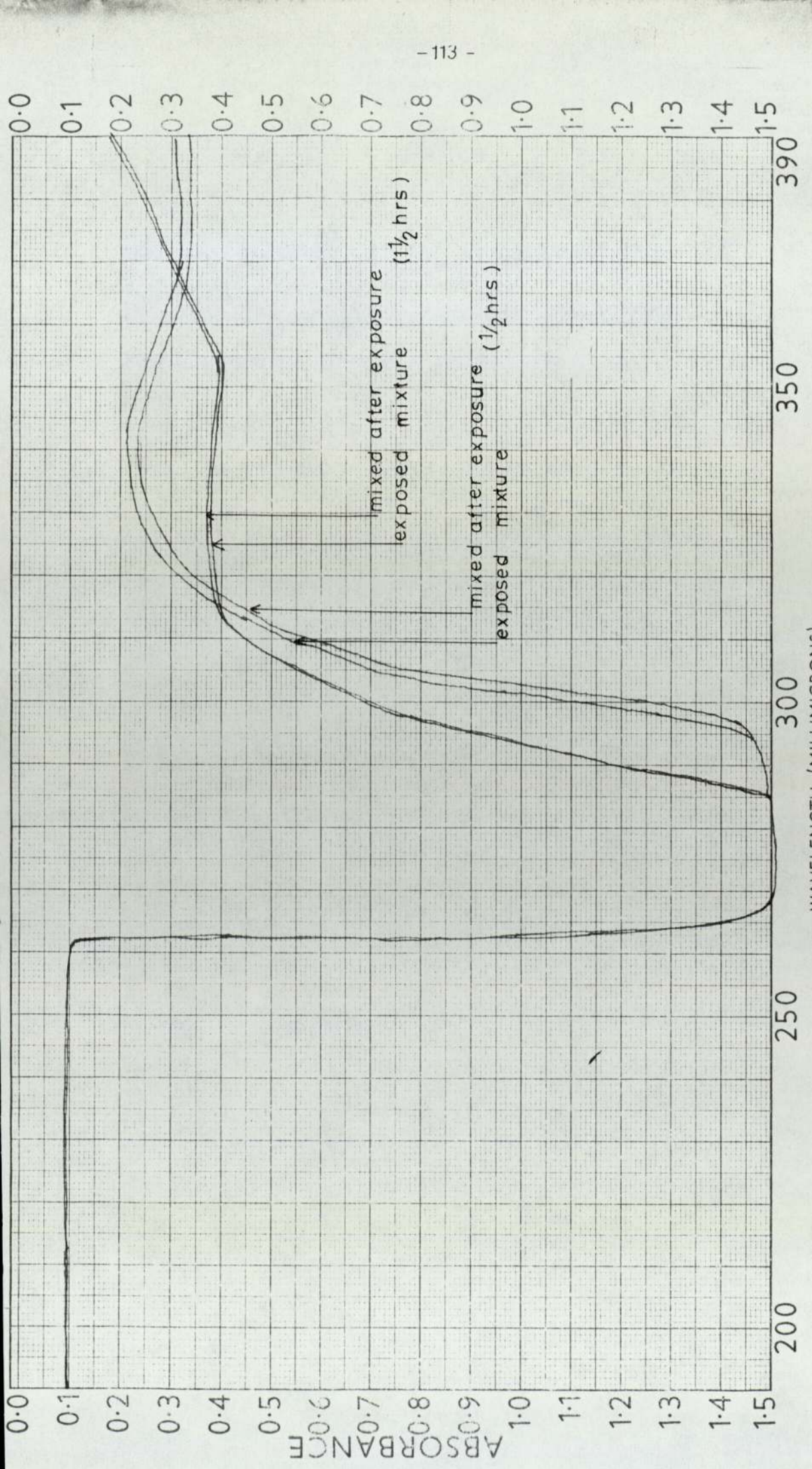

Figure (5.3,14a) Ultra-violet spectra of 0.005% BP and 0.003 $Ni(OX)_2$ in CCl_4, when exposed to UV light in the presence of oxygen.

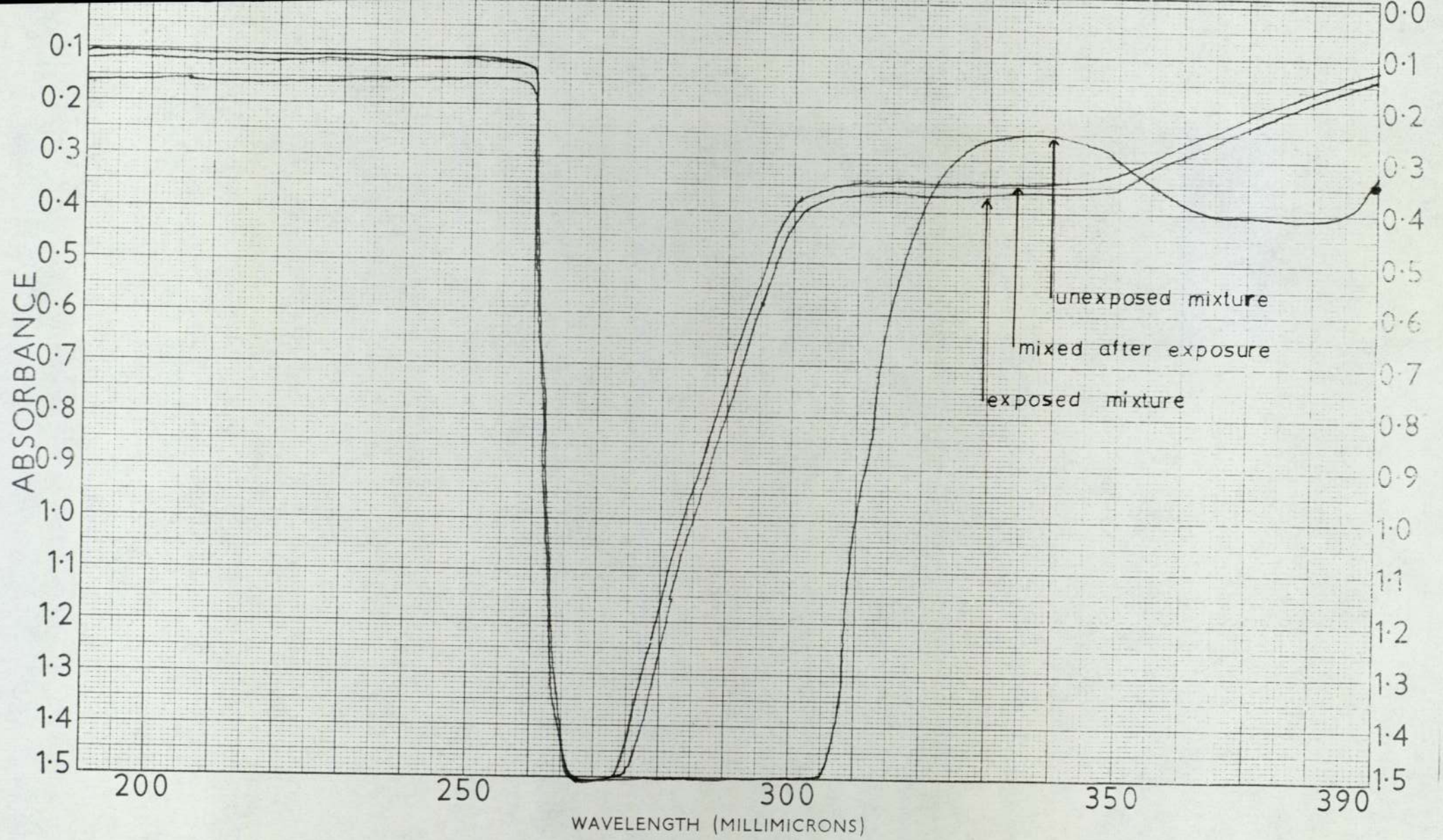

Figure (5.3.14b) Ultra-violet spetra of 0.005% BP and 0.003% $Ni(OX)_2$ in CCl_4, when exposed to UV light in the presence of oxygen for 21.4 hours.

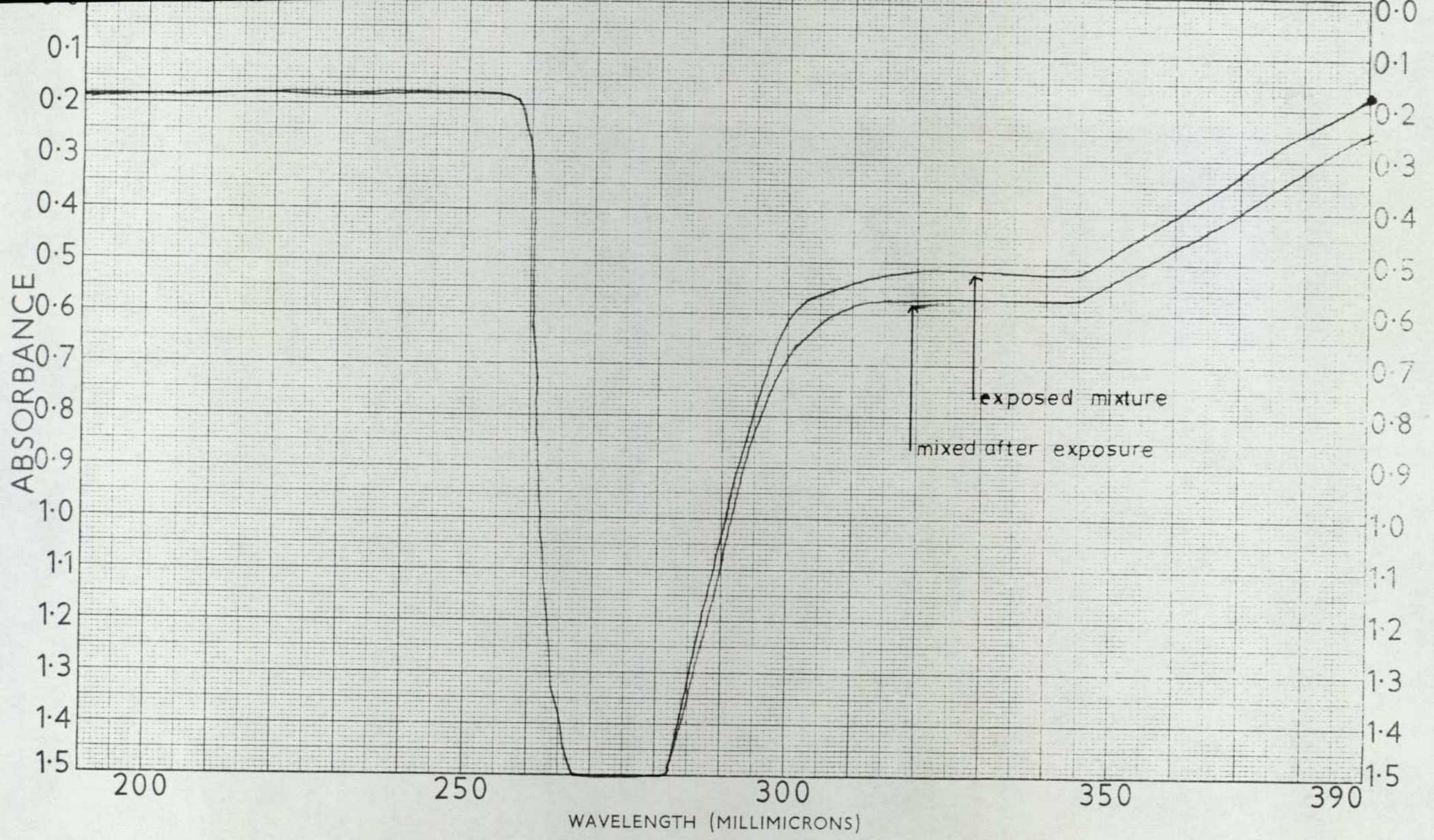

Figure (5.3.15) Ultra-violet spectra of 0.005% BF and 0.003% Ni(OX)2 in CCl4, when exposed to UV light under Nitrogen for 21.5 hours.

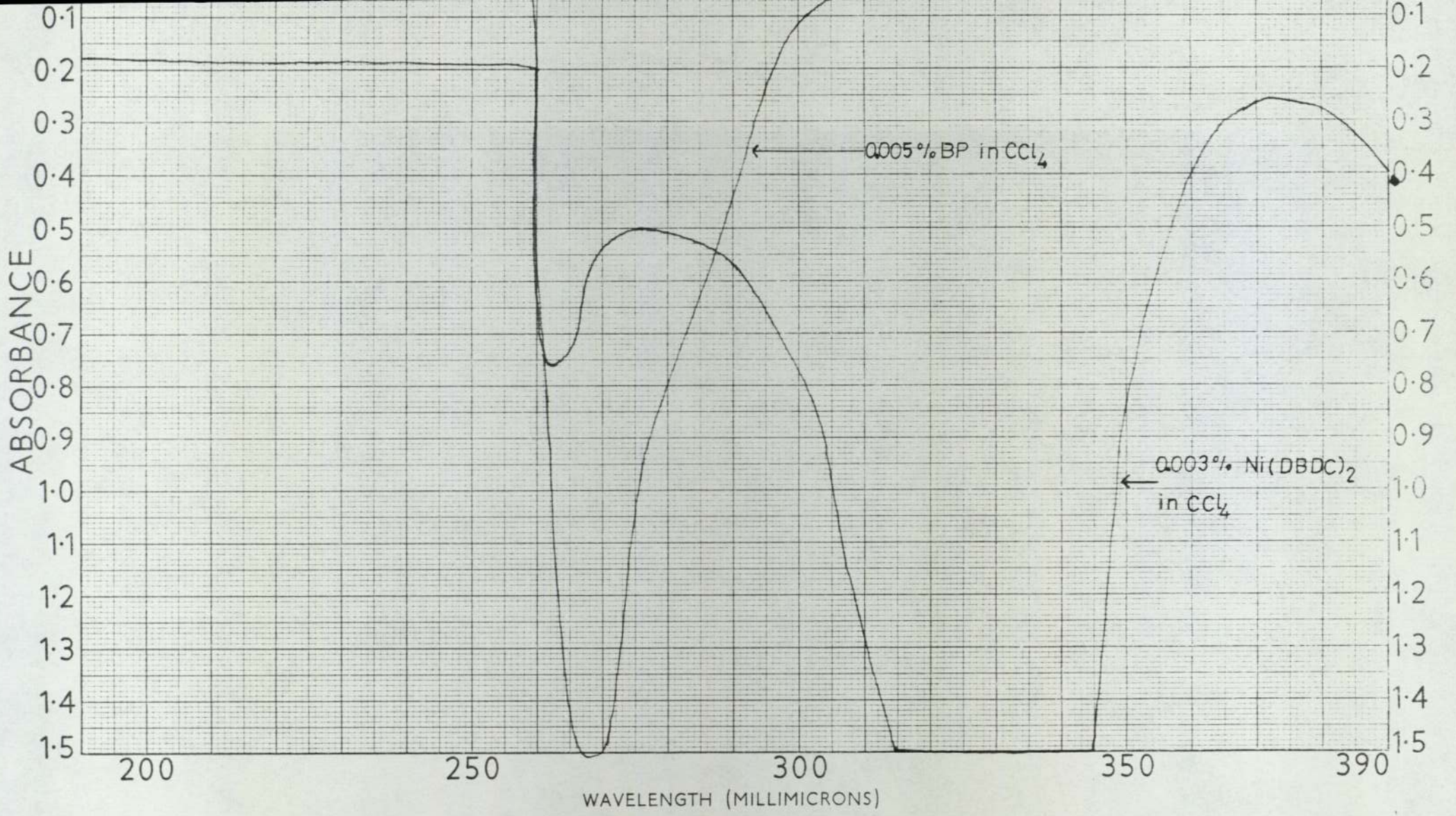

Figure (5.3.16) Ultra-violet spectra of BP and $Ni(DBDC)_2$ in CCl_4

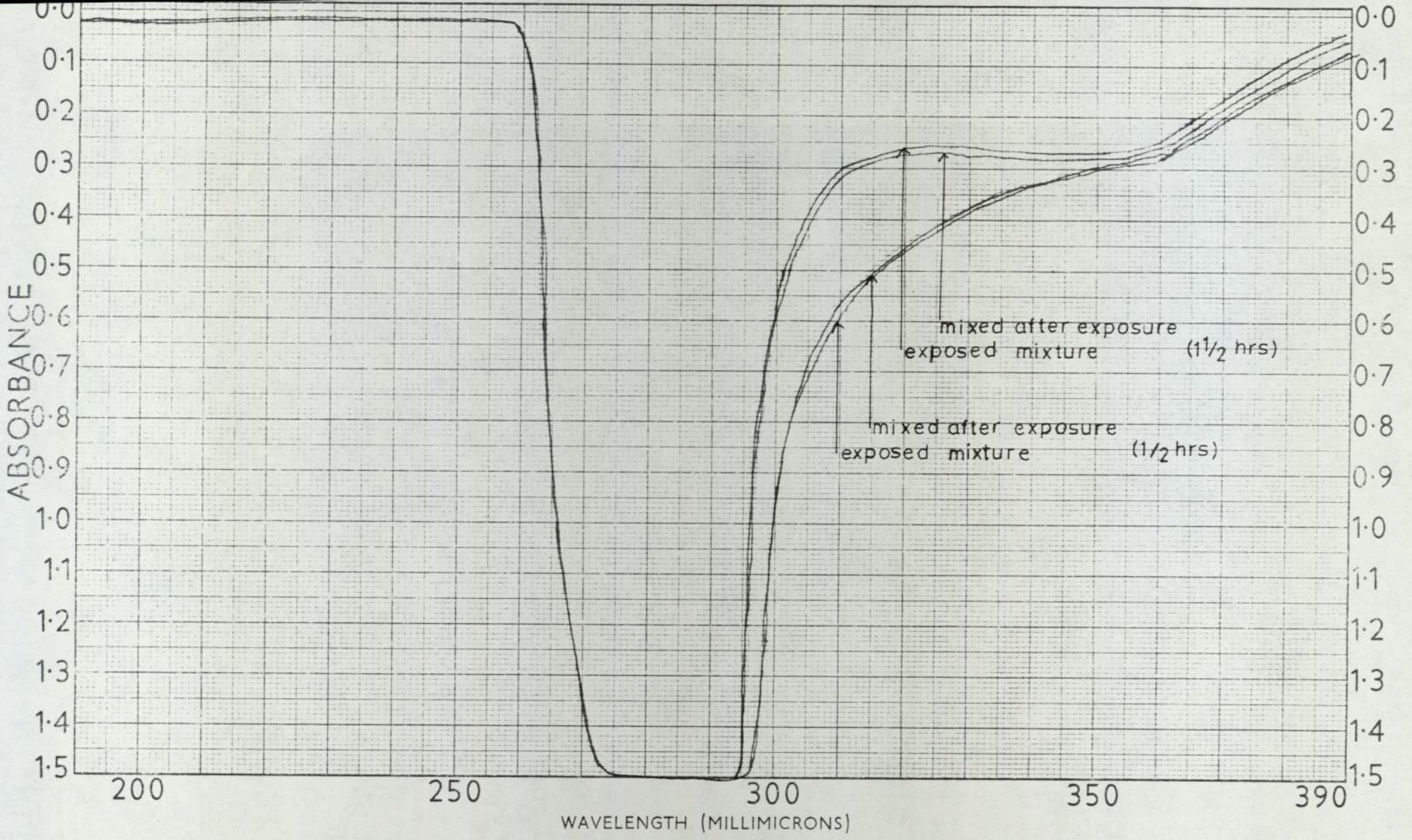

Figure (5.3.17) Ultra-violet spectra of 0.005% BP and 0.003% Ni(DBDC)2 in CCl_4, when exposed to UV light in the presence of oxygen.

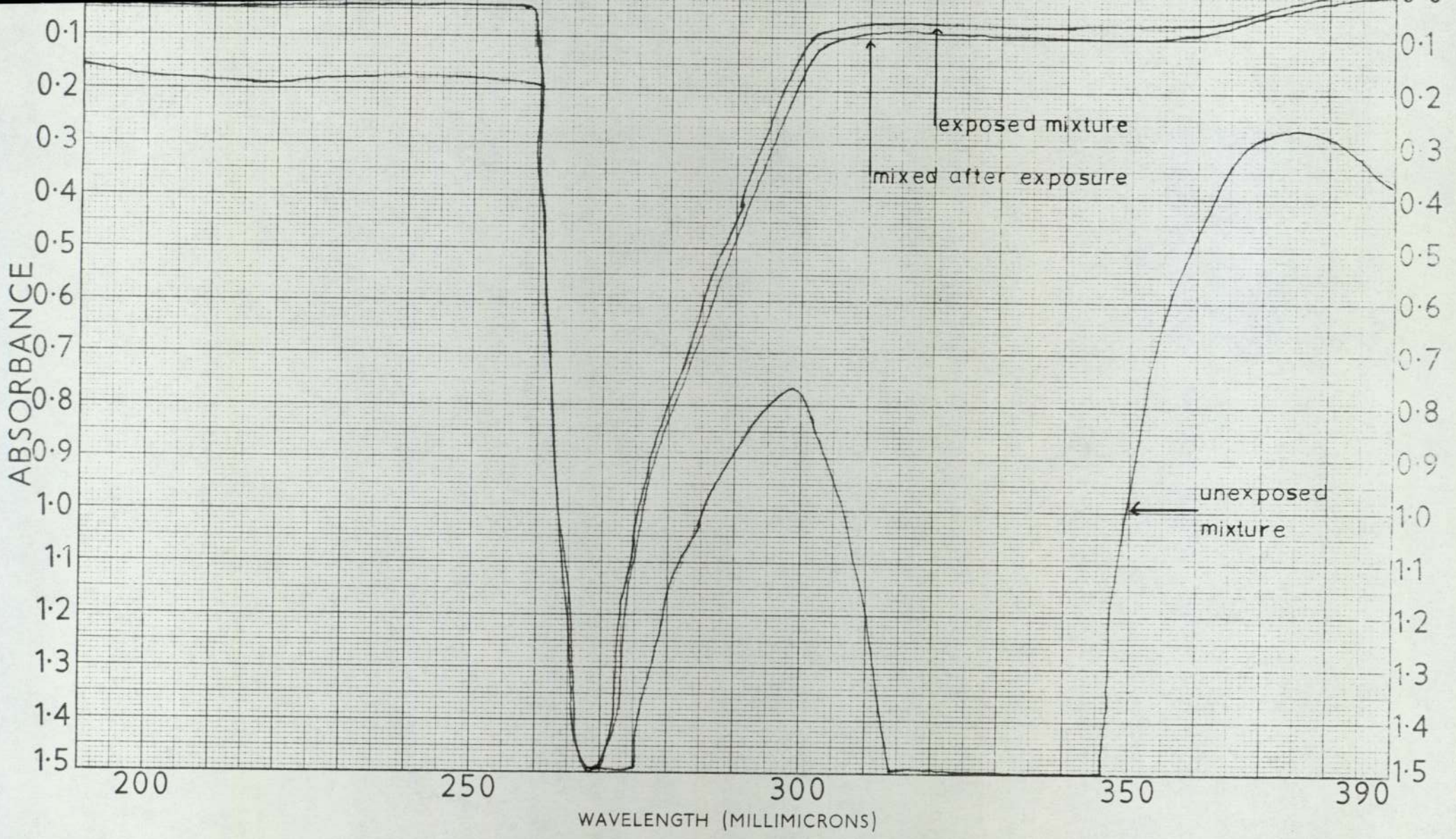

Figure (5.3.18) Ultra-violet spectra of 0.005% BF and 0.003% $Ni(DBDC)_2$ in CCl_4, when exposed to UV light in the presence of oxygen for 21.5 hours.

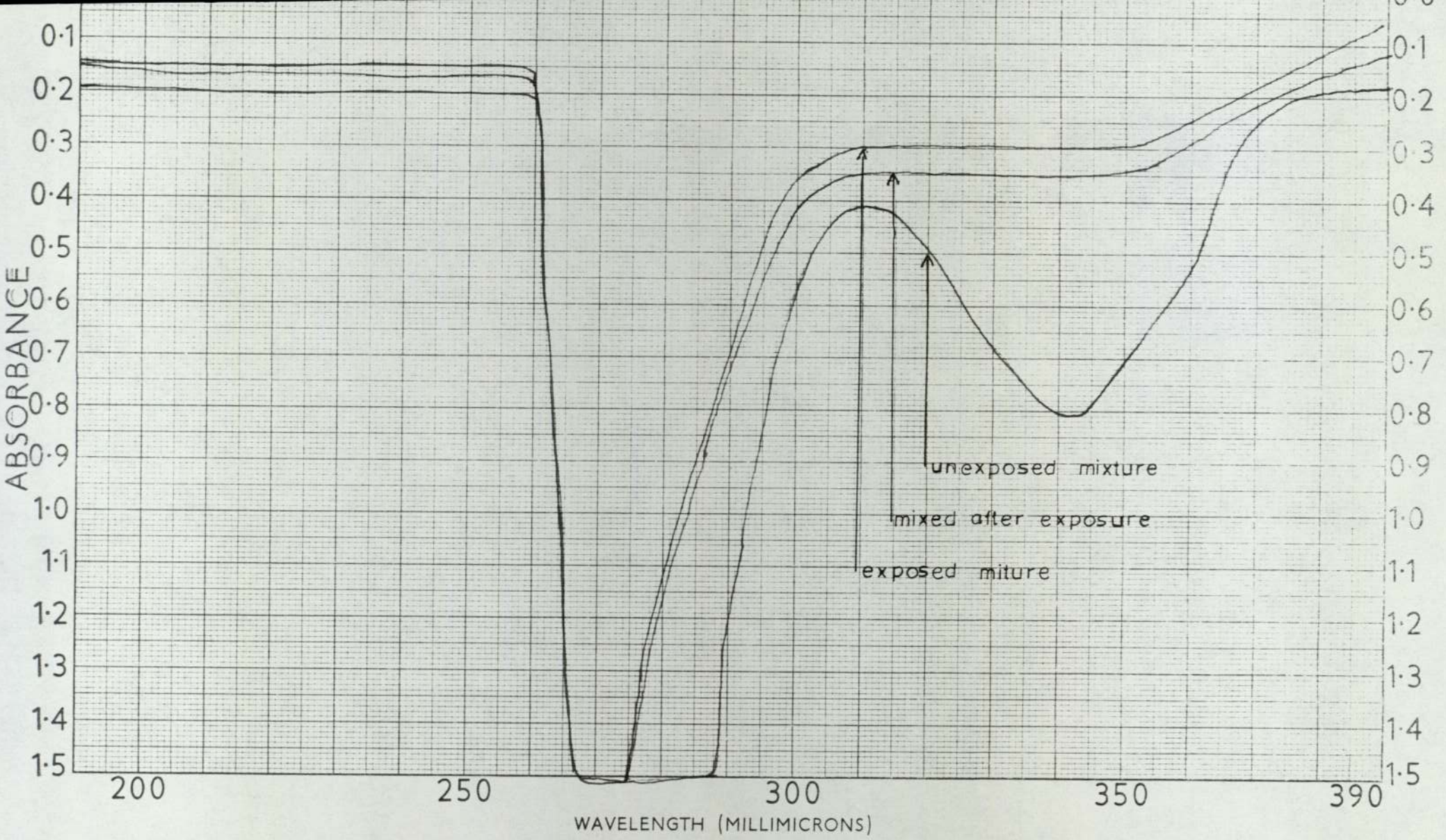

Figure (5.3.19a) Ultra-violet spectra of 0.005% BF and 0.003% $Cu(OX)_2$ in CCl_4, when exposed to UV light in the presence of oxygen for 23 hours.

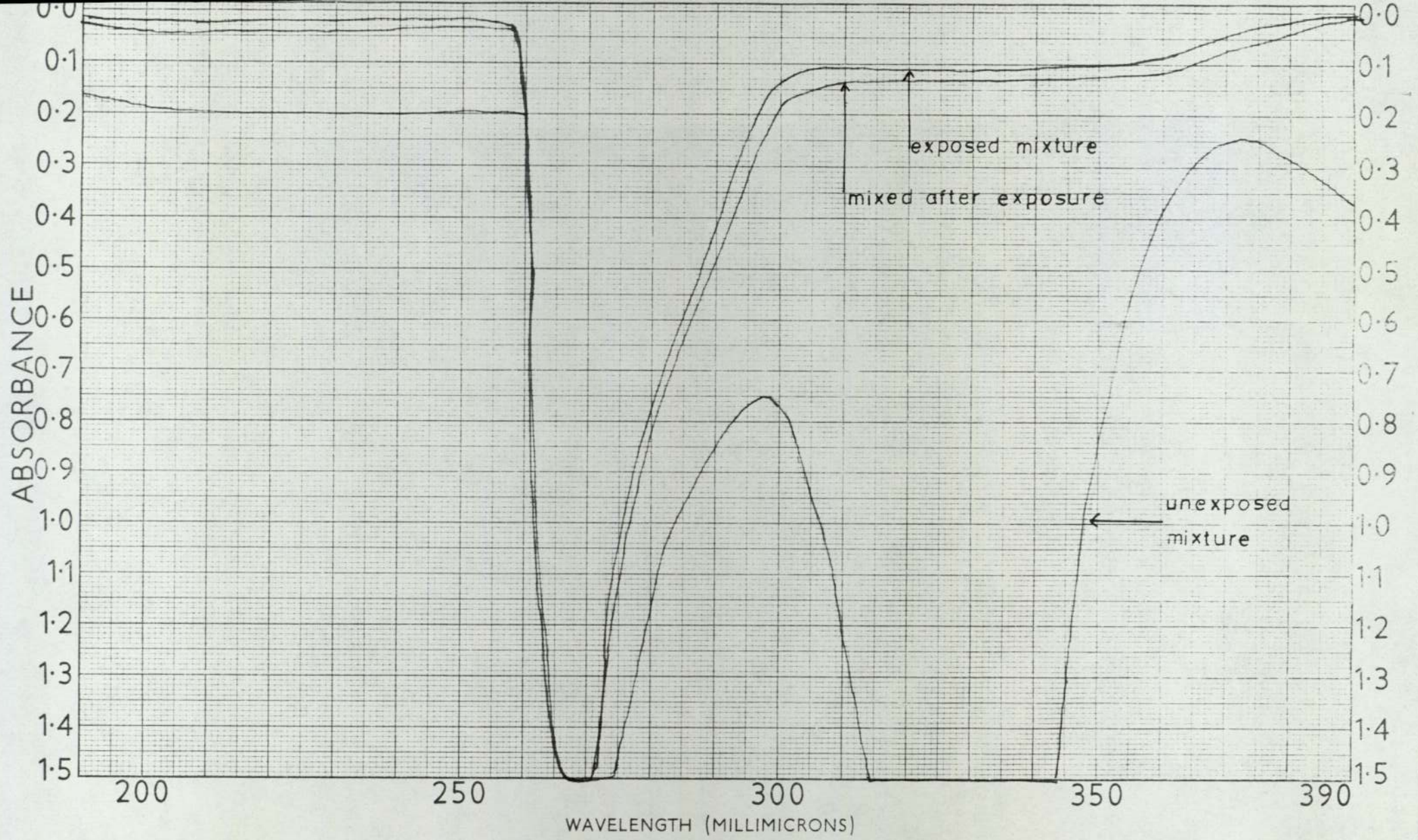

Figure (5.3.18b) Ultra-violet spectra Of 0.005 BF and 0.003 $Ni(DBDC)_2$ in CCl_4, when exposed to UV light in the presence of Nitrogen for 21.5 hours.

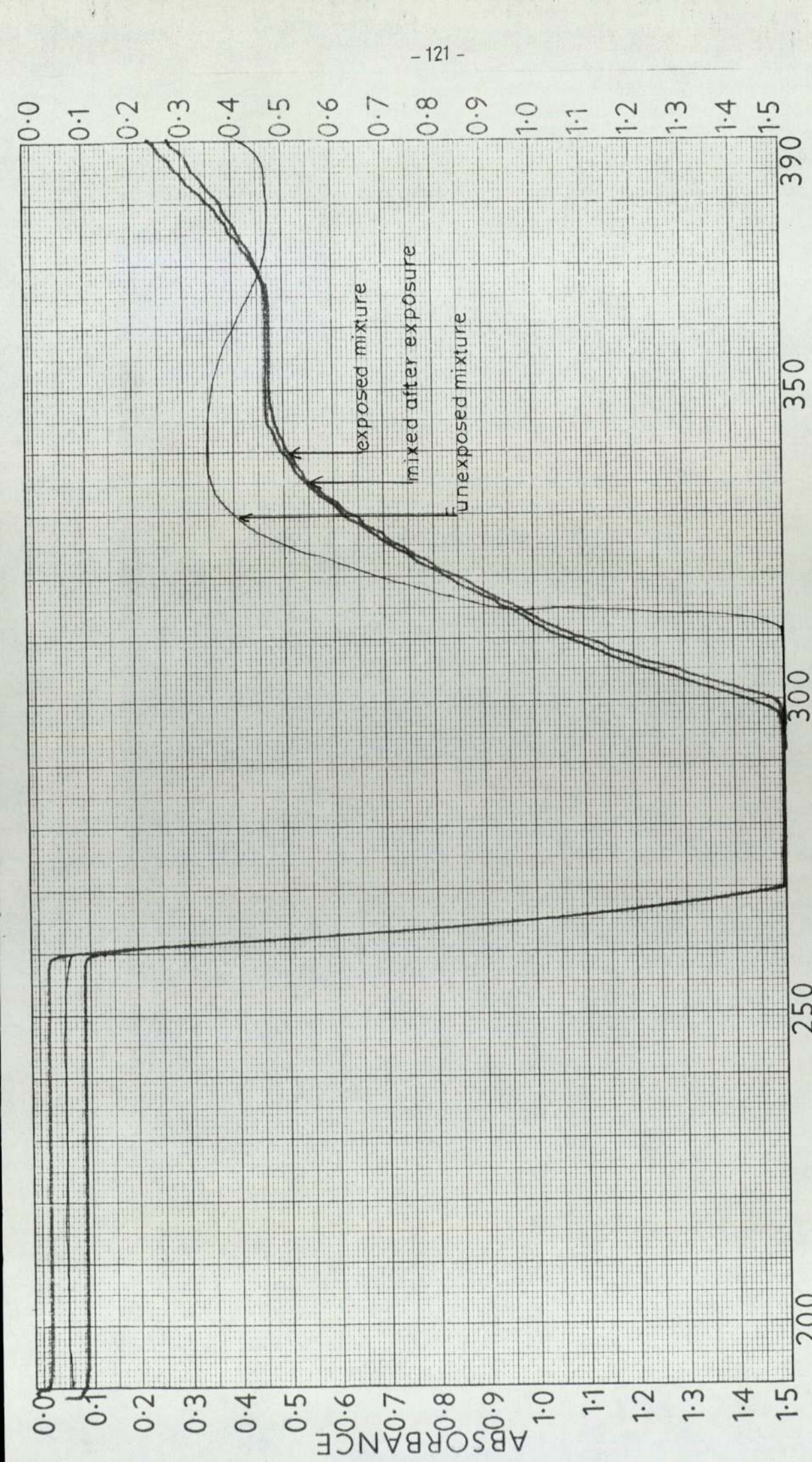

Figure (5. 3.20) Ultra-violet spectra of 0.5% BMK and 0.003% $Ni(OX)_2$ in CCl_4, when exposed to UV light in the presence of oxygen for 24 hours.

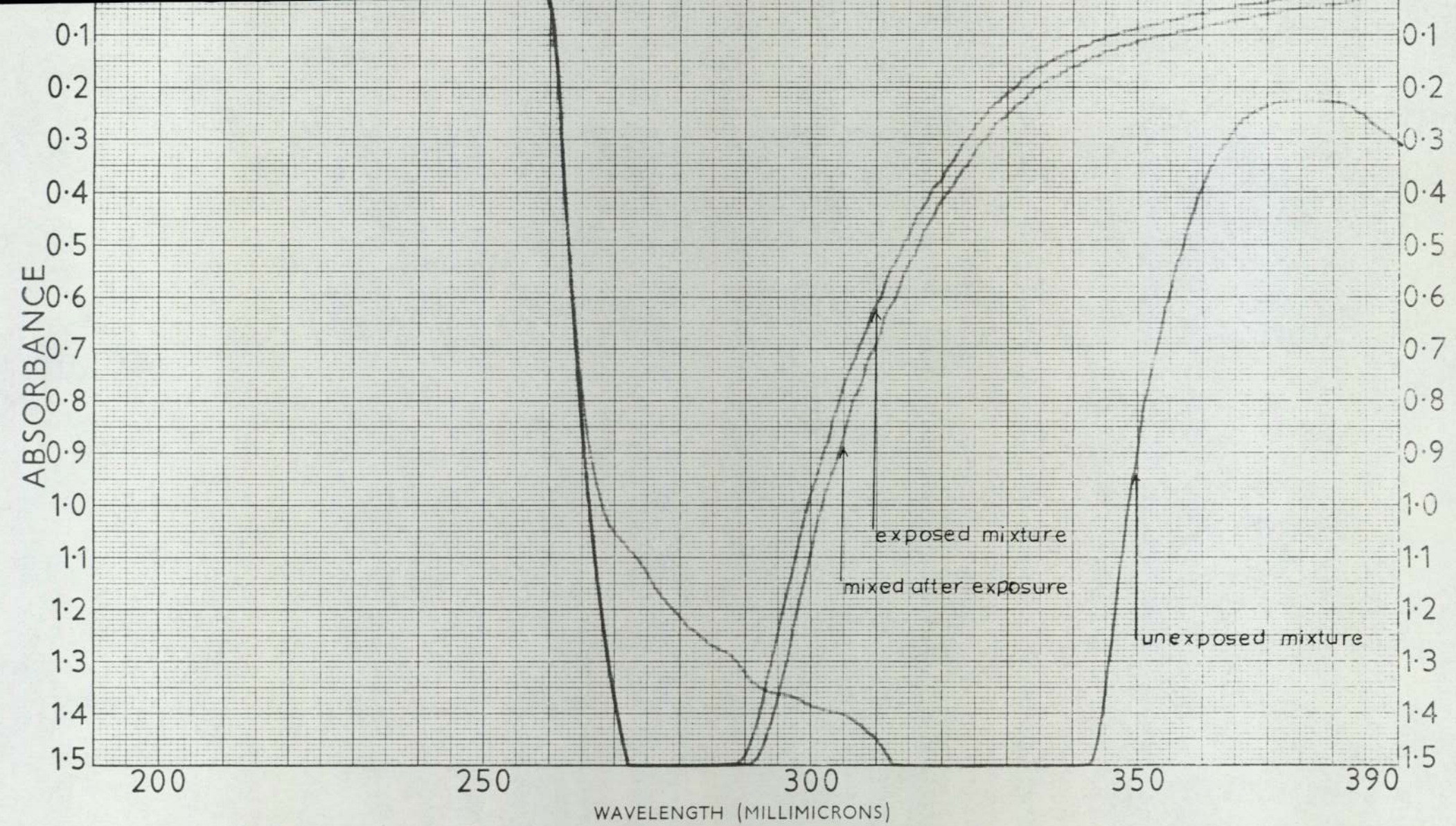

Figure (5.3.21) Ultra-violet spectra of 0.5% BNK and 0.003% $Ni(DBDC)_2$ in CCl_4, when exposed to UV light in the presence of oxygen for 22.3 hours.

Similar experiments were carried out with $Ni(DBDC)_2$ and $Cu(OX)_2$ in the presence of BP, oxygen and nitrogen. Figures (5.3.16) to (5.3.19). With both complexes the presence of the ketone or oxygen did not have any effect on their stability. Therefore they do not seem to quench either triplet carbonyl or singlet oxygen.

A similar experiment was carried out with BMK and $Ni(OX)_2$, and BMK and $Ni(DBDC)_2$. The spectrum obtained when the ketone and metal complex were exposed individually and mixed together was identical to the spectrum obtained of the mixture exposed for the same length of time. This was the same when the experiment was carried out under nitrogen or oxygen. Figures (5.3.20) and (5.3.21). A similar argument would lead to the same conclusions, that is the stability of $Ni(OX)_2$ is in no way effected by the ketone which could easily generate a triplet state when exposed to UV radiation. BMK having triplet energy higher than BP would more readily satisfy the requirements for quenching of triplet energy by $Ni(OX)_2$. (Chapter I). Also singlet oxygen if produced seems to have no effect on the stability of the complex.

If these metal complexes are successful in quenching the higher energy states of oxygen or carbonyl, then the metal complex itself will be raised to a higher energy state, which could relax back to its ground state by a number of different routes, namely by the emission of a photon of light (fluorescence), transforming the excitation into vibrational energy (internal conversion) or another alternative by chang[109] the spin of one of the electrons in the half filled orbitals and thereby become a

triplet state (inter system crossing). All these will be photophysical processes and hence photophysical quenching will be involved. However, if the excited quencher undergoes a chemical reaction,then the process will be chemical quenching.

Since these complexes change when exposed to UV, then there is no possibility for physical quenching to take place. The fact that the rate of decomposition of these complexes are the same in the presence of BP or oxygen seems to eliminate any possibility of photochemical quenching.

Figures (5.3.22) and (5.3.23) show the results from similar experiments with $Fe(OX)_3$ and BP. Here the stability of the iron oxime complex seems to be decreased by the presence of BP in the systems. This evidently supports the results shown in the previous chapter where $Fe(OX)_3$ is shown to act as a proxidant when BP was used as an initiator. This would mean that this complex is capable of producing radicals by photolysis which could act as initiators of oxidation. Singlet oxygen however does not seem to have a marked effect on the already unstable complex.

In a similar experiment with $Fe(OX)_3$ and BMK a difference in the spectrum of the $Fe(OX)_3$ complex was again observed. Figure (5,3.24) the difference here is not as marked as was with BP.

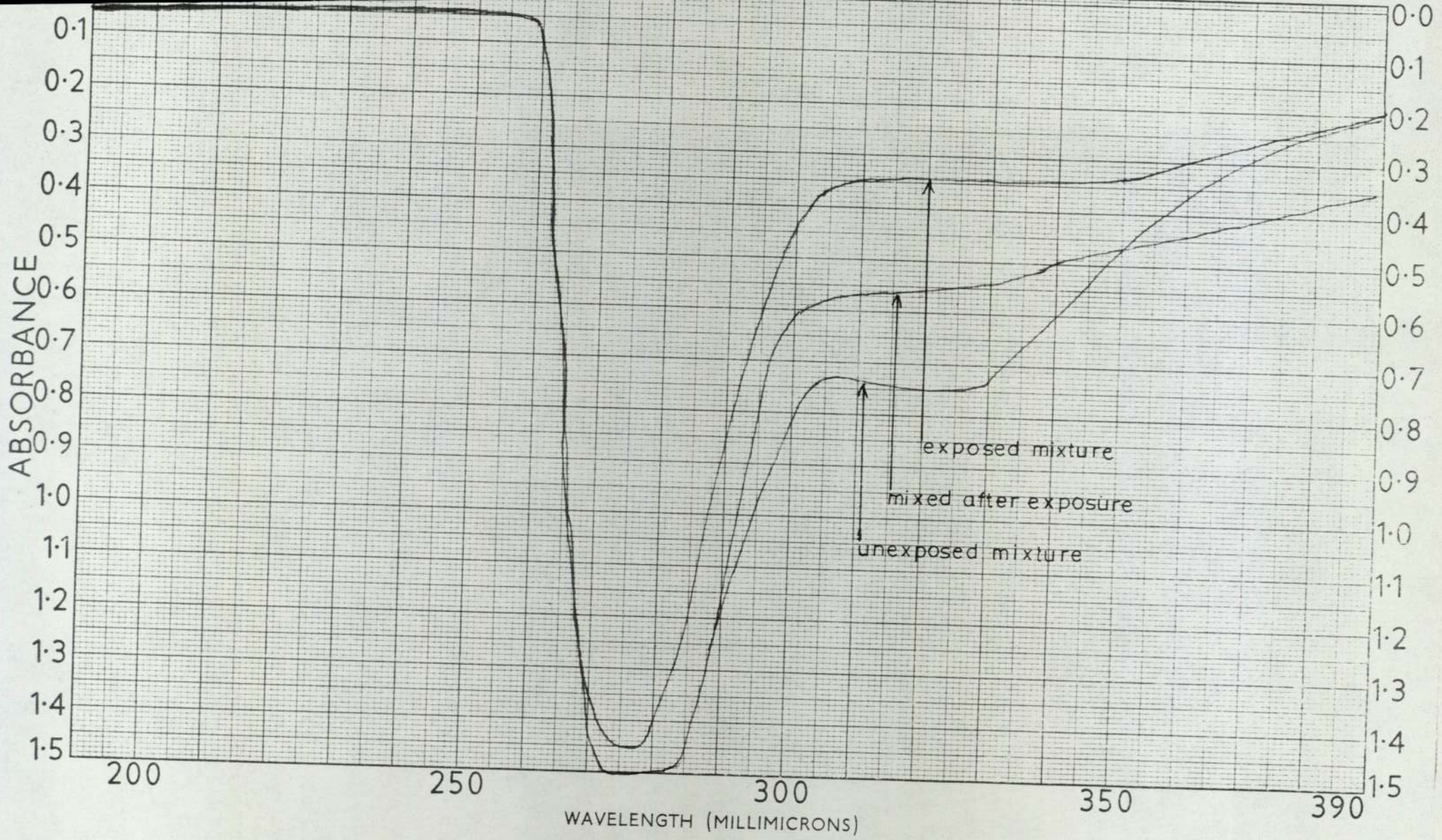

Figure (5.3.22) Ultra-violet spectra of 0.005% BP and 0.003% $Fe(OX)_3$ in CCl_4 , when exposed to UV light in the presence of oxygen for 5½ hours,

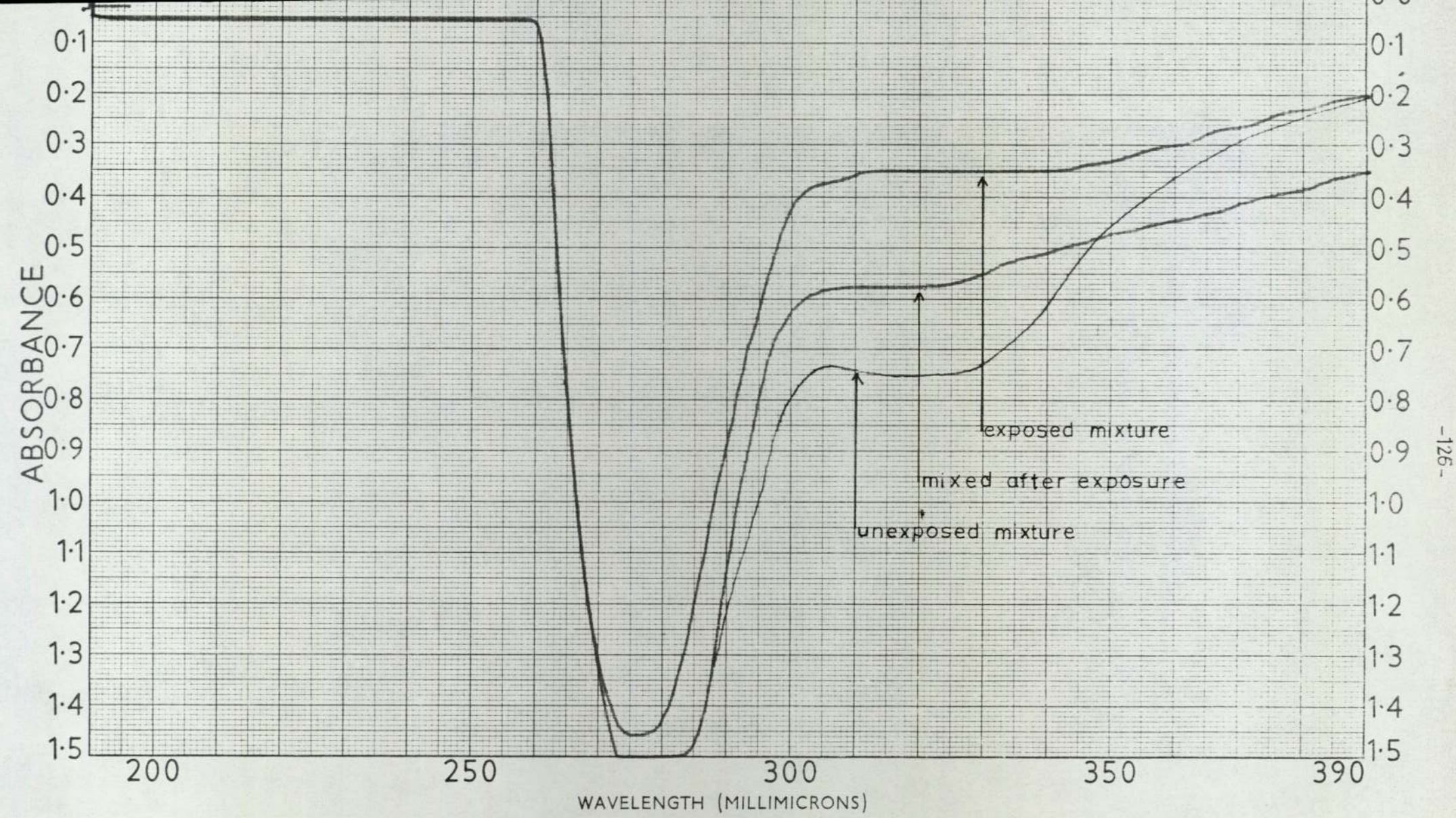

Figure (5.3.23) Ultra-violet spectra of 0.005% BP and 0.003% $Fe(OX)_3$ in CCl_4, when exposed to UV light in the presence of Nitrogen for $5\frac{1}{2}$ hours.

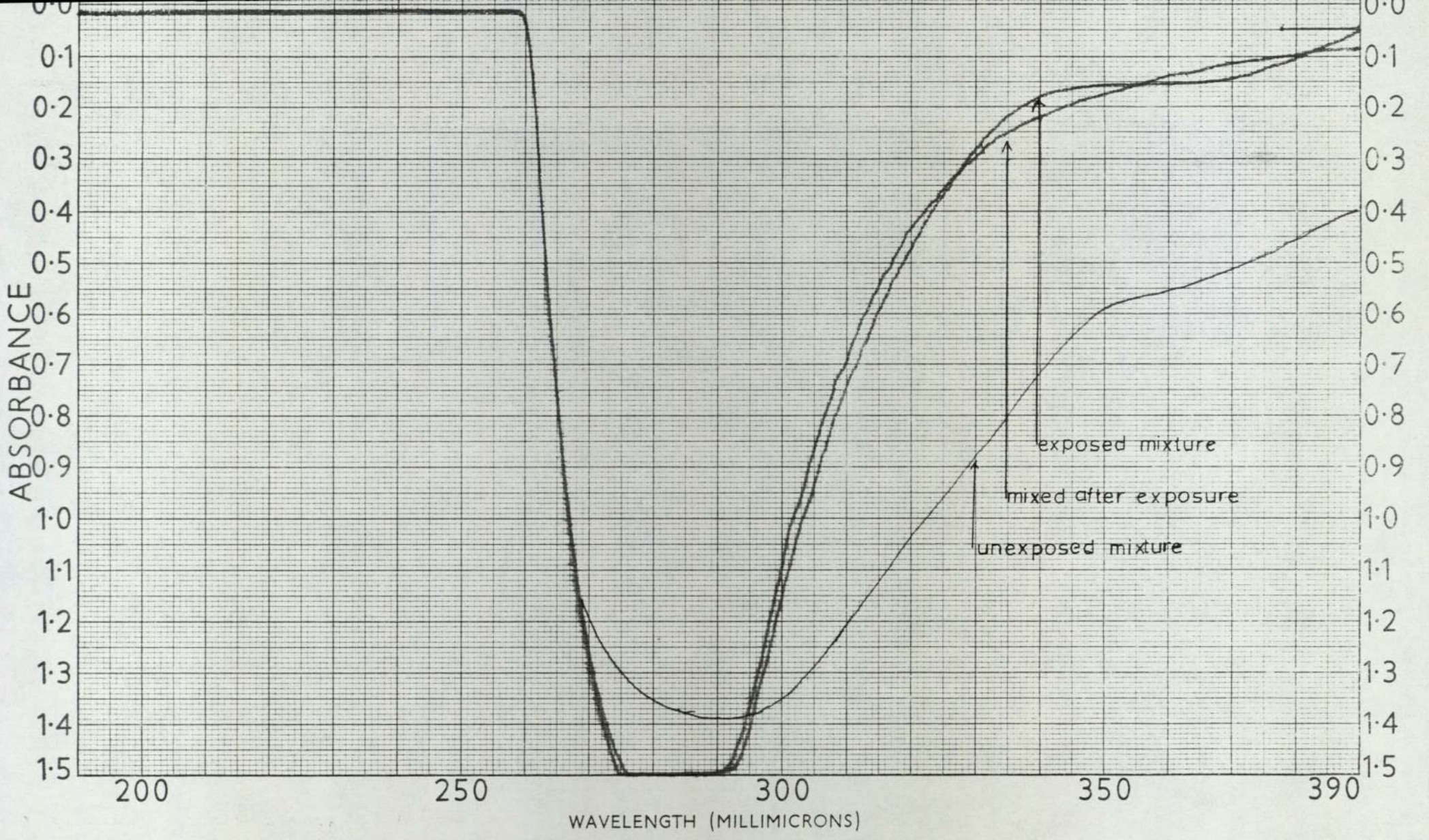

Figure (5.3.24) Ultra-violet spectra of 0.5% BMK and 0.003% $Fe(OX)_3$ in CCl_4, when exposed to UV light in the presence of oxygen for 18½ hours.

CHAPTER 6

REACTIONS OF METAL COMPLEXES WITH HYDROPEROXIDES

The results of oxygen absorption studies shown in Chapter four suggests that the stabilising activity of $Ni(DBDC)_2$ and $Ni(OX)_2$ is partly due to an interaction of these metal chelates with the hydroperoxides as well as screening, rather than by a quenching mechanism. In this chapter the reaction of these metal complexes are examined kinetically and by subsequent product analysis some of the kinetic parameters are determined.

6.1.1 Reactions of $Ni(OX)_2$ with hydroperoxides

100 ml of a solution containing 10^{-2}M%* CHP and 10^{-2}M%* $Ni(OX)_2$ in carbon tetra chloride was exposed to ultra-violet light in a three necked round bottom flask made out of quartz, figure (3.2.5). 4 ml solution of this was removed at regular one hour intervals and was analysed by Infra-red spectroscopy, (IR) thin layer chromatography (TLC) and gas liquid chromatography (GLC).

IR spectra were obtained with a Perkin Elmer 457 spectrophotometer. For TLC plastic sheets precoated with a layer of 0.25 mm thick silica gel were used. The samples taken out at regular intervals of time were run on the plates using the solvent system benzene, methyl ethyl ketone, water and formic acid, in the ratio of 900:100:94:4. This is the best solvent system for the phenolic products present in this reaction mixture[77].

* moles in 100 gms of solution.

Figure (6.1.1) Changes in the IR spectrum of a 1:1 mixture of CHP and $Ni(OX)_2$ when exposed to ultra-violet light. temperature 29±1.°c

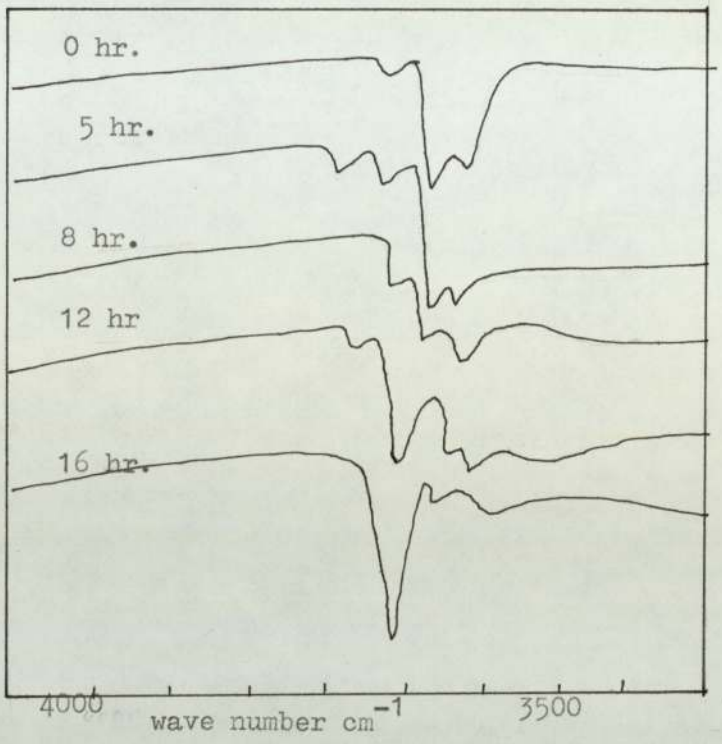

Figure (6.1.4) Changes in the IR spectrum of a 1:1 mixture of CHP and $Ni(OX)_2$ when exposed to UV light at 75±1°C

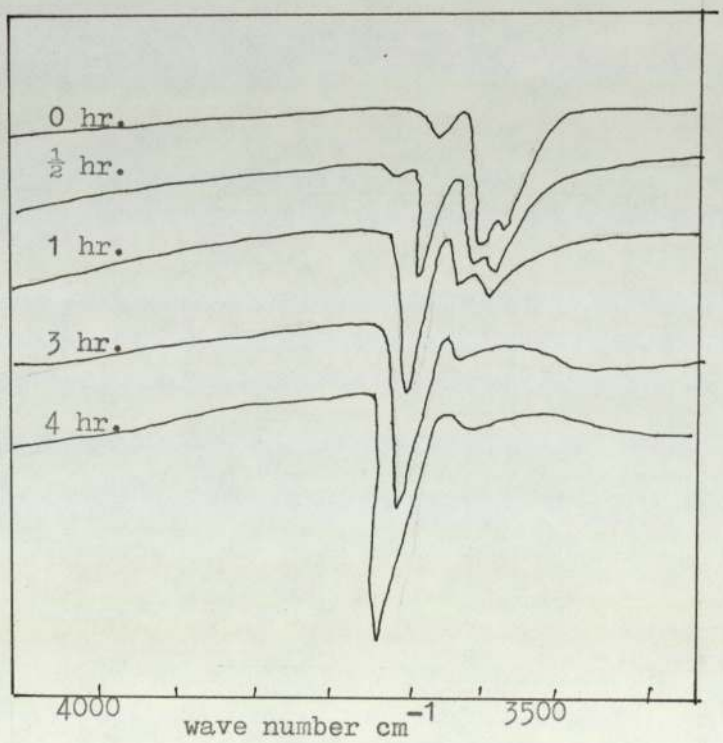

The plate was dried by blowing hot air and was sprayed with 5% Ferric chloride solution to identify the phenolic products present in the mixture.

To separate the carbonyl compounds by TLC 50% benzene in water was used. This was sprayed with 0.4% 2-4-dinitrophenyl hydrazine in 2N hydrochloric acid. The OXO compounds were revealed as intense yellow spots on a light yellow background.

The volatile products formed during the reaction were trapped by cooling in a mixture of dry ice in acetone and the resulting solution was analysed by mass spectra.

6.1.2 Results and Discussion

When a mixture of 10^{-2}M% CHP and 10^{-2}M% $Ni(OX)_2$ in carbon tetra-chloride were exposed to UV radiation, an IR spectrum of the mixture showed a gradual decrease in the intensity of the bands at 3520 cm^{-1} and 3550 cm^{-1} due to the O-H stretching of the hydroperoxide[78] followed by a gradual increase in intensity of the band at 3605 cm^{-1} due to cumyl alcohol[79], figure (6.1.1)

The phenolic products of the samples taken out at regular intervals were separated by TLC. This showed the presence of three different phenolic compounds in addition to the spots due to the original $Ni(OX)_2$ complex. These were identified by comparing with the rf values obtained with authentic samples and were found to be due to ortho-hydroxy aceto-phenone oxime (faint spots), O-hydroxy acetophenone and salicylic acid.

Ortho-hydroxy-acetophone oxime and ortho-hydroxy-acetophone appeared after the second hour of exposure to ultra-violet radiation. Figure (6.1.2), whereas the spots due to salicylic acid appeared after the solution had been exposed to UV light for three hours. These spots became more intense with time, while the spots due to o-hydroxy-acetophenone oxime and ortho-hydroxy acetophone first intensified until up to about five hours of exposure to UV light, and then decreased until the solution had been exposed for ten hours after which they disappeared completely. An approximate plot of these intensities with time is shown in figure (6.1.2).

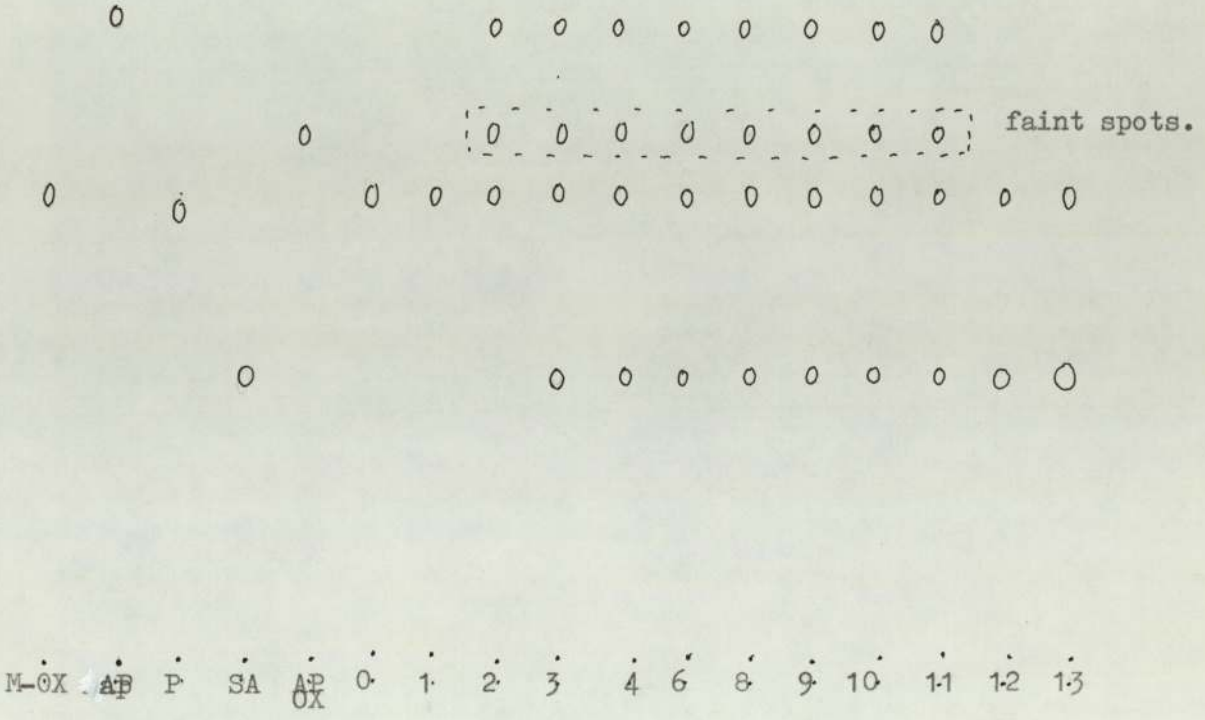

Figure (6.1.2)

TLC separation of a 1:1 mixture of CHP and $Ni(OX)_2$ when exposed to UV light, at 29±1°C. The numbers denote the time of exposure in hours.

M - OX = Nickel oxime complex

A - P = Orthohydroxy acetophenone

P = Phenol

SA = Salicylic acid

AP - OX= Ortho hydroxy acetophenone oxime.

A similar TLC separation with 50% benzene in water was used to identify the carbonyl compounds. Intense spots due to o-hydroxy acetophenone were identified in the samples from two to ten.

A separation of the soluble products by GLC confirmed the presence of cumyl alcohol and a small amount of acetophenone. In addition to this a considerable amount of an unknown compound was observed. Later on this was identified as methyl cumyl ether. Synthesis of methyl cumyl ether and a subsequent GLC separation helped to confirm this. The percentages are 88.81% cumyl alcohol, 6.52% acetophenone and 4.66% methyl cumyl ether.

A similar experiment was carried out with the same molar ratios at 75°C and exposed to UV radiation, the reaction was fast, all the products of oxidation of $Ni(OX)_2$ were observed in the fraction taken out in the first half hour. In addition to this traces of phenol were observed in the samples removed in the first two hours. The TLC analysis is shown in figure (6.1.3.)

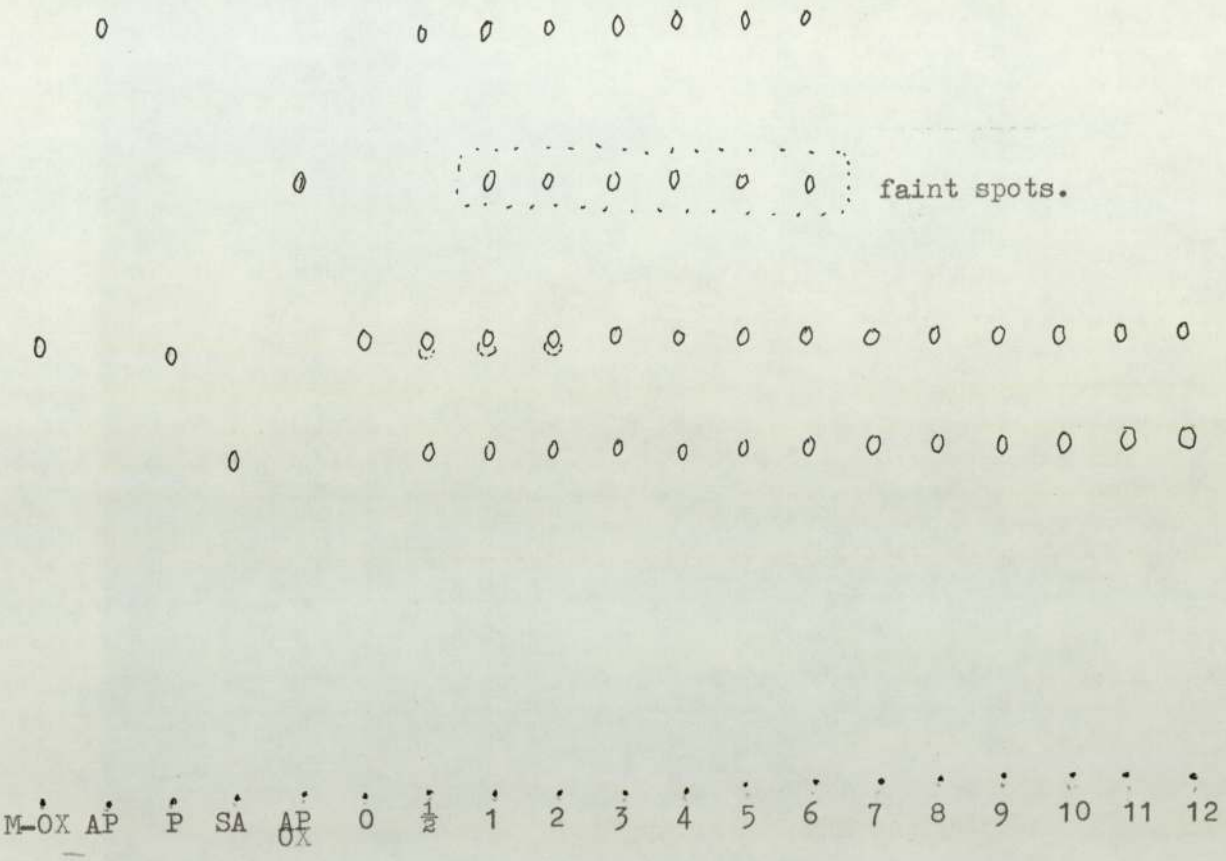

TLC separation of a 1:1 mixture of CHP and $Ni(OX)_2$ when exposed to UV radiation at (75°±1°C). Numbers denote the time of exposure in hours.

Figure (6.1.3.)

A separation of the soluble products by GLC gave 62.15% cumyl alcohol, 4.23% acetophenone and 33.62% cumyl methyl ether. Since this ether is formed by the oxidation of $Ni(OX)_2$ by cumene hydroperoxide this would mean that the oxidation rate is greatly increased by increasing the temperature.

Figure (6.1.4) shows the IR spectra of these samples. The disappearance of the bands at 3520 cm^{-1} and 3550 cm^{-1} paralleled the appearance of a sharp band at 3605 cm^{-1}. These changes were much more rapid than in the previous experiment where the temperature was only 29±1°C.

A similar experiment was carried out at 76°C in the absence of light, with a solution containing the same molar ratios of CHP and $Ni(OX)_2$. The samples removed at regular one hour intervals were analysed by IR, TLC and GLC. The changes in the IR spectra were qualitatively the same as when exposed to UV light. The disappearance of the bands at 3520 cm^{-1} and 3550 cm^{-1} paralleled the appearance of a sharp band at 3605 cm^{-1}, which is due to the O-H sketching of cumyl alcohol. These changes were much faster than the changes in the IR spectra of the experiment carried out in the presence of UV light at 29±1°C and much slower than the changes observed when the experiment was carried out in the presence of UV light at (75±1°C).

The products identified by TLC were the same as before, and traces of phenol were observed in the samples reacted for one and two hours. Figure (6.1.6).

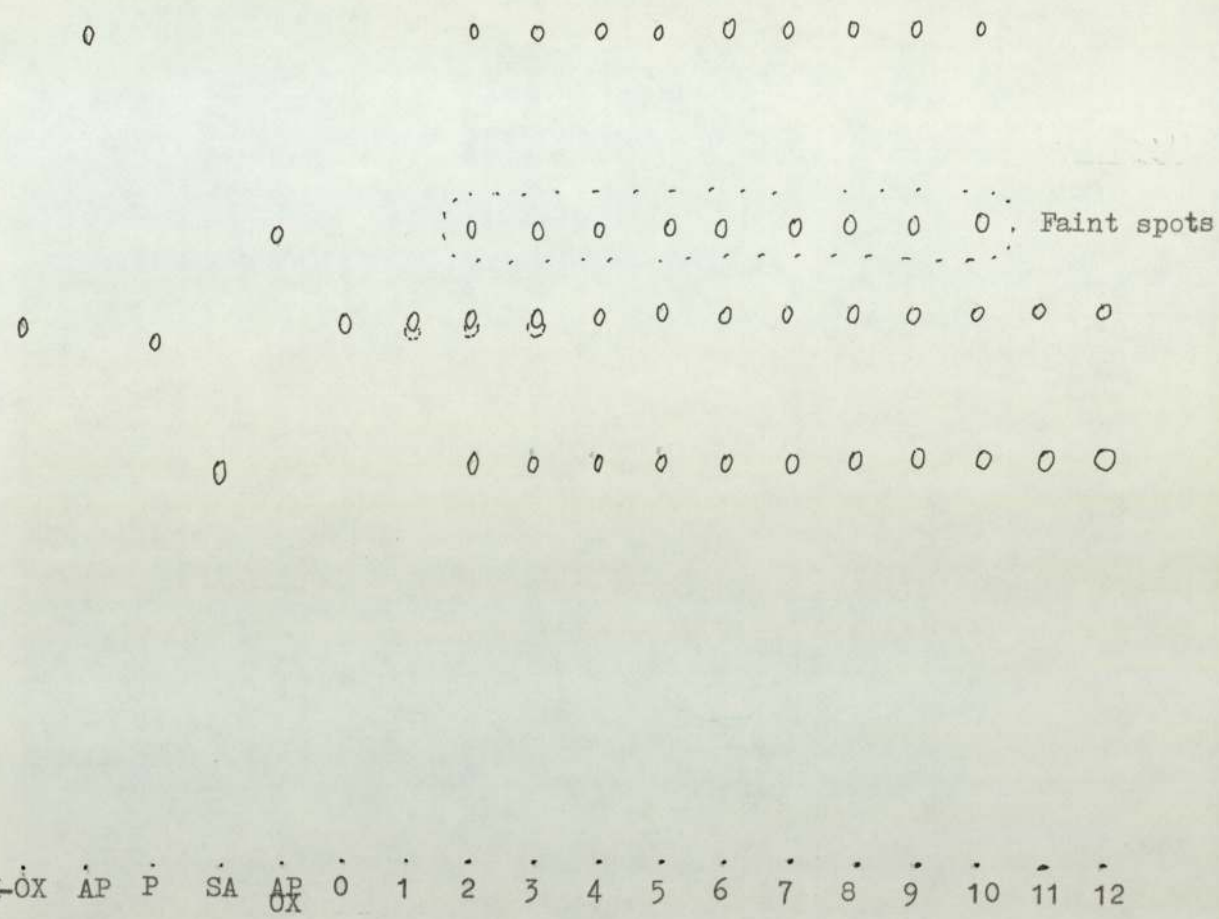

TLC separation of a 1:1 mixture of CHP and $Ni(OX)_2$ when heated to 75°C. Numbers denote the time of heating.

Figure (6.1.6)

An experiment with tertiary butyl hydroperoxide (TBH) and $Ni(OX)_2$ at equimolar concentrations were carried out under UV and also at 75°C. Samples were taken out at regular one hour intervals and were analysed by IR and TLC. As before the IR spectrum showed a regular decrease in the intensity of the band at 3560 cm^{-1} corresponding to the O-H stretching of TBH, with this a band appeared at 3620 cm^{-1}, which is due to the O-H stretching of tertiary butyl alcohol. After five hours of heating the

intensity of the band at 3620 cm^{-1} started to decrease and altogether disappeared in a few hours, figures (6.1.7) and (6.1.8). A closer analysis of the spectrum showed an appearance of a band of low intensity at 1625 cm^{-1}. This new band was identified as due to >C = CH_2 of isobutene formed by the dehydration of tertiary butyl alcohol. The formation of products at 75°C under UV light was faster than the reaction in the dark.

The products of the reaction were analysed by TLC. The oxidation products of $Ni(OX)_2$ namely, o-hydroxy acetophone and salicylic acid were observed but after a longer reaction time of five hours in the reaction under UV radiation, and about nine hours in the thermal reaction, whereas, with CHP oxidation products were observed after half an hour and two hours respectively in the two experiments. A TLC separation of carbonyl showed only the presence of O-hydroxy acetophone.

The volatile products formed during these reactions were trapped by cooling in a mixture of dry ice and acetone. An analysis of the resultant solution by mass spectra showed the presence of water and acetone in the reaction with CHP and $Ni(OX)_2$. In addition to these isobutene was observed when the reactants were TBH and $Ni(OX)_2$. No oxidation products of nitrogen were observed in the volatile products.

Similar reactions were carried out at 75°C and under ultra-violet light with CHP and $Ni(OX)_2$ molar ratio 2:1. An analysis of the products by TLC, IR and GLC showed the presence of oxidation products as before.

Figure (6.1.5) Changes in the IR spectrum of a 1:1 mixture of CHP and $Ni(OX)_2$ when heated to 75°C

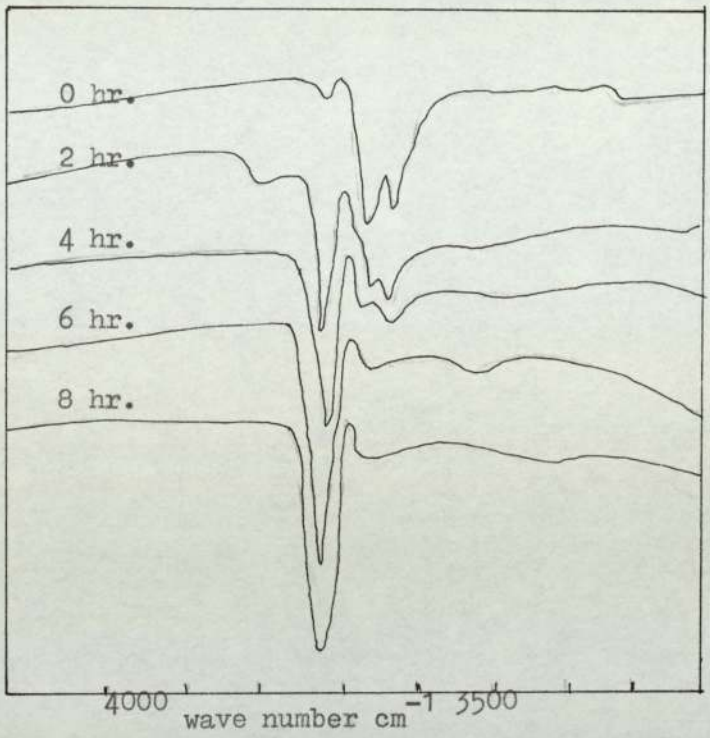

Figure (6.1.7) Changes in the IR spectrum of a 1:1 mixture of TBH and $Ni(OX)_2$ when exposed to UV light at 75±1°C

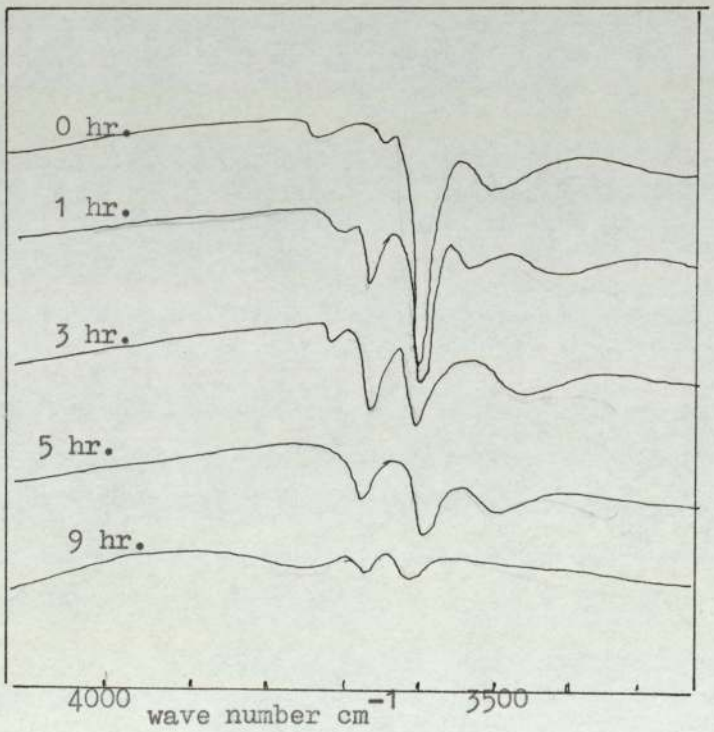

Figure (6.1.8) Changes in the IR spectrum of a 1:1 mixture of TBH and $Ni(OX)_2$ when heated to 75°C

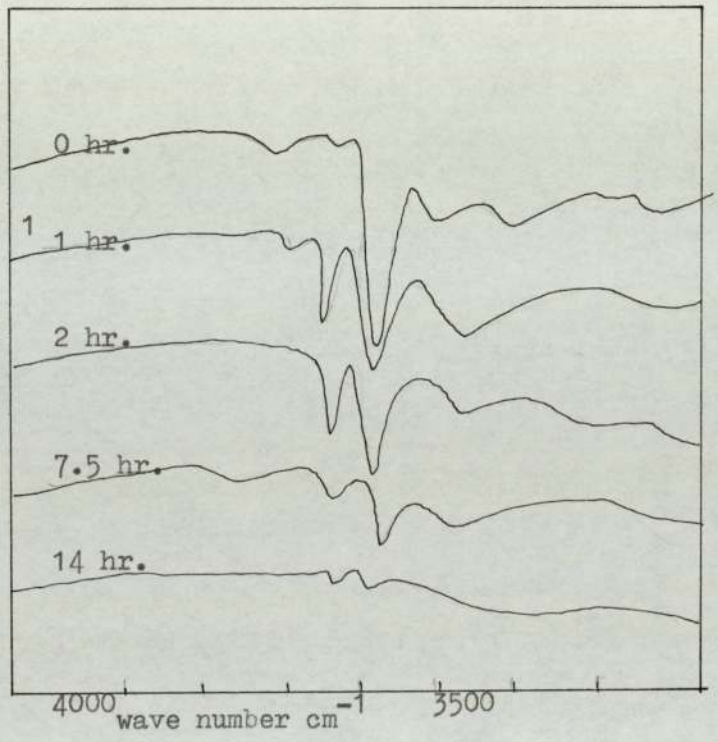

In all these reactions of $Ni(OX)_2$ with hydro-peroxides a greenish brown precipitate was formed. Attempts made to characterise this compound were not successful due to its sensitivity to air and moisture. This precipitate answered the test for nickel and liberated iodine from sodium iodide in isopropyl alcohol. This suggested the possibility of formation of an intermediate nickel complex by the displacement of an oxime ligand by a molecule of hydroperoxide. To confirm this an experiment was carried out with a solution containing identical molar concentration of CHP and $Ni(OX)_2$, to this the same molar concentration of the free ligand -hydroxy-acetophenone oxime was added. An analysis of this solution at regular intervals by IR and TLC did not show the presence of the products of oxidation of $Ni(OX)_2$. This suggests a reversible exchange of the ligand oxime by hydroperoxide[80].

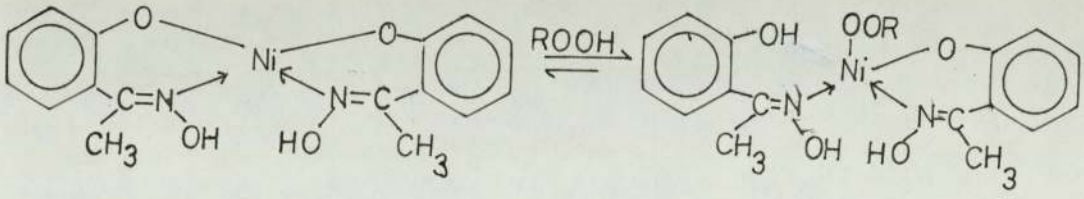

The free oxime so formed will undergo further reaction with hydroperoxide giving rise to the corresponding oxidation products.

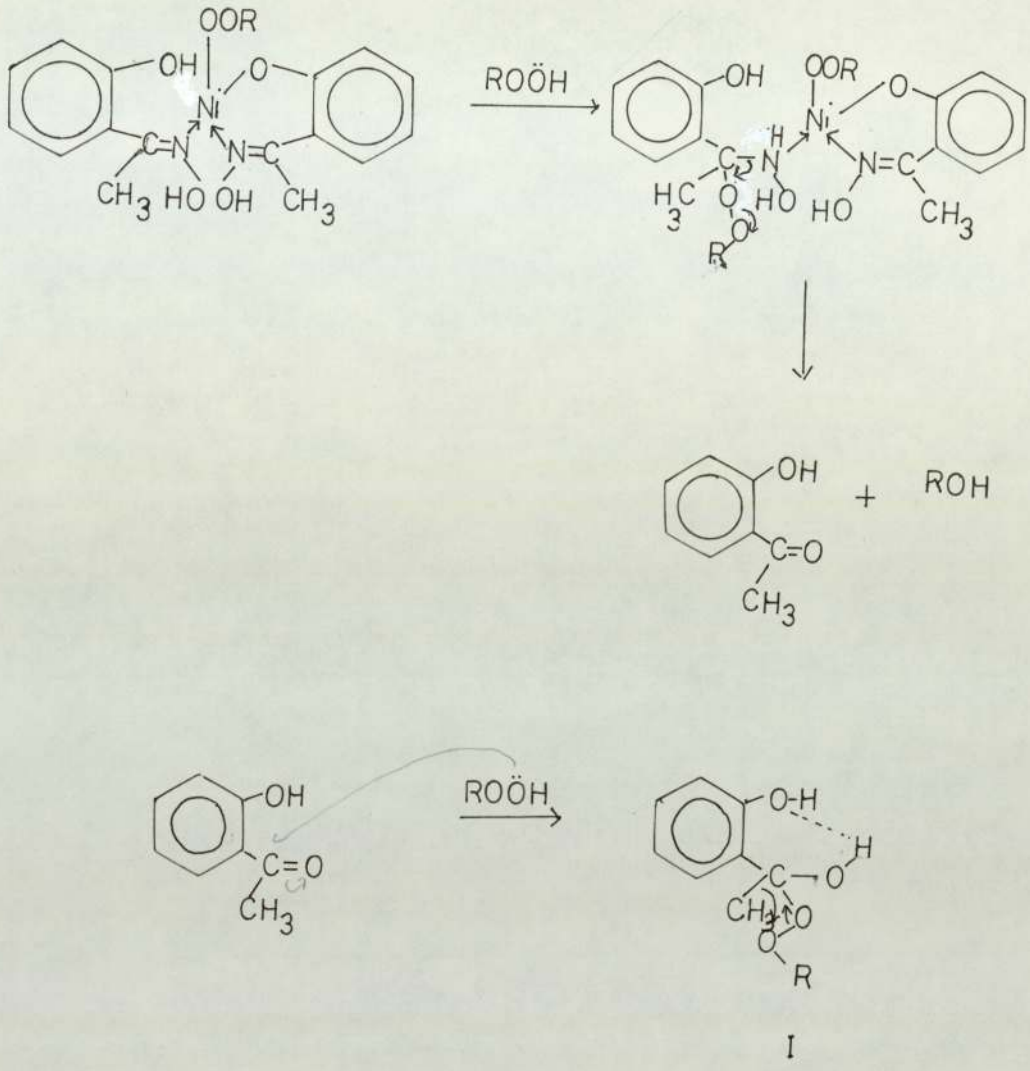

I

First the orthohydroxy acetophenone is formed which with another molecule of hydroperoxide will give rise to the transient intermediate compound I, which is stabilised with the formation of a six membered ring intermediate by hydrogen bonding. Hence the common Baeyer Villiger type of reaction[81] will not take place and instead the methyl group will migrate to the oxygen atom instead of the phenyl group, giving rise to cumyl methyl ether and salicylic acid.

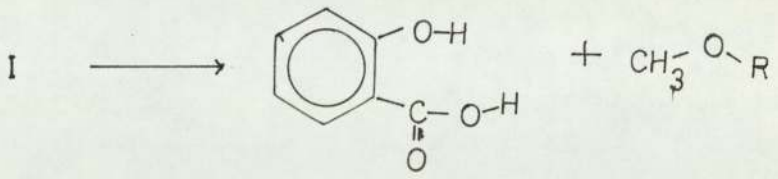

An attempt was made to study the kinetics of decomposition of hydroperoxides, but this was not successful due to the interference of the metal complex with the methods available for the quantitative estimation of hydroperoxides. These reactions will account for the stabilising activity of $Ni(OX)_2$ in addition to screening in the presence of hydroperoxides.

6.2 Reactions of $Ni(DBDC)_2$ with cumene hydroperoxide

Guillory and Becker[82] showed that the UV stabilising behaviour of $Ni(DBDC)_2$ is not due to a quenching of carbonyl triplet, but could be due to an interaction with singlet oxygen, as they found these complexes to disappear much more rapidly in the presence of oxygen than in its absence. However it is well known that metal dithiocarbamates are rapidly destroyed by hydroperoxides in a process which gives rise to an effective catalyst for hydroperoxide decomposition. The work by Scott et al.[44] showed that during the formation of the active catalytic species, $Ni(DBDC)_2$ in itself is destroyed with the formation of nickel sulphate.

The products formed by the decomposition of CHP vary, depending on the conditions and the nature of the additive used[83], strong Lewis acids react rapidly and exothermically to yield exclusively phenol and acetone by an ionic mechanism[84,85,86]. This could be represented schematically as follows.

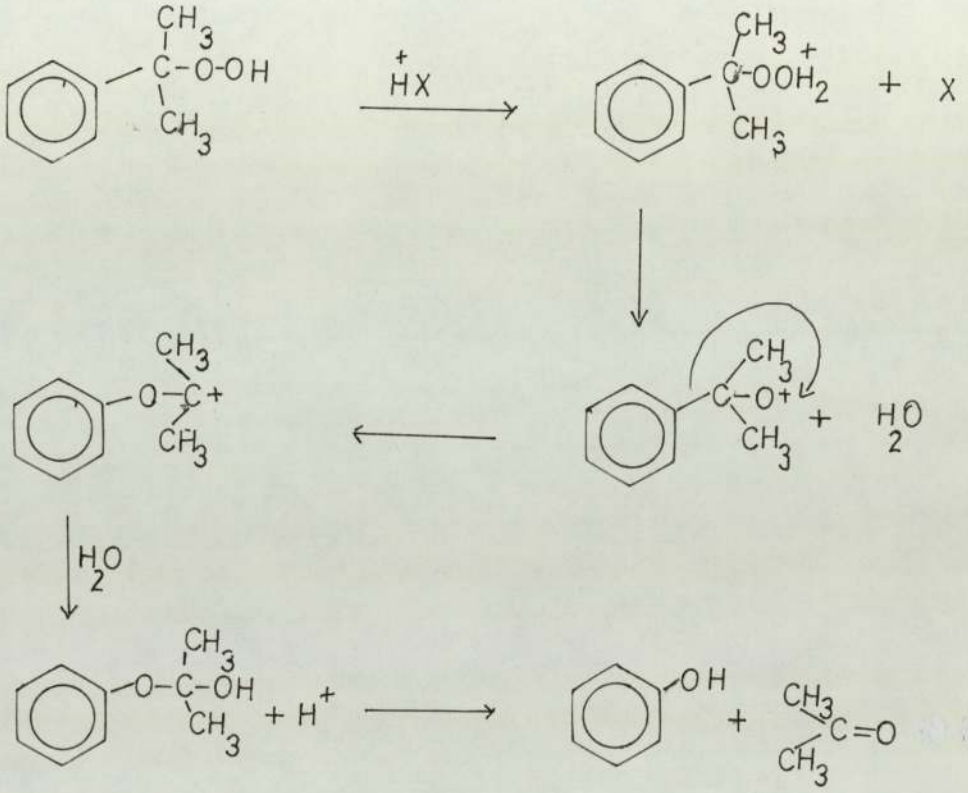

A homolitic decomposition of hydroperoxide may also occur, usually in the presence of transition metal ions. This takes place through the formation of α cumyloxy radicals[87] which leads to the formation of cumyl alcohol, acetophenone, dicumyl peroxide, methane and α-methyl styrene, and; less readily to the formation of methanol, dicumene and oligomers of α-methyl styrene. The following reaction scheme was proposed to account for the products formed[83,85,88].

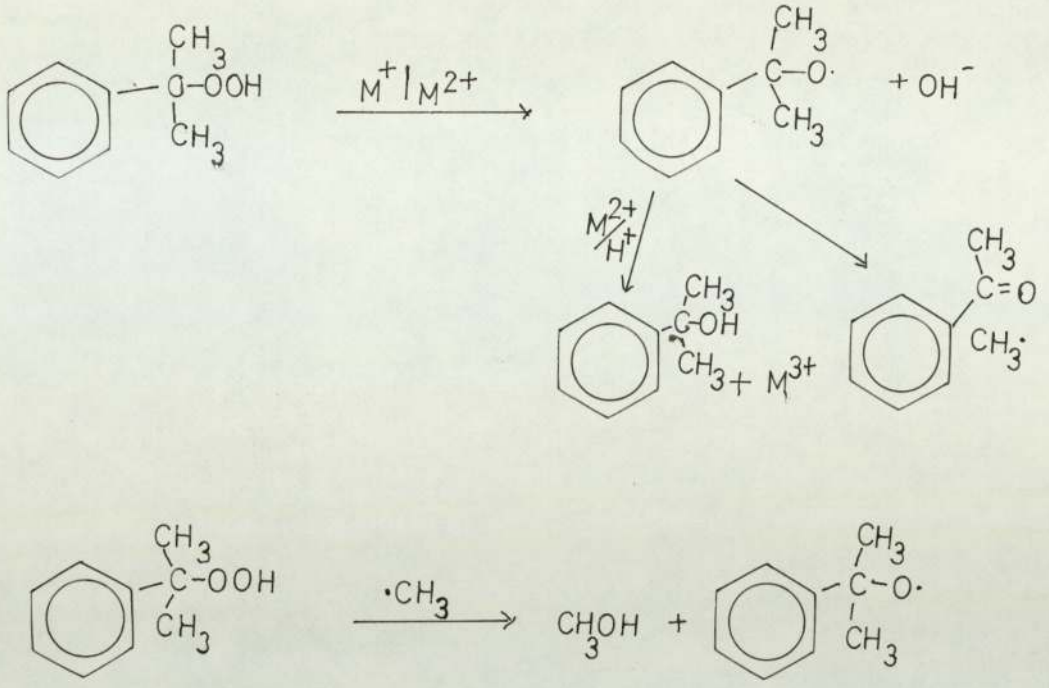

6.2.1 Thermal decomposition of CHP by $Ni(DBDC)_2$

Pure CHP in chlorobenzene was used which was treated with different concentrations of $Ni(DBDC)_2$ at 60°C. This reaction was carried out under nitrogen using the apparatus described in Chapter 3. The kinetics of the reaction was followed by measuring the amount of unreacted hydroperoxide at regular intervals of time, for this the iodometric method described in Chapter 3 was used. The decomposition of CHP in the absence of additive was also followed at 60°C.

The results shown in figures (6.2.1) and (6.2.2) were obtained by a plot of $\log \frac{(CHP)_t}{(CHP)_o}$ with time, and $1-\frac{(CHP)_o}{(CHP)_t}$ with time respectively. The second set of graphs show that the reaction is second order within the first few minutes, but was apparently first order for the rest of the time. However it is clearly seen that the rate constant is

Figure (6.2.1) First order plot for the decomposition of CHP by $Ni(DBDC)_2$

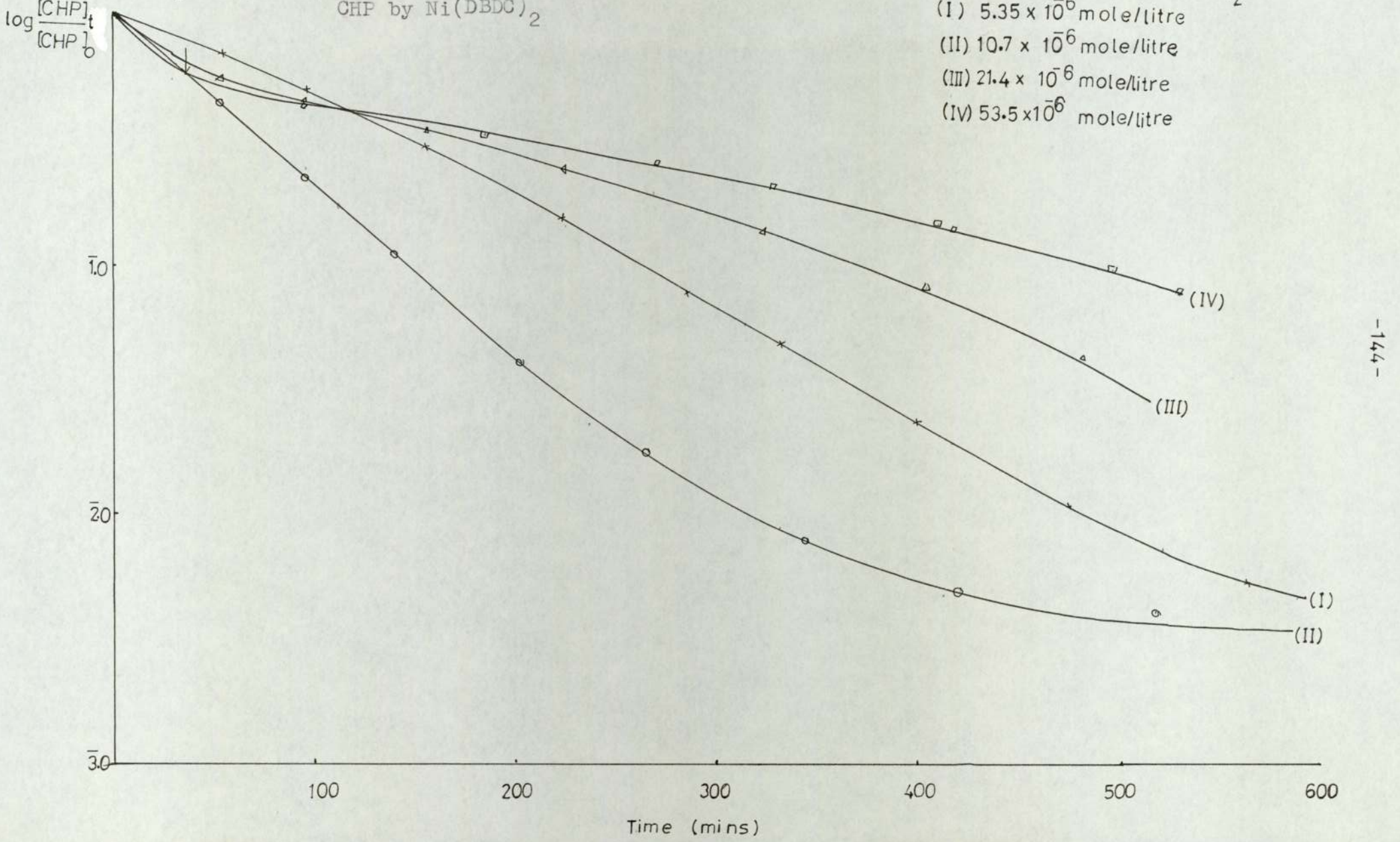

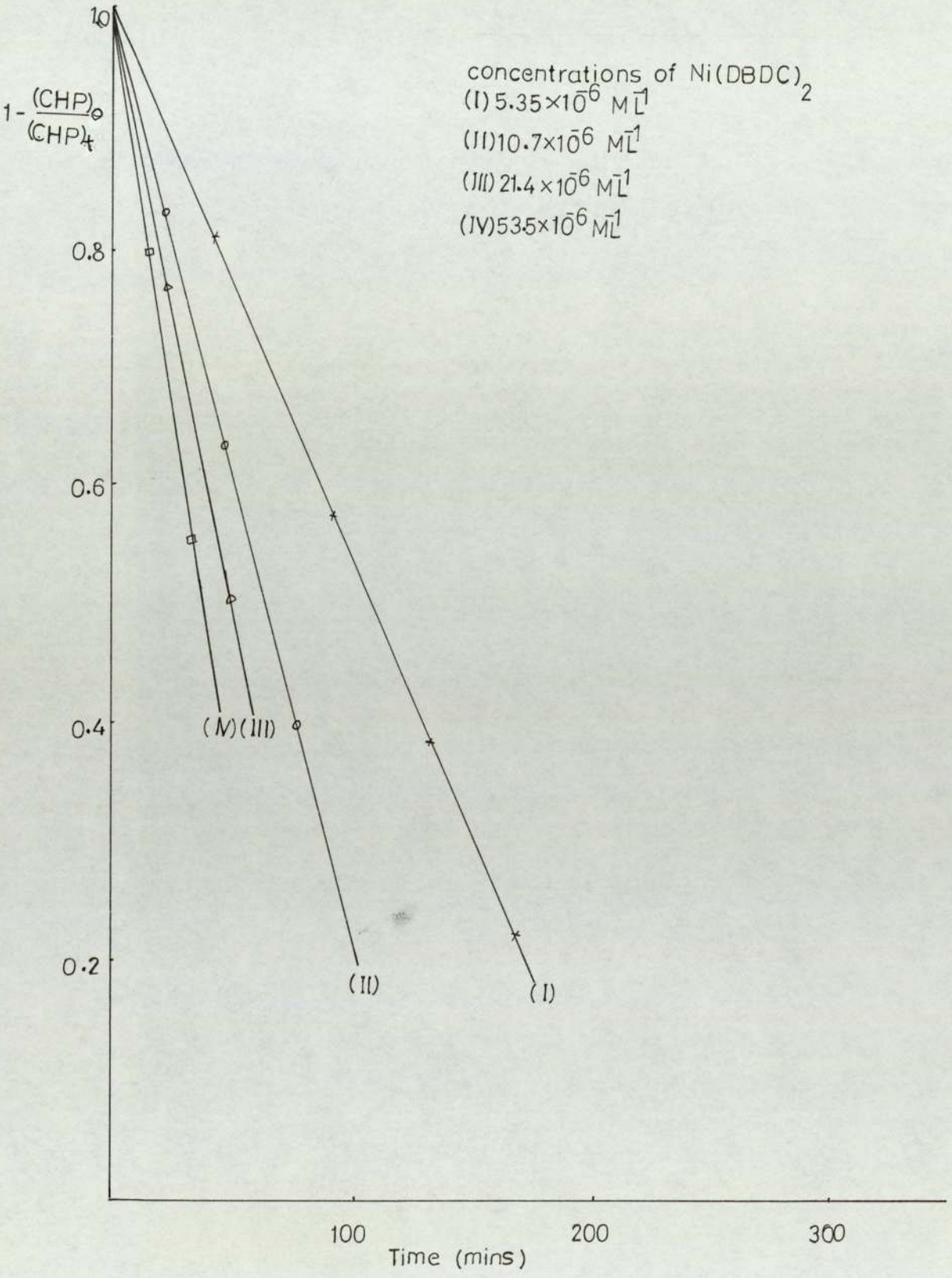

Figure (6.2.2) Second order plot for the decomposition of CHP by $Ni(DBDC)_2$

dependent on the initial concentration of metal complex, indicating a pseudo first order reaction of the type

$$-d\frac{(CHP)}{dt} = k_2(CHP)\ [M]^x \qquad (1)$$

Since low concentrations of the metal complex were used to reduce the hydroperoxides, this active species cannot be in excess, so that for the above kinetic scheme to hold, this species must function as a true catalyst.

A detailed study of the early stages of the interaction of hydroperoxide with different concentrations of $Ni(DBDC)_2$ in chlorobenzene showed the separation of nickel sulphate, accompanied by a rapid catalytic decomposition of the hydroperoxide figure (6.2.1.) With lower concentrations of $Ni(DBDC)_2$ [curves I and II] the hydroperoxide concentration was, ultimately reduced to zero whilst that of the control (without metal complex) remained unchanged. At higher concentrations of the metal complex ($>10^{-5}$M) a large amount of $Ni(SO_4)$ came down as a precipitate within the first few minutes of the reaction followed by a slower rate of decomposition of hydroperoxide showing that $Ni(SO_4)$ inhibits the decomposition of CHP.

The major products formed by the $Ni(DBDC)_2$ catalysed decomposition of CHP were 63.0% phenol and 24.6% acetone and is entirely as expected on the basis of a cationic decomposition namely phenol and acetone and not those expected from a transition metal catalysed decomposition which would give acetophenone as the major product in a radical forming reaction.

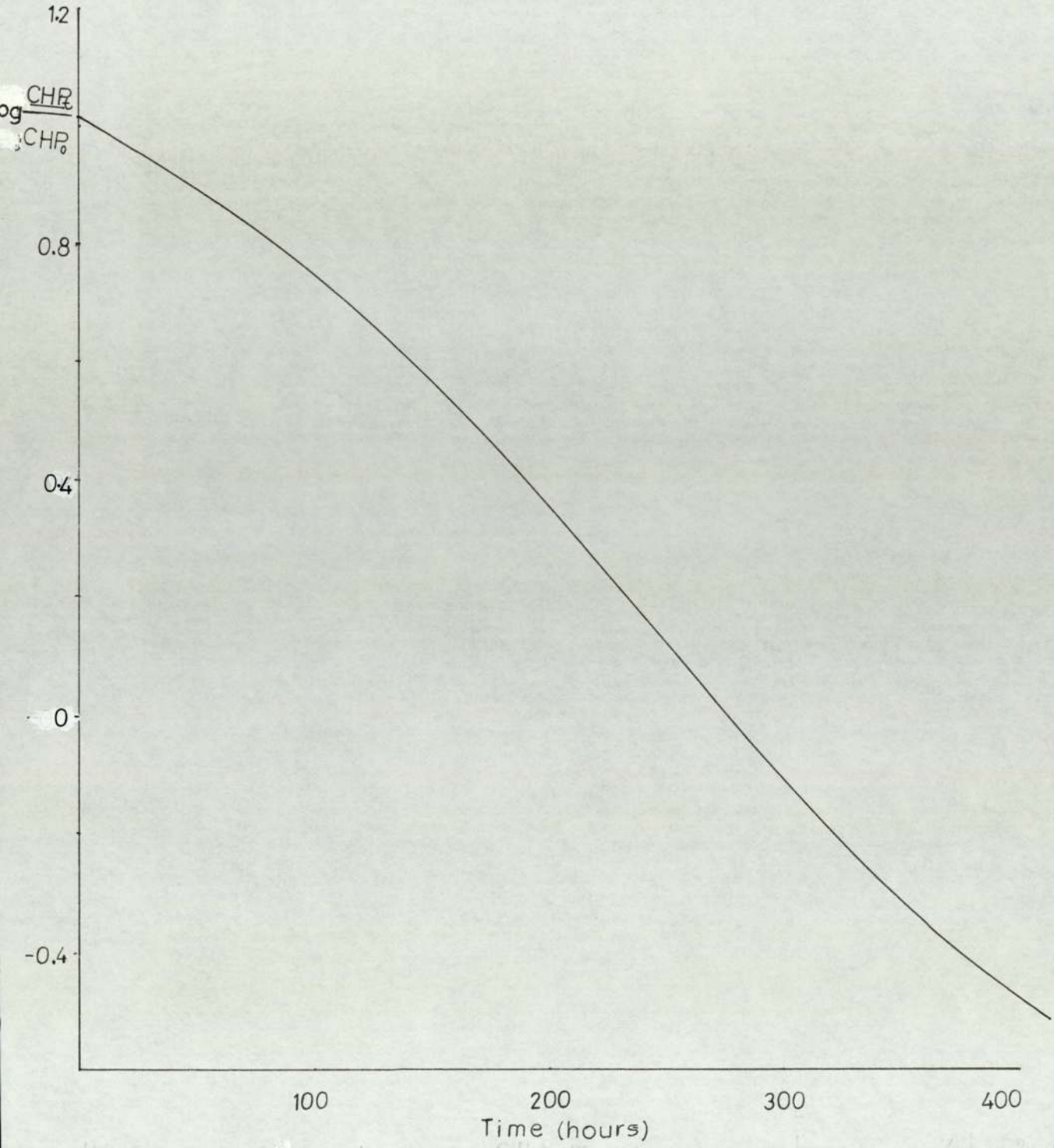

Figure (6.2.3) Kinetics of decomposition of CHP in Cumene by 0.025% $Ni(DBDC)_2$ at 59°C

This reaction was now repeated in an autoxidising solvent, cumene, at 59°C and here too the catalytic decomposition of CHP followed pseudo-first order kinetics, figure (6.2.3) and the major products were phenol and acetone, and hence the decomposition is by a cationic species. Furthermore the proxidant effects observed during the early stages of hydroperoxide initiated oxidation (Chapter 4) in the presence of $Ni(DBDC)_2$ together with a liberation of a gas from this during autoxidation as observed by Scott et al.[44] enabled them to propose that the agent responsible for the non radical hydroperoxide decomposition is sulphur dioxide or sulphur trioxide, formed by the oxidation of the metal dithiocarbomate by hydroperoxide.

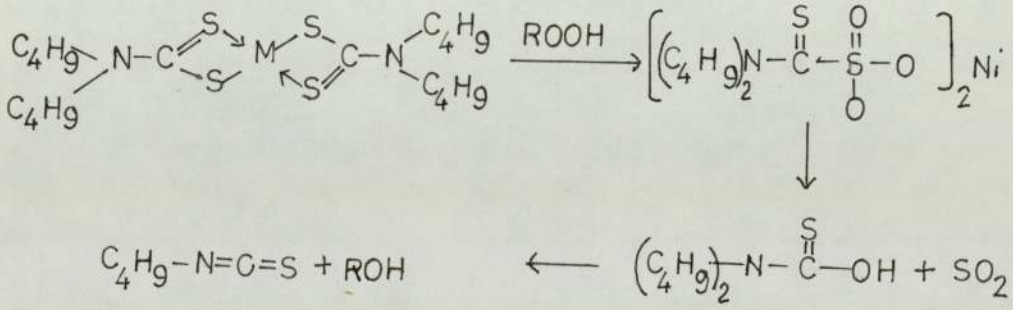

and the mechanism of decomposition of cumene hydroperoxide proposed was

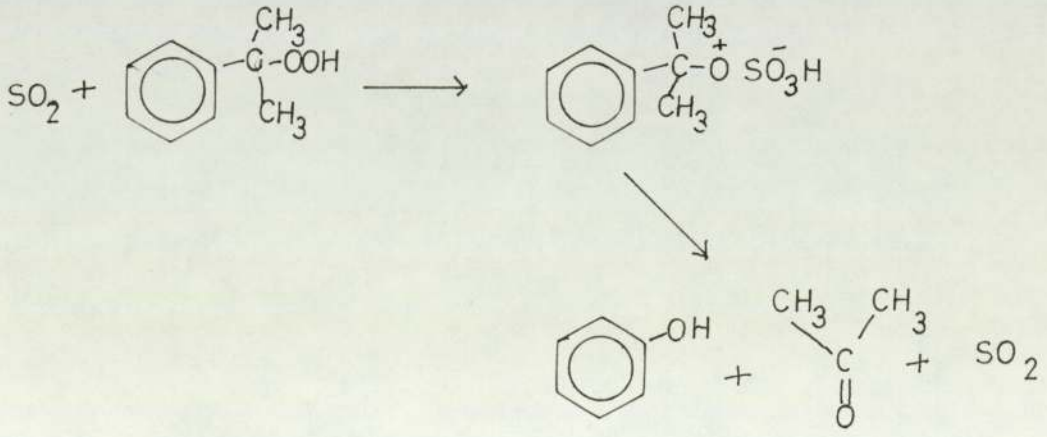

6.2.2 Decomposition of CHP by $Ni(DBDC)_2$ when exposed to ultraviolet light.

When 10^{-2}M of CHP were reacted with 10^{-4}M of $Ni(DBDC)_2$ under UV radiation a reaction identical to above was observed, but at a much slower rate. A plot of $\log \frac{(CHP)_t}{(CHP)_o}$ vs time is shown in figure (6.2.4) The reaction did not fit into either first order, second order or third order plot within the first 100 hours, after that it was evidently first order, but at a reduced rate compared to the thermal reaction. The reaction rate depends on the concentration of $Ni(DBDC)_2$ used. Therefore this too follows pseudo first order kinetics and hence follows the rate as given in equation (1).

Here too low concentrations of $Ni(DBDC)_2$ were used. This removed all the CHP, but took a longer time. This means that the process is catalytic and the active catalytic species is sulphur dioxide or sulphur trioxide. Nickel sulphate was detected as a greenish precipitate at the end of the experiment. An analysis of the products by GLC, when the reaction has gone to completion showed that the main products of decomposition were phenol and acetone as expected. Therefore the mechanism of the reaction is the same as in the previous case and the same reaction scheme should hold.

6.3 Kinetics of decomposition of hydroperoxides by carbonyl compounds

Although hydroperoxides are not UV chromophores they are found to be the key initiators in photoxidation of polyolefins. The cause for this is still the subject of speculation. Sedlar[89] has found that carbonyl

Figure (6.2.4) First order plot for the decomposition of CHP by $Ni(DBDC)_2$ under UV.

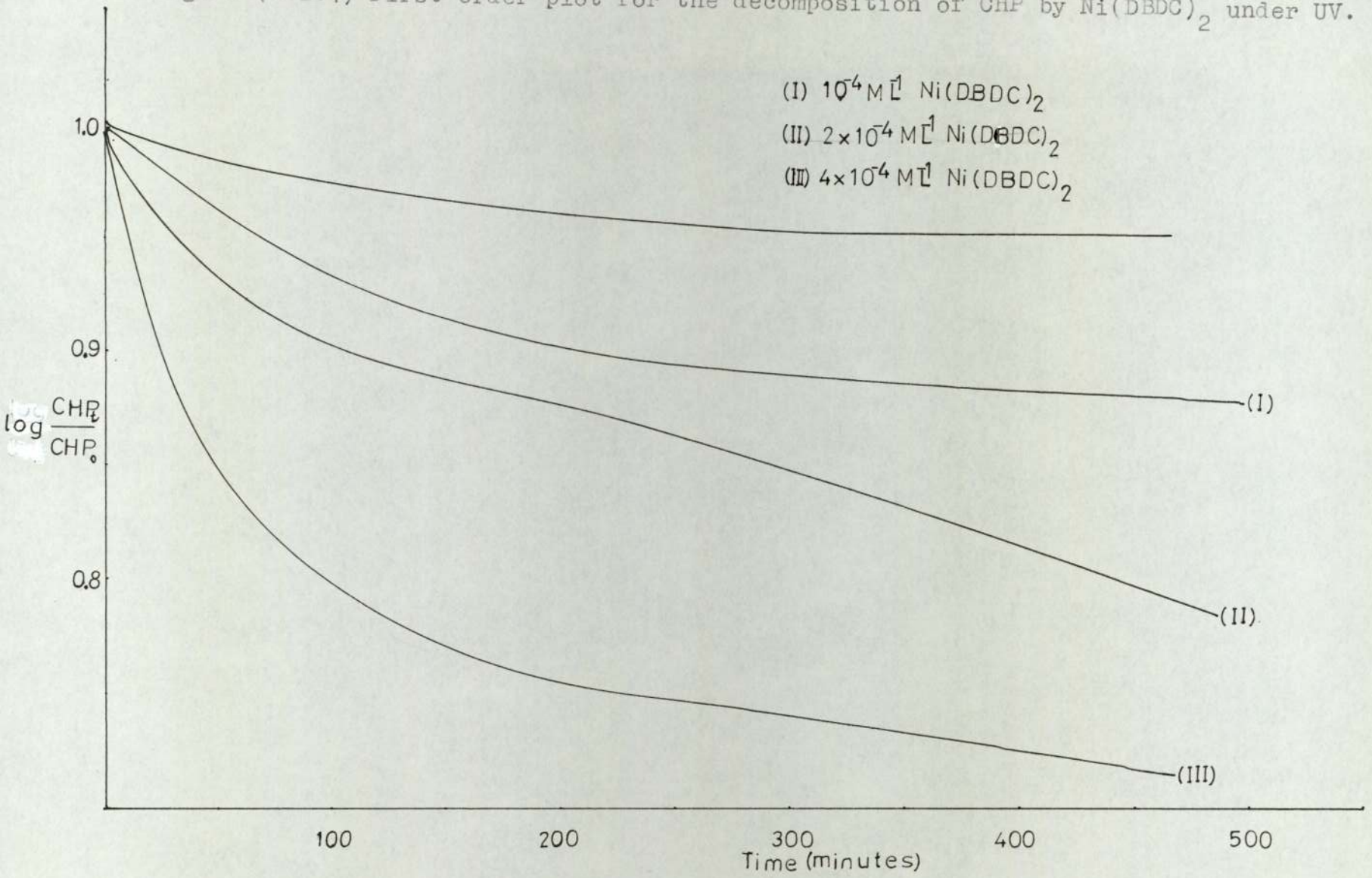

compounds can act as activators for the decomposition of hydroperoxides. Therefore the following studies were carried out where an attempt was made to evaluate the kinetics of decomposition of hydroperoxides in the presence of benzophenone.

Pure CHP in chlorobenzene was used, which was treated with different concentrations of benzophenone at 29±1°C and under ultra-violet radiation. With low concentrations of benzophenone the reactions were very slow and were almost identical to the rate observed with uncatalysed decomposition. However when stoichiometric quantities were used a faster rate of decomposition was observed. figure (6.3.1)

The major products formed during decomposition were analysed by GLC and were found to be cumyl alcohol and acetophenone. The percentages are 63% and 26.25% respectively. This would mean that the decomposition of CHP follows a free radical mechanism, and the following reaction scheme will account for all the products formed during the reaction.

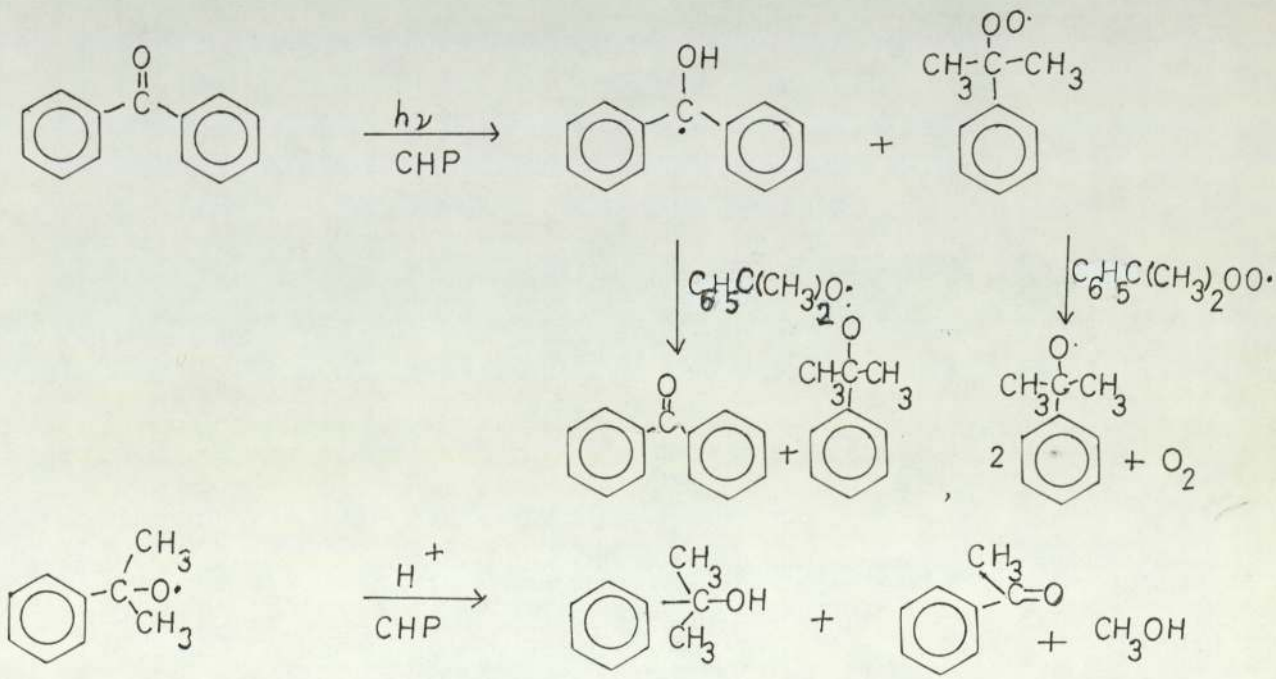

Figure (6.3.1) First order plot for the decomposition of CHP by BP.

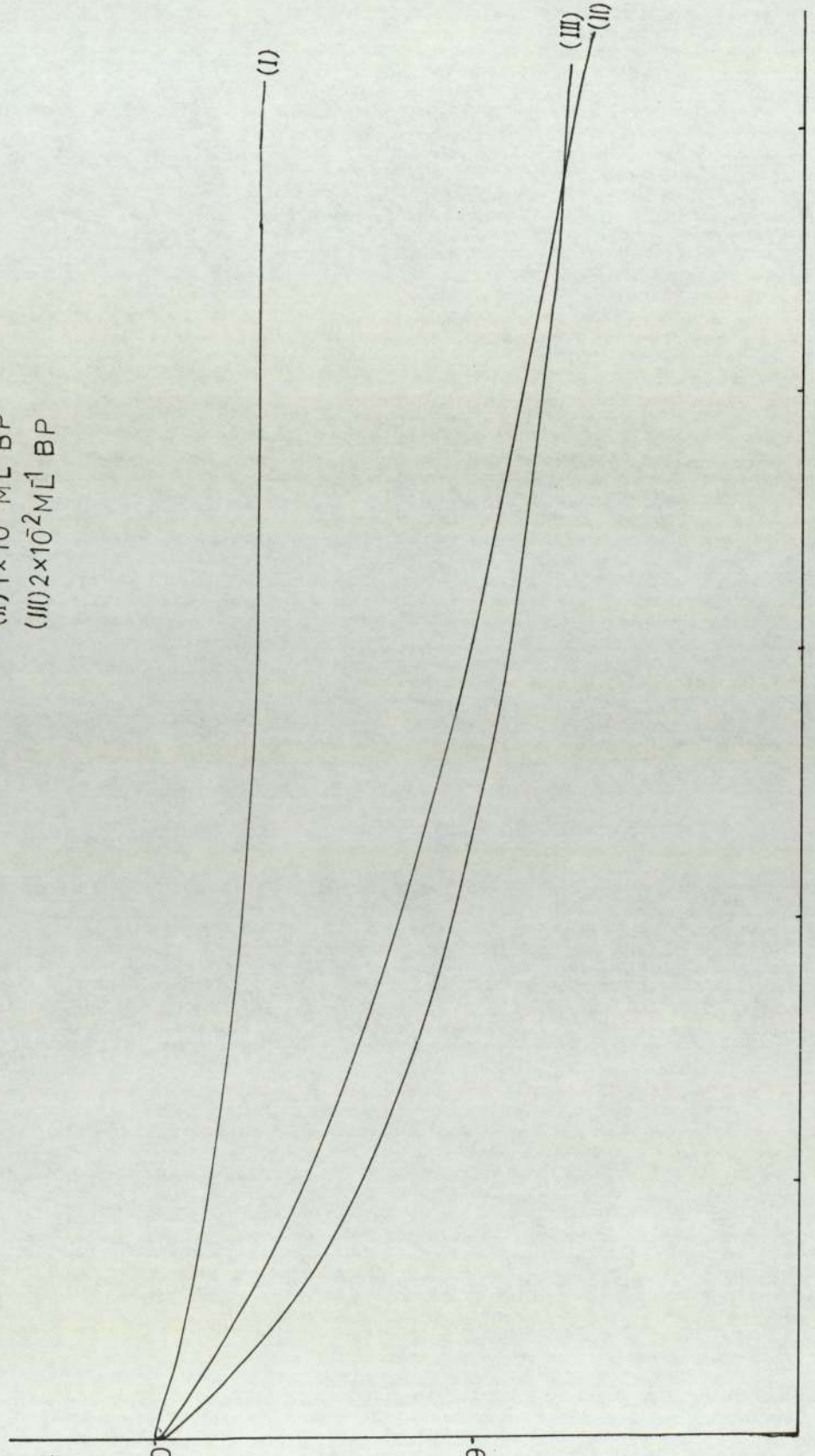

The IR spectrum of the final solution did not show the presence of benzophenone, which would mean that BP is removed by a subsequent side reaction.

CHAPTER 7

MECHANISMS OF STABILISATION OF POLYOLEFINS

In the previous chapters the effects of the nickel chelates on oxygen containing model systems were used to evaluate their mechanism of action. Similar studies were made on high density polyethylene (HDPE) low density polyethylene (LDPE) and Polystyrene (PS) and these results were correlated with the results obtained from the solution studies.

7.1 EXPERIMENTAL

Processing:

HDPE was processed at 200°C in a closed mixer in an atmosphere of nitrogen for five minutes, and was quenched in water immediately after mixing. This was compression moulded to films of thickness 8×10^{-3} inches at 160°C. LDPE and PS were processed under the same conditions at 160°C and were compression moulded into films of thickness 8×10^{-3} inches at 160°C.

These films were mounted on quartz slides and were exposed to ultra-violet radiation. Infra-red analysis was carried out using a PE 457 spectrophotometer; detailed procedure is given in Section (3.4.1).

Results and

7.2 DISCUSSION

Figures (7.2.1) and (7.2.2) show infrared spectra of HDPE (low pressure polyethylene) and LDPE (high pressure polyethylene). These show strong C-H stretching bands of the CH_2 group in the region 2800 - 3000 cm^{-1}. The bands due to CH_3 groups gives a symmetric stretching band at 2962 cm^{-1}[90] and a symmetric deformation band at [91] 1378 cm^{-1}. These bands are given by monomeric branched paraffin hydrocarbons with an intensity proportional to the number of chain ends. In LDPE, fig. (7.2.1) the intensities of these bands are much greater than could be accounted for by the ends of unbranched chains. They show that some of the molecules are branched. The entent of branching varies with polymerisation conditions, usually in commercial LDPE there are about 20 to 30 methyl groups per 1,000 carbon atoms[72]. In HDPE there are only about 7 methyl groups per 1,000 carbon atoms and branches occur at intervals of some 20 carbon atoms. In LDPE double bonds would be expected at some of the chain ends, and indeed bands at 909 cm^{-1} and 1640 cm^{-1} due to the group $RCH = CH_2$ are found. Unsaturation due to pendent methylene groups ($R_1R_2C = CH_2$) appear at 887 cm^{-1} and 1645 cm^{-1} which is not observed with HDPE where the unsaturated groups present are apparently all of the terminal ($RCH = CH_2$) or chain ($RCH = CHR'$) types[92]. The other bands observed are due to the oxygen containing functional groups in the region 1720 cm^{-1} due to C = O stretching. A hydroxyl -O-H band at 3,300 cm^{-1} is also found. The intensities of these bands increase when polyethylene is exposed to ultra-violet radiation in air and a measure of the carbonyl (C=O) intensity at 1721 is used as a measure of the oxidation of polyethylene. The groups present in HDPE and LDPE are summarised in Table (7.1).

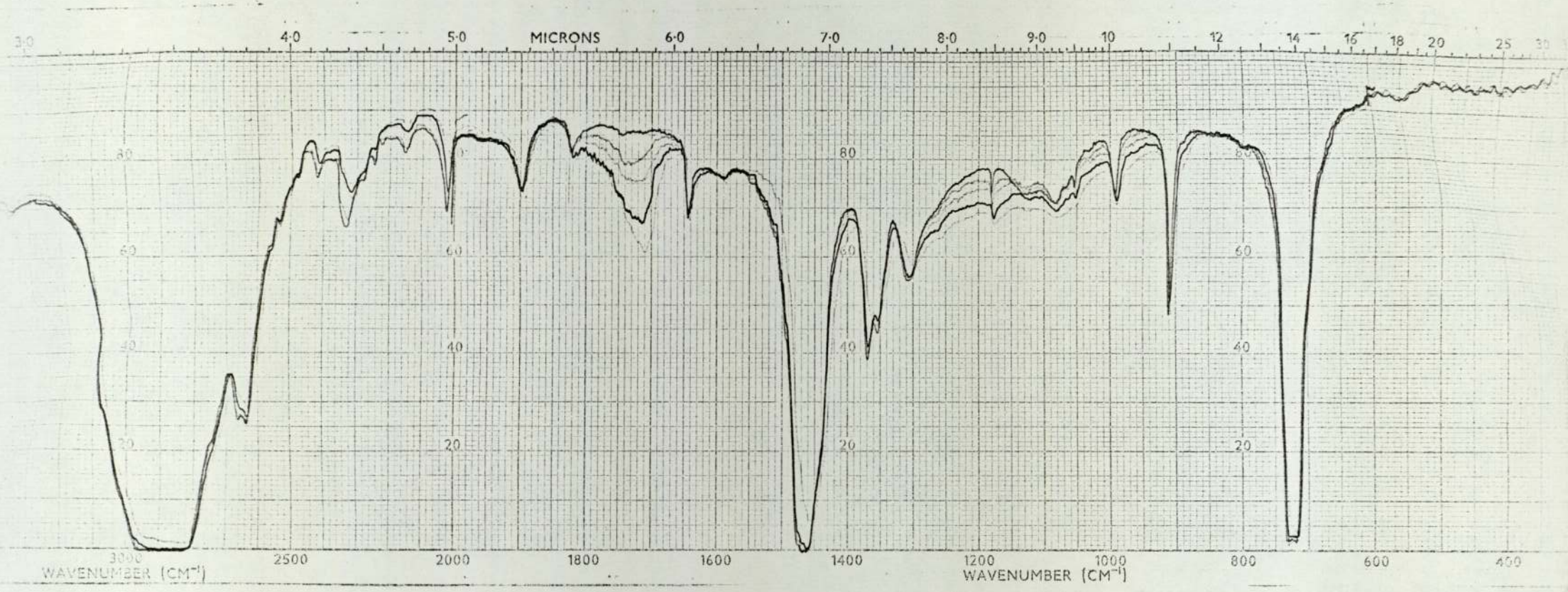

Figure (7.2.1) The Infra-Red spectrum of Hdpe.

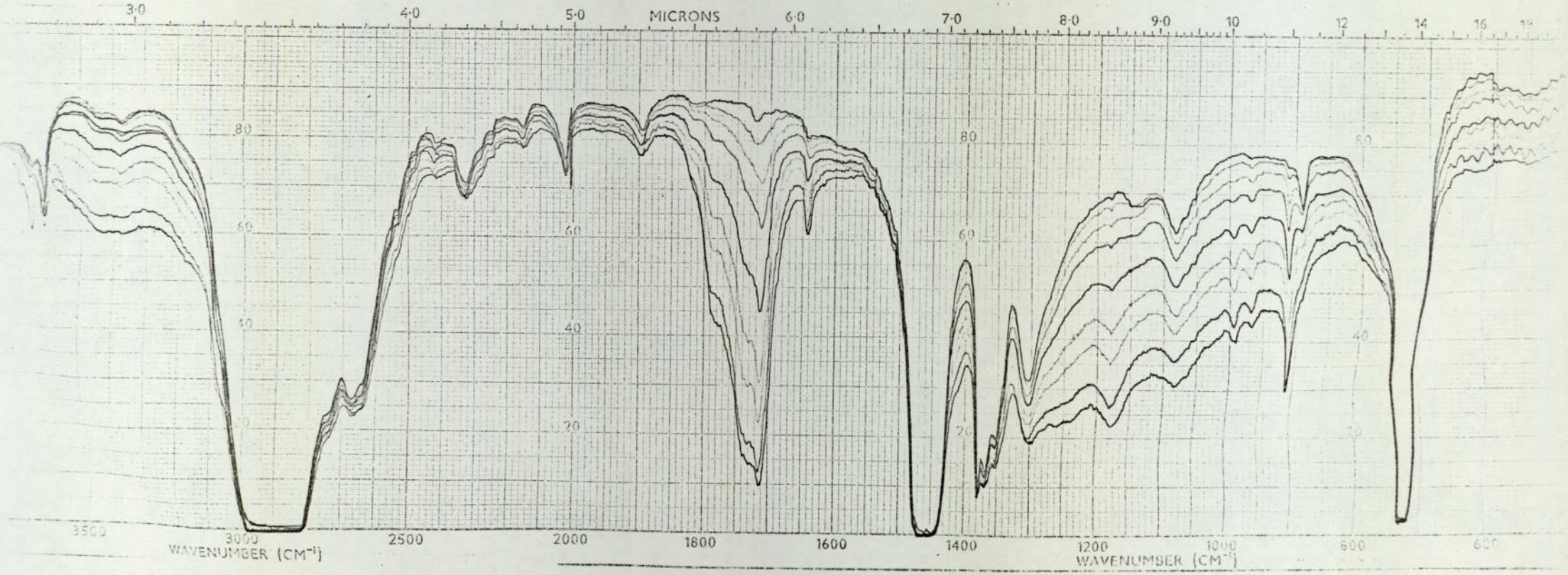

Figure (7.2.2) Infra-Red spectrum of Ldpe.

TABLE 7.1

Functional groups identified in HDPE and LDPE

Functional group	$\nu(cm^{-1})$	
	HDPE	LDPE
-OOH	3510	3510
-OH	3380	3380
-CH	2800-2980	2790-2990
-CH=CH-	1645	1645
$-CH_3$	1370	1380
$RC=CH_2$	909,990	909,1640
$\begin{matrix} R_1 \\ \diagdown \\ \quad C=CH_2 \\ \diagup \\ R_2 \end{matrix}$	-	887±1
$\begin{matrix} R_1 \\ \diagdown \\ \quad C = O \\ \diagup \\ R_2 \end{matrix}$	1720±1	1720±1
$\begin{matrix} R \\ \diagdown \\ \quad C = O \\ \diagup \\ CH_3 \end{matrix}$	1725±1	1725±1
-COOH	1710	1710-1713
-CHO	1735	1735
-COOR	1749±1	1748
$\begin{matrix} \quad O \\ \quad \parallel \\ -C \\ \diagdown \\ \quad OOH \end{matrix}$	-	1785

The effects of the absorbed UV light on the polymers have been interpreted as being due to free radical chain oxidation which finally leads to the cleavage of the polymer back bone, to cross linking and to the formation of small molecular fragments[93] and some unsaturation[18,94,95].

The most important initiation process involved in the early stages of the photoxidation of polyethylene has been shown to be hydroperoxide photolysis associated with the decay of vinylidene groups[96]. Carbonyl and vinylidene are good UV chromaphores present in polyolefines. An absorption of a photon by these will raise the energy of the molecule to an excited singlet state which by a process of intersystem crossing will subsequently produce a triplet excited state.

Photoxidation is characterised by the absence of autocatalysis and by the inefficiency of the radical chain terminators, such as phenolic antioxidants[97]. This has been attributed to a degradative mechanism with a high initiation rate and a short kinetic chain length. Trozzolo and Winslow[18] proposed a mechanism for the oxidative photo-degradation of polyethylene, based on the predominant role of the ketone groups. However recent work by Scott et al.[98] showed that the most important initiation process involved in the early stages of the photoxidation of polyethylene is hydroperoxide photolysis associated with the decay of vinylidene groups, which is then followed by the carbonyl photolysis occurring primarily by the Norrish type II process. This would clearly explain the inflexion observed in the carbonyl indices during the photoxidation of unsaturated HDPE and LDPE these are shown in figures (7.2.3) and (7.2.14) respectively. The initial part of the carbonyl formation curve has been shown to be due to hydroperoxide photolysis.

Figures (7.2.3) to (7.2.13) were obtained with various concentrations of $Ni(OX)_2$, $Ni(DBDC)_2$, UV(1084) and UV(531) used as additives and as screens at equivalent screening effectiveness in HDPE. All four compounds were found to be more effective as additives than as screening agents. The slightly lower values of carbonyl formation observed when $Ni(OX)_2$ is used as a screen could be due to reduced hydroperoxide photolysis. However when this is used as an additive the hydroperoxide derived carbonyl formation rate is considerably retarded. $Ni(DBDC)_2$, UV(1084) and UV(531) show similar effects to $Ni(OX)_2$ when used as a screen, but $Ni(DBDC)_2$ completely removes the hydroperoxide derived carbonyl growth curve when it is used as an additive this is consistent with the behaviour of $Ni(DBDC)_2$, which was shown to be a peroxide decomposing atnioxidant, (chapters 4 and 6). $Ni(OX)_2$ does not show this effect although it does react to some extent with hydroperoxides.

However when cyasorb UV(1084) and UV(531) are used as additives or screening agents for HDPE, the same inflexion is observed in the carbonyl indices, [figures (7.2.7) to (7.2.11)] indicating that a certain amount of hydroperoxide is produced during processing which gives the initial part of the carbonyl formation curve as in the unstabilised and screened samples. This fact is also reflected in their embrittlement times (Table 7.2). From this it is clear that the stabilising activity of UV(1084) and UV(531) is not by removing or inhibiting the formation of hydroperoxides. The embrittlement times of the screened samples are uneffected while the HDPE samples when stabilised with $Ni(OX)_2$, $Ni(DBDC)_2$ and UV(531) show more than a three fold increase in their embrittlement

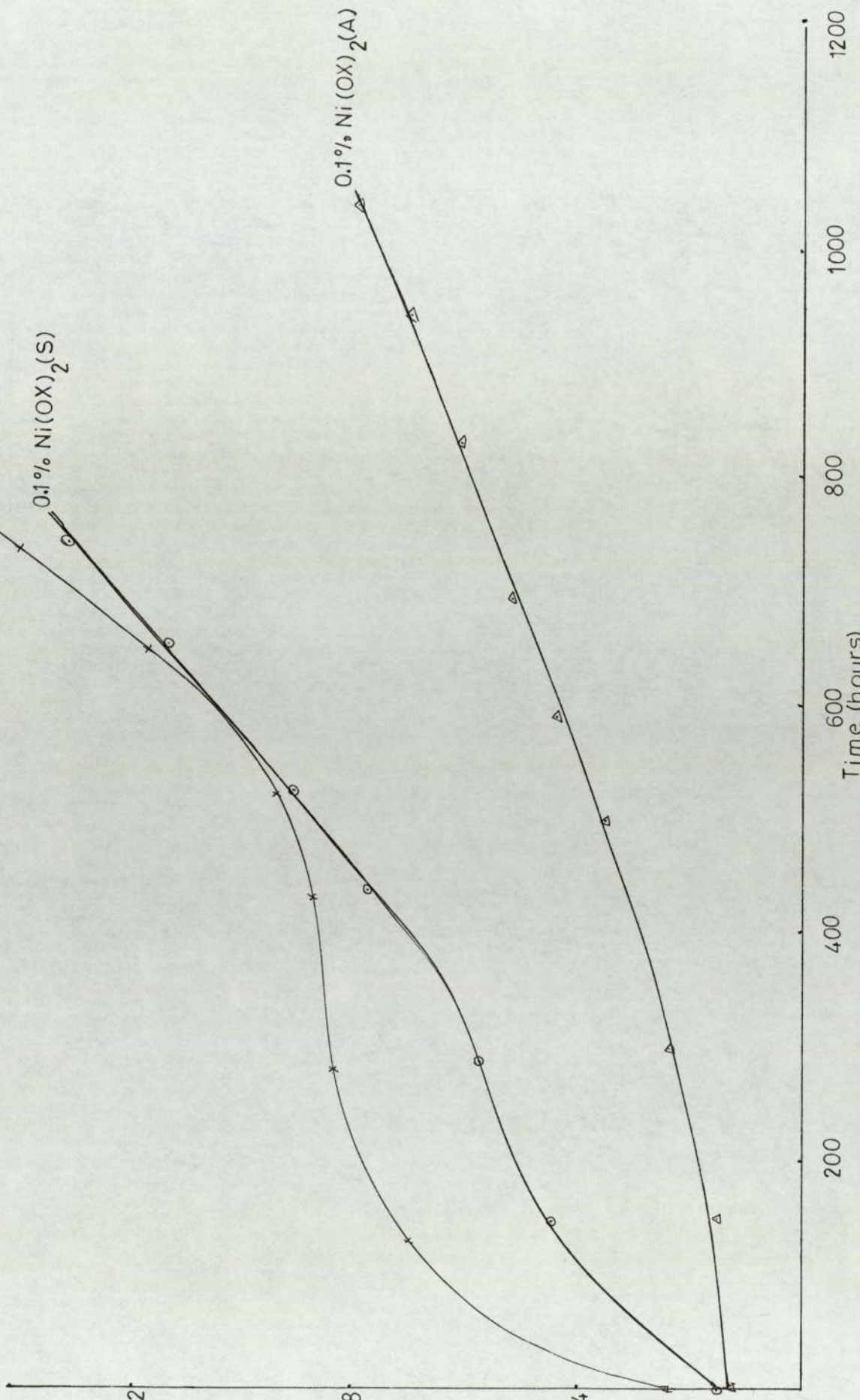

Figure (7.2.3) Change in Carbonyl Index with time of irradiation for HDPE.

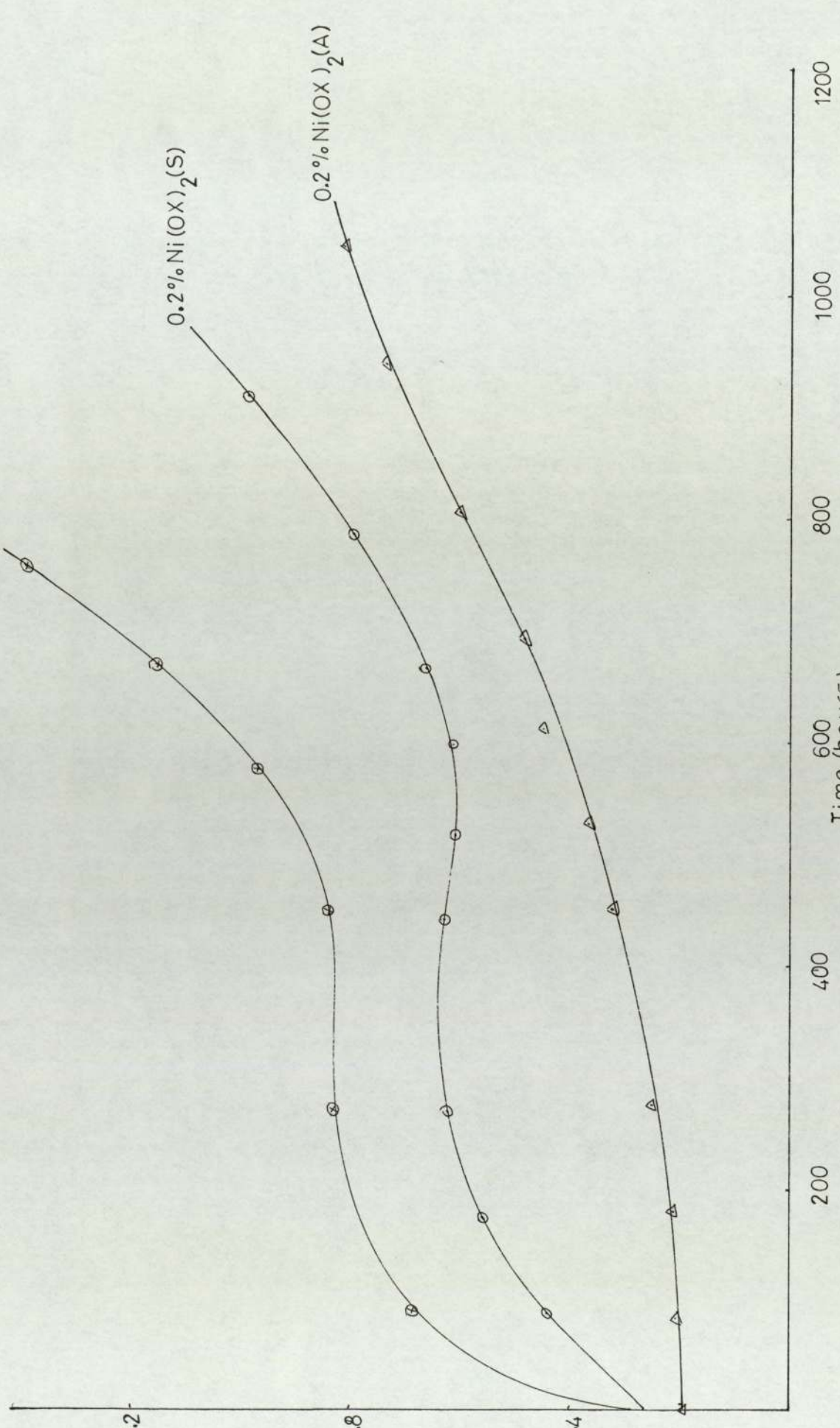

Figure(7.2.4) Change in Carbonyl index with time of irradiation for HDPE.

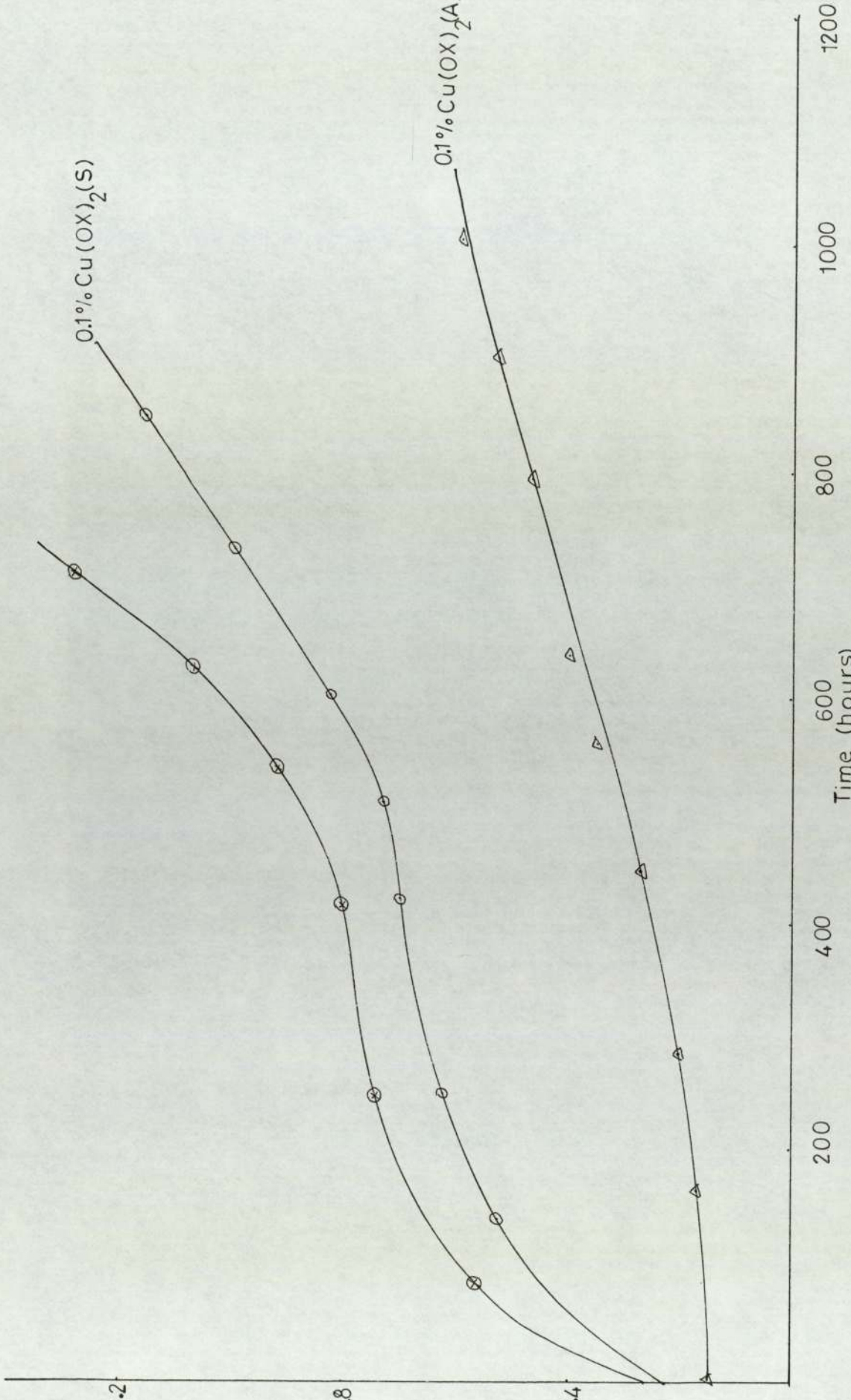

Figure (7.2.5) Change in Carbonyl Index with time of irradiation for HDPE.

7.2.5

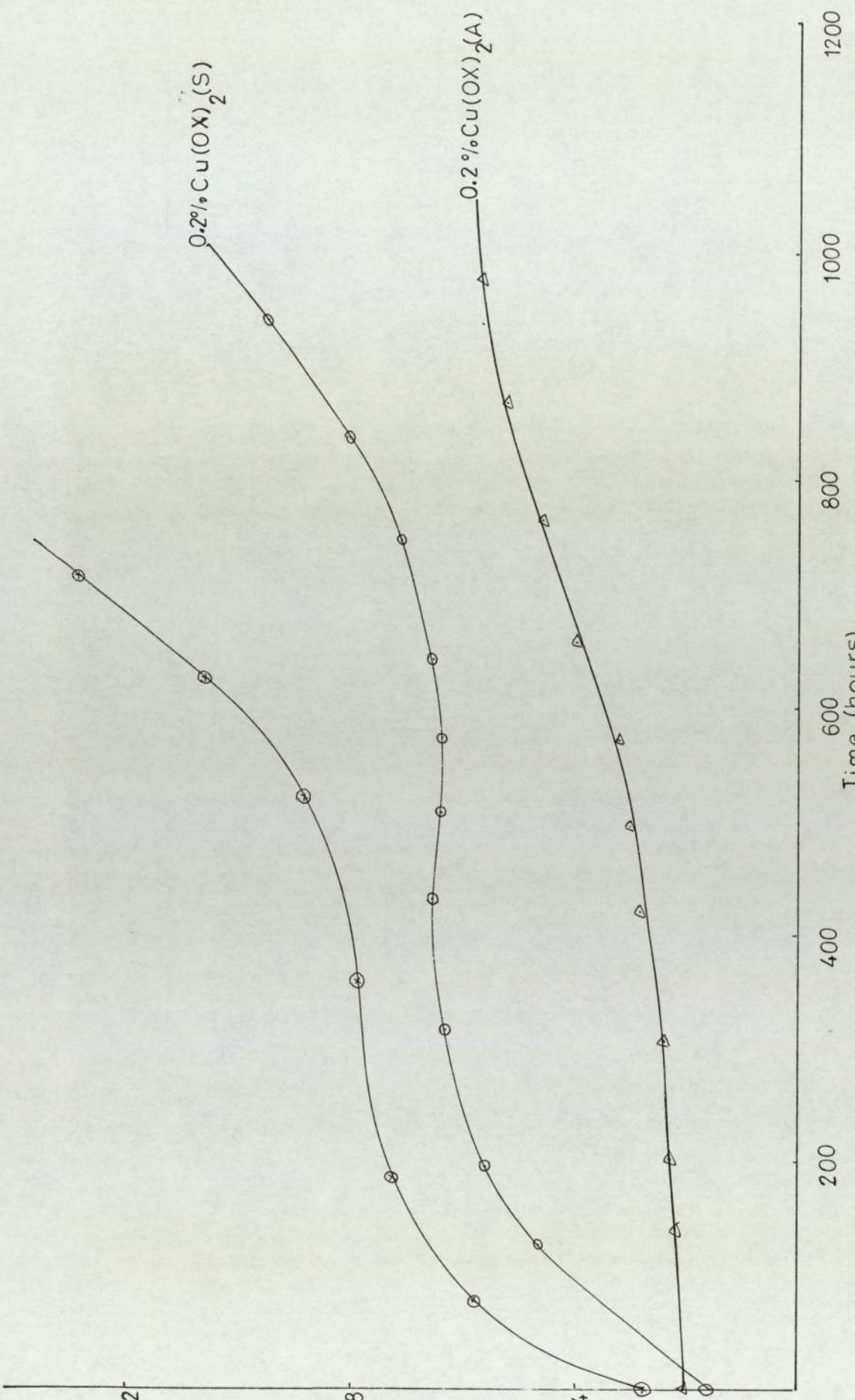

Figure (7.2.6) Change in Carbonyl Index with time of irradiation for HDPE.

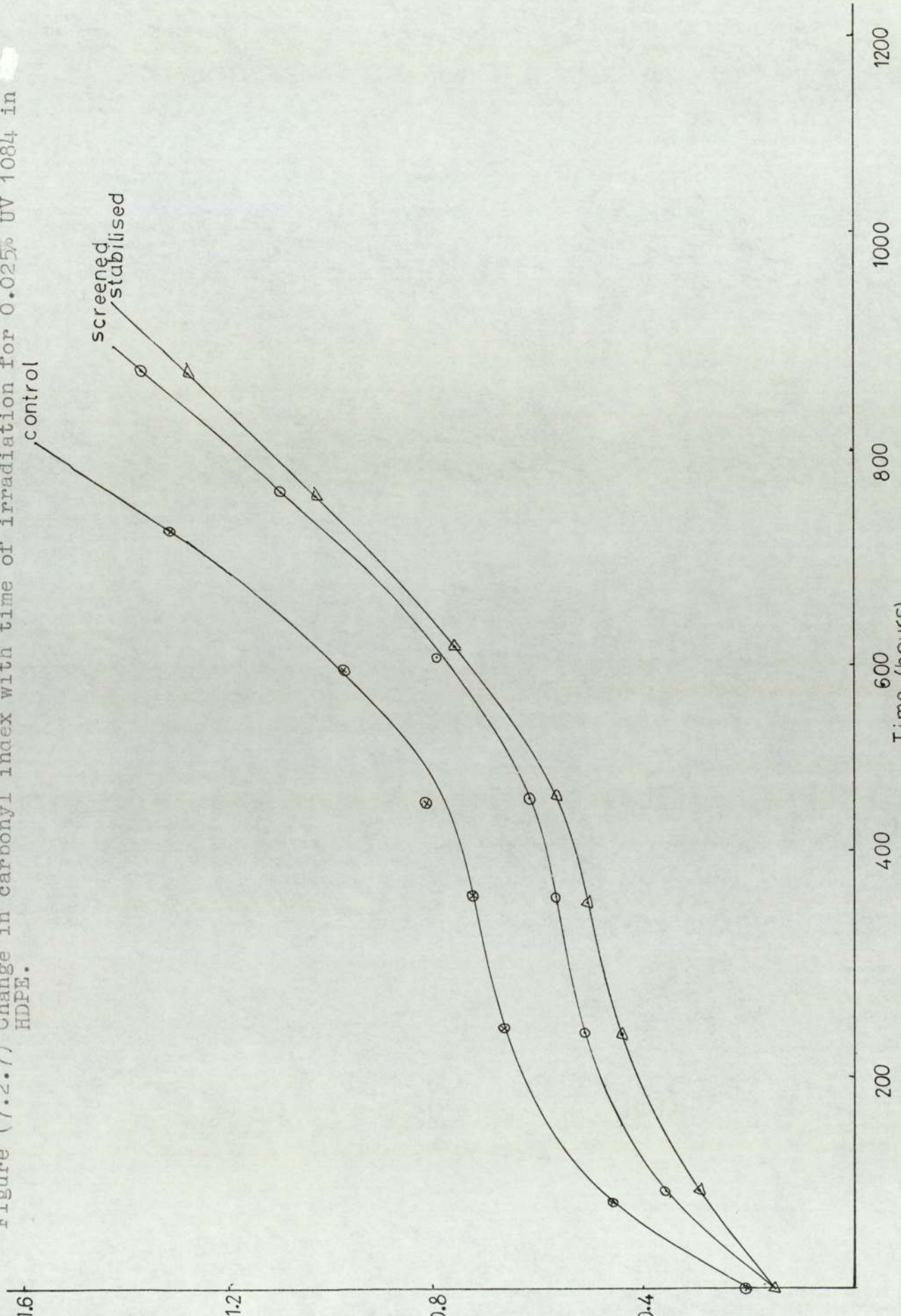

Figure (7.2.7) Change in carbonyl index with time of irradiation for 0.025% UV 1084 in HDPE.

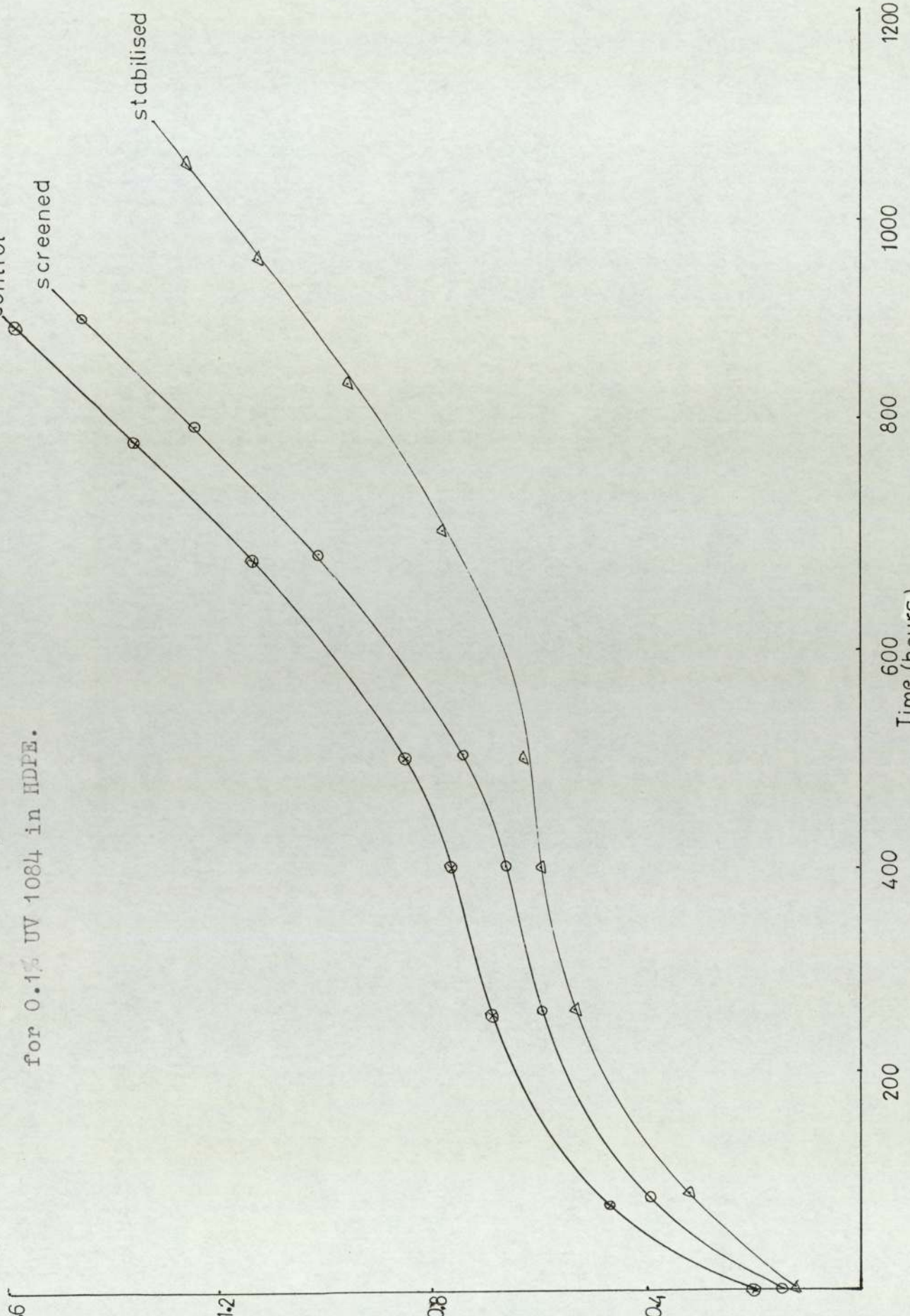

Figure (7.2.8a) Change in Carbonyl index with time of irradiation for 0.1% UV 1084 in HDPE.

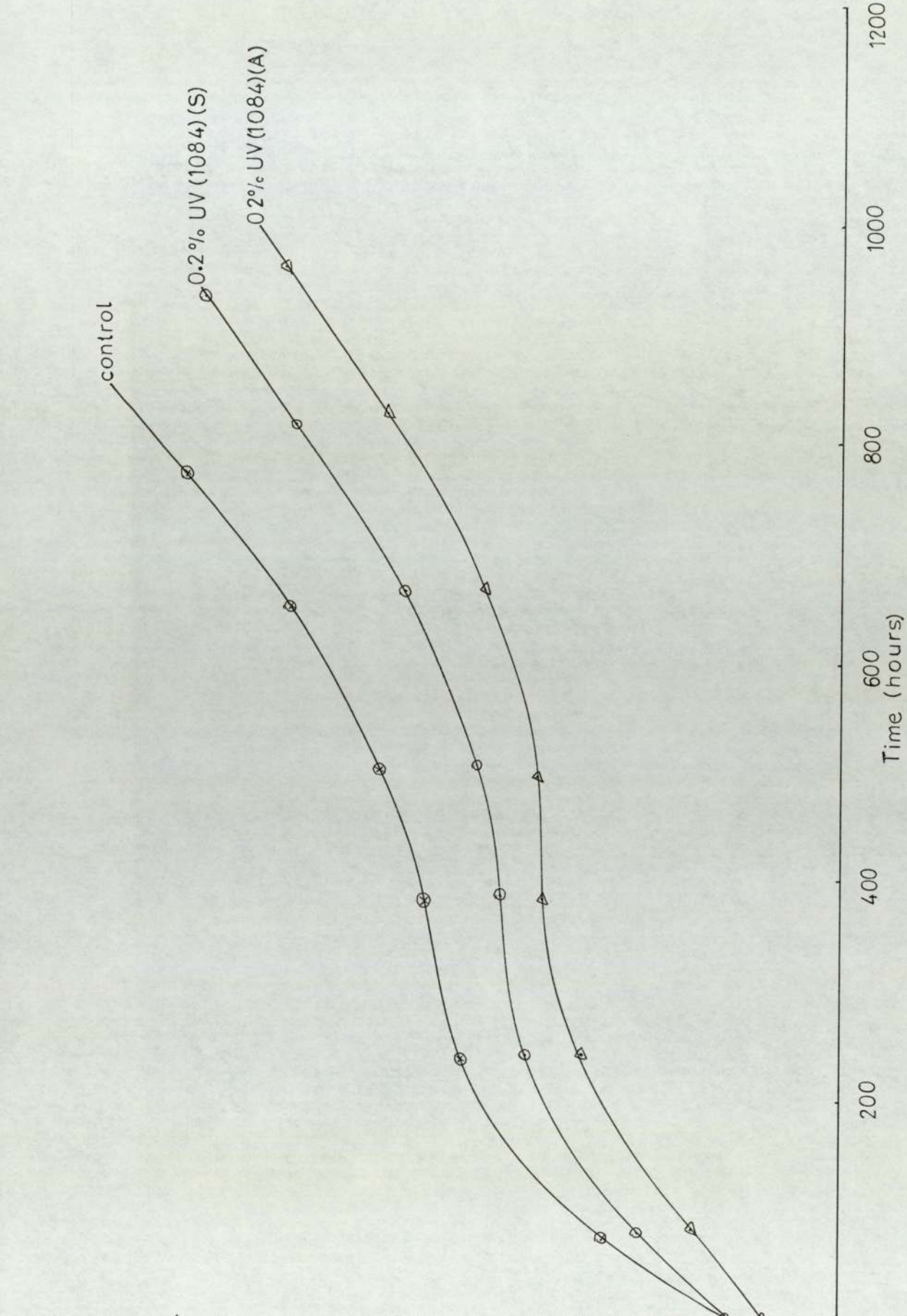

Figure (7.2.8b) Change in carbonyl index with time of irradiation for HDPE.

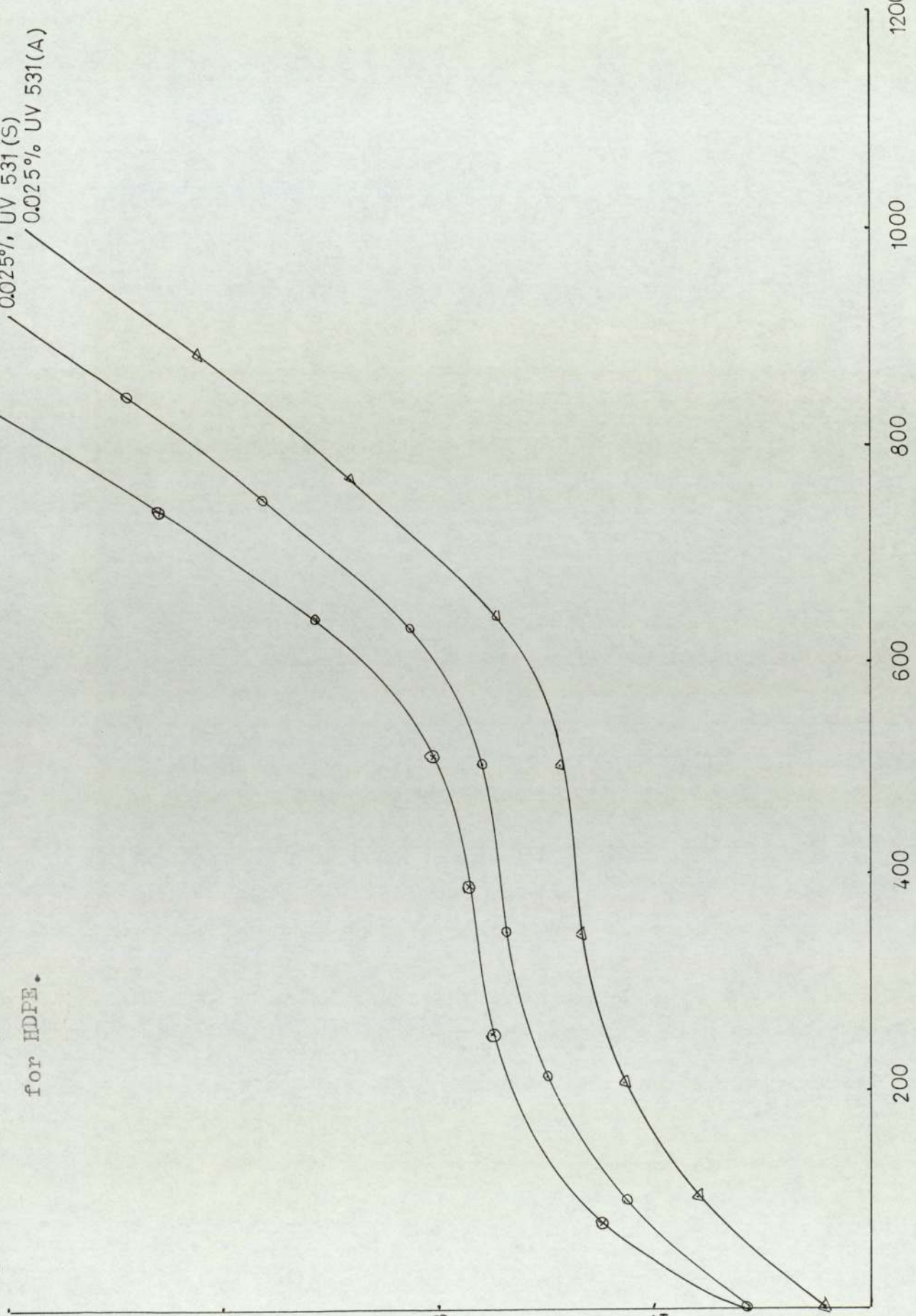

Figure (7.2.9) Change in Carbonyl index with time of irradiation for HDPE.

Figure (7.2.10) Change in Carbonyl index with time of irradiation for 0.1% UV 531 in HDPE.

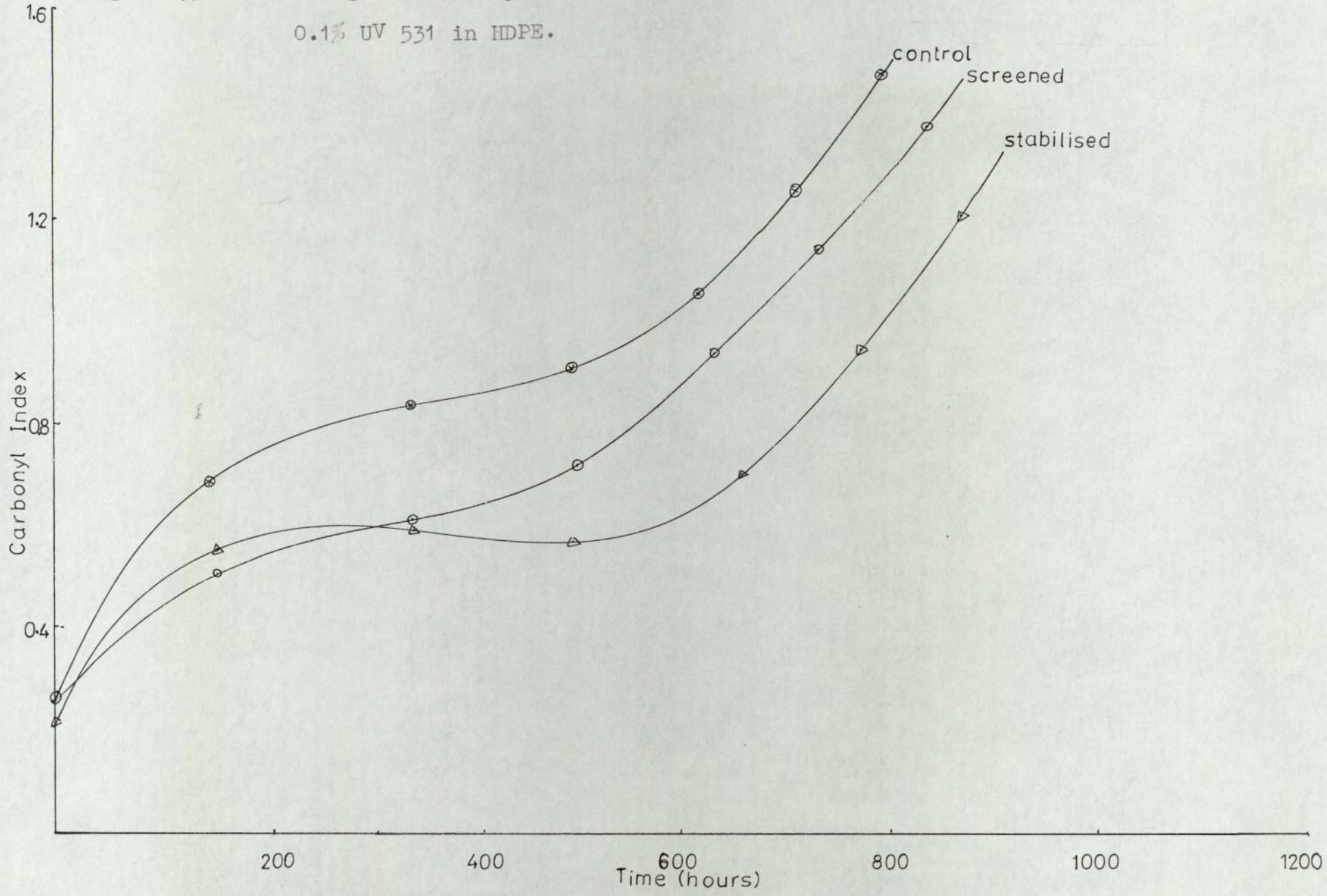

Figure (7.2.11) Change in carbonyl index with time of irradiation for 0.2% UV5 531 in HDPE.

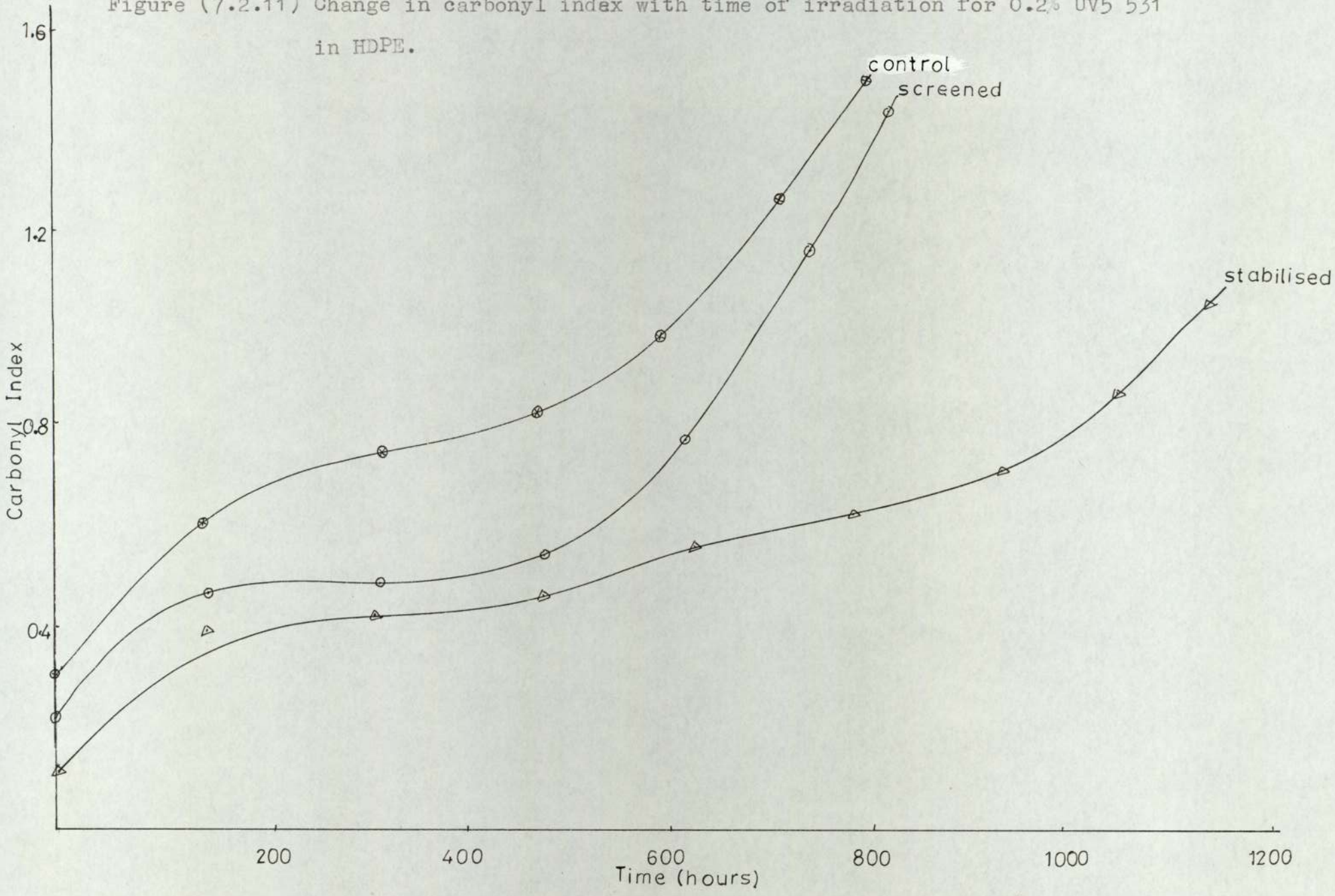

Fig. (7.3.2) Change in carbonyl index with time of irradiation for HDPE.

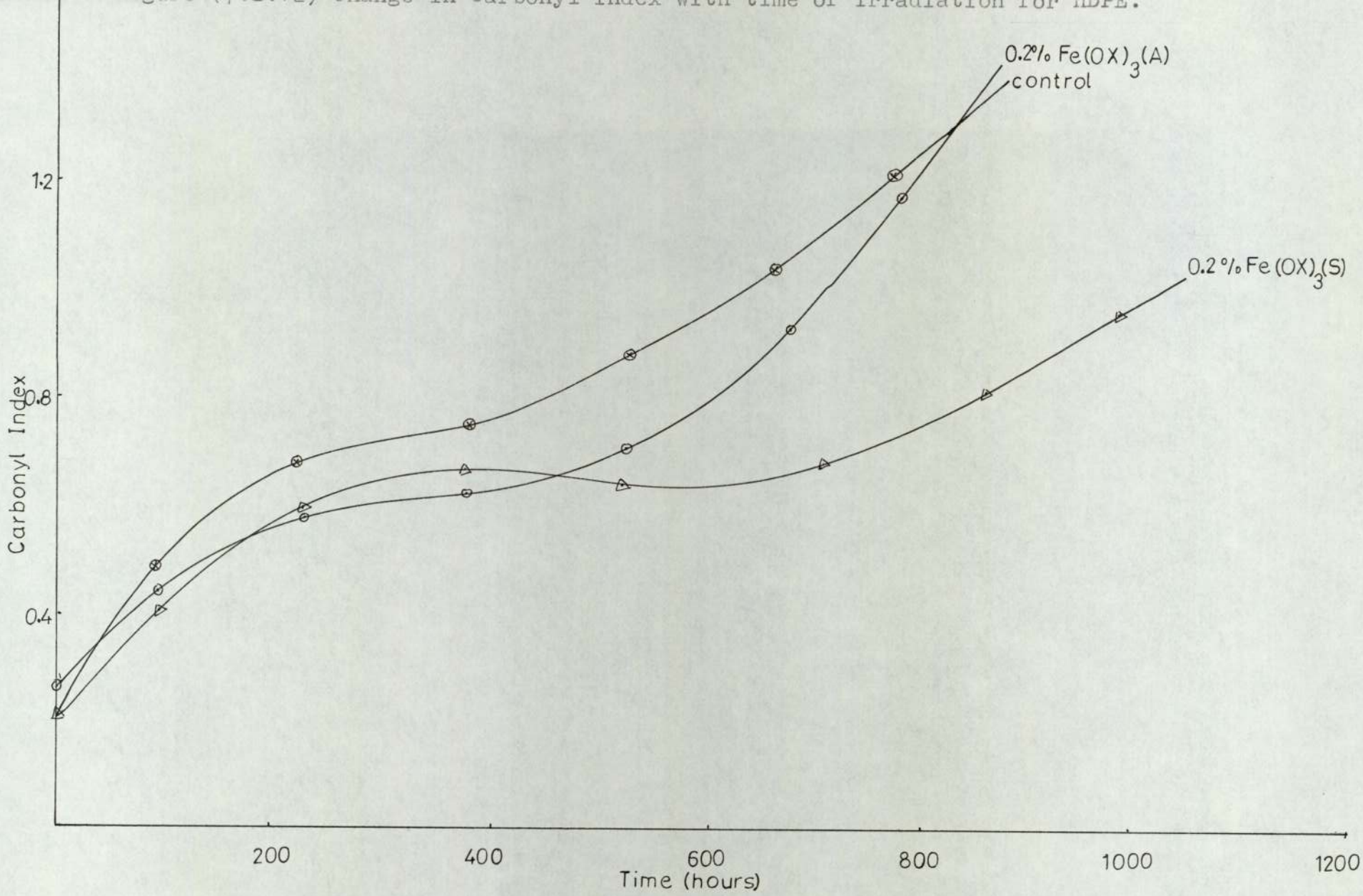

Figure (7.2.13) Change of Carbonyl index with time of irradiation for HDPE.

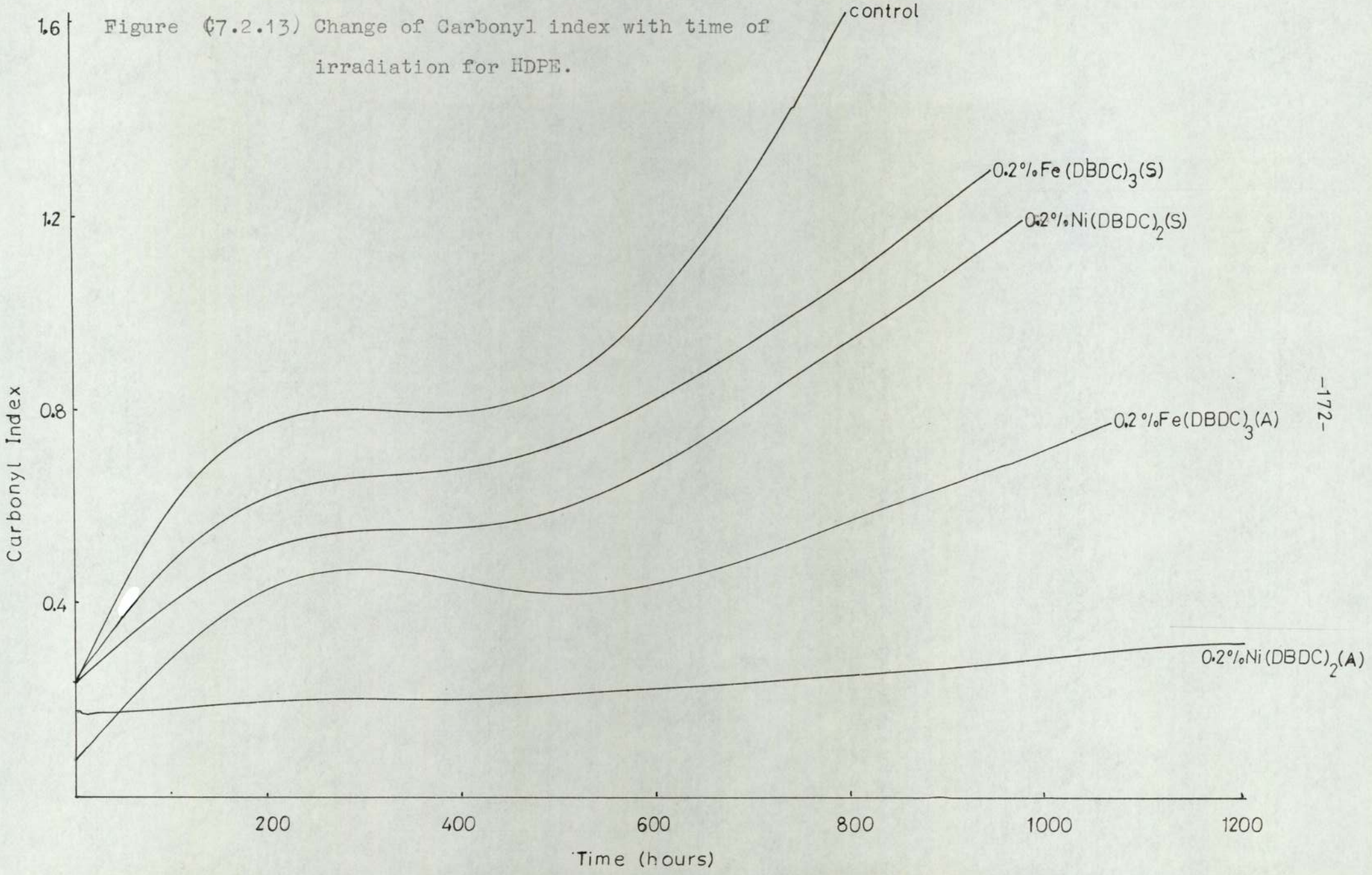

times. However 0.025% or 0.1% UV(1084) does not seem to import any stabilising activity as far as the embrittlement time is concerned. The values of carbonyl indices are slightly lowered. This is in very good agreement with the results observed with solution studies (Chapter 4).

The samples screened and stabilised with $Cu(OX)_2$ behaves in a similar manner to those screened and stabilised with $Ni(OX)_2$. The inflexion in the carbonyl index curve of the screened sample is due to the photolysis of hydroperoxides which is not observed in the stabilised sample. This would mean that $Cu(OX)_2$ too removes the hydroperoxides to a certain extent and hence the hydroperoxide derived carbonyls are not observed in the initial stages of photoxidation.

Figure (7.2.13) shows the variation of carbonyl index of HDPE when stabilised or screened with 0.2% $Fe(DBDC)_3$. These show the same inflexion due to the photolysis of hydroperoxides during the initial stages of photoxidation but $Fe(DBDC)_3$ seems to be a better stabiliser than a screen. Comparing this with the curves observed with $Fe(OX)_3$ Fig.(7.2.12), during the initial stages of photoxidation $Fe(OX)_3$ is a better stabiliser than a screen, however after a few hours of exposure to UV light the stabilised sample shows a rapid increase in the carbonyl index and exceeds the carbonyl index of the screened sample. The embrittlement times of the two samples are also the same. This is in agreement with the oxygen absorption curves shown in Chapter 4. The unexpected UV activating effect of the iron complex appears to be associated with its much lower thermal and photostability than the nickel and copper complexes.

Figure (7.2.14) The changes in functional group with time of irradiation for LDPE.

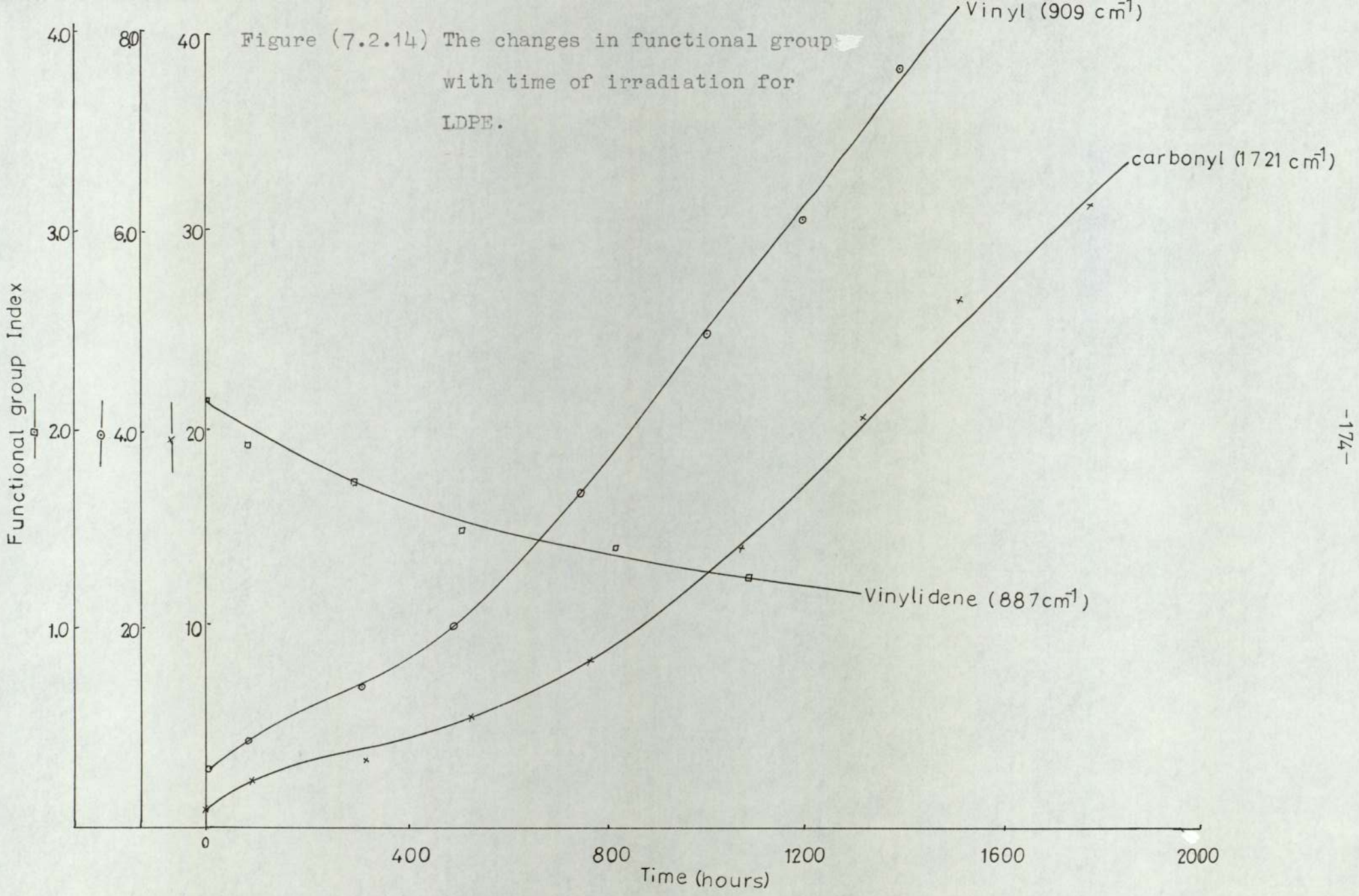

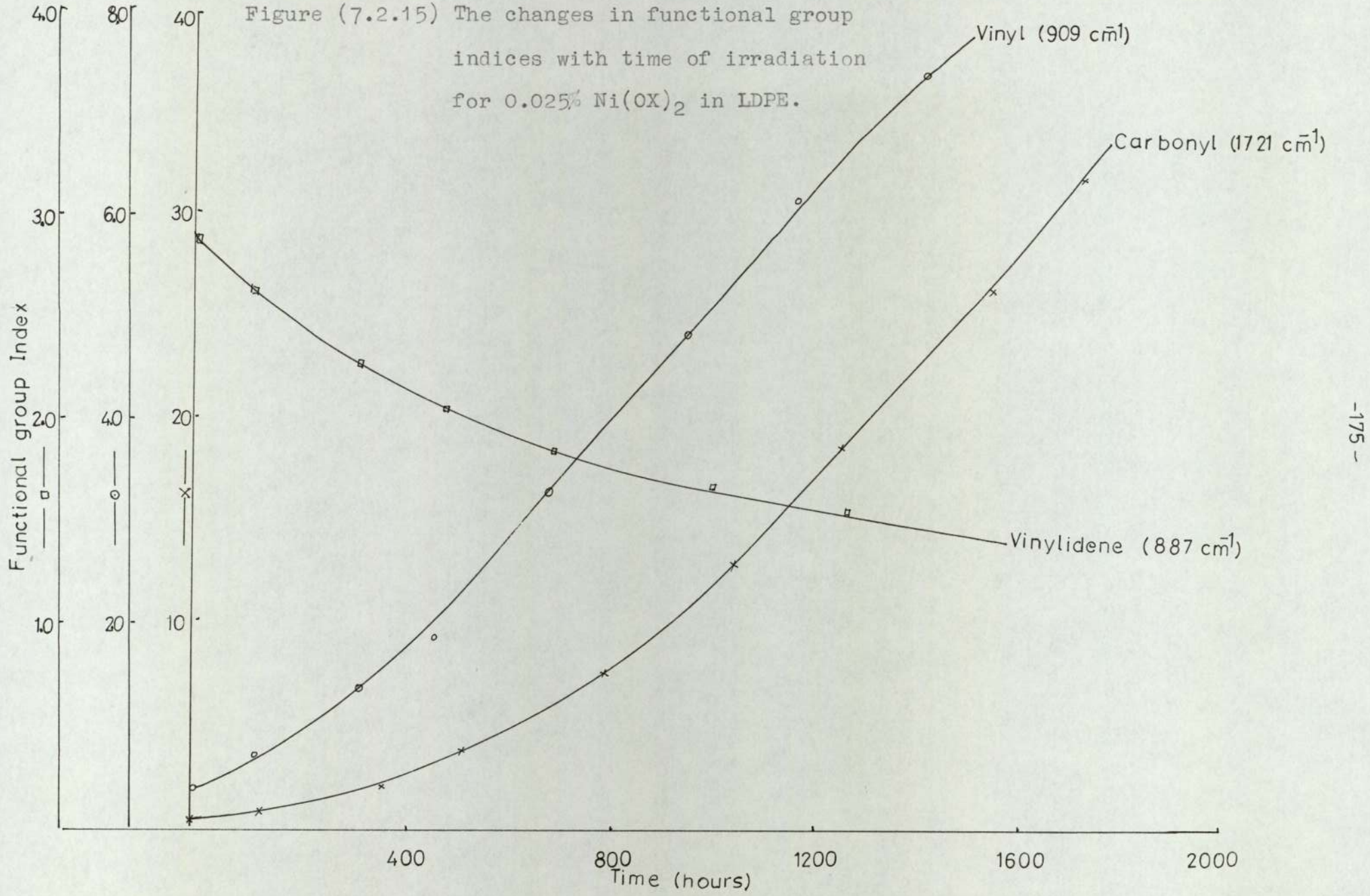
Figure (7.2.15) The changes in functional group indices with time of irradiation for 0.025% Ni(OX)2 in LDPE.
Vinyl (909 cm⁻¹)
Carbonyl (1721 cm⁻¹)
Vinylidene (887 cm⁻¹)
Functional group Index
Time (hours)
4.0
3.0
2.0
1.0
8.0
6.0
4.0
2.0
40
30
20
10
400
800
1200
1600
2000

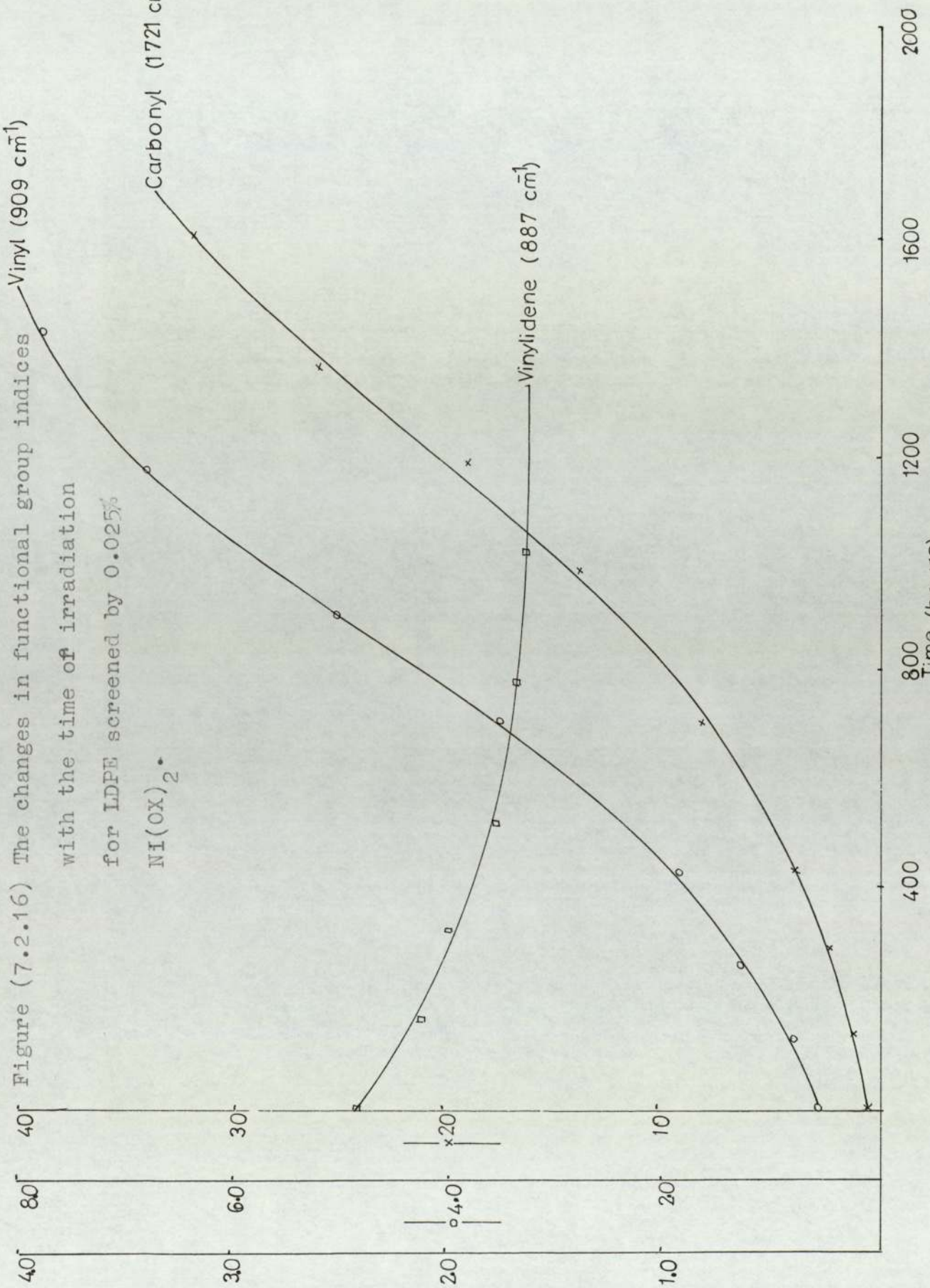

Figure (7.2.16) The changes in functional group indices with the time of irradiation for LDPE screened by 0.025% $Ni(OX)_2$.

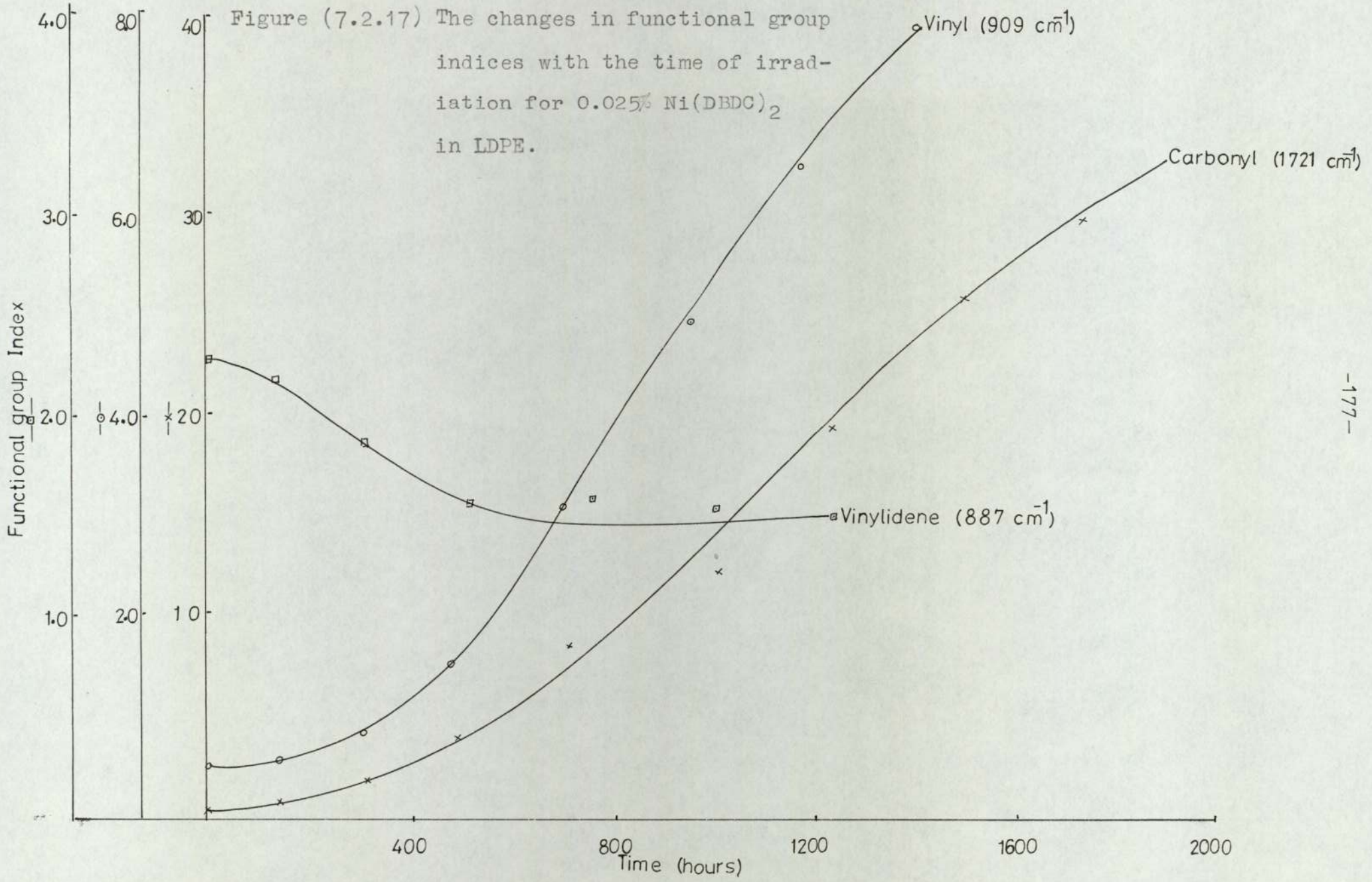
Figure (7.2.17) The changes in functional group indices with the time of irradiation for 0.025% Ni(DBDC)2 in LDPE.
Vinyl (909 cm-1)
Carbonyl (1721 cm-1)
Vinylidene (887 cm-1)
Functional group Index
4.0
3.0
2.0
1.0
80
6.0
4.0
2.0
40
30
20
10
400
800
1200
1600
2000
Time (hours)

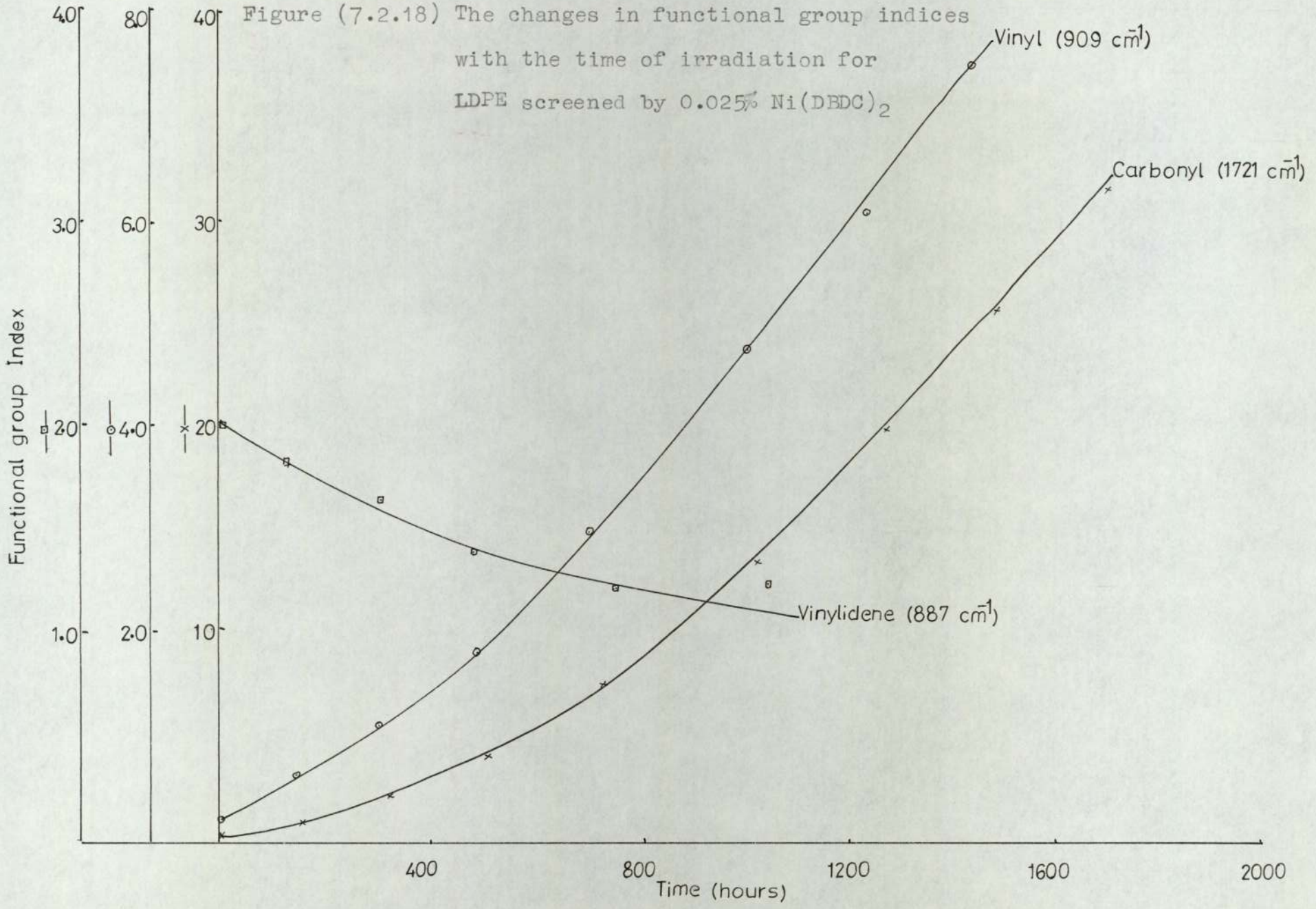
Figure (7.2.18) The changes in functional group indices with the time of irradiation for LDPE screened by 0.025% Ni(DBDC)2
Vinyl (909 cm-1)
Carbonyl (1721 cm-1)
Vinylidene (887 cm-1)
Functional group Index
Time (hours)
4.0
3.0
2.0
1.0
8.0
6.0
4.0
2.0
40
30
20
10
400
800
1200
1600
2000

Figure (7.2.19) The changes in functional group indices with the time of irradiation for 0.025% VU 1084 in LDPE.

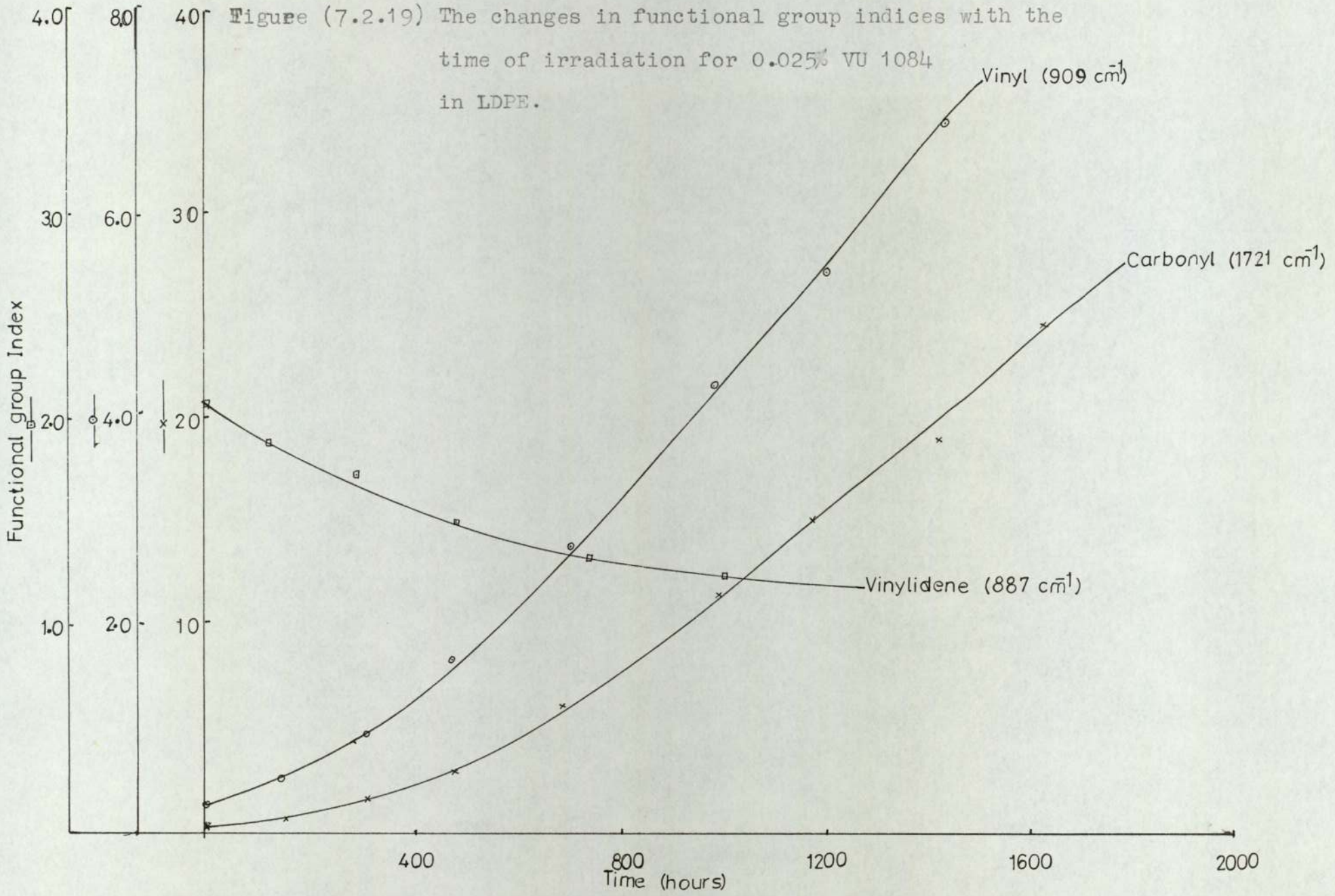

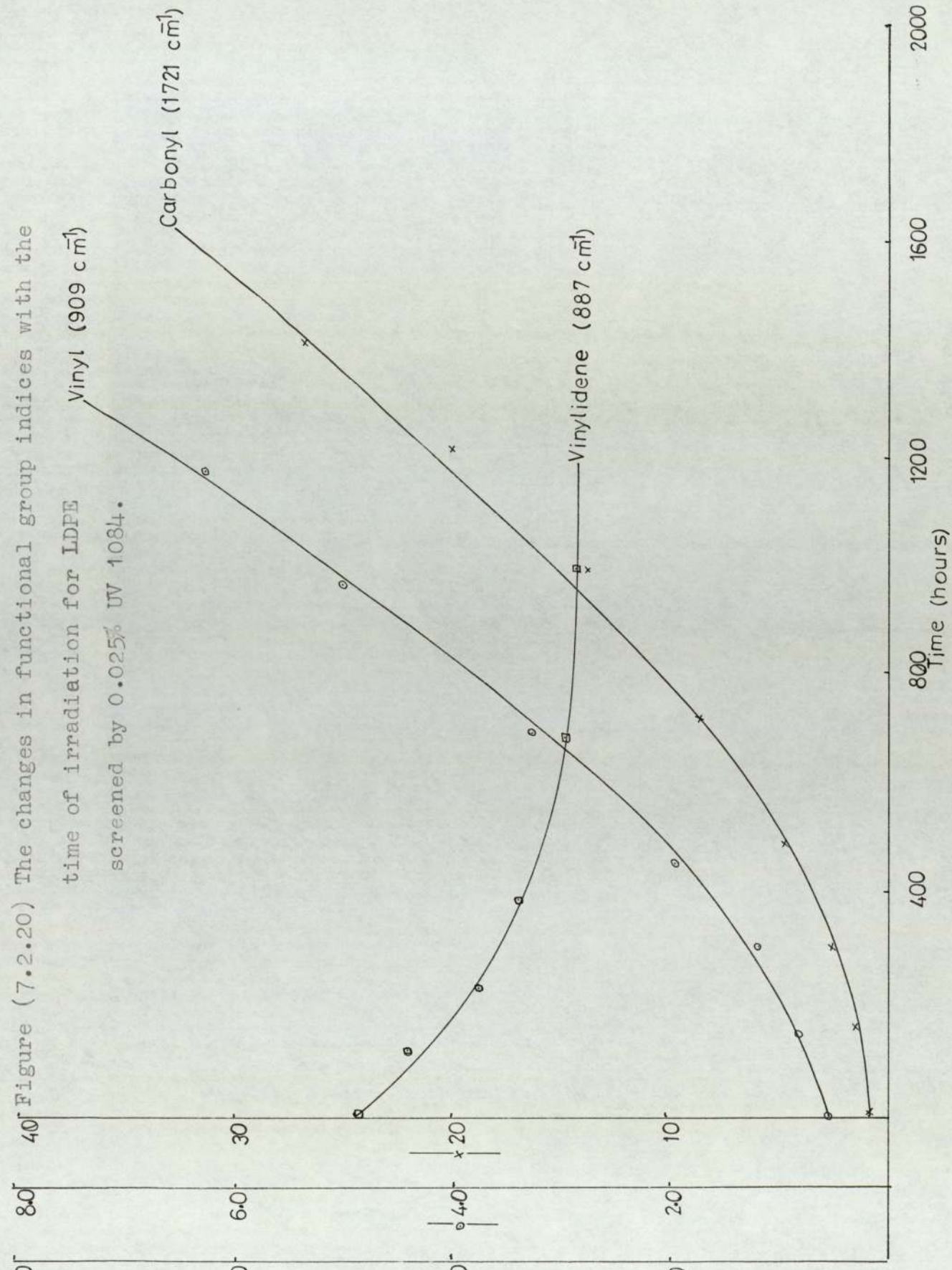

Figure (7.2.20) The changes in functional group indices with the time of irradiation for LDPE screened by 0.025% UV 1084.

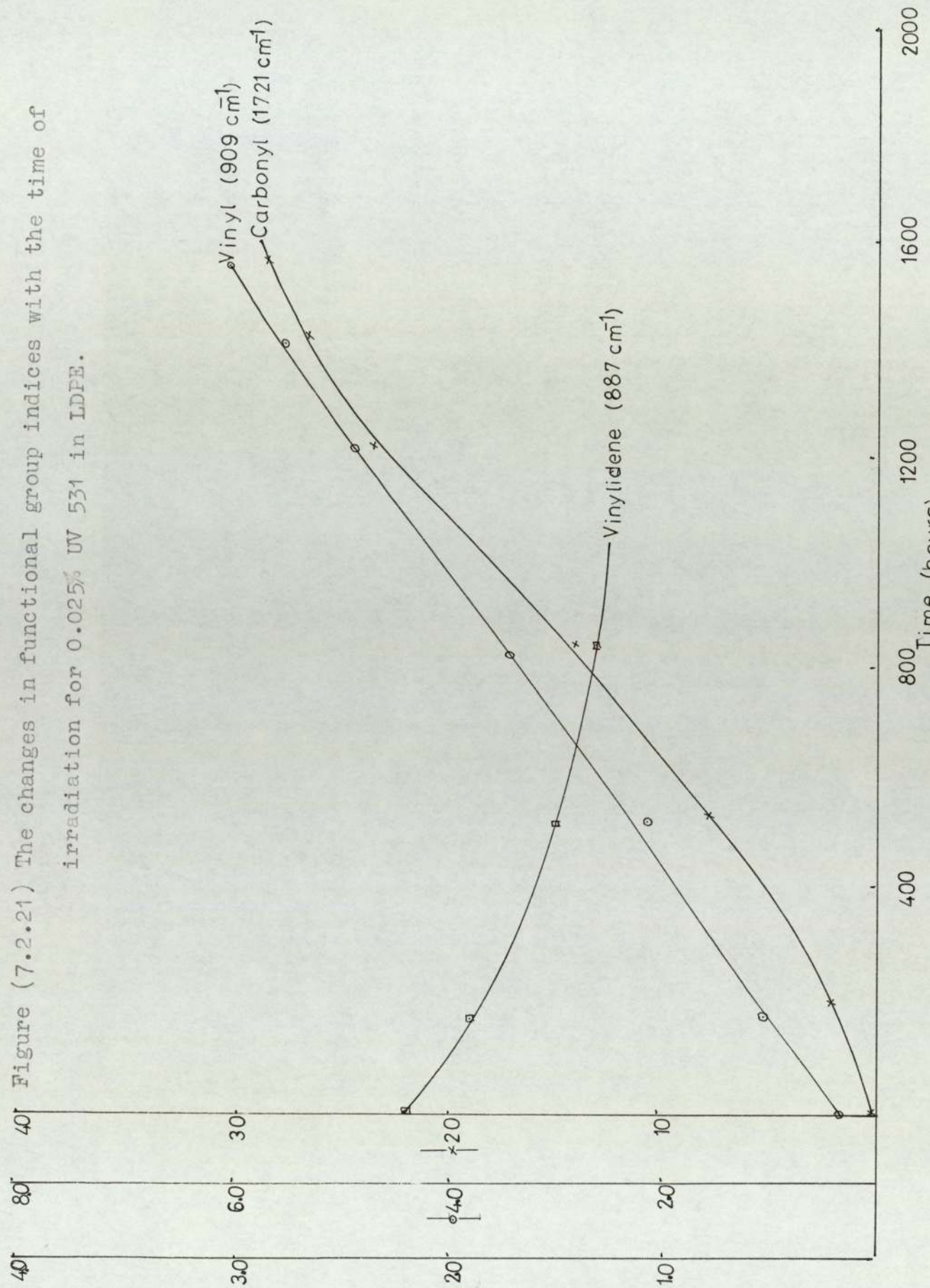

Figure (7.2.21) The changes in functional group indices with the time of irradiation for 0.025% UV 531 in LDPE.

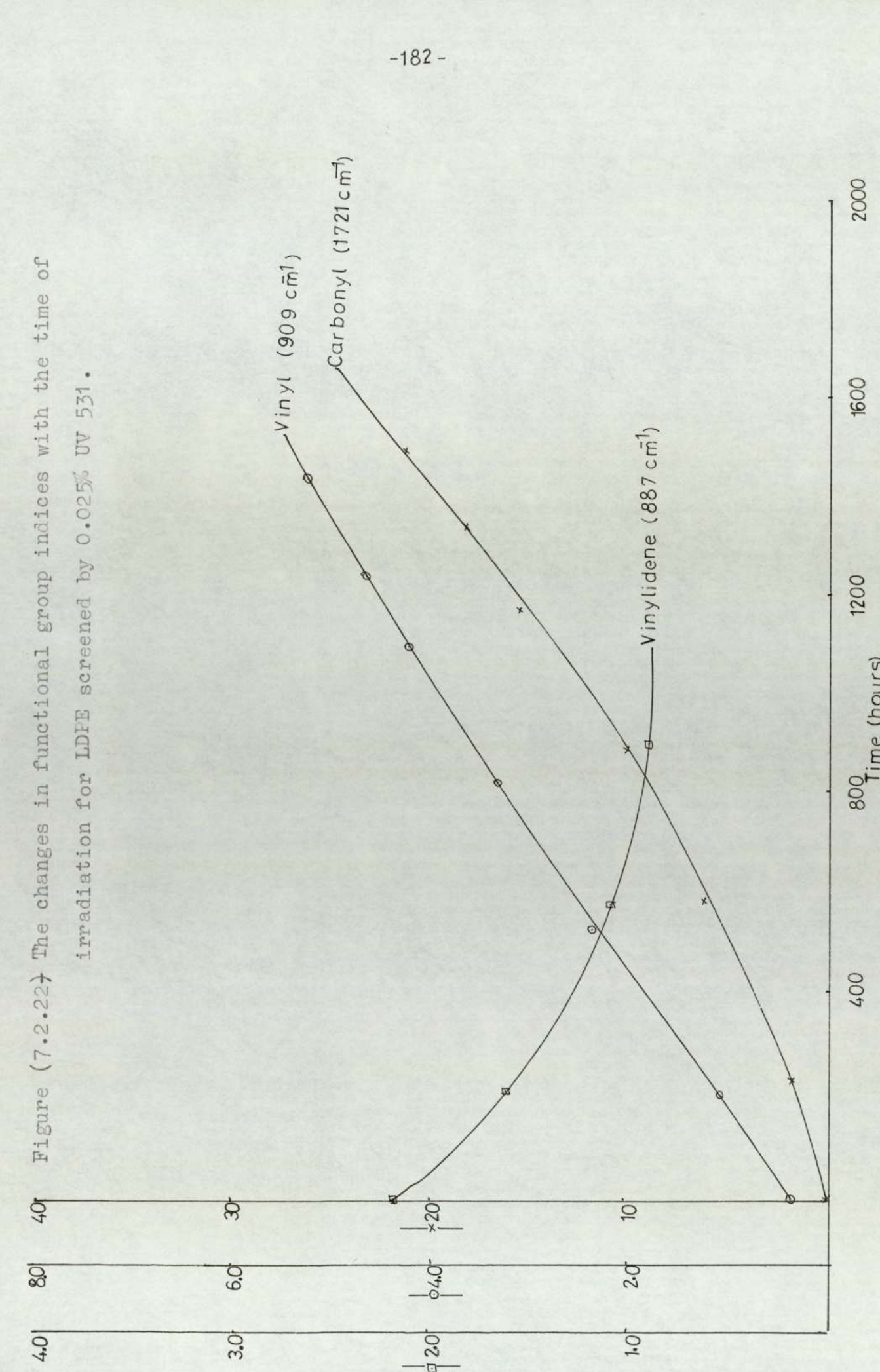

Figure (7.2.22) The changes in functional group indices with the time of irradiation for LDPE screened by 0.025% UV 531.

Inmildly processed LDPE samples Fig.(7.2.14) vinylidene groups (887± 1 cm^{-1}) initially present decay rapidly on UV irradiation and this precedes the formation of significant amounts of carbonyl. This suggests that vinylidene decay must be in some way associated with the photoinitiation step. The formation of vinyl (909 cm^{-1}) which is present to a much smaller entent in the processed polymer also parallels carbonyl formation and appears to be consequent upon it. This is the expected sequence of events if vinyl is formed by Norrish II breakdown of carbonyl. The formation of aldehyde, Figure (7.2.2) (band at 1785 cm^{-1}) and carboxylic (1185 cm^{-1}) are almost certainly a consequence of Norrish I photolysis of carbonyl. These support the earlier conclusion that once significant amounts of carbonyl are present in the polymer either as a result of thermal oxidation or by UV catalysed oxidation then they are involved in the photodegradation process, however the rapid disappearance of vinylidene suggests that other photo-oxidative reactions occur involving this group and that this process precedes carbonyl formation.

Figures (7.2.14) to (7.2.20) relates the changes in carbonyl, vinyl and vinylidene indices with exposure for stabilised and unstabilised LDPE. Films prepared from the polymers mixed with 0.025% $Ni(OX)_2$, 0.025% $Ni(DBDC)_2$ 0.025% cyasorb UV(1084) were irradiated and the carbonyl indices were measured at intervals. In the case of the unstabilised and screened samples (the samples containing hydroperoxides and vinylidine) there was a rapid increase in carbonyl formation due to the above photoxidation which destroys both vinylidene and hydroperoxide whereas the sample stabilised with 0.025% $Ni(DBDC)_2$ showed a short induction period in both

TABLE 7.2

Embrittlement times of HDPE, with the stabiliser used as an additive (A) or screen (S)

Complex	Concentration (gm/100gm polym)	Embrittlement time (hrs)
-	-	∿ 665
$Ni(OX)_2$ (A)	o.1%	> 2000
$Ni(OX)_2$ (S)	0.1%	∿ 665
$Cu(OX)_2$ (A)	0.1%	> 1835
$Cu(OX)_2$ (S)	0.1%	665
$Fe(OX)_3$ (A)	0.1%	∿ 665
$Fe(OX)_3$ (S)	0.1%	∿ 665
$Ni(DBDC)_2$ (A)	0.1%	> 2000
$Ni(DBDC)_2$ (S)	0.1%	∿ 665
$Fe(DBDC)_3$ (A)	0.1%	1835
$Fe(DBDC)_3$ (S)	0.1%	∿ 665
UV(1084) (A)	0.1%	∿ 665
UV(1084) (S)	0.1%	∿ 665
UV(531) (A)	0.1%	> 2000
UV(531) (S)	0.1%	∿ 665

the disappearance of vinylidene and formation of carbonyl as compared with the sample screened with 0.025% $Ni(DBDC)_2$. However the effect of 0.025% $Ni(OX)_2$ or 0.025% UV(1084) on the carbonyl formation or vinylidene disappearance rates were much less marked and showed little difference from the control. The differences between the stabilised and screened samples too were much less. Higher concentrations of the stabilisers would have been more effective. From this it follows that anti-oxidants which destroy peroxides or in some other way inhibits the oxidative chain reaction are likely to be much more effective in commercial polymers. Higher concentrations of these stabilisers in LDPE would have shown marked differences in their stabilities.

The IR spectra of polystyrene on UV irradiation are shown in figure (7.2.27). The oxidative photodegradation of polystyrene has been extensively studied. It has been shown[99,100] that oxygen preferentially attacks the α-hydrogens found on the backbone of the polystyrene chain and that the initial product is hydroperoxide[101]. However positive proof of the structure of the final product resulting from the decomposition of this hydroperoxide has not so far been found.

Several investigations[101,102] has postulated an acetophenone type of structure.

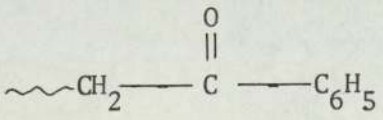

while others postulated an aromatic carbonyl similar to benzal acetophenone[100].

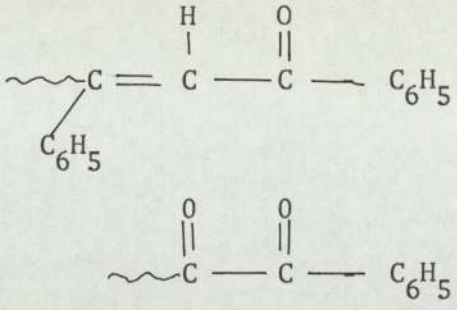

or a dicarbonyl compound

Intense sharp bands were formed at 1705 cm^{-1}, 1740 cm^{-1} and 1780 cm^{-1}, and continued to grow during degradation. The band at 1740 cm^{-1} was taken as a measure of oxidation with the band at 1940 cm^{-1} as the reference. Here the nickel dithiocarbamate complex seems to be less effective as a stabiliser in the latter stages of oxidation as compared to $Ni(OX)_2$ and UV(1084) complexes Figure (7.2.23). This may be due to the less peroxidation of the Polystyrene backbone during processing as compared to HDPE and LDPE. Also the absence of the prominent inflexion is the carbonyl index measurements observed in polyethylenes confirm this to a certain extent. However, figures (7.2.23) to (7.2.29) show similar differences in the stabilities of samples screened and stabilised respectively by the three complexes. These three complexes as additives seem to impart an additional stability to polystyrene other than screening. However no induction period to carbonyl formation was observed even though the rate of increase of carbonyl index was not uniform.

The formal similarity of the behaviour of the transition metal oximes with that of the dithiocarbomates argues a similarity in mechanism. However, these metal complexes are not catalytic peroxide decomposers and although some of them, mainly the nickel and copper complexes possess antioxidant properties their UV stabilising effect appears to be primarily due to UV

Figure (7.2.23) Carbonyl index vs time for polystyrene.

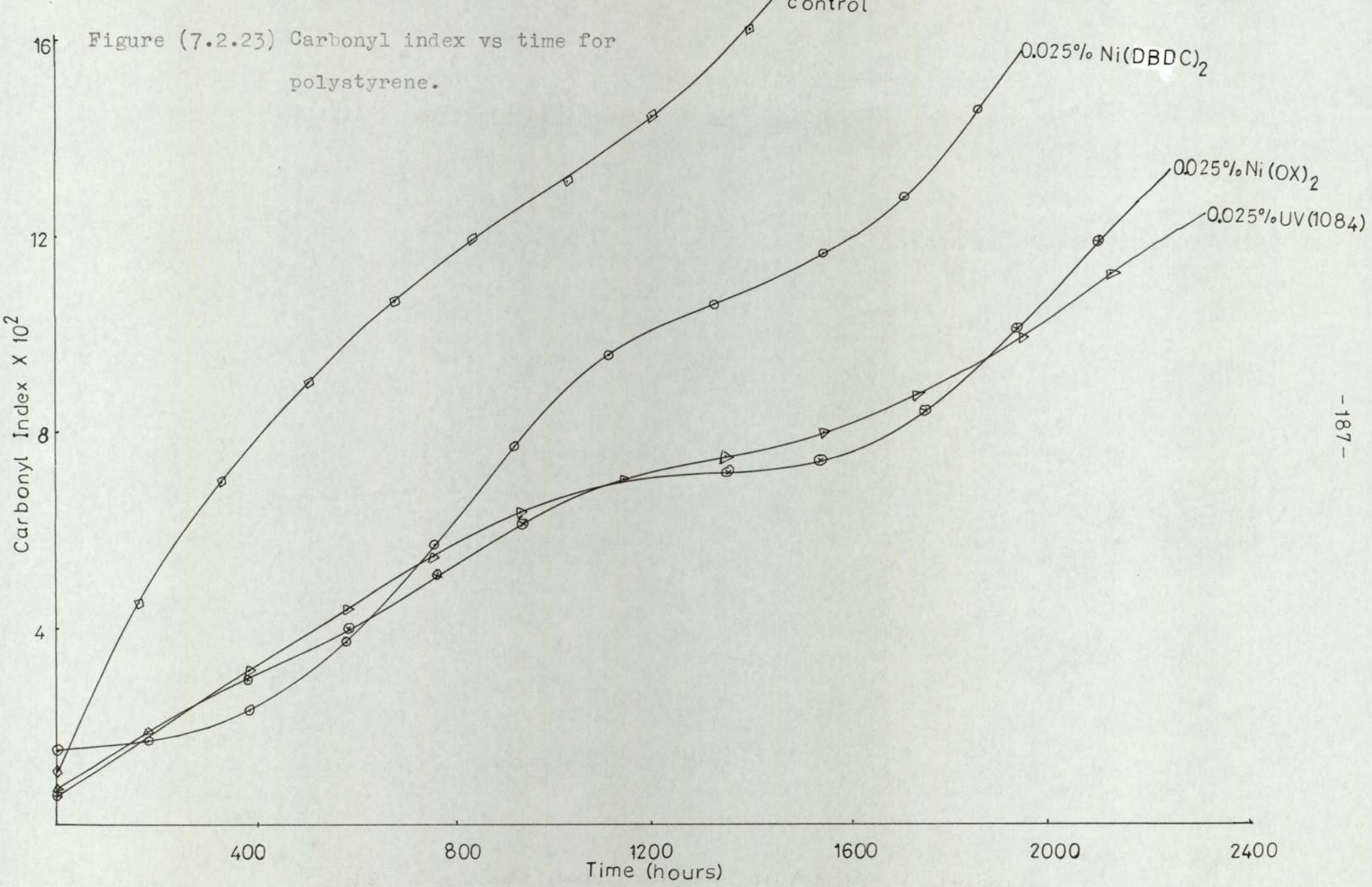

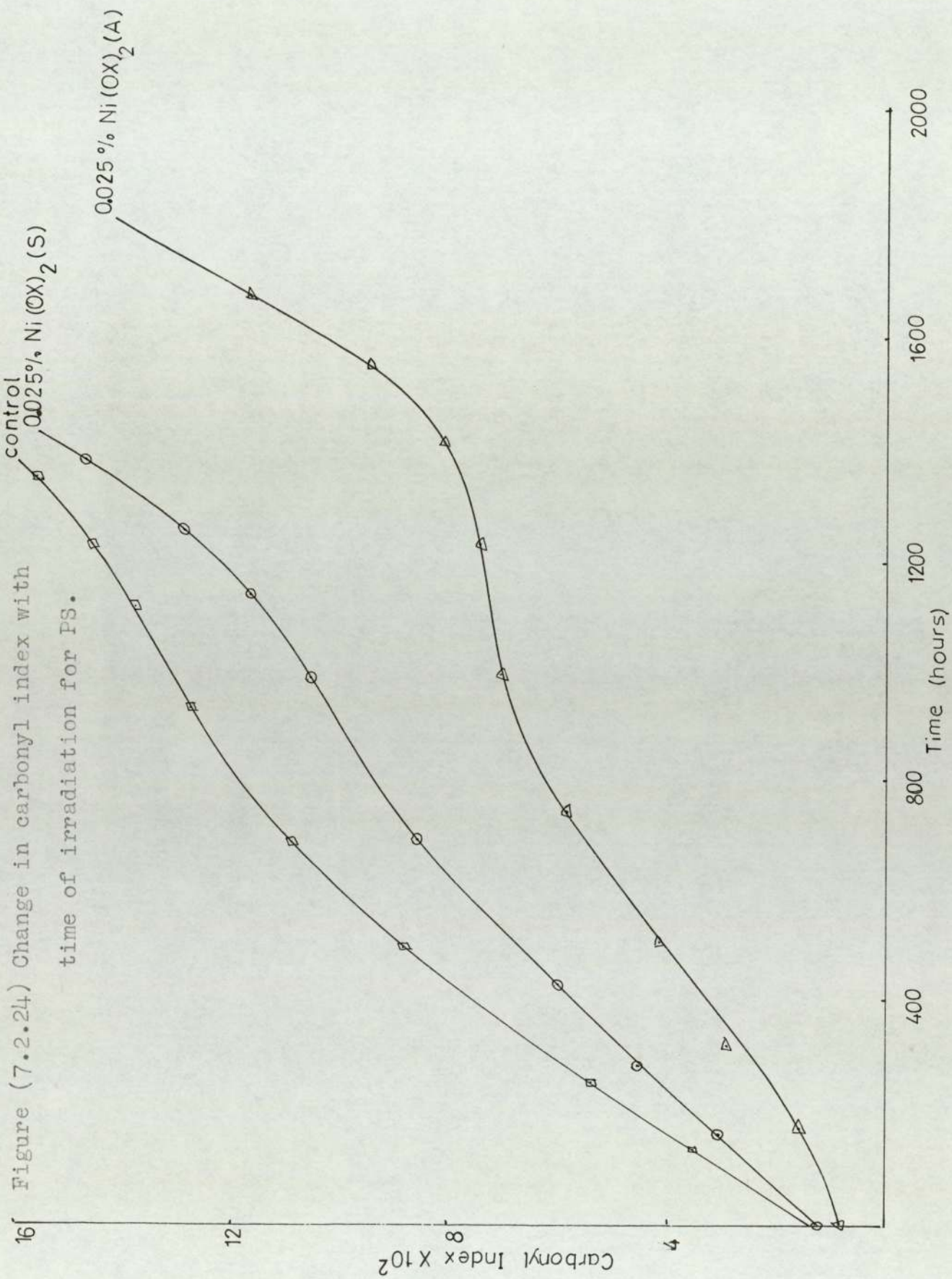

Figure (7.2.24) Change in carbonyl index with time of irradiation for PS.

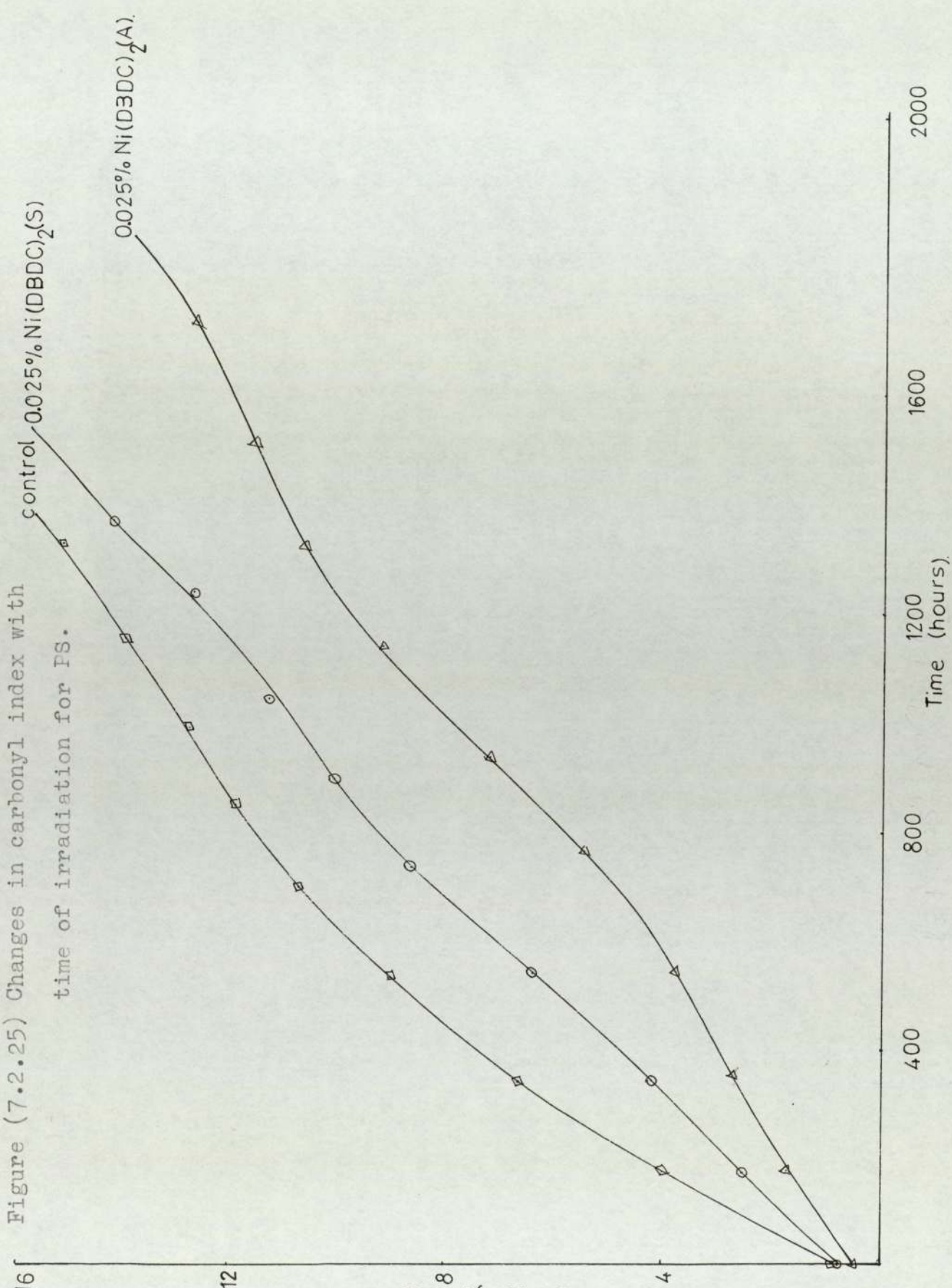

Figure (7.2.25) Changes in carbonyl index with time of irradiation for PS.

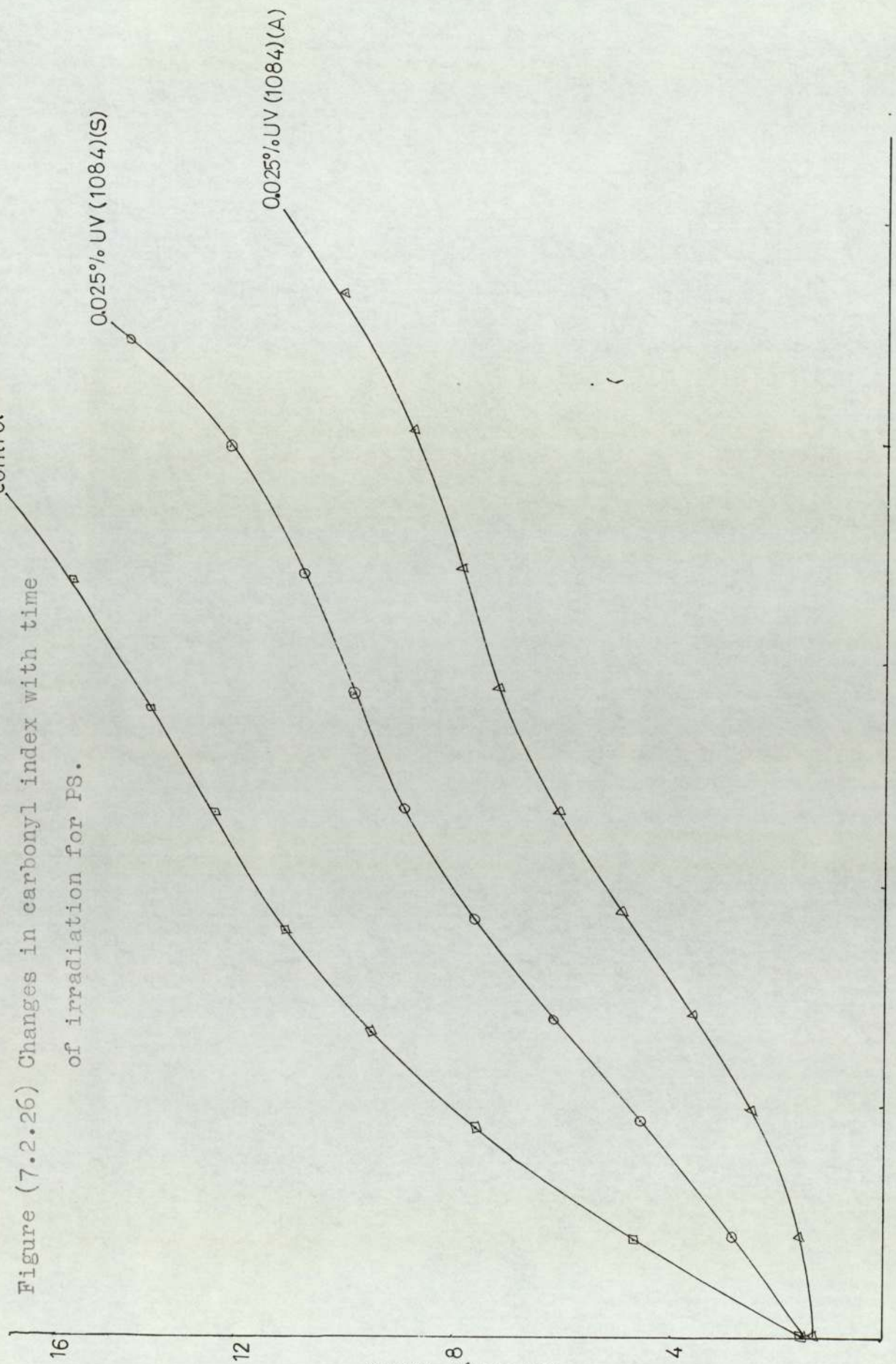

Figure (7.2.26) Changes in carbonyl index with time of irradiation for PS.

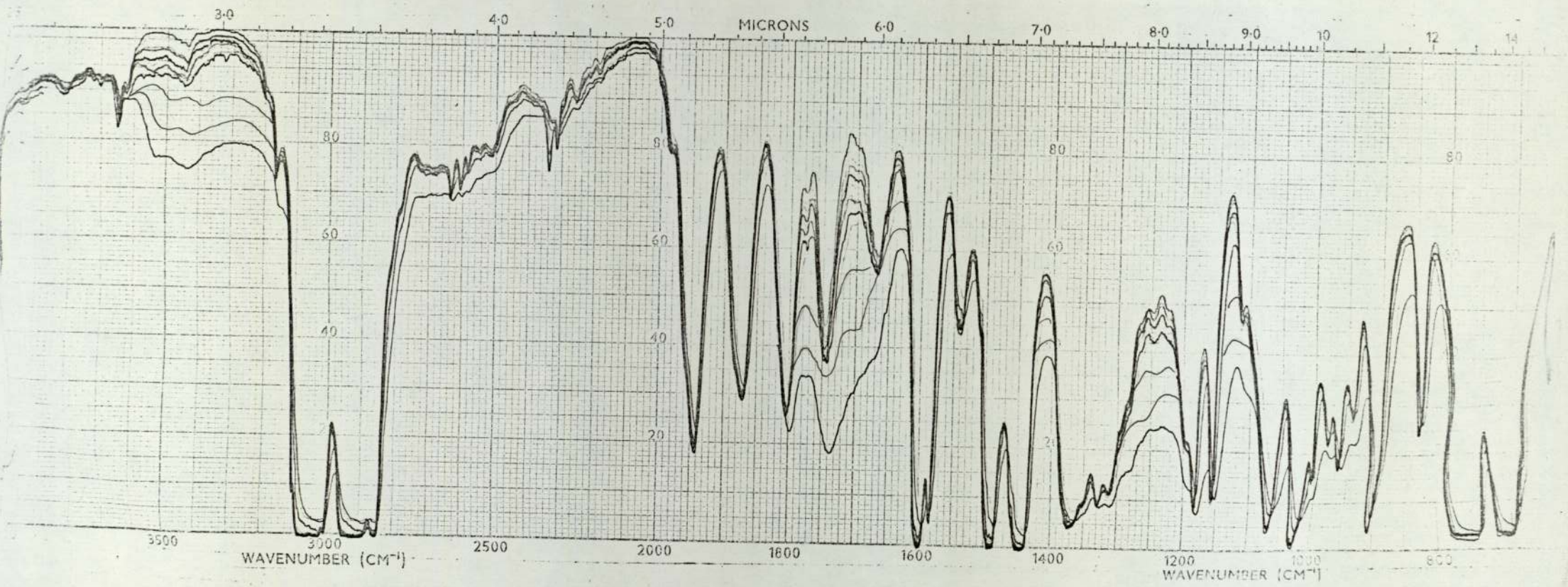

Figure (7.2.27) Infra-Red spectrum of PS.

screening (Chapter 6). The rapid change of the iron complex from a photostabiliser to a photo-activator]see figures (7.2.12) and (7.2.13)] again results from the photoinstability of the initially stabilising complex.

CONCLUSIONS AND SUGGESTIONS FOR FURTHER WORK

The work that has been described shows that the additives used influence the rates of oxidation and the formation of oxidation products in both polymers and model system.

All three nickel chelate compounds, $Ni(OX)_2$, $Ni(DBDC)_2$ and cyasorb UV(1084) were found to retard the oxidation initially by a process of screening the ultra-violet radiation. The order of effectiveness of these additives were found to be $Ni(DBDC)_2$ > $Ni(OX)_2$ > cyasorb UV(1084). There is a good deal of evidence to prove that the main stabilising activity of $Ni(DBDC)_2$ is due to its ability to decompose hydroperoxides. The kinetic measurements of this reaction and subsequent product analysis confirmed this reaction to follow first order ionic reaction giving phenol and acetone.

The behaviour of $Ni(DBDC)_2$ in high density polyethylene seems to be very similar to its effect on hydroperoxide and carbonyl formation in low density polyethylene. Carbonyl formation and vinylidene disappearance during UV irradiation are both inhibited by $Ni(DBDC)_2$. This is consistent with its behaviour as a hydroperoxide decomposes in model systems.

The behaviour of $Ni(OX)_2$ and $Cu(OX)_2$ were similar both in model systems and polymer studies. $Ni(OX)_2$ too reacted with hydroperoxides but not catalytically as in the case of metal dithiocarbomates. The instability of these complexes to UV radiation eliminates any possibility

of physical quenching of excited states of carbonyl and oxygen. The fact that benzophenone in the presence of oxygen does not seem to have any effect on the stability of the nickel chelates eliminates any possibility of photo-chemical quenching. The results from oxygen absorption studies confirmed the fact that these nickel chelates have no additional effect other than screening in a triplet activated model system. This is conclusive evidence that chemical quenching of the triplet excited state is not an important mechanism in the photostabilisation by these metal chelates.

$Ni(OX)_2$ was also shown to be a hydroperoxide decomposer but not in this case catalytic. This seems to agree very well with the carbonyl formations observed in high density polyethylene, where the hydroperoxide derived carbonyls were absent in the stabilised samples, and the evidence suggests that hydroperoxides oxidise the metal oxime to give ortho hydroxy acetophenone and salicylic acid as the major oxidation products and methyl cumyl ether as a biproduct in solution studies. This would explain the stoichiometric reaction between the complex and hydroperoxides and the lower stability activity of $Ni(OX)_2$.

UV(1084) appears to behave only as a UV screen when present as an additive in photoxidising cumene. There is no evidence that it has any additional function in either a triplet activated or hydroperoxide initiated photoxidation.

The absence of evidence of triplet carbonyl or singlet oxygen quenching effects in the photoxidation of cumene is at variance with the

previous theories put forward on the mechanism of action of these nickel complexes as UV stabilisers. The two initiator systems isobutyl methyl ketone and benzophenone makes the system applicable to both polyolefins and polystyrene respectively.

The results of these metal chelates as additives and screens in polystyrene were not very conclusive, due to the low concentrations of additives used. Higher concentrations of these should give marked differences in carbonyl indices. Also oxygen absorption studies of these polymers when stabilised and screened by the respective additives will be interesting.

The iron complex $Fe(OX)_3$ behaves as a delayed action photosensitizer both in polyolefins and model systems and this effect is due to the photolysis of the complex to give initiating free radicals.

To evaluate the photochemical reaction of the various additives it is necessary to find evidence for the production of free radicals under the influence of UV light. Electron spin resonance methods used in the present study were not successful therefore a chemical method by studying a reaction which proceeds via free radical mechanisms should be used. An example of this method is to study both the photo and thermal polymerisation of vinyl monomers, for example styrene using the photoactivator as a probable problem initiator.

REFERENCES

1. Munk, A.V. and Scott, J.R., Nature 177, 857 (1956)
2. Evans, D.F., J.C.S. 345 (1953).
3. Tsubomura, H. and Mullikan, R.S., J.A.C.S. 82, 5966, (1966).
4. Hoijfink, G.J., Act.Chem.Res. 2, 114, (1969).
5. Chien, J.C.W., J.Phys.Chem. 69, 4317 (1965)
6. Carlsson, D.S. and Robb, J.C., Trans.Farad.Soc. 62, 3403 (1966)
7. Betts, J.C. and Robb, J.C., Trans.Farad.Soc. 64, 2402 (1968)
8. Hutson, G.V. and Scott, G., Europ.Polym.J. 10, 45 (1974)
9. Baum, B., J.of Appl.Polym.Sci. 2, 281 (1959)
10. Kaplan, and Kelleher, P.G., J.Poly.Sci.Part B 9, 563 (1971)
11. Norrish,R.G.W. and Searby,M.H., Proc.Roy.Soc.(London) A 237, 464 (1956)
12. Bolland, J.L., Proc.Soc. A186, 218 (1946)
13. Bolland, J.L., Trans.Farad.Soc. 46, 358 (1950)
14. Briggs, P.J. and McKellar, J., J.Appl.Polym.Sci. 12, 1825 (1958)
15. Briggs, P.J. and McKellar, J., Chemistry and Industry, 622 (1968)
16. Harper, D.J., McKellar, J.F. and Turner, F.H., J.Appl.Polyp.Sci. 18, 2802 (1974)
17. Chien, J.C.W., Connor, W.P., J.A.C.S. 90, 1001 (1968)
18. Trozzolo, A.M. and Winslow, F.H., Macromolecules 1, 98 (1968)
19. Flood, J., Russel, K.E. and Wan, S.K.S., Macromolecules 6, 669 (1973)
20. Adamczyk, and Wilkinson, F., J.C.S. Faraday II, 68 (1972)
21. Carlsson, D.J., Suprunchuk, T. and Wiles, D.M., Macromolecules, 5, 654 (1972)
22. Carlsson, D.J., Suprunchuk, T. and Wiles, D.M., J.Polym.Sci. B11,6(1973)
23. Pivovarov, A.P., Ershov, U.A. and Lukovnikov, A.F., Soviet Plastics 10, 11 (1967)

24. Heller, H.J. and Blattman, H.R. Pure and Applied Chemistry 36, 141 (1973)

25. Cicchett, O., Adv.Polym.Sci. 1 70 (1970)

26. Adams, J.Q., J.A.C.S. 89:24, 6022 (1967)

27. Carlsson, D.J. Suprunchunk, T. and Wiles, D.M., J.A.P.S. 16, 615(1972)

28. Porter, G. and Wright, M.P., Discussions of Farad Soc. 27, 18 (1959)

29. McConnell, H., J.Chem.Phys. 20, 1043 (1952)

30. George, G.A., J.A.P.S. 18, 117 (1974)

31. Linschitz, H. and Sarkanen, K., J.A.C.S. 80, 4826 (1958)

32. Linschitz, H. and Pekkavieneu, L. J.A.C.S. 82, 2411 (1960)

33. Bell, J.A. and Linschitz, H., J.A.C.S. 85, 528 (1963)

34. Fry, A.J.R., Liu, S.U. and Hammond, G.S. J.A.C.S. 88, 4781 (1966)

35. Guillory, J.P. and Cook, C.F. J.A.P.S. Part A-1, 9, 1529 (1971)

36. Adams, J.Q. J.A.C.S. 89:24 6022 (1967)

37. Guillory, J.P. and Cook, C.F. J.A.C.S. 95, 4885 (1973)

38. Carlsson, D.J. and Wiles, D.M. J.Polym.Sci. 12, 2217 (1974)

39. Carlsson, D.J. Mendenhall, G.D., Suprunchunk, T. and Wiles, D.M.
J.A.C.S. 94,8960 (1972)

40. Guillory, J.P. and Cook, C.F. J.Polym.Sci.(Polym.Chem ed.)11,1927(1973)

41. Felder, B. and Schumacher, R. Angew. Macromol. Chem. 31, 35 (1973)

42. Flood,J., Russell, K.E. and Wan, J.K.S. Macromolecules 6, 669 (1973)

43. Scott, G. Atmospheric Oxidation and Antioxidants, Elsevier Amsterdam
(1965) a. page 41
b. page 116

44. Holdsworth, J.D., Scott, G. and Williams, D. J.A.C.S. 4691 (1964)

45. Colclough, T. and Cunnees, J.I. J.C.S. 4790 (1964)

46. Ingolot, K.U. Oxidation of organic compounds Advan.Chem.Ser. 75 - 1
American Chem.Soc. 296 (1968)

47. Mellor, D.C., Moir, A.B. and Scott, G. Europ.Polym. J. 9, 219 (1973)

48. Hutson, G.V. and Scott, G. Chem.and Ind. 725 (1972)

49. Naarmann, H. J. of Appl. Chemistry.

50. Vogel, A.I. Test book of Practical organic Chemistry, 3rd edition. p.721.

51. Gupta, B.D. and Mallik, W.U. J.of Indian Chem.Soc. 48 1(1973)

52. Rundle, and Parasok, J.Chem.Phys. 20, 1487 (1952)

53. Nakamoto, Margoshes and Rundle. J.A.C.S. 77, 6480 (1955)

54. Bline and Hadzi, J.C.S. 4536 (1958)

55. Weissberger, A(ed) Techniques of organic chemistry Vol.VII, 2nd edition. (interscience) 1955

56. Kharasch, M.S., Fono, A. and Nudenberg, W. J.Oxg.Chem. 16, 113 (1951)

57. Apparatus developed by R.P. Brueton, University of Aston in Birmingham.

58. Reference 43 page 99

59. Hirt, R.C. et al. J.Opt.Soc.Am. 50, 706 (1960)

60. Muir, R.D. and Graupner, A.J. Anal.Chem. 36, 194 (1964)

61. Wagner, C.D., Smith R.H. and Peters, E.D. Analyt.Chem. 19, 976 (1947)

62. Paul, K.T. RAPRA Bulletin, 2, 29 (1972)

63. Rugg, F.M., Smith, J.J. and Bacon, R.C. J.Poly.Sci. 13, 535 (1954)

64. Lohman, F.H. J.Chem.Educ. 32, 155 (1955)

65. Henniker, Infra-Red Spectrometry of Industrial Polymers (Academic Press) 161 (1967)

66. Ewing, Instrumental Methods of C hemical Analysis (McGraw-Hill) 82(1960)

68. Parker, C.A. and Hatchard, C.G. J.Phys.Chem. 63, 22 (1959)

69. Parker, C.A. Proc.Roy.Soc.(London) A220, 104 (1953)

70. Parker, C.A. Trans.Faraday Soc. 50, 1213 (1954)

71. Davies, Goldsmith, Gupta and Lester. J.C.S. 4920 (1956)

72. Autoxidation of Hydrocarbons and Polyolefins by Reich, L. and Stivale, S.S. Page 98

73. Hiah, R. Traylor, T.G. J.A.C.S. 87, 2766 (1965)

74. Factor, A., Russel, C.A. and Traylor, T.G. J.A.C.S. 87, 3692 (1965)

75. Traylor, T.G., Russel, C.A. J.A.C.S. 87, 3698 (1965)

76. Clark, H.C. and Odell, A.I. J.Chem.Soc. 520 (1956)

77. Paper chromatography edited by Huis, I.M. Macck. (Academic Press New York) p.252

78. Fundamentals of molecular spectroscopy by C.N.Banwell (McGraw-Hill Publishing Company Ltd. 1966) p.102

79. Applications of Abs rption spectroscopy or organic compounds by J.R.Dyer (Prentice-Hall, inc. 1965) p.40

80. Borga, Enchre, and Scott, G. in Press

81. Preference 43. page 57

82. Guillory, J.P. and Becker, R.S. J.Polym.Sci.(Poly.Chem.ed) 42,993 (1974)

83. Kharash, M.S., Fono, A. and Nudenberg, W. J.Org.Chem. 16, 113 (1951)

84. Hock, H., Lang, S. Ber 77B, 257 (1944)

85. Kharash, M.S., Fox, A. and Nudenberg, W. J.Org.Chem. 15, 748 (1950)

86. Seubolos, F.H. and Vaughan, W. J.A.C.S. 75, 370 (1953)

87. Scott, G. British Polymer Journal 3, 24 (1971)

88. Kharash et al. J.Org.Chem. 15, 763 (1950)

89. Sedlar , Private communication

90. Fox, J.J., Martin, A.E. Proc.Roy.Soc.(London) A175, 208 (1940)

91. Luongo, J.P. J.Polym.Sci. 42, 139 (1960)

92. Cross, L.M., Richards, R.B. and Willis, H.A. Discussions of Faraday Soc. 9, 235 (1950)

93. Guillet, J.E., Dhanray, J., Golemba, F.J., Hartley, G.H. from ref(80)

94. Pross, A.W., and Black, R.M. J.Soc.Chem.Ind. 69, 113 (1950)

95. Winslow, F.H., Matreyeck, W., Trozzolo, A.H. and Hansen, R.H. ACS Div, Polym.Chem. Polymer foreprints 9, 377 (1950)

96. Amin, M.U., Scott, G. and Tillekeratua, L.M.K. European Polymer Journal (1975)

97. Burgess, A.R., Natl.Bur.St.Circular 525, 149 (1953)

98. Scott, G. Lecture delivered at the American Chemical Society

99. Beachell, H.C.and Nemphos, S.P. J.Polym.Sci. 25, 173 (1957)

100. Wall, L.A., and Tyron, M. J.Polym.Sci. 62, 697 (1958)

101. Jelhink, J.Polym.Sci. 4, 1 (1949)

102. Grassie, N. and Wein, N.A. J.Appl. Polym. Sci. 9, 999 (1965)